Ships in an Artificial Force Field:

A Multi-agent System for Nautical Traffic and Safety

Proefschrift

ter verkrijging van de graad van doctor

aan de Technische Universiteit Delft,

op gezag van de Rector Magnificus prof. ir. K.C.A.M. Luyben,

voorzitter van het College voor Promoties,

in het openbaar te verdedigen op 13 mei 2014 om 10:00 uur

door Fangliang XIAO

Master of Science from Wuhan University of Technology

geboren te Wuhan, China

Dit proefschrift is goedgekeurd door de promotoren:

Prof. dr. B.J.M. Ale
Prof. ir. H. Ligteringen

Samenstelling promotiecommissie:

Rector Magnificus,	voorzitter
Prof. dr. B.J.M. Ale,	Technische Universiteit Delft, promotor
Prof. ir. H. Ligteringen,	Technische Universiteit Delft, promotor
Dr.ir. C. van Gulijk,	Technische Universiteit Delft
Prof. dr. ir. P. van Gelder,	Technische Universiteit Delft
Prof. ir. T. Vellinga,	Technische Universiteit Delft
Dr.ir. W. Daamen,	Technische Universiteit Delft
Prof. dr. J. Mou,	Wuhan University of Technology
Prof. dr. ir. S.P. Hoogendoorn,	Technische Universiteit Delft, reservelid

Dissertation
Ships in an Artificial Force Field: A Multi-agent System for Nautical Traffic and Safety

Authored and distributed by:

Fangliang Xiao
Delft University of Technology
Faculty of Technology, Policy and Management
Jaffalaan 5
2628 BX, Delft
The Netherlands

Cover image from: http://xiaba.shijue.me/stuff/5141755b4b7959dc570000ae.html
http://hdw.eweb4.com/out/1100696.html
Cover design by Chen Guo
Printed by CPI Wöhrman Print Service www.wps.nl
ISBN/EAN: 978-94-6186-300-3

ACKNOWLEDGEMENT

The result of being a PhD candidate in the Netherlands is much more rewarding than just the doctoral degree. The experience in the Netherlands has broadened my mind by understanding different ways of life and thinking. I have become more open to differences, as there are reasons behind the differences. The Dutch culture has made me understand the Chinese culture better and become more confident of the future. The benefits are much more than I can consciously list here. I couldn't have come so far without the support of the people around me. All my success owns to my supervisors, my colleagues, my friends, and my family.

First and foremost I would like to thank my promoter Prof. Ben Ale, who gave me the opportunity to carry out the PhD research in this university. I had all the freedom to try new ideas and cooperate with the interested people. He also encouraged me to improve my English and gave me all the opportunities to learn English. Every step of my progress was under his supervision.

My promoter Prof. Han Ligteringen played a very important role. He was great support to me. His guidance varied from academic research, different perspective of thinking, cultural discussions, and personal growth. He spent a lot of time on every detail of my work. Without his patience and encouragement, I couldn't have finished this thesis.

My daily supervisor, Coen van Gulijk, always assisted me with problems that I had. He taught me many skills in this academic world. This research would have become more difficult without him.

Interactions with colleagues were pleasant and rewarding. The ladies were kind and the men were supportive. Erika van Verseveld and Carla van Dongen relieved me from many administrative burdens. My officemate Zahra Rezvani supported me with many interesting discussions about research, culture, and life. Frank Guldenmund showed his understanding to my troubles and shared his ideas to overcome the obstacles. Paul Swuste shared his interesting stories and experiences to me. Matthijs Moorkamp translated the summary of the thesis. I also had interesting talks and interactions with other colleagues. I appreciate the group members who had nice meals together.

My friends in Delft brought me happiness and support. Haoliang Huang and Liangyue Ji accompanied with me during the most difficult first year in the Netherlands. I was always welcomed to their home whenever I was happy or not. Xiaogang Yang always shared his wisdom, sincere advice, and understanding of this world. Dan Liu and Jing Xiao brought me a lot of fun during their stay in the Netherlands. When friends are not listed here, it does not mean that they are not important to me. I think they will understand because they are friends.

Special thanks to the members of the doctoral committee who spent a lot of time on my thesis and gave their valuable comments. There were also other people who contributed to the thesis. Yvonne Koldenhof and her colleagues from the Dutch Maritime Research Institute (MARIN) provided the AIS data and were kind enough to allow me the use of their software "Show Route" for the data analysis. Lamber Hulsen, Cor van der Schelde and their colleagues from the Port of Rotterdam provided the hydrodynamic simulation results for currents using the Delft3D® software. Chen Guo helped me to design the thesis cover. Claire Taylor helped me with the language problems in the thesis. Many thanks go to Cees Timmers and Franca Post who gave various supports during my stay in Delft.

My family is always the source of strength. The good health that I inherited is invaluable. I haven't been sick during the four years with heavy workload. Good life habits are also inherited from my family which has increased the possibility of my success.

Fangliang Xiao, Delft, April 2014

SUMMARY

Ships in an Artificial Force Field: A Multi-agent System for Nautical Traffic and Safety

Ship accidents are part of the risk assessment for the design of ships, offshore infrastructures, and waterways. However, in reality it is difficult to get sufficient understanding and detailed information of the ship traffic. With the development of data collection and analysis, probabilistic risk models have been improved to better reflect the reality. With the development of computer-aided systems, simulation models have been used to understand the problems and mitigate the risks, since simulation is able to provide the details of interactions among components and characteristics of components within a complex system.

The main objective of this research is developing a simulation tool that provides information of detailed ship behavior in a specific navigational environment, on both the ship traffic level and the individual ship level, for safety analysis, decision making, planning of ports and waterways, and design of mitigation measures. In order to achieve the main objective of this research, the following research questions have been composed:

- What are the limitations in the existing methods for maritime risk analyses? What are the advantages of using a simulation method?
- How can we derive the information from AIS (Automatic Identification System) data and further utilize the information for simulating realistic ship behavior?
- How can we develop a realistic nautical traffic simulation model with detailed description of its methodology, concept, structure, calibration, and validation?
- How can we utilize the simulation in probabilistic risk analyses and further applications?

In this research, we have developed the Artificial Nautical Traffic System (ANTS) model for maritime safety. The simulation method proposed is able to provide realistic ship traffic behavior by using the agent based model and the artificial force field. The ODD protocol (Overview, Design concepts, Details) has been a great support for detailed description of its methodology, concept, structure, calibration, and validation. Ship AIS data is treated as real

world data, therefore the data have been analyzed and utilized. A Dutch case and a Chinese case have been studied to demonstrate model implementation, calibration, validation, and the applications.

The literature review has described the state-of-the-art on the probabilistic risk assessment (PRA) of maritime accidents. It is found that the approach has evolved roughly from statistical analysis, to analytical methods, then to a method based on networks, and finally to a simulation method, while some researchers combined several methods to solve complex problems. The simulation method showed its advantages in providing sufficient ship (traffic) details, realistic representation of ship behavior and environment, and evolving sufficient factors that need to be taken into consideration. The complex system of ship traffic that is subject of analysis cannot be sufficiently reproduced by the other methods. Therefore, it has been concluded that the simulation method is the best way to execute PRA with realistic detailed behavior on both ship traffic level and individual ship level, taking into account the influence of wind and currents.

The ODD protocol has been applied for the model development and description. It helps with presenting many elements in the multi-agent system in a standard form and supports systematic description of relevant elements in the simulation. Firstly, the structure of the model becomes clear and the processes of the model are better organized. Secondly, it helps in defining the stochastic characteristics of the agent-based model. Thirdly, it helps to explain the way that the individual ship behavior is transformed into traffic behavior. Fourthly, the sub-model element helps to describe the artificial force field model and other sub-models for ship movements.

The AIS data provides boundary inputs, information for model development, model calibration, and model validation. This thesis interprets the AIS data on both a ship traffic level and an individual ship level. AIS data is utilized for model calibration and validation. An innovative use of the correlation coefficient analysis has been introduced to identify the factors that determine the artificial forces and find the parameters in the equations.

The most innovative part of theory development is adopting and applying the multi-agent concept and artificial force field theory in the nautical traffic simulation model. Firstly, taking advantage of the multi-agent concept, the autonomous ships are able to perceive their local circumstances (encountering situations, waterway geometry), and make decisions to maneuver the ship based on regulations and common practices in ship navigation. The autonomous nature of the agents showed advantages on both an individual ship level and a ship traffic level. On an individual ship level, the individual ship behavior is realistic and reflects the proper characteristics of the ship. On a ship traffic level, the simulation showed the statistical characteristics of the traffic. Secondly, the multi-agent system has the potential to reflect interactions (e.g. evasive behavior), emergent situations (e.g. different situations for collision avoidance), and stochastic characteristics (a number of random

variables to get stochastic ship behavior), which are lacking in most of the existing ship traffic simulation models. The decision making process for ship maneuvering is mimicked using artificial forces for collision avoidance behavior of ship interactions. The forces are based on properties of the ships and their environments such as the dimensions of the ships, speed, ship types, encountering situations, and the shape of the water channel. Head-on forces, overtaking forces, and the forces from waterway boundaries are developed based on statistical analysis of ship encounters. The artificial forces determine the rudder angle for the ship to change the course and avoid collision, and finally to achieve a new lateral position with balanced forces. Note that the forces not only enable the ship to avoid collision, but also reflect the regulations on collision avoidance and common practices to represent realistic ship tracks that are similar to reality.

The ANTS model has been implemented for both a Dutch case and a Chinese case. For validation, the traffic level of simulation output is compared to the reality for both cases. On individual ship level, three head-on encounters and three overtaking encounters are compared. The results show that the simulation outputs are similar to reality.

Applications for probabilistic risk analysis of accidents have been provided using the model. The probabilities of grounding, close encounters and collisions can be determined, based on simulation runs that cover sufficient length of time (e.g. a full year). Future situations with a larger density of ship traffic can also be predicted. Those applications demonstrate the possible ways of further using the ANTS model for safety analysis.

SAMENVATTING

Schepen in een kunstmatig krachtenveld: een multi-agent model voor nautisch verkeer en nautische verkeersveiligheid

Bij het ontwerp van schepen, offshore constructies en waterwegen worden risico-inventarisaties gemaakt waarbij ongevallen met schepen een belangrijk onderdeel zijn. Het blijkt echter lastig om voldoende gedetailleerde informatie te verzamelen over het scheepvaartverkeer. Er worden probabilistische risicomodellen (PRA) gebruikt die een beter inzicht in de veiligheid geven. Deze risicomodellen zijn in de afgelopen jaren verbeterd door ontwikkelingen op het gebied van data verzameling en data analyse. Met de ontwikkeling van computer systemen zijn simulatiemodellen toegepast waarmee de problemen beter begrepen worden en risico's beperkt worden. Dit was mogelijk doordat simulaties het mogelijk maken in complexe systemen de details van interacties tussen componenten en de eigenschappen van die componenten te geven.

Het hoofddoel van dit onderzoek is het ontwikkelen van een simulatie instrument dat in staat is, zowel op het niveau van het scheepvaartverkeer als het niveau van individuele schepen, informatie te leveren over het detailgedrag van schepen in een bepaalde navigatieomgeving. Dit instrument kan worden ingezet voor veiligheidsanalyses, besluitvorming, ruimtelijke planning van havens en waterwegen en het ontwerp van risicoverlagende maatregelen. Om het onderzoeksdoel te realiseren zijn de volgende onderzoeksvragen geformuleerd:

- Wat zijn de beperkingen van de bestaande methoden op het gebied van maritieme risico analyses? En wat zijn de voordelen van het gebruik van een simulatie methode?
- Hoe kunnen we informatie aan AIS (Automatic Identification System) ontlenen en gebruiken voor het simuleren van realistisch scheepvaartverkeer?
- Hoe kunnen we een realistisch scheepvaartverkeersmodel ontwikkelen met een gedetailleerde beschrijving van methodologie, gebruikte concepten, structuur, kalibratie en validatie?
- Hoe kunnen we deze simulatie inzetten voor probabilistische risicoanalyses en andere toepassingen?

In dit onderzoek is het Artificial Nautical Traffic System (ANTS) ontwikkeld voor maritieme veiligheid. De voorgestelde simulatiemethode maakt het mogelijk om het gedrag van het scheepvaartverkeer realistisch weer te geven door gebruik te maken van een “agent based model” en een kunstmatig krachtenveld. Het ODD protocol (Overview, Design concepts, Details) is hierbij gebruikt om een gedetailleerde beschrijving op te stellen van de methodologie, concepten, structuur, kalibratie en validatie. Hierbij zijn AIS data beschouwd als “real world” data en om die reden geanalyseerd en toegepast. Een Nederlandse en een Chinese casus zijn gebruikt om de implementatie, kalibratie, validatie en toepassingsmogelijkheden van het model te demonstreren.

In de literatuurstudie is de state-of-the-art beschreven van probabilistische risico-inventarisatie methoden (PRA) voor maritieme veiligheid. Hierbij hebben we gevonden dat de methodiek grofweg een ontwikkeling heeft doorgemaakt van statistische analyses, via analytische- en netwerk methoden naar methoden gebaseerd op simulaties, waarbij sommige onderzoekers een combinatie toepasten voor het oplossen van complexe problemen. De simulatiemethode heeft hierbij voordelen omdat het in staat is voldoende details van schepen (en scheepsverkeer) mee te nemen en omdat voldoende relevante factoren meeneemt om het gedrag van schepen en hun omgeving realistisch weer te geven. Het complexe systeem van het scheepvaartverkeer kan niet voldoende nauwkeurig worden gereproduceerd door de andere methoden. Om die reden hebben is geconcludeerd dat de simulatiemethode de beste manier is om PRA uit te voeren met een gedetailleerd beeld van het gedrag van schepen en het scheepvaartverkeer waarbij ook de invloed van wind en stroom meegenomen kan worden.

Het ODD protocol is toegepast voor het ontwikkelen en het beschrijven van het model. Deze methode is geschikt voor het in een standaardvorm presenteren van de vele elementen in een “multi-agent” systeem en helpt bij de systematische beschrijving van de relevante elementen in de simulatie. Ten eerste wordt de structuur van het model duidelijk en kunnen de processen binnen het model beter worden georganiseerd. In de tweede plaats helpt het in het definiëren van de stochastische eigenschappen van het model. Ten derde wordt het eenvoudiger het gedrag van individuele schepen naar dat van het scheepvaartverkeer te vertalen. En tenslotte maakt het gebruik van “sub-modellen” het mogelijk het model voor het kunstmatige krachtenveld te beschrijven, evenals andere submodellen voor het manoeuvreergedrag van de schepen.

De AIS data leveren randvoorwaarden voor de simulaties, informatie voor het ontwikkelen van het model, het kalibreren van het model en tenslotte voor model-validatie. Hierbij hebben we de AIS data gebruikt voor zowel informatie op het niveau van het scheepvaartverkeer als het niveau van individuele schepen. Beide data-groepen zijn gebruikt voor kalibratie en validatie. Voor de calibratie is op innovatieve wijze gebruik gemaakt van

correlatie coëfficiënt-analyse om de factoren in het kunstmatige krachtenveld en de parameters in de vergelijkingen te bepalen.

Het meest vernieuwende aspect van theorieontwikkeling in deze studie is het toepassen van het “multi-agent” concept en de theorie over kunstmatige krachtenvelden in een maritiem verkeerssimulatiemodel. Ten eerste is het door het “multi-agent” concept mogelijk dat autonome schepen de lokale omstandigheden (ontmoetingen en vaarweg geometrie) waarnemen en kunnen manoeuvreren op basis van verkeersregels en de algemene navigatiepraktijk. De autonomie van deze “agents” geeft voordelen op zowel het niveau van individuele schepen als het niveau van het scheepvaartverkeer. Individuele schepen gedragen zich hierdoor realistisch in de simulatie en vertonen de juiste eigenschappen. Daarnaast vertoont het gesimuleerde scheepvaartverkeer de juiste statistische karakteristieken. Ten tweede heeft het “multi-agent” systeem de mogelijkheid interacties (zoals ontwijkend gedrag), noodsituaties (zoals het voorkomen van aanvaring), en stochastische eigenschappen weer te geven, die in de meeste bestaande scheepvaartsimulatiemodellen ontbreken. Het besluitvormingsproces voor het manoeuvreren van schepen is hierbij nagebootst door toepassing van kunstmatige krachten bij het voorkomen van aanvaring. Deze krachten zijn gebaseerd op de eigenschappen van de schepen en hun omgeving zoals afmetingen, snelheid, scheepstypen, ontmoetingssituaties en de vorm van de waterweg. De krachten bij kop-kop ontmoeting, bij inhalen en de krachten als gevolg van de oevers van de waterweg zijn gebaseerd op een statistische analyse van scheepsontmoetingen. De kunstmatige krachten bepalen de roerhoek om de koers te wijzigen en een aanvaring te voorkomen, en vervolgens een nieuwe positie te bereiken waarin de krachten weer in evenwicht zijn. Daarbij moet opgemerkt worden dat de krachten tevens het vaarreglement ter voorkoming van aanvaring zijn meenemen om een zo realistisch mogelijke afspiegeling van scheepsbewegingen te krijgen.

Het ANTS model is toegepast op een Nederlandse en Chinese casus. Voor validatie van het model is de modeluitvoer in beide casussen vergeleken met de werkelijke gegevens. Op het niveau van individuele schepen zijn drie kop-kop ontmoetingen en drie inhaalmanoeuvres vergeleken. De resultaten laten zien dat de gesimuleerde uitvoer te vergelijken is met de werkelijke scheepsbewegingen.

Toepassingen op het gebied van probabilistische risico-analyse van ongevallen zijn gepresenteerd met gebruikmaking van het model. De kans van stranding, “near misses” en aanvaringen kunnen berekend worden op basis van simulatieruns met voldoende lengte in de tijd (bijvoorbeeld één jaar). Toekomstige situaties met grotere scheepsdichtheid kunnen ook worden voorspeld. Deze toepassingen demonstreren de mogelijke manieren waarop het ANTS model ingezet kan worden voor veiligheidsanalyses.

TABLE OF CONTENTS

LIST OF TABLES

LIST OF FIGURES

TERMS AND SYMBOLS

This section shows an overview of terms and symbols that are used in the main content of the thesis. The terms used in this thesis are based on the definition by Webster (1992). The Roman symbols other than the parameters listed in Table 6-1, Table 6-2, Table 6-3, and Table 6-4 are listed in Table 1. Other symbols appeared in the thesis are listed in Table 2. The symbols in the literature review (Chapter 2) are not listed, as the symbols are defined in the concerned paragraph.

Waterway and vessel terms defined by Webster (1992)

BERTH	A place where a vessel is moored at a wharf or lies at anchor
CHANNAL	Part of a watercourse used as a fairway for the passage of shipping. May be formed totally or in part through dredging.
FAIRWAY	The main thoroughfare of shipping in a harbor or channel; although generally clear of obstructions, it may include a middle ground (that is, a shoal in a fairway having a channel on either side) suitably indicated by navigation marks (such as buoys)
PORT	A place in which vessels load and discharge cargoes or passengers. Facilities in developed ports normally include berths, cargo handling and storage facilities, and land transportation connections. Normally a harbor city, town, or industrial complex.
WATERWAY	A water area provides a means of transportation from one place to another, principally a water area providing a regular route for water traffic, such as a bay, channel, passage or canal, and adjacent basins and berthing areas. May be natural, artificial, or a combination of both.
BARGE	A heavy, no-self-propelled vessel designed for carrying or lightering cargo.

PILOT The person piloting (directing and controlling the maneuvering of) the vessel. In actual vessel operations, the pilot could be a licensed independent pilot, master or qualified deck officer.

SHIP A self-propelled, decked vessel used in deep-water navigation.

TUG A strongly built vessel specially designed to pull or push other vessels.

VESSEL A general term referring to all types of watercraft including ships, barges, tugs, yachts, and small boats.

List of Symbols

Table 1 Roman symbols other than the parameters listed in Table 6-1, Table 6-2, Table 6-3, and Table 6-4

a	Ship speed acceleration (m/s^2)
B	ship beam (m)
$\mathrm{B_a}$	the hull area above the waterline (m^2)
$\mathrm{B_w}$	the hull area below the waterline (m^2)
$\mathrm{C_b}$	block Coefficient
C_i	the consequence of an accident in a given time
d	ship draught (m)
$\mathrm{D_{head-on}}$	"Distance to act" for a head-on encounter (m)
$\mathrm{D_{overtaking}}$	the distances to act for a overtaking encounter (m)
$\mathrm{D_{overtaking\_after}}$	the distances to act after a overtaking encounter (m)
$\mathrm{Exp(mu)}$	exponential distribution with mean $(1/\mathrm{mu})$
$\mathrm{F_{bank}}$	the force from the starboard bank of the channel
$\mathrm{F_{bank,p}}$	the force from the port bank of the channel
$\Delta\mathrm{F_{bank}}$	change in force from the starboard channel bank
$\Delta\mathrm{F_{bank,p}}$	change in force from the port channel bank
$\mathrm{F_{head-on}}$	force comes from another ship within a head-on situation
$\mathrm{F_{overtaking}}$	force makes the overtaking ship shift to port
$\mathrm{F_{overtaken}}$	force makes the overtaken ship shift to starboard
K	constant
K'	the correction modulus for shallow water
K	one of the maneuverability indices, a larger K means a good ability to change the course of the ship
K′	one of the non-dimensional form of maneuverability indices
L	distance to the port boundary of the channel (m)
LOA	Length overall (m)
Ld/A_R	rudder area ratio
N	number of ship passages in a certain period of time
$\mathrm{N_A}$	number of collision candidates in a period of time
$\mathrm{N_C}$	number of collision occurrences in a period of time
$\mathrm{N_{daily}}$	daily number of ship arrivals
$\mathrm{N_E}$	number of grounding *with engine failure* occurrences in a period of time
$\mathrm{N_R}$	number of grounding *with rudder failure* occurrences in a period of time
$\mathrm{N_{weekly}}$	weekly number of ship arrivals
$\mathrm{P_C}$	the probability that further evasive action by any means has failed

P_{hourly}	ratio of average hourly number of ship arrivals, which is used to describe the hourly differences of ship arrivals
P_i	the probability of i-th accident in a given time
$\boldsymbol{R}$	risk
R	distance to the starboard boundary of the channel (m)
ΔR	a random residual (the discrepancy between theory and practice for head-on force) (m)
ΔR_3	a random residual (the residual from regression for the distance from starboard channel boundary after encountering) (m)
R^2	coefficient of determination
R_{daily}	daily residuals from regression
R_E	average accident rate for each occurrence of engine failure
R_{EF}	failure rate of main engine
R_G	the accident rate for each occurrence of rudder failure
R_{RF}	failure rate of rudder system
R_{weekly}	weekly residuals from regression
S_n	the distance between the two adjacent crossing-lines (m)
S_p	speed of a ship (m/s)
T	one of the maneuverability indices, a larger T indicates the ship has a better ability to keep its course
T_E	the average time for each ship passage in the studied area
T_R	the average time for each ship passage in the studied area
T_{st}	the time constant of the ship deceleration
T'	one of the non-dimensional form of maneuverability indices
t	time spent after engine failure (minutes)
t_n	is time stamp at crossing-line number n (s)
Δt	time step in the simulation (s)
TI_n	The time interval for the ship number n (s)
TA_n	the time of arrival for the ship number n (s)
v_n	vessel speed at crossing-line number n (m/s)
Δv_n	ship speed change between two adjacent crossing-lines at crossing-line number n (m/s)
V_0	the ship speed at the beginning of the engine failure (kn)
V_a	wind velocity relative to the ship (m/s)
V_c	current velocity (m/s)
V_g	ship speed over ground (m/s)
V_s	the ship velocity in wind (kn)
V_T'	the drift velocity of the ship by wind (m/s)
V_w	wind speed (m/s)
(x_i, y_i)	ship position in the simulation

Table 2 Other symbols appeared in the thesis

δ	rudder angle (degree)
γ	rate of turning (degree/second)
Φ_i	heading of the ship (degree)
$\aleph(\mu, \sigma^2)$	normal distribution with mean (μ) and standard deviation (σ)
μ	mean of normal distribution
σ	standard deviation of normal distribution
Θ	phase position in a tidal cycle
$\Delta\Theta$	phase difference for two adjacent hours

1. INTRODUCTION

1.1 Research motivation

This research looks into the problems of the risk of ship collision and ship grounding with ever increasing ship traffic in confined waterways such as ports and inland waterways, driven by the increasing needs of waterborne transportation that supports a dynamic economy. Ship accidents are part of the risk assessment for the design of ships, offshore infrastructures, and waterways. Understanding the detailed information of the ship traffic in the waterway is needed to reduce the maritime risks. There are two dimensions to be proactive in both design phase and operational phase of an infrastructure. The first dimension is the probabilistic design process, where a better-designed waterway can reduce the chance of ship collisions. The other dimension is the operational phase when the infrastructure is already there. Risk analysis can play an important role in the operational guidance for the traffic. There are also two dimensions for risk analysis, which are probability and consequence. A better design or improved operational guidance can reduce the probability of accidents and/or the consequences of collision.

However, in reality it is difficult to get sufficient understanding and detailed information of the ship traffic. There are two reasons for this. One is that the ship traffic is a dynamic system that is very complex. The other is the lack of information to learn from accidents since only accidents that involve large amounts of damage are reported in the public domain. To overcome these difficulties, detailed information of ship behavior is needed.

Previously, there are analytical methods (Wang et al., 2006) and the models based on networks (e.g., Fuzzy Logic (Priadi et al., 2012), Bayesian Networks (Szwed et al., 2006), and Neural Networks (Łącki et al., 2012)) for risks assessment for the design of ships, offshore infrastructures and waterways. The prime driver for the risk analysis is the probability of accidents. Therefore, analytical methods were developed to calculate that probability (e.g. the (AASHTO, 2004) model). However, analytical models lack detailed descriptions of real-life ship movements (Li et al., 2012b, Xiao et al., 2010). The models based on networks are still dependent on historical data and expert opinions.

A simulation tool has been used for several decades as a way to provide detailed ship behavior when the information required cannot easily be obtained from the real world. Following the first simulation approach by Davis et al. (1980), in recent years two different types of simulation models were developed, one for ship traffic simulation and the other for individual ship simulation. For ship traffic, Hasegawa et al. (2000) developed SMARTS (Marine Traffic Simulation System) for ship traffic in ports. However the routes and waypoints are predetermined and dynamic collision avoidance behavior was not the focus. A different simulation model with dynamic ship movements with different ship types and ship sizes has been developed for the Gulf of Finland (Goerlandt et al., 2011). However, the behavior of individual ships is simplified to implement the collision avoidance. This is because the hydrodynamic behavior of the individual ships and the human influences are very complex. For individual ships, the interaction with other ships and the role of human interventions are important. Dynamic ship movements can be simulated with manned ship-handling simulators (e.g. the Mermaid 500 at MARIN). One of the drawbacks is that normally only scenarios with certain extreme circumstances are simulated using the system. Another disadvantage is that the interactions between ships are based on expert judgment. And different traffic patterns and uncertainties in the waterway are difficult to be reflected by this system, because the simulations are time consuming and the equipment is expensive (Webster, 1992).

Therefore the model requirement should be a realistic reproduction of the individual ship behavior and the entire traffic, as none of the existing models achieves this. The ANTS model is an agent based simulation system using artificial force field theory to describe the details of the ship traffic and collision candidates. The simulation method proposed is able to provide realistic ship traffic behavior. In this sense, it provides information that not only statistically reflects the ship behavior on a ship traffic level, but also provides realistic ship behavior on an individual ship level. On a ship traffic level, the ships are made to behave in a traffic pattern similar to reality. On an individual ship level, the ship behavior is based on regulations and common practices that are derived from AIS (Automatic Identification System) ship tracks. More importantly, the individual ship behavior is a result of multiple influences from encountering situations and weather conditions.

The ANTS model is only applicable in restricted waters so far. However, the method introduced in this thesis can be used to develop submodels that are suitable for a wider perspective (such as in the open sea area). The focus of the ANTS method is restricted water, because the geometry is an important factor and statistical data are scarce, while the models for open sea are more reliable.

1.2 Research questions

The main objective of this research is developing a simulation tool that provides information of detailed ship behavior in specific navigational environment on both the ship traffic level and the individual ship level for safety analysis, decision making, planning of ports and waterways, and design of mitigation measures. In order to achieve the main objective of this research, the following research questions have been composed:

- What are the limitations in the existing methods for maritime risk analyses? What are the advantages of using a simulation method?
- How can we derive the information from AIS data and further utilize the information for simulating realistic ship behavior?
- How can we develop a realistic nautical traffic simulation model with detailed description of its methodology, concept, structure, calibration, and validation?
- How can we utilize the simulation in probabilistic risk analyses and further applications?

1.3 Research approach

The approach is divided into three components, (i) finding the gaps in the latest knowledge and designing a new method to fill these gaps, (ii) developing a realistic simulation to fulfill the main objective, and (iii) using the simulation model to demonstrate its potential. The approach can be elaborated as follows:

1.3.1 Literature review

This thesis studies the state of the art literature on probabilistic risk assessment (PRA) of the nautical traffic and waterway-related infrastructures. Based on the literature, gaps in the existing methods can be found. In this way, a solid basis of knowledge can be formulated for the work that will be carried out afterwards.

1.3.2 Data collection and analysis

The AIS data is collected and analyzed to obtain statistical data on the ship behavior and better understanding of the ship traffic in the waterway. The AIS data is field data that adequately describes “reality”. The information on environmental conditions such as wind, current, and visibility should be collected from the authorities.

The results of the AIS data analysis provide boundary inputs, information for model development, model calibration, and model validation. The AIS data analysis also concerns the characteristics of the ship behavior on both a ship traffic level and an individual ship level. This thesis studies the way the ship interactions influence the ship traffic. Possible effects on

the ship behavior resulting from many influences should be identified, which include local regulations, local navigational circumstances, encounters, wind, current, and visibility. Other characteristics such as the LOA (Length Overall), speed and the gross tonnage of the ship should also be categorized and taken into account in describing ship behavior.

1.3.3 Detailed description of the model methodology, concept, structure, calibration, and validation

There are many methods and models that could achieve part of the research objective. The challenge is to select the most suitable method. This thesis should provide solid arguments to support the choice of the simulation method to achieve the main objective. Finally, all the methods and concepts should be consistent within a framework in which every element and sub-model is clearly described and fitted.

On this basis a new model for maritime safety has been developed, Artificial Nautical Traffic System (ANTS). The ANTS model can be used to simulate realistic ship traffic to derive probabilistic risk analyses for maritime traffic. It is expected that the ANTS model may also be applicable in many other studies, such as assessing the effectiveness of new rules for the waterway, port and waterway design, and finding proactive ways to mitigate collision risk in busy waterways.

The ANTS model is an agent based simulation system using artificial force field theory to describe the details of the ship traffic and collision candidates. The simulation method proposed is able to provide realistic ship traffic behavior. In this sense, it provides information that not only statistically reflects the ship behavior on a ship traffic level, but also provides realistic ship behavior on an individual ship level. On a ship traffic level, the ships are made to behave in a traffic pattern similar to reality. On an individual ship level, the ship behavior is based on regulations and common practices that are derived from AIS ship tracks. More importantly, the individual ship behavior is a result of multiple influences from encountering situations and weather conditions.

For the model calibration, the parameters are tuned and ranges are provided for the variables in the models. There are always differences between reality and a simulation. A good simulation must ignore the irrelevant factors and concentrate on the important factors that are relevant to represent reality. So, the simulation results must be presented in a suitable form (by either illustrations or tables), to allow comparison with real life data.

For validation, case studies in waterways in the Netherlands and in China have been carried out to test the model. The navigational conditions and regulations are very different when comparing the Dutch case and the Chinese case. Therefore a study area is selected for each case to prove the validity of the agent-based artificial force field model. This thesis compares

the simulation outputs with the AIS data on both a ship traffic level and an individual ship level. The success of the both cases can show the universal applicability of the ANTS model.

1.3.4 Studies for utilizing the simulation

Case studies are presented to illustrate the applications of the ANTS model in the probabilistic risk analysis of accidents. With the simulation output, the way that the individual ship behavior develops into accidents can be studied, thus overcoming the lack of detailed registration in accident records. The model needs to be able to simulate the situations of interest to see what can happen, including future situations or other situations of interest. The case studies provide the way that information can be derived to support the decision making and the development of mitigation measures.

1.4 Thesis contributions

The literature study provides an overview and shows the gaps in previous methods. This thesis states that the simulation method is better for reproducing reality and providing the detailed information needed for risk analyses. The detailed information is difficult to derive with analytical methods. Many elements of risk analysis obtained from previous analytical methods are included in the simulation model. What is special in this model is that the wind, currents, and detailed information on the navigational environment are included.

The main contribution in this research is introducing the artificial force field theory and an agent based model to reproduce individual ship behavior and its integration into ship traffic, taking advantage of the AIS ship tracks to understand the ship behavior on both a ship traffic level and an individual ship level. The decision making process of the officer on watch reproduced by artificial forces is more realistic and reasonable. This avoids behavior that comes from a “black box” from which the result is not fully understandable. Finally, the model represents ship behavior that reflects the regulations and common practices of the waterway.

The data analysis has provided quantitative descriptions of the ship behavior. Encountering situations are also analyzed for model development. In addition, the AIS data is used to understand the ship behavior including the human factor, which is objective evidence rather than an expert’s opinion. The results of the AIS data analysis provide a sound basis for the definition of artificial forces and the development of the multi-agent simulation.

This thesis sets a framework to incorporate the elements that need to be considered in the nautical traffic simulation. The most important principle is the constitution of the ship traffic from behavior of the individual ships based on local navigational circumstances. The situations an individual ship is in are constantly changing, and the individual ship is

constantly responding to these changes. Within the framework, the sub-models for realistic ship movement can be made compatible.

The proposed simulation tool can provide detailed information to improve the safety of the concerned waterway. Firstly, simulations can be used in designing and optimizing the waterway layout to ensure the safe passage of ships. Secondly, simulations can assist in organizing the ship traffic, thus reducing the nautical risk. Finally, the safety and efficiency of the ship traffic performance can always be improved by better understanding the ship traffic, provided with the information from the simulation outputs.

1.6 Outline of the thesis

The thesis consists of five parts. These are a literature review, the data analysis, the model development and description, the case studies, and utility of the simulation.

First of all, the thesis has discussed a number of models that exist in the literature, and finally leads this research into developing a simulation model for probabilistic risk assessment (Chapter 2). Secondly, there are a number of concepts and theories for developing the model. The theories include methods on AIS data analysis (Chapter 3 and Chapter 4), multi-agent concept (Chapter 5), and artificial force field theory and model development (Chapter 5 and Chapter 6). Thirdly, AIS (Automatic Identification System) data is treated as an important basis for the model development. The details of the AIS data analysis are provided in concerned Chapters (Chapter 3, Chapter 4, and Chapter 6). Fourthly, this thesis utilizes the ODD (Overview, Design concepts, Details) protocol for the model structure and detailed description for the complexity, including the structure (Chapter 5) and details (Chapter 6). Finally, both the Dutch case and Chinese case are studied with the use of ANTS model (Chapter 7 and Chapter 8). The model is validated by comparing the output and the historical data for the studied area. The structure of the chapters can be found in Figure 1-1.

The contents of the thesis are:

Chapter 1, Introduction

Chapter 2, Review of the literature on maritime risks

Chapter 3, AIS data analysis

Chapter 4, Influence of visibility, wind, and currents

Chapter 5, Multi-agent concept for simulation

Chapter 6, Submodels in a multi-agent simulation

Chapter 7, Model Setup, calibration and validation

Chapter 8, Case study of the Chinese waterway

Chapter 9, Utilizing the simulation for probabilistic risk analysis

Chapter 10, Conclusions and recommendations

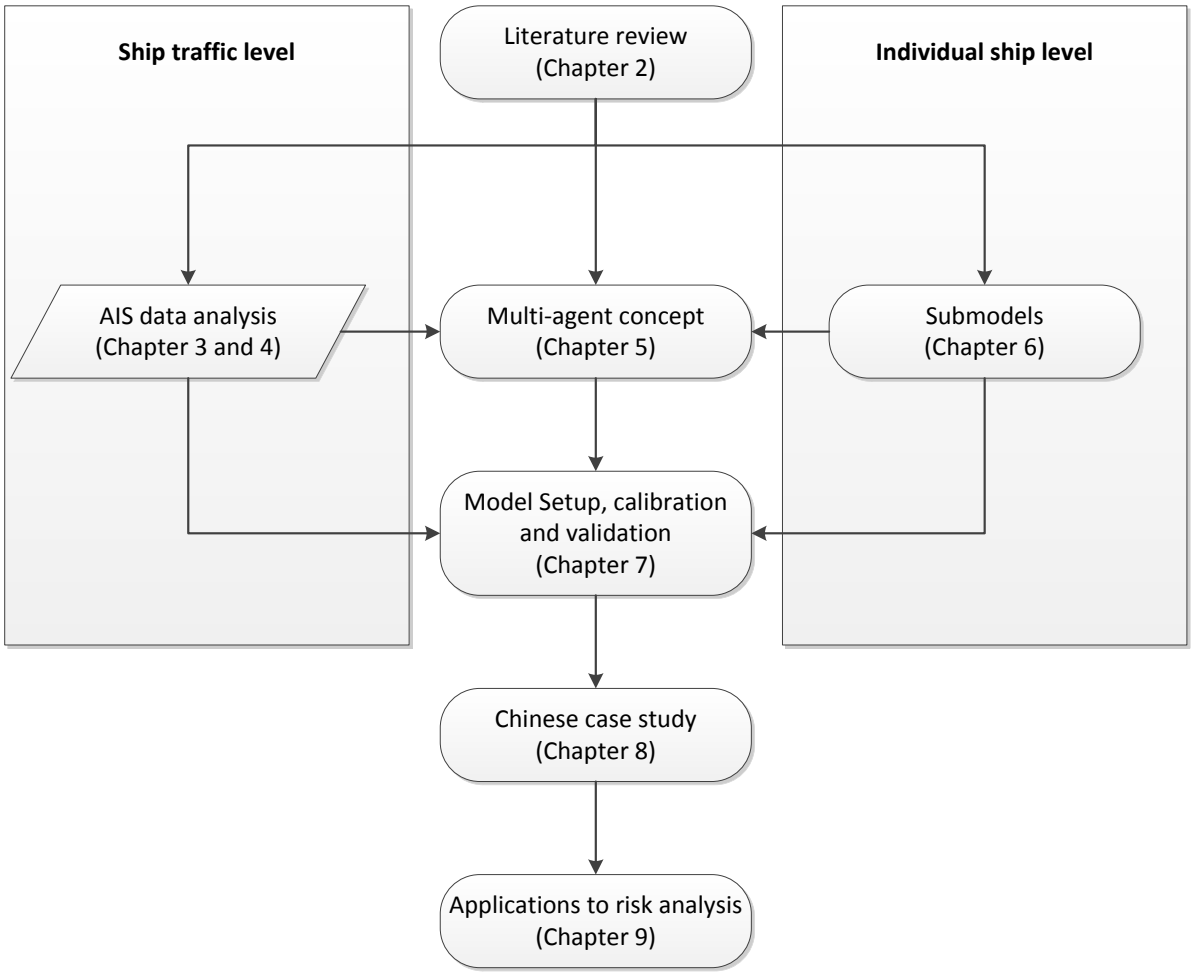

Figure 1-1: Flowchart for the relationships of the chapters

2. REVIEW OF THE LITERATURE ON MARITIME RISKS

2.1 Introduction

This chapter treats the existing literature for the probabilistic risk assessment (PRA) of nautical traffic and waterway related infrastructures. Probabilistic research of ship collision is a part of the research on risk assessment and the design of ships, offshore infrastructures and waterways (Gucma, 2009). There are many methods which were developed for calculating the probability of collision as well as the consequence prediction (Gardenier, 1983, Geng, 2007, Laheld, 1983, Larsen, 1983, Ylitalo, 2009). With worldwide development of the methods for the ship collision risk assessment, it is found that the methods are evolving over time. This thesis differentiates the methods into four categories: statistical methods, analytical methods, network based methods, and simulation methods.

2.2 Statistical Methods

2.2.1 Method Introduction

Normally, accident statistics are derived from historical accident databases to get the probability of disasters. A typical example was conducted by the PIANC (The World Association for Waterborne transport, Navigation, Ports, Waterways) to derive the probability of bridge collision by ships (PIANC, 2001).

The causes of the collisions are also derived from statistics. The causes of collision can be divided into three main groups: human error (approximately 64%), technical failure (21%) and extreme circumstances (15%) (van Manen et al., 1998). Human error is the main source of ship position aberrancy. However, collisions often stem from a combination of human error, technical failure or extreme circumstances. The human factor is not well taken into consideration in the existing models for risk analysis. There are studies that try to statistically interpret human factors as an element in risk analyses. The human element is studied in collision events (Trucco et al., 2008), maneuvering behavior (Bin, 2006), human performance

with different environmental conditions (Hänninen et al., 2010), and ship operation (Itoh et al., 2004, Zheng et al., 2009). However, statistical interpretation still lacks the details that reflect the process how human error results in an accident. The way ship crew's behavior affects the probability of collision should be further studied.

2.2.2 Discussion

The advantage of statistical method is that it is easy to understand and simple to apply. But the disadvantage is that consistent databases are not always available, and the historical data may not reflect what could be happening in the future with different conditions. Therefore, this simple and direct method is restricted by insufficient of historical data.

2.3 Analytical Methods

When the database of accidents is not available, analytical methods are a substitute for PRA. Analytical methods are based on statistical data of ship and bridge collision accidents, the local navigational environment and knowledge of ship navigation. Given a causational factor, then the probability of accidents can be calculated. This method has been widely used in calculating probability of incidents (Gucma et al., 2008, Roeleven et al., 1995, Ylitalo, 2010). The models are introduced below.

2.3.1 AASHTO Model

2.3.1.1 Model description

As described in the AASHTO (American Association of State Highway and Transportation Officials) report, the expression of the annual frequency of collapse of a bridge is (AASHTO, 2004):

$$\mathrm{AF} = (\mathrm{N})(\mathrm{PA})(\mathrm{PG})(\mathrm{PC}) \qquad (2 - 1)$$

Where, AF = annual frequency of the collapse of a bridge element due to a given N; N = annual number of vessels classified by type, size, and loading condition which can strike a bridge element; PA = probability of vessel aberrancy; PG = geometric probability of a collision between an aberrant vessel and a bridge pier; PC = probability of bridge collapse due to a collision with an aberrant vessel. In this formula, the probability of a collision event is:

$$\mathrm{P} = (\mathrm{N})(\mathrm{PA})(\mathrm{PG}) \qquad (2 - 2)$$

The number of vessels, N, could have different values for different classifications of vessels. PA can be determined by a statistical method or an approximate method. The statistical method is based on historical database which includes all kinds of vessel aberrancy. The approximate method is based on the formula:

$$PA = (BR)(RB)(RC)(RXC)(RD) \quad (2 - 3)$$

Where: PA = probability of aberrancy; BR = aberrancy base rate; RB = correction factor for bridge location; RC = correction factor for current acting parallel to vessel transit path; RXC = correction factor for cross-current acting perpendicular to vessel transit path; RD = correction factor for vessel traffic density.

In this method BR is a given number. The BR for ships is 0.6×10^{-4}; and for barges, BR should be 1.2×10^{-4}. RB is a factor for bridge location, ranging from 1.0 to 2.0 depending on river bending. RC and RXC are numbers slightly larger than 1.0 depending on the current velocity. RD is based on the traffic density, which ranges from 1.0 to 1.6 depending on the traffic density in the waterway.

As described in the AASHTO model, the geometric probability, PG, is based on geometric distribution of ship traffic and pier position. It is recognized that the aberrant vessel distribution perpendicular to the centerline of vessel sailing path can be expressed by a normal distribution, see Figure 2-1. The geometric probability, PG, is taken as the area under the normal distribution bounded by the pier width and the width of vessel (AASHTO, 2004). The centerline of vessel sailing path is the location of the mean of the normal distribution. PG shall be determined by the Beam of each vessel category (BM) and the width of the bridge pier. The annual data of ship traffic distribution should be collected from the AIS data, radar observation or personal observations.

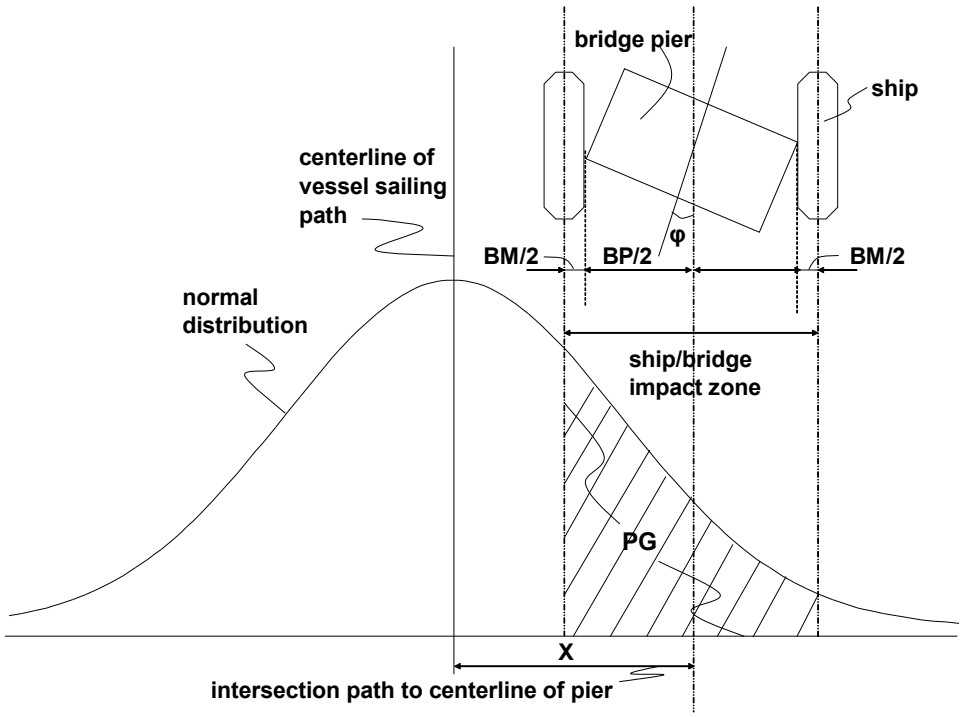

Figure 2-1 Geometric Probability of Pier Collision, based on (AASHTO, 2004)

2.3.1.2 Discussion

The AASHTO model is easy to apply. However, this model is only applicable in the US, because some parameters in the equation were derived from databases of American waterways. So the same parameters could not be directly used in the waterways of another country. For example, BR (aberrancy base rate) was given as 0.6×10^{-4} for a ship and 1.2×10^{-4} for a barge. These values could be different in a country in Europe or Asia. This means the aberrancy rate in a specified waterway should be examined by investigating the local historical databases or expert opinions.

2.3.2 Kunz's Model

2.3.2.1 Model description

Kunz (1998) introduced another simplified mathematical model to calculate the probability of a collision event, based on the relative position between vessels and a bridge pier when the failure occurs. In this model, the failures are assumed to happen randomly and to occur under the influence of various independent causes and conditions, which include human errors, mechanical failures, environmental conditions, traffic density, ship characteristics, waterway characteristics and defects in the waterway. Normal distributions can be found in the model to describe the random variables with reference to the expectation value. The random variables are the ships course deviation with angle φ and the stopping distance x (Figure 2-2). The original equation for the distribution of deviations angle is:

$$F_{\varphi}(\varphi) = \frac{1}{\sqrt{2\pi}\sigma_{\varphi}} \int_{-\infty}^{\varphi} \exp\left\{-\frac{(\varphi-\bar{\varphi})^2}{2\sigma_{\varphi}^2}\right\} d_{\varphi} \qquad (2 - 4)$$

And the distribution of the stopping distance x is written as:

$$F_x(x) = \frac{1}{\sqrt{2\pi}\sigma_x} \int_{-\infty}^{x} \exp\left\{-\frac{(x-\bar{x})^2}{2\sigma_x^2}\right\} d_x \qquad (2 - 5)$$

The probability of a collision course and the probability of the stopping distance x being smaller than the position s before collision, can be found by calculating F_{φ} and F_x for each position s along the approach track of the ship. The collision model is written as:

$$v = N \cdot \int (d\lambda/ds) \cdot W_1(s) \cdot W_2(s) ds \qquad (2 - 6)$$

Where, v is the collision probability; N is the number of passing ships (a linear relationship between the passage frequency and the numbers of accidents is assumed); $(d\lambda/ds)$ is the failure rate per travel unit; $W_1(s) = F_{\varphi}(\varphi_1) - F_{\varphi}(\varphi_2)$, which is the probability of a collision track; $W_2(s) = 1 - F_x(s)$, which is the probability of not being able to stop (or make an evasion) before collision.

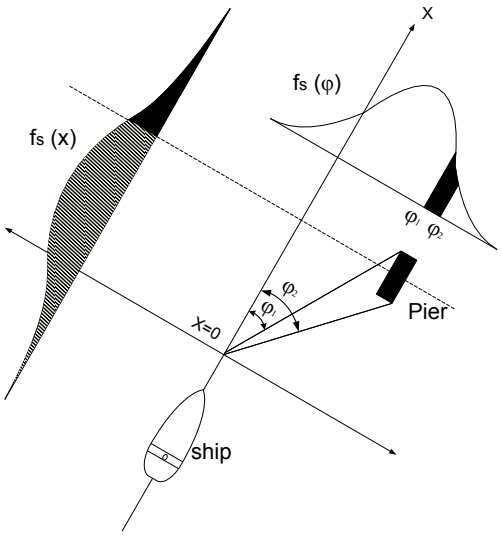

Figure 2-2 Kunz's Mathematical collision model (based on (Kunz, 1998))

In the estimation of the failure rate, the specific locations and environmental conditions within the waterway should be taken into account in the analysis. A global number in specific waterways is used in the more common situation when information is lacking. For instance, if the mean value of failure rates for German waterways, which is between 1.4 and 6.0 [acc. / (ship · year sailing time)], is combined with the sailing time of individual ship when passing the bridge, a failure rate $d\lambda/ds$ can be found. For estimating a more specific failure rate a regression analysis is recommended, which takes into consideration a long time period, preferably since the bridge was constructed.

2.3.2.2 Discussion

Kunz models ship and bridge collision in more detail. An additional normal distribution is used to describe the stopping distance of vessels. Different classifications of the ship can lead to different results for the probability of collision. For example, the stopping distance distribution will be different for different ships. However, several values in the model need to be evaluated for a specific application, because those values could be different for different characteristics of waterways, different location of bridge and different types of vessels.

There are many parameters that need to be considered in this model. These parameters can make the estimation more accurate. However, in practice, it means more statistical data analysis or assumptions. These parameters could also be different in different waterways. This makes the application more complicated than the AASHTO model, in which many parameters are predetermined. Moreover, the model specifies that failures occur under the influence of human errors, mechanical failures, environmental conditions, traffic density, ship characteristics, waterway characteristics and defects in the waterway. However, the way that the factors affect ship traffic and consequently accidents is not described in detail.

2.3.3 Eurocode Model

2.3.3.1 Model description

The Eurocode model (Vrouwenvelder, 1998) is similar to the AASHTO model. In the model, there is a co-ordinate system (x, y) (Figure 2-3). The x coordinate, which is curved, follows the centerline of the traffic lane. The y coordinate stands for the horizontal distance from the center line to the structure, that is located at the point (0, d) and potentially could be collided. The occurrence of ship aberrancy is modeled as an inhomogeneous Poisson distribution. Then, the probability of a collision event is expressed by:

$$P_c(T) = nTP_{na} \int \int \lambda(x)\, P_c(x,y) f_s(y) dxdy \qquad (2 - 7)$$

Where T = period of time under consideration; n = number of ships per time unit; P_{na} = the probability that a collision is not avoided by human intervention; $\lambda(x)$ = probability of failure per unit travelling distance; $P_c(x,y)$ = conditional probability of collision, given initial position (x,y); $f_s(y)$ = distribution of the initial ship position in y direction.

For an indication of λ, an example was provided: 28 ships were observed to hit the river bank in a period of 8 years and over a distance of 10 km, with a ship density of 8000 ships per year in the waterway of Nieuwe Waterweg near Rotterdam in the Netherlands, leading to $\lambda = 4 \times 10^{-6}$ per ship per km.

2.3.3.2 Discussion

The Eurocode model is not exactly the same as the AASHTO model. Firstly, an inhomogeneous Poisson distribution is introduced in the model, which takes into account the potentially dangerous area in the waterway. It is apparent that failure rate is affected by the size of the dangerous area. Therefore the size of the potentially dangerous area should be determined, provided the historical data is available. Secondly, the x coordinate is curved, instead of the straight centerline of the vessel sailing path in the AASHTO model. This model assumes that the ships are always navigating with a constant horizontal distance to the center line. Lastly, $P_c(x,y)$ is another factor that affects the outcome. Its value differs from point to point and is complicated to determine. It also changes with navigational circumstances and types of vessels. The variation of $P_c(x,y)$ is similar to Kunz's model.

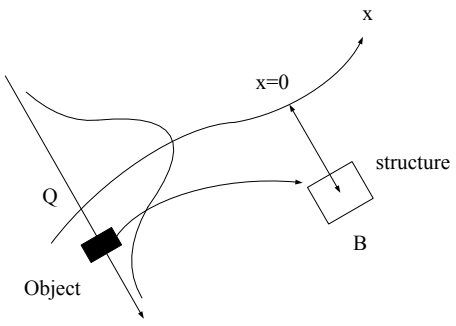

Figure 2-3 Ingredients for probabilistic collision model in Eurocode (Based on (Vrouwenvelder, 1998))

2.3.4 Pedersen's Model

2.3.4.1 Model description

Pedersen's model (Pedersen, 2002) is evolved from Larsen's model (Larsen, 1993). In the case of the Great Belt Link, the collision frequency (F_{Total}) is determined on the basis of four accident categories (Pedersen et al., 1998):

$$F_{Total} = F_{Cat,1} + F_{Cat,2} + F_{Cat,3} + F_{Cat,4} \quad (2 - 8)$$

The four categories are:

Category 1 Vessel traffic distribution is comprises 99% of the traffic that is Gaussian distributed and 1% that is uniformly distributed across the Eastern Channel. Accidents are due to human error, steering gear or the propulsion system.

Category 2 Ship that fail to make a proper change of course at a way point before passage.

Category 3 Vessels making evasive maneuvers in encounter situations near bridge and eventually collide with bridge. The number of encounter situations is derived from ship domain theory (Frandsen et al., 1991).

Category 4 Drifting ships that do not following the normal route. It is assumed that drifting ships originate from the normal route and direction in which they move is distributed over 360°, and the longitudinal axis of the ship is transverse to the direction of motion (see Figure 2-4).

Mathematical expressions are given for the risk calculation in each of those four categories. The model applied to calculate the expected rate ($F_{Cat,1}$) of serious collisions for a part between A to B of a bridge segment was given (Pedersen, 2002):

$$F_{Cat,1} = \frac{1}{T}\sum_i \frac{1}{V_{a,i}} \int_0^{V_{max,i}} \int_A^B \int_0^T P_{c,i} q_i V_i B_i R_i \, dt dx dV_i \quad (2 - 9)$$

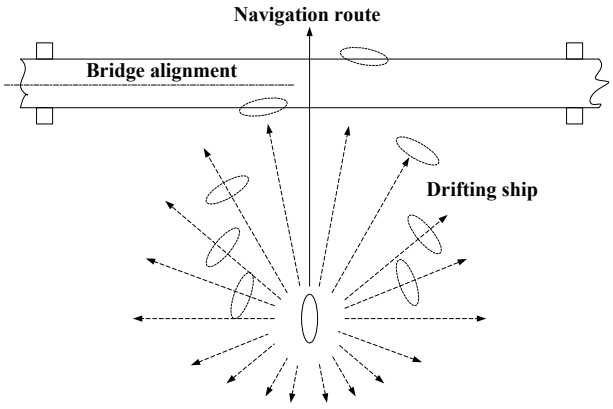

Figure 2-4 Ship drifting sideways toward a bridge line, accident category 4 (based on (Pedersen, 2002))

Where $V_{a,i}$ = average speed of ship class i; $V_{max,i}$ = maximum speed of ship class i; $P_{c,i}$ = causation factor, i.e. the probability of a collision if the ship is on a collision course (Frandsen et al., 1991); q_i = traffic density function of the ships given by the number of ships and the Gaussian distribution described above; the unit is the number of ships per unit area; V_i = distribution of speed of the ships; B_i = simple geometrical collision indicator function, which is 1 when the ship strikes a pier or a girder and 0 when the ship either passes through the bridge line without collision or grounds before it reaches the bridge line; R_i = severity of the collision; this factor depends on the ship collision crushing force, i.e. type, ship size, ship velocity, the strength of the bridge structure and a number of other parameters; T = time; x = axis along the bridge line.

A similar formula to calculate $F_{Cat,2}$ was not given in the paper, but in the earlier literature of Pedersen (Pedersen et al., 1993), a parameter P_o (probability of omission to check position of ship) was added in the equation to calculate $F_{Cat,2}$. $F_{Cat,3}$ and $F_{Cat,4}$ are small contributions, and their importance depends on the individual case. A computer based ship simulation was used in the practice of bridge design in this case. Finally the bridge span was enlarged to decrease the value of $F_{Cat,3}$.

2.3.4.2 Discussion

In Pedersen's model, the collision frequencies are categorized and studied individually. Similar categories were also applied to collision risk with offshore wind farms (Biehl et al., 2007). The model is used in the design process of large span bridges situated in the sea, where sea going ships transit underneath. But whether this model can be applied for the design of smaller bridges across rivers should be further examined. The encountering situation is taken into account, except overtaking. However, the fact is that overtaking could happen in the bridge area if no rules prohibit that. Further, weather conditions like wind and current effects on the ship movements are not considered in this model.

2.3.5 Drift Model

2.3.5.1 Model description

In the design process of the Su-Tong Bridge in China, a new model was developed to calculate the probability of collisions between ships and the bridge for cases in which the ships go out of control in the bridge area (Fang et al., 2009). As is shown in Figure 2-5, if drift width of a ship is larger than the available width of the channel, collision might occur. The motion of the ship which is out of control is illustrated in Figure 2-6.

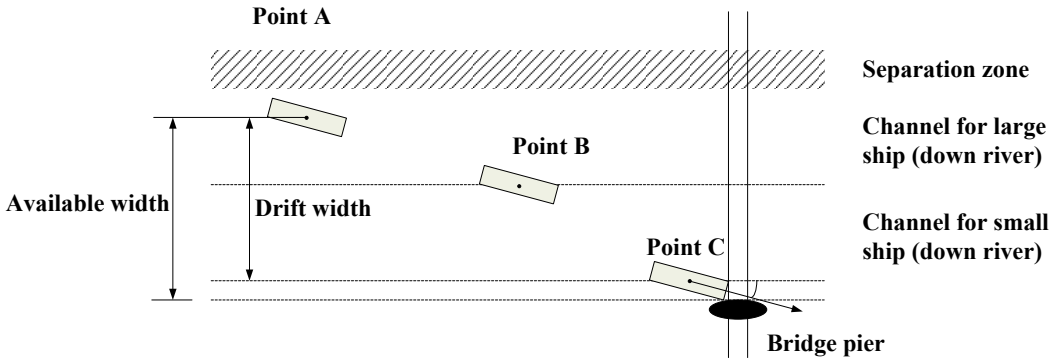

Figure 2-5 Ship and bridge collision event (based on (Fang et al., 2009))

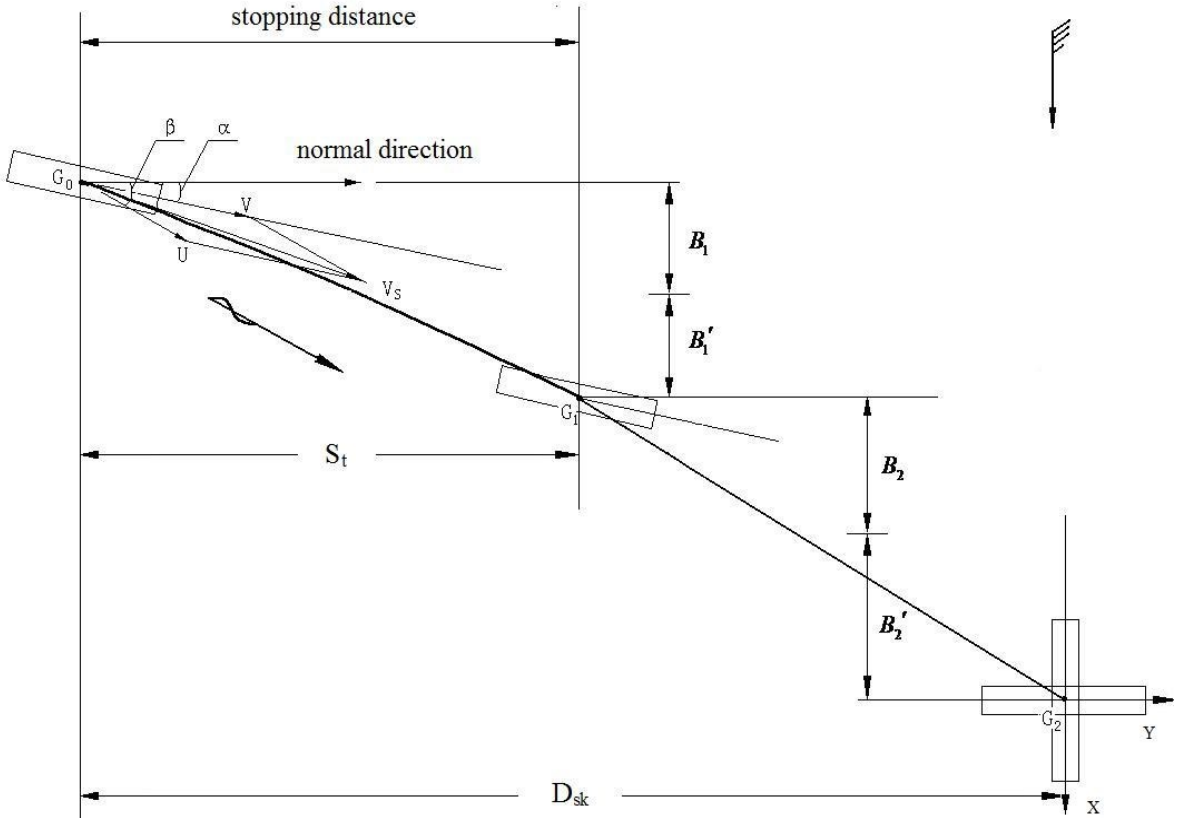

(a) $D_{sk} > S_T$

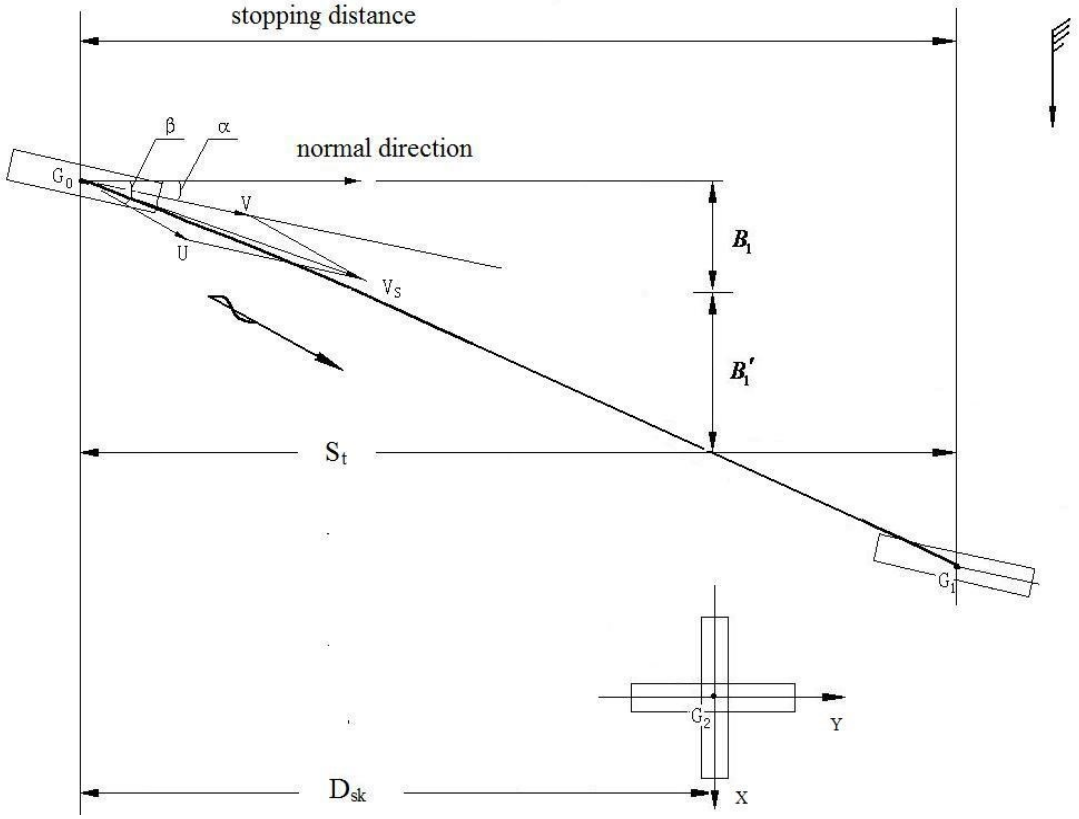

(b) $D_{sk} < S_T$

Figure 2-6 Motion steps for the ship that is out of control (based on (Fang et al., 2009))

The ship motion is caused by inertia, wind and current. There are two cases considered in the model (Fang et al., 2009):

Case 1, when $D_{sk} > S_T$, the total drift is:

$$B = B_1 + B_1' + B_2 + B_2' \tag{2 - 10}$$

Case 2, when $D_{sk} < S_T$, the total drift is:

$$B = B_1 + B_2 \tag{2 - 11}$$

Where: D_{sk} is distance between the point of losing control and bridge transect; S_T is projection on axis y of the stopping distance resulting from stopping ability and current. B_1 is the drift on axis x caused by the current within stopping period; B_1' is the drift on axis x caused by wind within the stopping period; B_2 is the drift on axis x caused by the current without inertia; B_2' is the drift on axis x caused by the wind without inertia.

The drift on axis x induced by current can be calculated by empirical formulas:

$$B_1 = v_0 \cdot T_{st} \cdot \left(1 - e^{-T/T_{st}}\right) \cdot \sin\alpha + U \cdot T \cdot \sin\beta \tag{2 - 12}$$

$$B_1' = K \cdot K' \cdot \sqrt{\frac{B_a}{B_w}} \cdot e^{-0.14 v_a} \cdot v_{a1} \cdot T \quad (2 - 13)$$

Where v_0 = ship speed when the ship is out of control; T_{st} is time constant of ship deceleration, and $T_{st} = c/\ln 2$, the constant c can be found from the Table 2-1 by ship displacement; α = the angle between the normal direction and ship course (degrees); β = the angle between normal direction and the direction of ship's motion (degrees); U = current velocity; v_a is average ship velocity within stopping period(m/s); v_{a1} is the relative wind velocity within stopping period (m/s); T = elapsed time between the time the ship started being out of control to the time the ship drifts with the current without inertia, which can be derived:

$$v = v_0 \cdot e^{-t/T_{st}} \quad (2 - 14)$$

$$T_{st} = c/\ln 2 \quad (2 - 15)$$

Where v is instantaneous speed; v_0 is ship speed at the beginning of the engine failure; T_{st} is time constant of ship deceleration; t = time spent after engine failure.

Where, $K \in (0.038, 0.041)$; K' is correction modulus for shallow water, which is indexed in Table 2-2; B_a is hull area above waterline (m^2), while B_w is hull area below waterline (m^2); V_s is ship velocity in wind (kn); V_a is wind velocity relative to ship (m/s). The wind speed relative to ship can be calculated by:

$$\overrightarrow{V_a} = \overrightarrow{V_s} + \overrightarrow{V_w} \quad (2 - 16)$$

In which $\overrightarrow{V_s}$ is the ship speed, and $\overrightarrow{V_w}$ is the wind speed.

Table 2-1 Time constant for different displacement (disp.) (based on (Fang et al., 2009))

Disp. (t)	C (min)	Disp. (t)	c (min)	Disp. (t)	c (min)	Disp. (t)	c (min)
1000	1	~21000	6	~66000	11	~136000	16
~3000	2	~28000	7	~78000	12	~152000	17
~6000	3	~36000	8	~91000	13	~171000	18
10000	4	~45000	9	~105000	14	~190000	19
~15000	5	~55000	10	~120000	15	~210000	20

Table 2-2 Correction modulus for ships in shallow water K' (based on (Fang et al., 2009))

Water depth (H)/real draught (d)	1.1	1.5	2.0
K' for ordinary cargo ships	0.6	0.7	0.8
K' for very large ships (C_b >0.8)	0.5	0.6	0.7

B_2 is the drift on x axis induced by the current without inertia:

$$B_2 = U \cdot t_p \cdot \sin\beta = S_p \cdot \tan\beta \quad (2 - 17)$$

$$t_p = S_p/U \cdot \cos\beta = (D_{sk} - S_t)/U \cdot \cos\beta \quad (2 - 18)$$

$$S_p = U \cdot t_p \cdot \cos\beta = (D_{sk} - S_t) \quad (2 - 19)$$

$$S_t = v_0 \cdot T_{st}(1 - e^{-T/T_{st}})\cos\alpha + U \cdot T \cdot \cos\beta \quad (2 - 20)$$

Where, t_p is the drifting time without inertia; S_p is the drift distance on axis y caused by the current without inertia.

B_2' is the drift distance on x axis caused by wind without inertia:

$$B_2' = K \cdot K' \cdot \sqrt{B_a/B_w} \cdot V_{a2} \cdot t_p \quad (2 - 21)$$

Where, V_{a2} is relative wind velocity, m/s; Ship speed, considering influence of current when losing control:

$$V = \sqrt{(v_0\cos\alpha + U\cos\beta)^2 + (v_0\sin\alpha + U\sin\beta)^2} \quad (2 - 22)$$

In this model, a ship losing control does not mean that the ship will collide with bridge. Whether a collision happens or not, depends on fairway condition, current, wind, positions of piers, etc. The shaded areas shown in Figure 2-7 are dangerous areas, in which the ships that are out of control have a chance to collide with the bridge. It is assumed that the probability of losing control is uniformly distributed, so the collision probability is:

$$P_{collision} = \frac{A_{danger}}{A_0} \quad (2 - 23)$$

Where, A_0 is the area in which ship navigates. The ships are classified by tonnage and ships are assumed to navigate according to local regulations; A_{danger} is the dangerous area, in which a loss of control can result in collision with the bridge, and this area is determined by factor of wind, current, ship speed etc.

2.3.5.2 Discussion

The drift model takes into consideration ship categories classified by tonnage. The whole process of drifting, which is influenced by wind and currents is described in detail. The probability of collision is calculated as the proportion of dangerous area of each ship categories. More detailed categories can further include angle of collision and ship type (Samuelides et al., 2008). The drawback of this model is that the distribution of vessel position and probability of vessel aberrancy are not taken into account. The ship traffic is assumed to be equally spread in the waterway, and this is not in accordance with practice.

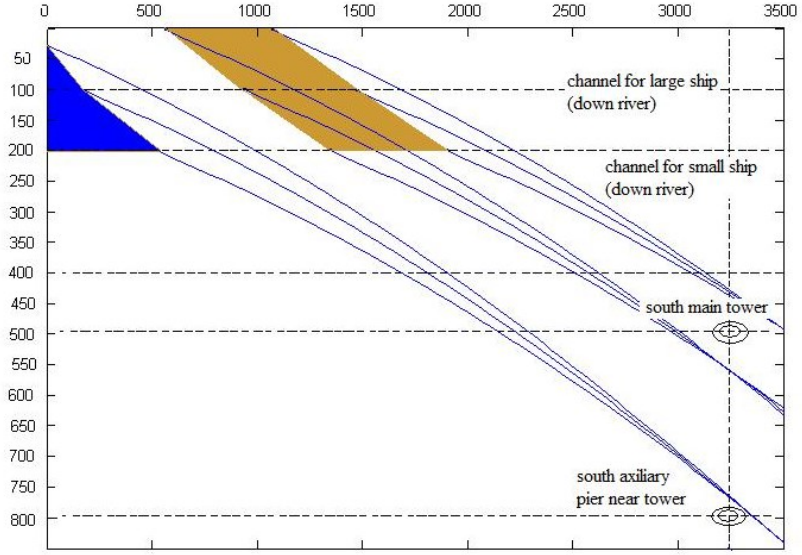

Figure 2-7 An example for dangerous area in drift model (based on (Fang et al., 2009))

2.3.6 Three Random Variables model

2.3.6.1 Model description

Based on the AASHTO model and Kunz's model, Geng et al. (2008) has developed a new model in the study of Chinese ship bridge collision problems (Geng et al., 2008, Lin et al., 2007, Wang et al., 2010). There are two detailed parameters added into Kunz's model. Firstly, the impact of water level changes has been taken into consideration. The frequency of a certain water level in a year should be multiplied by the probabilities of collision event for the specific water level. Then, the weighted sum of probability for different water level conditions becomes more realistic. Secondly, the aberrant vessel distribution perpendicular to the centerline of vessel sailing path is taken into consideration, which is adopted from AASHTO model. In this model, the probability of a collision event per year can be calculated by:

$$P_c = \sum_{i=0}^{n} \alpha_i P_{wi} \qquad (2 - 24)$$

Where: P_c = the probability of collision event per year; α_i = the proportion of time with water level i in a year; P_{wi} = the probability of collision event under the specific water level condition.

There is a coordinate system (x, y) as indicated in Figure 2-8. The x coordinate stands for the horizontal distance perpendicular to the centerline of vessel sailing path. The y coordinate stands for the distance parallel to the centerline of vessel sailing path. So, the collision model is:

$$P_{wi} = \sum_{j=1}^{n} N_j \int_{\mu_x-3\sigma_x}^{\mu_x+3\sigma_x} f(x) \int_0^D \lambda(s)[1 - F(s)] \int_{\theta_1}^{\theta_2} f(\theta) d\theta dy dx \qquad (2 - 25)$$

Where: N_j = annual number of vessels in category j; $f(x)$ = the distribution of vessel position in x direction; $\lambda(s)$ = probability of aberrancy per unit travelling distance. $F(s)$ = the probability of ship stopping before collision; $f(\theta)$ = the distribution of the deviation angle θ. $f(x)$, $f(\theta)$, and $F(s)$ are expressed in formula below:

$$f(x) = \frac{1}{\sqrt{2\pi}\sigma_x} \exp\left\{-\frac{(x-\mu_x)^2}{2\sigma_x^2}\right\} \quad (2 - 26)$$

$$f(\theta) = \frac{1}{\sqrt{2\pi}\sigma_\theta} \exp\left\{-\frac{(x-\mu_\theta)^2}{2\sigma_\theta^2}\right\} \quad (2 - 27)$$

$$f(s) = \frac{1}{\sqrt{2\pi}\sigma_s} \exp\left\{-\frac{(x-\mu_s)^2}{2\sigma_s^2}\right\} \quad (2 - 28)$$

$$F(s) = \int_{\mu_s-3\sigma_s}^{s} f(s)ds \quad (2 - 29)$$

When the ship is in area A, and $X < X_0 - BP/2 - BM/2$:

$$\tan\theta_1 = \frac{X_0 - \frac{BP}{2} - \frac{BM}{2} - X}{D - Y + BM} \quad (2 - 30)$$

$$\tan\theta_2 = \frac{X_0 + \frac{BP}{2} + \frac{BM}{2} - X}{D - Y} \quad (2 - 31)$$

When the ship is in area B, and $X_0 - BP/2 - BM/2 < X < X0 + BP/2 + BM/2$

$$\tan\theta_1 = \frac{X_0 - \frac{BP}{2} - \frac{BM}{2} - X}{D - Y} \quad (2 - 32)$$

$$\tan\theta_2 = \frac{X_0 + \frac{BP}{2} + \frac{BM}{2} - X}{D - Y} \quad (2 - 33)$$

When the ship is in area C, and X > X0 + BP/2 + BM/2:

$$\tan\theta_1 = \frac{X - X_0 - \frac{BP}{2} - \frac{BM}{2}}{D - Y + BH} \quad (2 - 34)$$

$$\tan\theta_2 = \frac{X - X_0 + \frac{BP}{2} + \frac{BM}{2}}{D - Y} \quad (2 - 35)$$

Where, X = the ship position along x direction; X_0 = the bridge pier position along x direction; BP = the width of bridge pier; BM = beam of mid-ship.

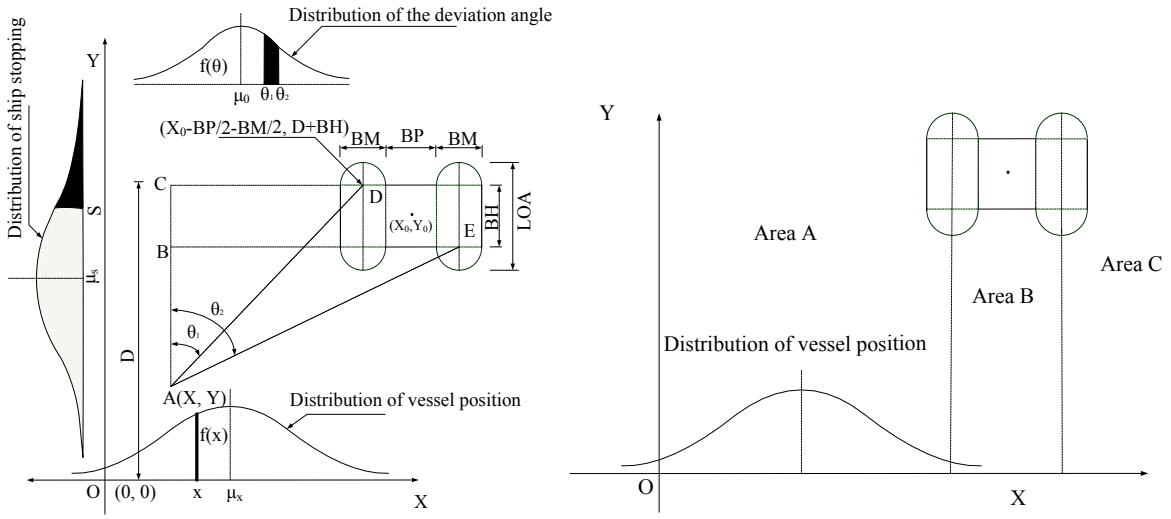

(a) Ingredients in the model (b) Three cases of intervals for calculus

Figure 2-8 Three random variables collision model (based on (Geng et al., 2008))

2.3.6.2 Discussion

This model takes most factors into consideration. Three random variables reflect the mechanism of ship and bridge collision, which takes advantage of both AASHTO model and Kunz's model. However, more random variables means more complicated process for application. More data and more analysis are needed. Further, some navigational factors such as wind and current are not reflected in the model.

2.3.7 Comparison of the Analytical Methods

The most reasonable and reliable approach to determine PA (probability of vessel aberrancy) should be based on long term accident statistics. However, when there is no adequate database, as stated by Wang et al. (2010), the AASHTO model is the most widely used model for calculating the probabilities of collisions, because of its simplicity and practicality. AASHTO has given estimates of PA, which is derived from American data. Whether that kind of data can be used in other regions of the world should be further investigated. The worldwide applicability issue could be the problem of every model mentioned above.

Further, most of the models do not take into consideration of wind, visibility, navigational aids and other factors of navigational circumstances. Currents and river bending are considered by adding corrections in the AASHTO model. Only the Drift Model takes into account the estimated effect of wind, current, and water depth. A comparison of the elements considered in each model is given in Table 2-3. The elements in the table are derived from the models mentioned above. Analytical models are compared, thus it is pointed out that these models lacked in the detailed description of the ship movements (Li et al., 2012b, Xiao et al., 2010).

Table 2-3 Comparison of the factors considered in the models

Risk factors	Risk elements	AASHTO model	Kunz's model	Eurocode model	Pedersen's model	Drift model	Three random variables model
Bridge factor	Pier / object Position	√	√	√	√	√	√
	Span of bridge	√	√	-	√	√	√
	Pier / object dimensions	√	√	-	√	√	√
Navigational circumstances	Wind	-	-	-	-	√	-
	Current	√	-	-	-	√	-
	Tide	-	-	-	-	√	-
	Water depth	√	-	-	√	√	√
	Visibility	-	-	-	-	-	-
	Bending channel	√	-	√	-	-	-
	Ship traffic density	√	-	√	√	-	-
Ship factor	Ship dimension	√	-	-	√	√	√
	Probability of vessel Aberrancy	√	-	√	√	-	-
	Distribution of vessel position perpendicular to normal route	√	-	√	√	-	√
	Ship deviation angle	-	√	-	-	√	√
	Stopping distance Distribution	-	√	-	-	√	√
	Failure rate per unit travel unit	-	√	√	-	-	√
	Speed of the ships	-	-	√	√	√	-
	Ship categories / classification	√	-	√	√	√	√
Human Factor	Human error	-	-	√	√	-	-

Kunz's model, the Eurocode model and the Three Random Variables model can mimic the critical steps for a ship to collide. For a vessel which is completely out of control, the drift model can reflect the whole process of the movement. However, for describing the ship behavior like collision avoidance, changing speed, or course alteration, the models shows weakness in describing the dynamic behavior of a nautical traffic system.

Kunz's model, the Eurocode model and the Three Random Variables model are very similar. The ship distribution is considered in all three models. But the formula of $P_c(x, y)$ (conditional probability of collision) given initial position (x, y) in Eurocode model was not provided, and that makes the model less practical than the AASHTO model. Kunz's model and the Three Random Variables model specifies the method to calculate $P_c(x, y)$, in which ship deviation angle ϕ and the stopping distance x were given as two variables. But only a single ship route was considered in the Kunz's model, rather than several. This is not the

case in Yangtze River of China. There are several routes in the Yangtze River for ships to navigate, and the routes are also interconnected. In addition, the distribution of ship path is not considered in the model. The Three Random Variables model has the advantage to take more elements into consideration.

Pedersen's model has advantage in the design process of a large span bridge situated in the sea. However, there are disadvantages compared with other models. Firstly, overtaking encounters are not considered in the model. Secondly, the effects of wind and current are not considered. Further, the ships drifting direction is considered as evenly distributed over 360°. These are simplifications compared with the Drift Model, in which the drifting ship moves under the force of wind and current.

Human factors have not been fully understood as an element in the probabilistic risk analysis. Human factor analysis should be studied and can be built in the model to calculate the probability of incidents.

2.3.8 Summary and Discussion

This section has presented an overview of several methods on modeling the probability of ship collision events, mostly for the presence of bridges, from a study of the available literature. The other kinds of probabilistic risks like groundings in shallow water or collisions with wind farms are based on the analytical models have been introduced in Section 2.3. After treatment of historical background, procedure, advantages and disadvantages of each model, comparisons are made for the risk elements that are considered in the existing analytical models. Consequently, the following conclusions are made for further development of the model: firstly, with the development of the models, more and more risk elements are taken into consideration in the models. A further development of the model should take into consideration all risk elements listed in Table 2-3. Moreover, the detailed description of the ship movement is needed. Secondly, more detailed categories of ships based on ship types, ship tonnages, ship dimensions, as well as ship maneuverability needs to be taken into consideration to make the model more accurate. Thirdly, different encountering situations must be taken into account. Sometimes, the position aberrancy of a collision candidate is caused by collision avoidance, especially in busy waterways. In addition, ship collisions may result in further collisions with bridges or other structures in busy waterways. So, further development of the model must include all those causes of accidents realistically. Fourthly, the effects of wind and currents need to be taken into account. The wind and currents are not only able to cause position aberrance and a larger swept path, but also can drive the ships that are not under control into collision (e.g. Drift Model). Therefore, the influence of the wind and currents needs to be examined and considered.

The presented models are basically aimed for designing and protecting bridges rather than protecting ship traffic. There are other similar analytical models that aimed for waterway

designs or wind farms are not introduced, e.g. the SAMSON model (Koldenhof et al., 2009). Further development of the models should deal with the ship collisions in restricted waterways from a ship traffic perspective, in order to reduce risk of collision, and to give guidance to mitigation methods for accidents.

2.4 Model based on networks

2.4.1 Fault Tree and Event Tree analysis

Fowler et al. (2000) used Fault Trees and Event Trees to estimate the risks. The methodology is based on results from the Commission of the European Communities (CEC) project "Safety of Shipping in Coastal Waters" (SAFECO). Figure 2-9 shows the diagram of the MARCS model to calculate the frequency and consequence of marine accidents, which contains statistical data, Fault Tree and Event Tree. Case studies are presented, however some data is based on simplifications and assumptions. The Fault Trees in the cases give insight into the full causational relation of the accident which enables the modeling of risk control options. In this method, some of the frequencies like the collision frequency at a location, frequency of powered grounding, probability of drift grounding, probability of structural failure, and probability of fire and explosion are also determined by different analytical methods.

According to the author the result of the analysis shows well (within a factor of 2) to reasonable (within a factor of 5) agreement with the historical data on frequencies of ship accidents. Several reasons contributing to the discrepancies between the results of the analysis and the historical data are addressed. Firstly, the data of historical accidents only contained serious incidents, which is less than the frequency of actual accidents. Moreover, fishing vessels, naval vessels, and pleasure craft are not taken into account. Secondly, some of data like structural failure frequency and fire occurrence rate are based on worldwide historical data, which may not be the same for the studied area. Thirdly, some values are determined by expert judgment and also bear certain discrepancies. Moreover, as is stressed by the author, the proposed method intends to give an illustration of the concept and not (yet) accurate results.

2.4.2 Bayesian networks as a tool

Bayesian networks show potential in maritime risk analysis and decision making in the PhD research of Friis-Hansen (2000). With the help of a software system, the Bayesian networks accomplish several calculations in the maritime risk model. The Bayesian network is constructed by a network of variables which is similar to the fault tree diagram. Compared to the fault tree, the Bayesian network is able to deal with more complex interactions. The Bayesian approach showed great power in the following ways (cases): a tool for cost-optimal inspection planning, a reliable model for upheaval buckling of trenched marine pipelines, an

effective detection system as regards misfire and exhaust valve leaks in marine diesel engines, risk analysis comparable to event tree analysis, and an algorithm for learning the topology and the probabilities through extracting knowledge from a database. It is demonstrated that the Bayesian networks are able to combine other probabilistic models consistently, and Bayesian networks have data mining ability and updating ability.

A relative simple diagram of a Bayesian model for human organization factor based ship operation (Hu et al., 2008) illustrates the characteristics of the method, see Figure 2-10. As was addressed by the author, the diagram could be built exponentially larger and more complicated than the diagram shown in the figure. However, even in the most complicated diagram, the Bayesian approach showed operability and transparency.

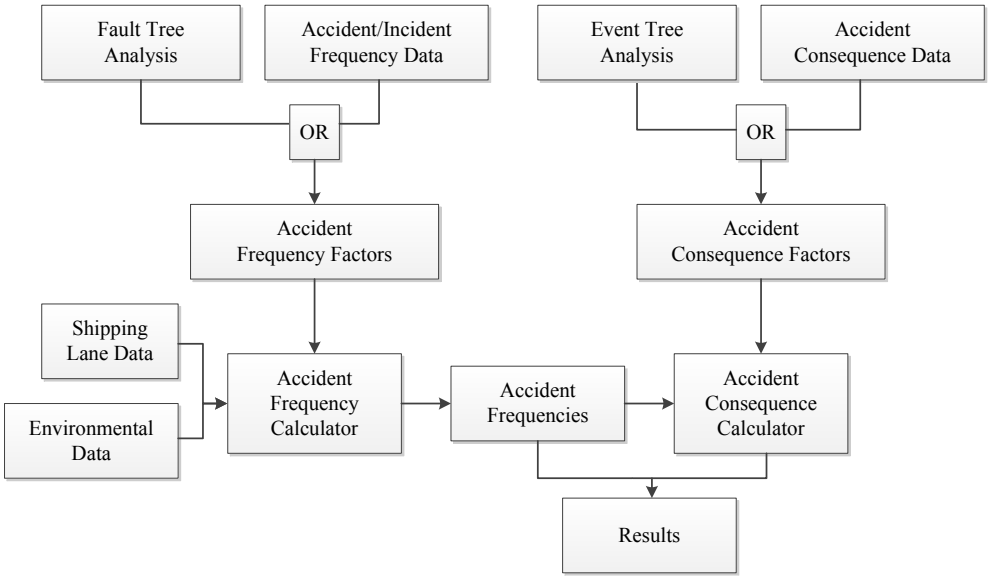

Figure 2-9 Block diagram of MARCS

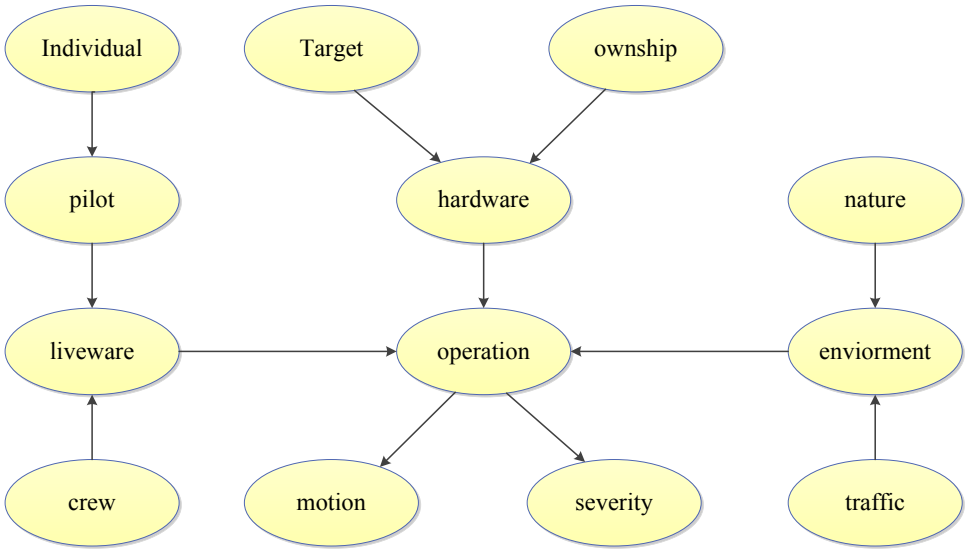

Figure 2-10 Visual Bayesian Network for HOF-based system of ship operation

In the maritime field, the Bayesian network is always combined with other methods for safety assessment. Szwed et al. (2006) applied Bayesian methodology for accident probabilities using paired comparison to elicit expert judgments for passenger ferry system in the US. Merrick et al. (2006) developed a Bayesian framework for addressing uncertainty which was combined with expert judgment for risk assessment in maritime transportation. This framework also has potential applicability to areas other than maritime risks, e.g. port security or aviation safety (Ale et al., 2009) where uncertainty is a problem.

However, as was stated by Hänninen et al. (2010), after applying Bayesian network for causation probability of incidents, it was found that this approach also suffered disadvantages. First of all, long term statistical analysis of ship traffic data is needed to guarantee a good result. Secondly, human performance affects the results, and validity of the network parameters is crucial for realistic estimations of collision probability. Thirdly, the Bayesian approach cannot adapt to seasonal differences of ship traffic which affect the results.

2.4.3 Fuzzy logic approach

With the combination of Analytic Hierarchy Process (AHP) and Fuzzy Logic System, Priadi et al. (2012) developed a decision tool for ship handling difficulty level. The Fuzzy Logic System part includes ship condition, ship handling facility condition, navigation condition and weather condition. For high level of uncertainty systems in the feasibility and concept design stages of maritime systems, a safety model using fuzzy logic approach for modeling various design variables was presented by Sii et al. (2001). Similar to Bayesian networks, this approach also can include experts' decision and knowledge, and various sources of information into the fuzzy logic inference process, see Figure 2-11. The fuzzy logic system also involves expert decisions in the model, which is subjective. Another problem is that sometimes the predications are vague (Parikh, 1994).

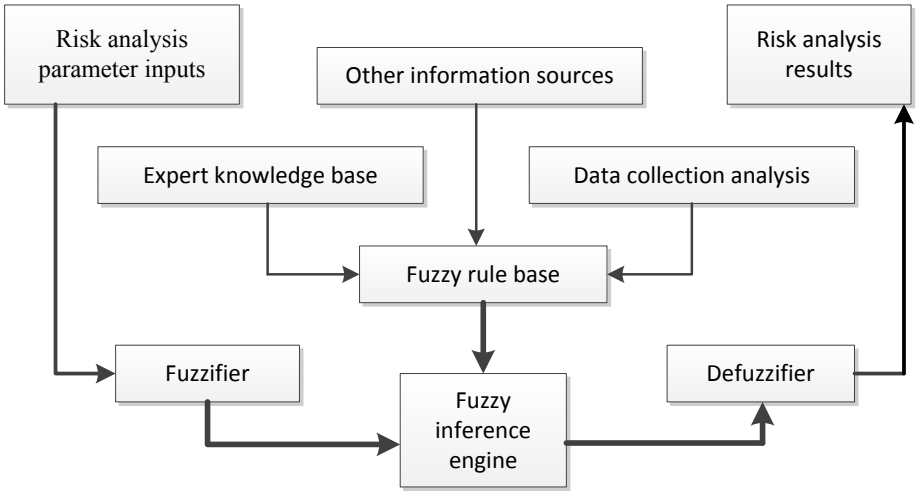

Figure 2-11 An overview of the safety model for risk analysis using fuzzy-logic-based approach

2.4.4 Discussion

The models based on networks produce detailed probability in each step of the incidents. With sufficient data, these models can always produce a result for prediction. However, these models are still dependent on historical data and expert opinions. Other than that, the networks can neither predict the details of ship behavior in normal situations nor indicate consequences of a single factor to ship behavior. Therefore no mitigation measures can be developed based on these methods.

2.5. Simulation method

With the obvious deficiencies in previous methods, researchers have developed realistic simulations to collect information needed. There are a lot of successful traffic simulations in different fields of transportation, such as road traffic, pedestrian behavior, flight traffic, as well as ship traffic. However, the characteristics of the ship traffic are very different.

Maritime researchers have found different ways to solve problem in different kinds of ship simulation. There are ship handling simulators, fast time simulations, and ship traffic simulations. In the following pages, we are going to discuss about the advantages and disadvantages in the existing ship simulations.

2.5.1 Ship handling simulator

A ship handling simulator is a computer aided machine system which enables performing in-house ship navigation with simulated hydrodynamic ship movements, simulated visual environment and real ship bridge man-machine interfaces. The advantage is that a ship handling simulator presents a very realistic bridge system which is able to mimic real navigation experience at sea (or on the waterway). The virtual reality is based on the characteristics of the technology below:

- Hydrodynamic model of ship movements
  The mathematical maneuvering model is able to respond to environmental conditions (wind, current, and visibility) and navigational orders (rudder and engine) with various hydrodynamic forces. Some latest simulators can even represent other special phenomena for a ship like suction, squat, trim and towing. Different maneuvering characteristics will depend on the simulated ship type, dimensions, navigation status (speed, course, draft) and environmental conditions.

- Large scale 3D visual projection aided by visual software
  3D visual projection is able to represent realistic 360° navigational environments including weather conditions, geographical conditions, and traffic conditions. Weather conditions incorporate rain, fog, snow, spray, day and night etc., which have

an impact on the visibility of the officer onboard. Geographical condition stands for the navigational 3D space that the ship is navigating in, including length, width, depth, and curvature of the waterway. The visual projection tries to visualize the other vessels in the waterway which the officer on board is trying to avoid. However, traffic condition is always a weak point for ship handling simulator. The other vessels in the traffic (target vessels) follow a predefined track with predefined speed. This is not a realistic representation of real ship traffic, even though the waypoints and speed can be modified by the instructors.

- Realistic in-house man-machine interfaces
  The ship bridge system provides a realistic man-machine interface which contains all the equipment needed onboard. The hardware equipment includes heading indicator, course indicator, ARPA, electronic chart, GPS, Loran-C, VHF-set, chart table, telegraph, and rudder etc. Man-machine interface represents a realistic bridge system to enable a realistic maneuvering and communication process.

There are many different kinds of ship handling simulators around the world. But the main function of the simulators is similar. A more detailed explanation of a Dutch ship handling simulator (e.g. the Mermaid 500) at MARIN (Maritime Research Institute Netherlands) can be found in (van der Rijken, 2008).

A ship handling simulator can be used for training purposes, maritime engineering design, and research. Ship officers and ship pilots can use this tool to develop skills for ship navigation and other operations. Webster (1992) gives a full description on using ship handling simulator on ports and waterway feasibility design. There are also discussions about the validity of simulation as a design technique, relative risks of passage, and other quantitative factors affecting cost and operability of waterway. Other researches use ship handling simulator to address the risk problems of human factors.

Although the ship handling simulator is a powerful and economic tool in designing better waterway and ports, reducing risks and training, there are limitations in this approach. As stated by Nguyen (2008), there are three aspects that need to be further improved in ship handling simulator. The three challenging aspects are ship maneuvering performance at low speed, bank effects and ship-channel interaction, and ship-ship interaction. The ship-ship interaction mentioned in the thesis is about the complex hydrodynamic interactions.

However, the different encountering situations and ship avoidance behavior are always beyond the scope of investigation, while these are important especially in busy waterways. The costs of experts and availability of the large simulator is also a constraint for its usability and accessibility.

2.5.2 Fast-time simulation

Fast-time simulation is a cheaper option for single ship simulation. It is provided with software installed on a single PC by which the ship behavior in the concerned waterway is simulated. It takes less simulation time and human intervention than ship handling simulator since it is a simplified version. However this will jeopardize the results compared to the ship handling simulator. Due to its simplicity and economization, it is often used as a substitute of ship handling simulator to get insight into the safety issues.

A good example of a Fast-time simulator is named SHIPMA developed by MARIN and Deltares[1]. In the SHIPMA program, the vessels are steered by auto-pilot for track keeping or in the harbor maneuvering mode for typical harbor maneuvers. Hydrodynamic derivatives (Abkowitz type) are used for the movement of different ship type, coupled with wind influence, bank effects, drift, and tug assistance. Different characteristics of ship behavior can be simulated based on need. The external influences like current and bathymetry are computed with other software. Results like ship positions, track, course and heading, rudder angle, speed, and other external conditions are recorded during the simulation, which can be plotted using DELFT-GPP afterwards.

2.5.3 Ship traffic simulation

Ship traffic simulation is very different from the simulation approaches mentioned above. Besides representing single ship behavior, it needs to include ship avoidance behavior in the waterway, especially in the confined busy waterway. In this approach, the ship interactions in collision avoidance, regulation conformity, and traffic management need to be considered. Ship traffic simulation exceeds the ship handling simulator's ability to consider single vessel safety on ship passage in extreme conditions, and it provides the possibility to consider all the conditions and situations which can happen in reality. This enables a safety assessment process in calculating all the possible probabilities of many kinds of accidents. There are different methods to simulate ship traffic, and this section will present those different ship traffic simulation models in detail. The advantages and limitations in the existing models will be mentioned.

2.5.3.1 Domain and Arenas theory for simulation

The first traffic simulation model evolved from the widely discussed domain theory. Ship domain is a predefined area around a ship that should remain clear of other ships. Pietrzykowski et al. (2009) introduced more details about ship domain, as there are a number of different kinds of ship domains with different shapes in the literature. In ship traffic simulation, Davis et al. (1980) modified concept of ship domain from Goodwin (1975) into "arena", which is a continuous domain retaining the concept of weighting of different

[1] "Fast-time Simulators" from http://www.marin.nl/web/Facilities-Tools/Simulators/Simulator-Facilities/Fasttime-Simulators.htm

sectors of Goodwin's domain. When a ship comes within range of a ship domain, a ship avoidance behavior can be simulated based on expert judgment. Simple speed change also can be simulated.

Discussion:

Ship domain and arenas theory are the most original methods to study ship traffic in the maritime field. Ship domain theory is still being discussed by scholars, especially in search of a universally applicable ship domain. The ship domains are evolving into different shapes. It gives thoughts for the other type of simulation model.

2.5.3.2 OFI (opportunity for incident) model

The OFI model uses a dynamic simulation method to count the occurrences of the various incidents scenarios which could happen in the concerned waterway (van Dorp et al., 2001). The consequence and probability will be subsequently processed based on the simulation result. In the end, risk management recommendations can be made for improving safety level of the ships. In the simulation, many factors for incidences are considered as variables. Those variables are ship route, ship class, type of interaction, proximity of interacting vessel, wind speed, wind direction, and visibility.

The core of the model as applied by van Dorp is the method to count the possible incidents by simulating the ship encountering on map. The maps were converted to bitmaps in the program, and the movement of the vessels including the ferries (the object of safety assessment) can be accurately represented on the background map of San Francisco Bay. Then the generated vessels in the same route can encounter with each other in the simulation. Finally, the interaction model counts the number of interactions among ships. The interaction model determines whether the vessels really interact with each other in an encountering situation based on the Closest Point of Approach method. The default setting in the model is that vessel within half a nautical mile of the ferry is counted as interacting, whereas vessel passage at more than half a mile distance or more than five minutes sailing time is not counted (Merrick et al., 2003). The data generated will be further processed in the safety assessment.

The OFI model is only a part of the modeling approach for the system of collision risk model, which consists of 6 stages of causal chain: root / basic cause, immediate cause, triggering incidents, accidents, consequences, and impacts. The OFI model combines situational and organizational factors in a given time, provided with all the factors for incidences. The historical data and expert judgment are also important supplements in the risk assessment. Some of the inputs in the simulation are derived by Bayesian networks (Merrick et al., 2005).

The complete procedure, model of the system simulation and the role of the simulations can be found in the Prince William Sound Risk Assessment (Harrald et al., 1998, Merrick et al.,

2000, Merrick et al., 2002), the Washington State Ferry Risk Assessment (Grabowski et al., 2000, van Dorp et al., 2001), and other literature published subsequently based on the previous projects (Merrick et al., 2003, Merrick et al., 2005, Merrick et al., 2006, van Dorp et al., 2011).

Discussion:

Many methods have been used in the complete procedure of nautical risk assessment. This contributes to formulating a complete system that provides elements to be considered in risk assessment for nautical incidents. Traffic simulation is an important element in the complete procedure. However, the traffic simulation model is only used for counting the incidents. In other words, the dynamic ship traffic behavior and collision avoidance is not addressed sufficiently. This makes the model greatly dependent on expert judgment and Bayesian networks. Without these the simulation cannot sufficiently reflect the realistic traffic and directly produce the probability of the accidents.

2.5.3.3 SMARTS (Marine Traffic Simulation System)

SMARTS was developed using SAFES (Ship Auto-navigation Fuzzy Expert System) by Hasegawa et al. (2000). SMARTS creates or deletes marine traffic according to the statistical data of the traffic as well as the destination and departure gates. After a ship is created, the route, waypoints, and other parameters are determined. The ship positions are updated at each time step. The ship navigation including collision / grounding avoidance maneuvers are governed by a fuzzy expert system. The simulation method was applied in simulating ship traffic in Osaka Bay.

Discussion:

This nautical traffic simulation provides ship interactions. However, the interactions based on fuzzy expert system are not described in detail. The effectiveness of the collision avoidance is not clear. In the multi-encountering situation, the ability to represent the real word practice is unknown. The route of the ships is predetermined, however in practice the ship tracks show a lateral spatial distribution rather than a fixed line of route. Furthermore, the environmental conditions are not taken into account.

2.5.3.4 Istanbul Strait simulation

The simulation model investigates the behavior of ship traffic based on different scenarios, ship arrival and waiting time, which gives guidance to ship traffic information in the future (Köse et al., 2003). There are five subsystems in the model. The subsystems are traffic flow from different directions, two information systems representing big ships, and simulation of bad weather conditions. All the subsystems are connected by a network. An important feature is that the passage of a big ship (with length larger than 200 m) will prevent traffic from the opposite direction from passing the strait. On a whole, this traffic simulation is a

good tool to determine the strategy for ship entry in the Istanbul Strait. Ulusçu et al. (2009) presents more details on using a mathematical risk model to estimate the risks of the Strait of Istanbul. In the study, the whole strait is divided into 21 slices to estimate the risk of ship traffic in each slice using mathematical models. Expert opinions are gathered for collision probabilities when data was lacking.

Discussion:

The Istanbul Strait simulation solved a local problem in management and quantifying risks. It is designed for traffic management. However, it is not capable to simulate realistic ship behavior and ship avoidance behavior in the strait. So, it has little ability for safety assessment of the ship traffic.

2.5.3.5 MARTRAM (Marine Traffic Risk Assessment Model)

Pimontel (2007) presents a ship traffic simulation program MARTRAM developed and used by Royal Haskoning to qualitatively analyze maritime safety in restricted waters. Before the simulation, the different ship type, dimensions, vessel speed, and safety domain are derived from 24 hour of real traffic data. However, pilot boats, tugs, and dredgers at work are not included in the model. The route of the ship passage is predefined in the simulation. During the simulation, the vessels are generated in the starting points of a route. These vessels proceed along the predefined routes and maintain a predefined distance to the centerline of the navigational channel. These distances vary with the channel width. However, a small proportion of vessels navigate along the center of the channel, or even to the port side.

In collision avoidance, the safety domain is used. The safety domains are predefined for each vessel based on vessel dimensions. However, the vessels carrying hazardous cargo are not treated differently. When another vessel invades a predefined safety domain, a collision avoidance maneuver will be activated, which is only speed reduction. As addressed by the author, predefined ship courses result in a “narrow route” in the simulation, as indicated by the model evaluation, which limites the reality of the simulation. MARTRAM also counts the number of safety domain invasions (encounters) as an indication of collision risk. The number of encounters in the simulation is significantly larger than the same observed in AIS. This discrepancy also shows the limitation of the model.

Pimontel (2007) concluded that: “the existing maritime traffic simulation programs are not able to accurately model collision probability. Also doubts are expressed about the suitability of using vessel safety domains for the identification of encounters in areas of restricted water.” Another suggestion by the author is to investigate the point that the ships really start the behavior for collision avoidance.

Discussion:

The MARTRAM model solves some of the risk problems in the confined waterway. Many types of ships with different dimensions can be generated in the simulation, which is a great advantage especially when it is coupled with AIS data observation. Moreover, different routes and encountering situations are generated based on observed data and local geometry of the waterway, which is a big achievement. However, there are aspects that need further development in the simulation. First of all, the predefined ship safety domain is not realistic for a ship encountering situation, as the ship officer on board judges the situation which is a complex human factor. Secondly, the vessel avoidance behavior is modeled only by speed change, which is not realistic. A dynamic change of speed and course in an encountering situation would be more realistic. Thirdly, grounding risk is not reflected in the simulation. Last but not least, environmental conditions like wind, visibility, and current are not reflected sufficiently.

2.5.3.6 MDTC based ship traffic model

The MDTC (minimum distance to collision) model uses discs to represent vessels, which looks similar to the Arenas model introduced above (Goerlandt et al., 2011, Montewka et al., 2010). The difference is that hydrodynamic simulation is implemented in the ships maneuver. Based on a series of ship encountering simulations, MDTC and CD (Collision Diameter) values are computed. Those values are used in the Pedersen's model to determine the probability of a ship collision. Rather than by the analytical method as in Pedersen's model the collision candidates are calculated by ship traffic simulation. In the ship traffic modeling, different types of ships are generated with different position distribution, speed distribution, course distribution based on data analysis. In this way, the collision candidates are computed and counted in different encountering situations and areas in the traffic simulation. Ultimately the estimation of the collision frequency can be calculated with the MDTC based model.

What is innovative in the model is determining the Minimum Distance To Collision, which is a substitute of the parameter "collision diameter" (CD) in the Pedersen's model (Kujala et al., 2009). This enables a more accurate and reasonable calculation of collision candidates in probabilistic modeling. The MDTC is based on radius of two vessels (two discs). And the MDTC is a parameter related to the ship type and encountering angle. If the distance between two vessels is less than MDTC of this specific situation, a collision accident happens, no matter what evasive action is taken on board. The Figure 2-12 represents vessel discs and MDTC.

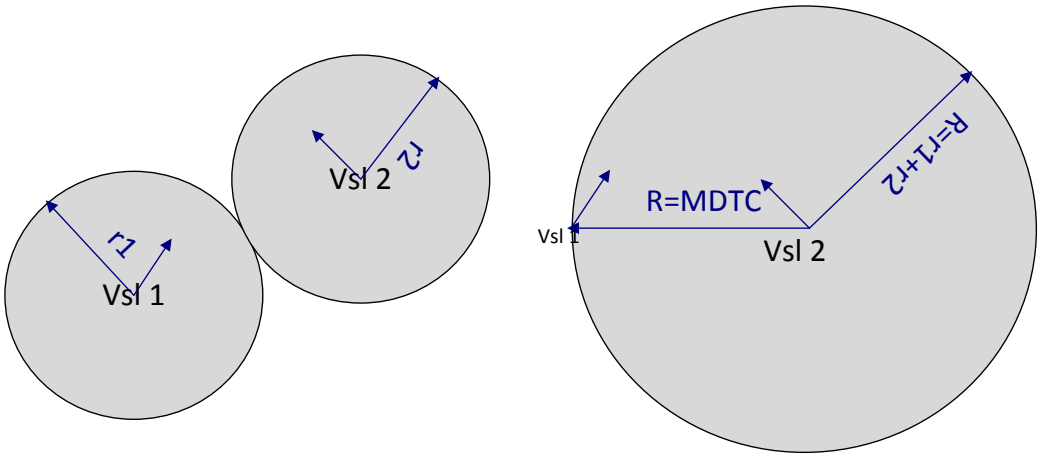

Figure 2-12 Representation of vessels as discs and definition of collision situation (based on (Montewka et al., 2010))

The MDTC is determined by using a hydrodynamic model of ship motion and different encountering situations with different types of ships. 3 types of vessels (container, passenger ship, and tanker) are taken into consideration, which constitute 9 meeting scenarios. Those scenarios include two container ships with the same size (or with different size), two tankers with the same size (or with different size), two passenger vessels, two Ro-Ro carriers, passenger ship with tanker, passenger ship with container ship, Ro-Ro with container ship. In each scenario, 17 kinds of crossing angles from 10° to 170° with 10° increments are carried out for simulation. After the simulation, the MDTC values for different crossing angles are calculated based on the tracks of the different hydrodynamic simulations with different scenarios. Finally, the values of MDTC and CD with different meeting angles are shown. The ship dynamics model is validated for three ship types by comparing the turning circle performance. The ship course and speed during turning are validated with good agreement.

There are several assumptions by the author in conducting the simulation:

- Initially the vessels are proceeding at full sea speed;
- The vessels are fully laden;
- The vessels start their maneuvers simultaneously;
- The settings of the steering gear and propulsion during the maneuver are constant;
- The initial course of vessel A is always 360° and vessel B changes her initial course in each consecutive trial by 10°;
- The initial relative bearing from vessel A to vessel B is 45 ± 2° starboard;
- Only the “turning away maneuvers” performed by means of rudder are considered;
- The influence of weather conditions is omitted;
- The curvature of the Earth is omitted because of the small distances being considered.

Discussion:

MDTC based model gave a good indication of the least distance needed for evasive action in a certain encountering situation, and it also provides a CD value which can be used in the Pedersen's model. The simulation result of CD value is more realistic than the same in the previous analytical method. However, as the author indicates, the assumption of blind navigation in the geometrical model doesn't reflect the fact that the ships can avoid each other in real traffic. This avoidance behavior includes several aspects. Firstly, the ship officers on board can take evasive actions to avoid collision well before the MDTC value calculated in this method is reached. Secondly, the ship officer can take avoidance action by giving a rudder angle to port side in emergency, which is good seamanship in practice. Whereas, only "hard a starboard" is supposed to be the rudder action in the MDTC based model. Thirdly, another effective evasive action is slowing down the vessel. Especially, when two ships encounter each other with 90° crossing angle, the ship on the portside can choose slowing down to avoid collision. However, in the MDTC model, always "hard a starboard" is applied on the rudder, and therefore the MDTC needed becomes very large (about five times LOA). This not only exaggerates the risk in the calculation, but also is not realistic in practice, especially in a busy and confined waterway when there is no room for turning. Last but not least, there are a lot of assumptions in the simulation which impede a realistic representation of practice. In reality, vessels don't start maneuvers simultaneously. Especially in a cross encountering situation, the "Give-way vessel" should take action to avoid collision and the "Stand-on vessel" should keep speed and course, which conforms to COLREGs. Weather conditions cannot be omitted especially in the open sea.

2.5.3.7 Neural networks and fuzzy logic based simulation

In the ship traffic simulation, one problem is to solve the collision avoidance function for each individual ship, especially in a multi-encountering situation in confined waterways. Ahn et al. (2012) proposed to model collision avoidance of ship with neural networks and fuzzy logic. Collision risk inference system and membership function are developed by marine traffic rules and maneuverability of the ship using fuzzy logic. Many scenarios of encountering situation have tested the advantage of this method.

Discussion:

This method takes advantage of expert system, neuro-fuzzy algorithm and neural network, and DCPA and TCPA are also consistently calculated. The complexity helps for realistic avoidance behavior of two or three ships in encountering situation. However, the complexity of the computation also can limit the number of ships in the simulation. For a realistic traffic simulation, the applicability of this method needs further verification.

2.6 Conclusions

This chapter reviewed existing methods for the probabilistic risk assessment of maritime accidents. Those methods include statistical methods, analytical methods, network based methods and simulation methods. The advantages and disadvantages for each method have been discussed in this chapter.

The statistical method is a simple and direct forward way for risk analysis, and this method is widely used in other methods. Most of the analytical methods are developed for bridges, while those methods are also applicable for other waterway related infrastructures. The models based on networks produce results based on existing probabilities and expert opinions. The simulation methods take advantage of the methods mentioned above. The statistical methods, analytical methods, and network based methods can either provide parameters for the simulation, or all those models serve as submodels for specific elements in a risk analysis. Simulations are considered to be an indispensable part of maritime recent risk analysis. Different simulations catch different elements in reality.

However, other methods are developed because often there is insufficient historical data to apply statistics. After reviewing the existing analytical methods, it is concluded that the most desirable model should take into consideration all risk elements listed in Table 2-3 to get more realistic results. The ships should be categorized into more detailed groups. The encountering situations and collision avoidance behavior should be taken into account with the effects from wind, current and visibility. The models based on networks cannot provide many details for improving the safety level of the ship traffic. The existing simulation methods are either weak in reproducing realistic collision avoidances on traffic level or weak in reproducing realistic individual ship movements.

Notwithstanding these limitations of existing simulation model, it is concluded, based on the comparison of the different methods, that the desired model for maritime risk analysis should be a simulation method that combines both traffic level and individual ship level of details, taking account of regulations and common practices in the waterway and catching as many elements in reality as possible.

3. AIS DATA ANALYSIS

AIS (Automatic Identification System) data has been a great support for this research. It functions as field data and supports input information (Chapter 3), and serves in model development (Chapter 6) and model validation (Chapter 7 and Chapter 8).

The AIS data analysis concerns the characteristics of the ship behavior on both a ship traffic level and an individual ship level. Ship characteristics such as the LOA (Length Overall), speed and the gross tonnage of the ship should be categorized and taken into account. On the ship traffic level, the characteristics of ship behavior include traffic density, spatial distribution, speed distribution, course distribution for different categories of ships. On the individual ship level, the analysis includes the collision avoidance for different characteristics of ships. This thesis studies the way the ship interactions influence the ship traffic. Possible effects on the ship behavior resulting from many influences should be identified, which include local regulations, local navigational circumstances, encounters, wind, current, and visibility.

AIS data provides aggregated data in the sense that it includes the effects of human decision making, environmental elements like wind and currents, and nautical regulations. The AIS data helps modeling real life traffic behavior in a way that is impossible in the existing models. After interpretation of the ship tracks provided by AIS data, information of ship traffic behavior is derived that is characterized by the mean values and statistical distributions of position, speed, heading, and time interval between two consecutive ships for different types and sizes of ships. Change in ship speed in the channel is also based on AIS data.

3.1 Introduction of AIS system

The AIS system transmits information of the sailing status of ships. The AIS equipment automatically broadcasts information from the vessel to an AIS ship receiver or an on-shore receiver through VHF (Very High Frequency) in a limited geographical space. That information includes ship position (from GPS), ship course, ship heading, ship rotation angle, ship speed, loading status, location and altitude of AIS antenna, ship type, navigation status, destination, time stamp, together with an unique identification number MMSI (Maritime

Mobile Service Identity) (Harati-Mokhtari et al., 2007). This information can be displayed on the monitor of other ships or the VTS (Vessel Traffic Service) center. The received AIS data can be used for additional lookout and collision avoidance onboard. It also can be used in a VTS center for traffic safety and efficiency by assisted target tracking. Moreover, nautical safety authorities also save the data for further research like accident investigation or analyzing the traffic status. In addition, researchers use historical AIS data to study the characteristics of vessel traffic to further improve safety and efficiency. Historical data analysis is used in this study to form the basis for a realistic simulation of ship traffic in the confined waterway.

The quality of the AIS data analysis depends on the AIS equipment. There are two types of ship borne mobile AIS equipment, Class A and Class B. The major difference is that Class A system is compulsory installed on the vessels larger than 300 gross tonnages engaging in international voyages, cargo ships larger than 500 gross tonnages not engaging in international voyages, and passenger ships. AIS equipment is not compulsory for some small ships, for which Class B system is simpler and lower cost equipment. Small ships without AIS equipment are not in the AIS data. However they can affect the behavior of large ships in encounters. The time interval for reporting depends on the type of equipment and the ship's dynamic conditions. The details can be found in Table 3-1 and Table 3-2 (IALA, 2010). As demonstrated in the tables, the accuracy of observed behavior change of ships depends also on the time intervals.

Harati-Mokhtari et al. (2007) mentioned errors concerning static information and dynamic information from AIS: for MMSI number, 2% of the information was found erroneous; For vessel type, different studies (VTS-based AIS study and Data-mining AIS study) showed 74% and 56% of discrepancy respectively between AIS data and reality; for navigational status, 30% of ships was displayed incorrect; for dimensions, there was about 18% incorrect information; the reliability of other dynamic information like position, course and speed would need to be further investigated.

However, based on experiences on AIS data analysis of the study area in the Port of Rotterdam, the information of positions, course and speed are more reliable there. Only a very small proportion of signals show ambiguous positions, e.g. navigating outside of the channel. This is not a problem since the ambiguous positions can be eliminated in the statistical analysis. Missing several signals for a single ship track is another kind of problem for data analysis. However, there are always single ship tracks without missing signals that can be chosen for analysis. Finally, information of small ships which are not equipped with AIS cannot be included in the AIS data analysis. This proportion of ships needs to be further analyzed and compensated for in a simulation model.

Table 3-1 Class A ship borne mobile equipment reporting intervals

Ship's dynamic conditions	Nominal reporting interval
Ship at anchor or moored and not moving faster than 3 knots	3 min
Ship at anchor or moored and moving faster than 3 knots	10 s
Ship 0-14 knots	10 s
Ship 0-14 knots and changing course	3 1/3 s
Ship 14-23 knots	6 s
Ship 14-23 knots and changing course	2 s
Ship > 23 knots	2 s
Ship > 23 knots and changing course	2 s

Table 3-2 Reporting intervals for equipment other than class A ship borne mobile equipment

Platform's conditions	Nominal reporting interval
Class B "SO" ship borne mobile equipment not moving faster than 2 knots	3 min
Class B "SO" ship borne mobile equipment moving 2-14 knots	30 s
Class B "SO" ship borne mobile equipment moving 14-23 knots	15 s
Class B "SO" ship borne mobile equipment moving > 23 knots	5 s
Class B "CS" ship borne mobile equipment not moving faster than 2 knots	3 min
Class B "CS" ship borne mobile equipment moving faster than 2 knots	30 s

3.2 Recent study on AIS data analysis

3.2.1 AIS data analyses of the Port of Rotterdam

Mou et al. (2010) analyzed AIS data of the North sea around the Port of Rotterdam, and he focused on the correlation between Closest Point of Approach (CPA) and other ship characteristics like ship dimensions, ship speed, and ship course. The histogram of speed and normal regression showed the distribution of speed in the area. And the histogram of heading indicates the number of ship candidates for encountering situations. Regression models were given to indicate the statistical relationship between CPA and LOA (Length Overall), and statistical relationship between CPA and speed. Finally, the paper checked the risk analysis result by using AIS ship tracks and SAMSON model provided by MARIN to show the advantages of the SAMSON model.

De Boer (2010) analyzed AIS data in a case study around Maasvlakte I of the Port of Rotterdam (Figure 3-1). Differences in average vessel paths and average vessel speed between incoming vessels and outgoing vessels were studied for different sizes of ships. The averaged vessel path is compared with different conditions, including normal condition, external influences from wind, current and visibility. The result showed that vessel paths were influenced by the crosswind and crosscurrent. However, there was no significant influence found on ship behavior from visibility, which could be resulting from lack of data. Ship encountering was briefly addressed.

Shen (2012) succeeded De Boer's work and further examined the pattern of the vessel traffic behavior by AIS data analysis. Other than the data from the location of Maasvlakte I, she also analyzed data at the Botlek area (Figure 3-1) which was away from Maasvlakte I. Comparisons of the results for both locations were used to check whether the waterway geometry had an influence on the vessel traffic behavior. Shen analyzed the spatial distribution for different classes of container ships to compare the similarities and differences. The result showed that the spatial distribution was influenced by the waterway curvature and the waterway width. There was also evidence that the ships preferred to stay closer to the center of the waterway when the ships were navigating in the waterway bend. Furthermore, the influence of wind, currents and visibility was studied. The influence of the wind was examined for both locations in the study. The crosswind did shift the vessel paths to the lee side, and a slight vessel speed change could be found. However, those differences were found to be very small (less than 5% of channel width).

3.2.2 AIS data analyses of the Gulf of Finland (GOF)

Data analyses were conducted in Finland. Statistical analyses with figures and histograms were presented for the characteristics of the ship traffic in GOF. Those studies evolved from Pedersen's model, which was further adapted to the local geographical conditions.

Kujala et al. (2009) used distributions and associated probability density functions from the histograms derived from AIS data to represent the ship traffic in a risk calculation using a mathematical method. First of all, the crossing area was observed from the AIS ship tracks on a map. Secondly, crossing angles for different types of vessels (passenger ships, cargo vessels, tankers, high-speed-crafts) were calculated. Finally, for different types of vessels the associated number of passages, average velocity, average length, and average width were derived from the AIS data.

Montewka et al. (2010) further analyzed the details of the ship traffic in the concerned area. Rather than using normal distributions, he proposed a number of distributions to describe the vessels' dimensions, spatial distribution, velocity distribution and course distribution. The Chi-square test was used to choose among the different continuous distributions to describe the speed and course of the ships. For length and beam modeling, a triangular distribution is used with upper and lower limit. Large discrepancies were found between the fitted continuous distributions and discrete values of spatial distributions derived from the AIS. So, discrete values of distributions were finally used to describe the spatial distribution of ship traffic.

Goerlandt et al. (2011) further developed a simulation model for ship collision probability with improved results from AIS data analysis. They included the fact that the number of vessel passages is different in different months, different days, and even different hours. So, a non-stationary Poisson process is used to describe the departure time distributions.

Further, missing ships in the AIS were also compensated for in the simulation later on. During simulation, they also implemented a Gaussian distribution to determine the positions of the vessels.

3.2.3 Discussion

AIS data analysis of the Port of Rotterdam and the Gulf of Finland provided the basis for AIS data analysis in this thesis. Firstly, the AIS data can provide the average value or histograms to describe the characteristics of the ship traffic, which include ship position, ship speed and ship course. Secondly, different continuous distributions can be used to describe the histograms. Statistical tools like the Chi-square test can be used to select the continuous distributions with the best fit to the histograms. Thirdly, the ships can be further categorized into different types and sizes to compare the differences. Fourthly, external influences from wind, currents and visibility should be examined. Finally, the data analysis should take into account the number of vessel passages in different months, different weeks, different days, and even different hours.

3.3 AIS data analyses in the Port of Rotterdam

3.3.1 Introduction of the AIS data studied

In this case, a nearly straight waterway in the Port of Rotterdam is chosen. The studied area is about 2.8 km length of channel with a center point at (51° 54' 13.77"N, 4° 16' 19.07"E), as shown within the red rectangle in Figure 3-1. The Dutch Maritime Research Institute (MARIN) provided the data and was kind enough to allow the use of their software “Show Route” for the data analysis.

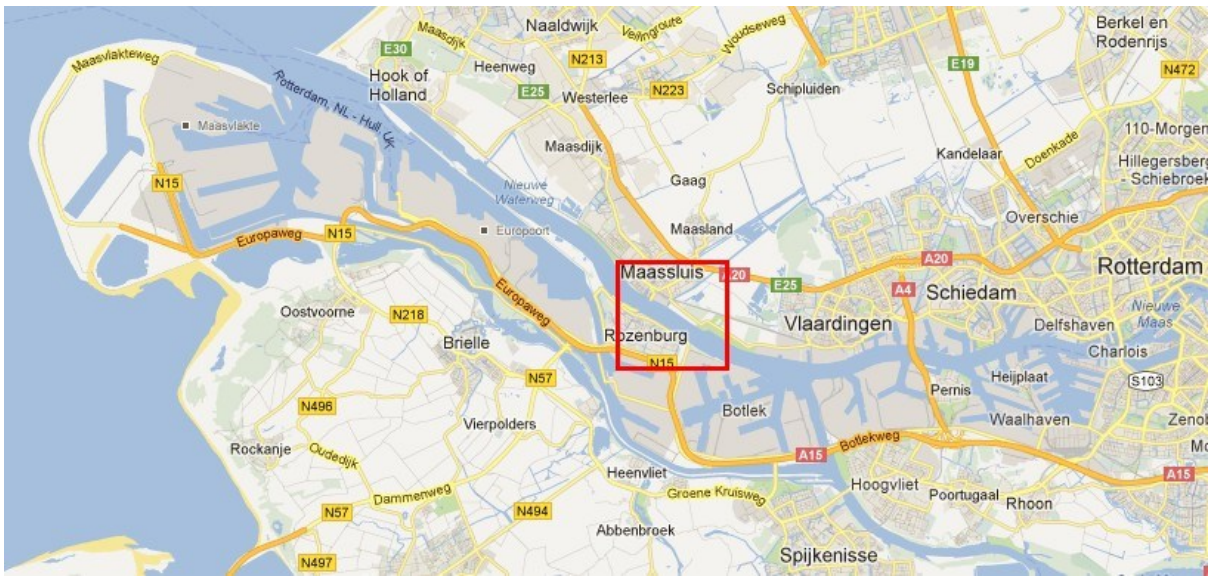

Figure 3-1 The study area in the Port of Rotterdam

The software “Show Route” is able to transfer the raw AIS data into a database with a detailed dataset of the status of ships. These data can be sorted according to ship type and class (size), and analyzed by common statistical methods. In the following data analysis, only data samples with incoming ships are analyzed. The outgoing ships have similar characteristics as the incoming ships. Incoming and outgoing are specific expression for the direction of ship passages. A vessel with incoming direction means that the ship comes into the waterway from the open sea. An outgoing vessel is sailing to the sea.

28 months of AIS data from 01/01/2009 to 01/05/2011 are used for data analysis. The numbers for different types of ships are shown in Table 3-3. There are 17 different types of ships that are using the waterway, but it is not necessary to simulate the behavior of the types of ships with infrequent passages. So the ship types are further aggregated into fewer categories as shown in Table 3-4. There are several reasons for the types of ships being aggregated in this way. Firstly, there is a large quantity of GDC (General Dry Cargo) ships, container ships and chemical ships. Those types of ships need to be analyzed separately. Secondly, there are not many LPG, LNG, and oil tankers, but they may have large consequences after collision, such as explosion or pollution, which is similar to chemical ships. So, those ships are combined with chemical ships. Thirdly, the numbers of tugs, RoRo ships, and dredgers are not small, and they have a special behavior in the waterway. So these ships are investigated independently. Tugs are highly maneuverable when they are not attached to other ships, and they become vulnerable when attached. Dredgers behave differently during operation from not being in operation. For RoRo ships carrying people on board, the consequence of an accident can be severe. Due to these different features, tugboats, RoRo ships, and dredgers have been analyzed separately. Lastly, there are 7836 ship passages for which ship type information is missing. So, these ships have also been analyzed independently.

Crossing-lines perpendicular to the channel have been selected to derive the data for the behavior of ship traffic. We can also observe the changes of those characteristics throughout the waterway. The crossing-lines help recording the data of ships provided by the AIS information. The AIS information is retrieved as if the information was recorded at the crossing-lines. There are 9 crossing-lines selected for analysis, which are named crossing-line 1 to crossing-line 9 from the left to the right of Figure 3-2. The statistical tools used in this study are described in Appendix I.

Table 3-3 Number of ships with different types in studied AIS data

Type	Number	Percentage
General dry cargo ships	12474	23.12%
Container ships	11353	21.05%
Chemical ships	9767	18.11%
Tugs	3119	5.78%
RoRo	3089	5.73%
Dredgers	2339	4.34%
Oil tanker	1087	2.02%
Miscellaneous	1094	2.03%
Bulker	879	1.63%
LPG	650	1.20%
Passenger of ferry	98	0.18%
Supply	70	0.13%
Recreation	55	0.10%
Pilot	11	0.02%
LNG	8	0.01%
Ore-bulk-oil carrier	8	0.01%
Fishing ships	5	0.01%
Unknown ship type	7836	14.53%
total	53942	100.00%

Table 3-4 Aggregated ship types with number of passages

Type code	Type	Number of passages	Percentage
I	General dry cargo ships	12474	23.12%
II	Container ships	11353	21.05%
III	Chemical ships, LPG, LNG, Oil tanker	11512	21.34%
IV	Tugs	3119	5.78%
V	RoRo	3089	5.73%
VI	Dredgers	2339	4.34%
VII	Others	2220	4.12%
VIII	Unknown ship type	7836	14.53%
-	Total	53942	100.00%

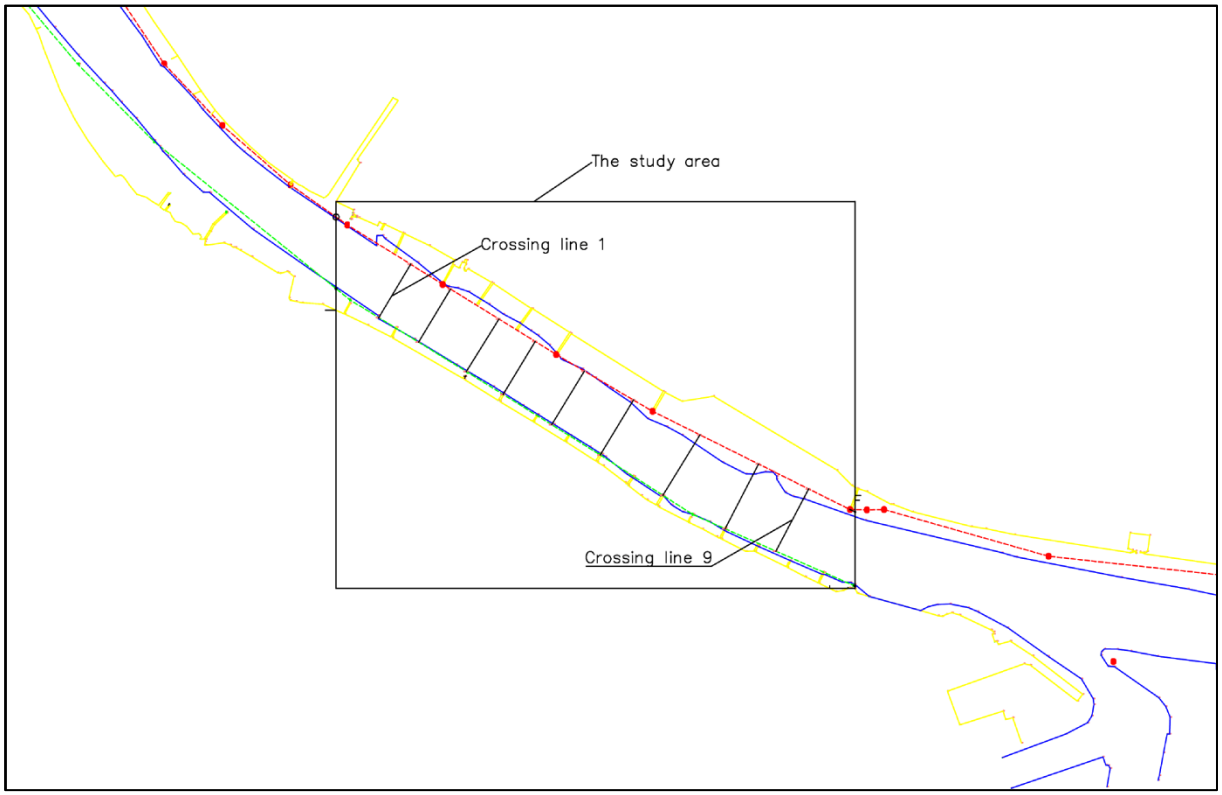

Figure 3-2 Locations of 9 crossing-lines in the study area (the crossing-line 1 and crossing-line 9 are indicated in the figure; the red lines and green lines are the boundaries of the waterway; the blue lines indicates the -10m depth contour; the yellow lines shows the channel banks)

3.3.2 Traffic density

Traffic density affects the number of encountering situations, which further affects the safety level in the waterway. The traffic density is described by the number of ship passages in a certain time period, and the distribution of the time interval between two ships. For example, if the number of ship passages per week is large, the traffic is dense. The time interval between the passages of two ships is another measure for the traffic density in the studied area. If the time intervals are large, the number of ships will be small. On the contrary, if the time intervals are small, we have dense ship traffic. Generally, we expect more accidents in dense traffic. This study helps to reproduce realistic variations of traffic density over the year, the month, the week, the day, and the hour in the simulation.

In order to know the variations of traffic density, this study analyzed two years of AIS data in the studied area. It is found that the number of ship arrivals is different in different time periods, based on observation of 46140 incoming ship arrivals in the time period from 01/01/2009 to 31/12/2010, 730 days altogether.

3.3.2.1 Monthly ship arrivals

For different months, the data is divided into 24 months. So there are 30 days in each "month". The ship passages in different months are shown in Figure 3-3.

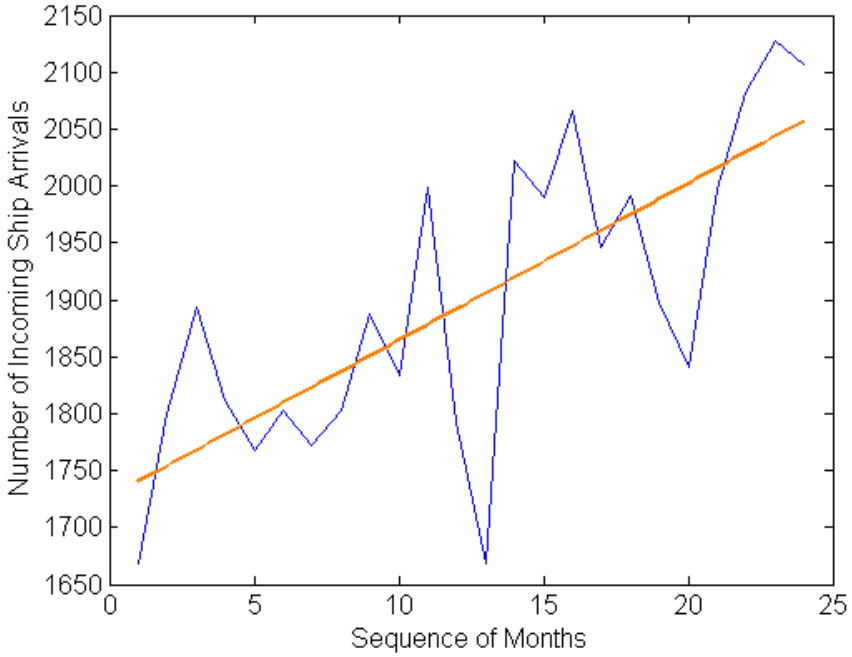

Figure 3-3 Ship arrivals on incoming direction in each month (24 months data)

The ship arrivals in different months are different. First of all, there is an increasing trend for the number of ship arrivals. Secondly, the ship traffic is dense in the season of spring and autumn, and the traffic decreases in the summer. However, the increases and decreases are not much (normally within 200 passages per month). Thirdly, there is an extreme low in every January.

Two factors might be the reasons of the increasing trend, which seems to be contrary to the economic situation during these years. One is that more inland barges are installed with AIS equipment's. The other factor is that the inland barges always have multiple shifts of berth for unloading the cargos at different locations in the port for a single voyage.

3.3.2.2 Weekly ship arrivals

There is a weekly fluctuation in the number of ship passages in the studied waterway (Figure 3-4). 103 complete weeks, from Monday to Sunday, are found in the 730 days of data. The incomplete weeks are not included in the analysis. The numbers of ship arrivals are different from week to week, but the increasing density of ship traffic is clear.

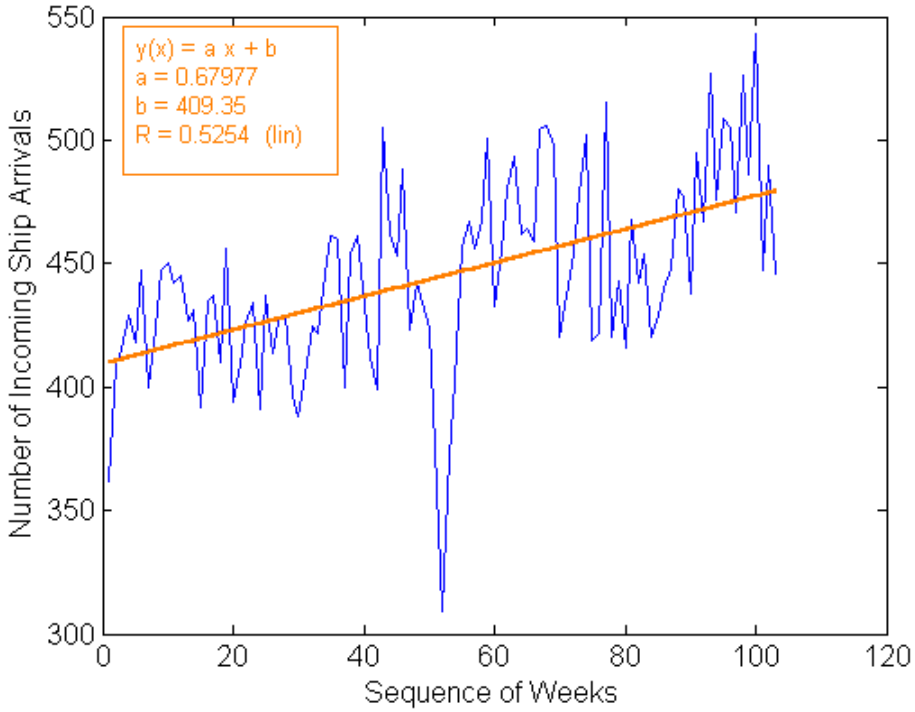

Figure 3-4 Ship arrivals on incoming direction in each week (103 weeks of data)

In order to approximate the numbers of ship passages in the simulation, two steps are taken to develop the equations for the weekly ship passages. Linear regression and residual approximation are used for that purpose. The same methods are also used to approximate other variables in this thesis.

Firstly, MATLAB® Curve Fitting Tool is used to fit the data with a straight line. Then a linear model is derived with coefficients:

$$\mathrm{F(x)} = \mathrm{a} * \mathrm{x} + \mathrm{b} \tag{3 - 1}$$

Where, $\mathrm{a} = 0.6798\,(0.4625, 0.8971)$, $\mathrm{b} = 409.4\,(396.3, 422.4)$, with 95% confidence bounds. This is clearly not a good approximation, as the coefficient of determination (R^2) is 0.276, which is very small. SSE (Sum of Squared Error) is 110300, which is very large. This discrepancy can be also observed from the Figure 3-4.

The second step is analyzing the residuals from the regression line. After analysis, the probability density function of normal distribution for the residuals is derived as:

$$\mathrm{R}_{weekly} = \aleph(\mu_{weekly}, \sigma^2_{weekly}) = \aleph(0, 32.9^2) \tag{3 - 2}$$

Therefore, the weekly number of ship arrivals for nautical traffic simulation is:

$$\mathrm{N}_{weekly}(\mathrm{x}) = 0.68\mathrm{x} + 409.4 + \mathrm{Y}, \text{ where } \mathrm{Y} \sim \aleph(0, 32.9^2) \tag{3 - 3}$$

where x stand for the number of the week which is simulated, $\aleph(\mu, \sigma^2)$ means normal distribution with mean (μ) and standard deviation (σ).

The credibility analysis with statistical tests for generating weekly variances of ship arrivals can be found in Appendix II.

3.3.2.3 Daily ship arrivals

The number of passages in each day is different. However, there is a trend that the daily number of ship passages is increasing throughout the year. The ship generation process needs to reflect both the increasing trend and daily fluctuation of ship arrivals. In order to generate statistical significant data for the number of ship passages in the simulation for each day, we divide the daily random number generation process into two steps. Firstly, we average the number of ship passages in weeks into each day of the weeks. This process not only guarantees the total number of ship passages in the whole year, but also reflects the increasing trend. Secondly, the daily differences from the average daily number can be generated by random normal process. Using MATLAB® function "normfit ()" to derive the mean and variance with 95% significant level, the probability density function of normal distribution for the daily residual is:

$$\mathrm{R}_{daily} = \aleph\left(\mu_{\mathrm{daily}},\ \sigma^2_{\mathrm{daily}}\right) = \aleph\left(-0.15,\ 9.85^2\right) \quad (3 - 4)$$

Where μ_{daily} stands for the mean and σ_{daily} stands for the standard deviation, with confidence interval of [-0.87, 0.57] and [9.36, 10.38] respectively. So, the number of ships in different days can be generated in the simulation using the function:

$$\mathrm{N}_{\mathrm{daily}}(\mathrm{x}) = \mathrm{R}_{daily} + \frac{\mathrm{N}_{weekly}(\mathrm{x})}{7}, \text{ where } \mathrm{R}_{daily} \sim \aleph\left(-0.15,\ 9.85^2\right) \quad (3 - 5)$$

x stands for the number of day which is simulating.

The credibility analysis with statistical tests for generating weekly variances of ship arrivals can be found in Appendix III.

3.3.2.4 Hourly ship arrivals

We can also observe the frequency of arrivals throughout the day in the two years, and find differences in different hours, see Figure 3-5. Especially at 6 am and 14 pm, the peak hours will result in more frequent encounters. And this phenomenon will be reflected in the simulation. The daily ship arrivals must be divided into every hour by the proportion of ship arrivals in one day, $\mathrm{P}_{\mathrm{hourly}}$.

3.3.2.5 The time intervals between ships

In the data base, the ship records are recorded by time sequence. So, time intervals (TI) can be obtained from the database very easily by Equation (3 - 6), which is a simply subtraction of the time of arrival (TA) of two sequential ships.

$$TI_n = TA_n - TA_{n-1} \quad (3 - 6)$$

In order to examine the distribution of time intervals, a histogram can be made. As was shown in Figure 3-6, the x axis stands for the time intervals (in seconds). And the y axis is the number of the ships. So, in order to approximate the time intervals in the simulation, an exponential curve can be fitted to the histogram and results in SSE of 0.0001566 and R-square of 0.9894:

$$f(x) = a * \exp(b * x) \quad (3 - 7)$$

Where, $a = 0.03102(0.03078, 0.03126)$, $b = -0.0007729(-0.0007814, -0.0007645)$, with 95% confidence bounds.

Applying Chi-square test the goodness-of-fit is rejected at 5% significant level. This proves that the time interval distribution does not really conform to the exponential distribution. However, the exponential distribution is still used for generating random numbers to approximate time intervals. This is because after having tried several other distributions the exponential distribution proves to be the best one.

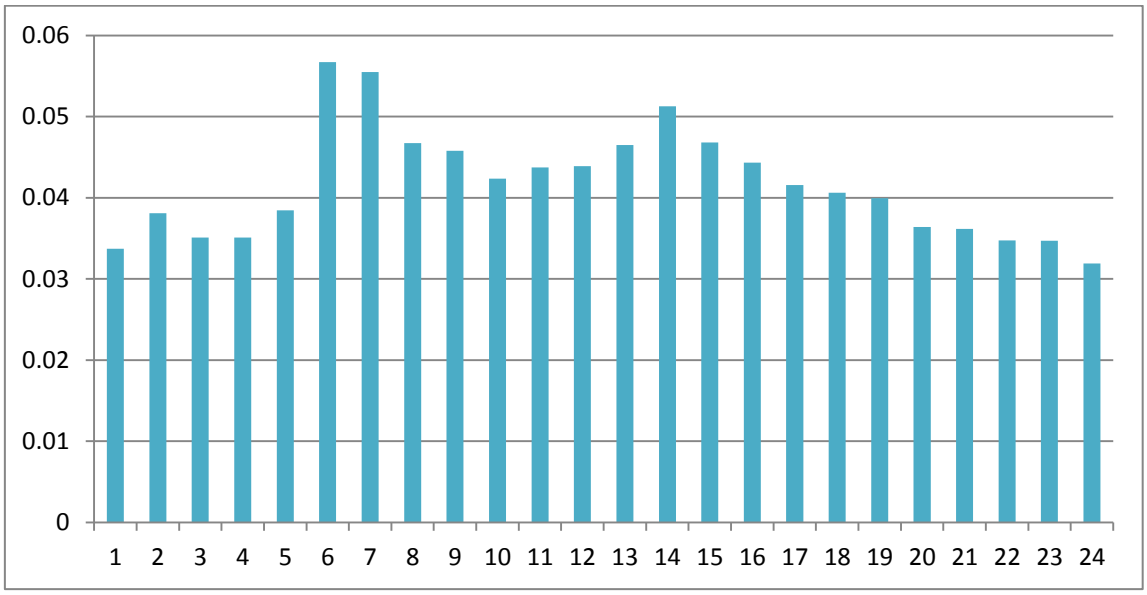

Figure 3-5 Hourly proportion of ship arrivals in one day

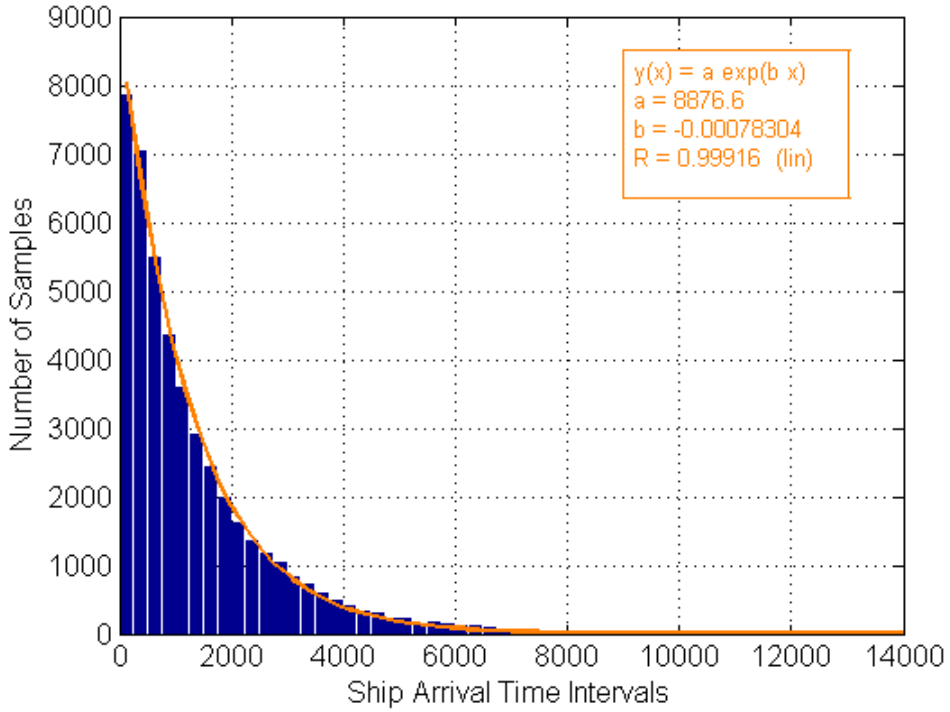

Figure 3-6 Ship arrival distribution of time interval (64140 samples)

As a result, the time interval of ship arrivals is determined by two variables. One is the daily fluctuation of number of ship arrivals, and the other one is the exponential distribution of time intervals. When the daily number of ship has been generated, the time interval between two ships generated ($\mathrm{TI_n}$) will be:

$$\mathrm{TI_n} = \mathrm{P_{hourly}} * \mathrm{N_{daily}(x)} * E \text{ , where } E \sim \mathrm{Exp(mu)} \qquad (3 - 8)$$

Where, $\mathrm{P_{hourly}}$ is the ratio of average hourly number of ship arrivals, which is used to describe the hourly differences of ship arrivals; $E \sim \mathrm{Exp(mu)}$ is the random process to generate a random number from exponential distribution with parameter mu.

3.3.3 Ship traffic behavior for different ship types and categories

3.3.3.1 Ship categories based on gross tonnage

Ships behave differently based on the characteristics of the individual ships. Especially in confined waterways, ships proceed with caution to avoid accidents, which is a result of good seamanship. The officer on watch determines the speed and track of the passage considering the characteristics of the own ship and the environment by experience. Therefore, different ships have different ways to adapt to their local situation. The dynamic behavior of the ships depends on the static characteristics of the ships. In order to study the dynamic characteristics (e.g. position, speed) in detail, we classified the vessels by type, and then we further classified the vessels by tonnage.

For example, container ships in Table 3-4 are further classified into 5 groups by gross tonnage (Table 3-5). It is observed that the ships with similar gross tonnage have similar ranges for lateral positions on the crossing-line. Therefore, the container ships are categorized into 5 groups. Figure 3-7 shows the boundaries of different categories of ships with lines. The classifications based on gross tonnage for each type of the ship other than container ships are presented in Appendix IV. The averaged vessel path and speed for different categories of ships are provided in Appendix V.

The data analyses in this chapter are conducted for different types and sizes of ships. However, with some exceptions only results of incoming container ships with category of gross tonnage less than 5100 GT are selected to show the characteristics of ship traffic. The results for the remaining categories of ships are similar, showing normal distribution to fit the histograms of lateral position and speed. The means and standard deviations are transferred as boundary input of the simulation, which can be found in the tables in Appendix IX. The histograms relate to the crossing-line 1, which is located at the left boundary of the "study area" shown in Figure 3-2.

Table 3-5 Categories for container ships by gross tonnage

Class	Class 1	Class 2	Class 3	Class 4	Class 5
Gross tonnage (t)	<5100	5101-12000	12001-20000	20001-38000	>38000

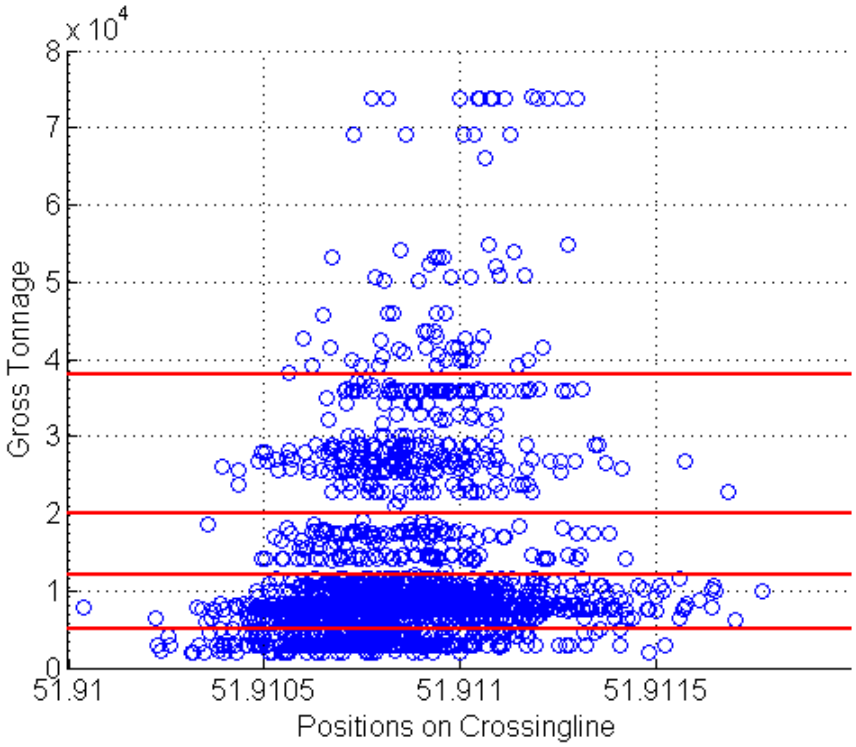

Figure 3-7 Scatter points of ship position and gross tonnage for type II (based on 2000 passages)

3.3.3.2 Spatial distribution perpendicular to the channel

Figure 3-8 shows the histogram of the lateral position distribution of container ships less than 5100 GT that are extracted from the AIS database. The x-axis is the non-dimensional lateral distance from the centerline of the waterway (0 stand for position of centerline, while 0.5 deviation stands for the position of starboard channel boundary), and the y-axis gives the fraction of ship numbers. The histogram comprises 31 bars which cover 80% of the waterway width. As the navigable waterway width is about 270 m, each bar in the histogram covers a width of about 7 meters. The graph shows that most of the ships were navigating on the starboard side of the waterway. Also most of the ship traffic prefers to stay closer to the centerline rather than to the channel bank. A small proportion of ships navigate on the port side of the waterway, which is dangerous, because they are navigating on the wrong side of the waterway where ships with an opposite direction can come close by and they have little time for collision avoidance. The normal curve appears to fit the histogram well. This normal distribution can be further used to allocate the lateral positions of the ships generated at the boundary of a future simulation model.

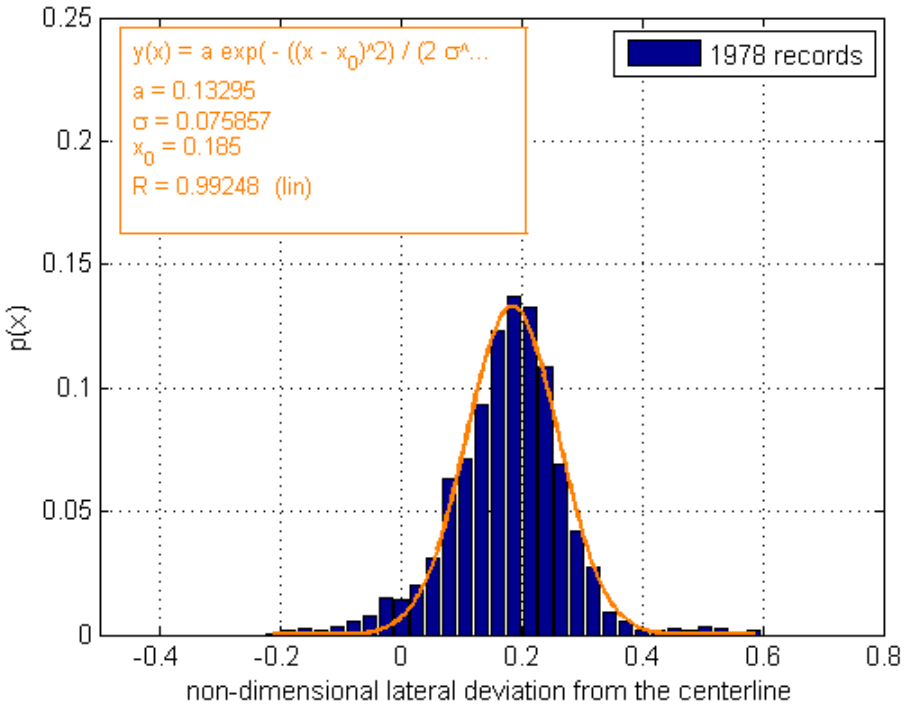

Figure 3-8 Spatial distribution for incoming containers at the crossing-line number 1 (less than 5100 GT, 1978 passages)

3.3.3.3 Speed distribution of ships

Different ships maneuver with different speeds, see Figure 3-9. A normal distribution fits the speed histogram. The speed of ships varies in a range from 5 kn to 15 kn, with a mean value of 10.7 kn and a standard deviation of 1.2 kn. Few ships are navigating with a speed less than 5kn or larger than 15 kn. This means most of the ships do not navigate at full speed, and the ships are expected to change speed based on different situations during passages.

A ship will navigate with a safe speed in the waterway. The chosen speed reflects the safe speed in a specific situation under normal circumstances. Especially in a busy channel, the OOW (Officer on Watch) should select a speed which guarantees the safety of the ship. So, the ship speed is determined by many factors, such as the experience of the OOW, characteristics of OOW, ship position, ship condition, ship dimensions, ship type, encountering situation, weather condition and characteristics of the waterway. As a result, each ship will sail with its own speed as is required by the concept of “good seamanship”, which results in the large variation of speed.

3.3.3.4 Course distribution of the ships

As is shown in Figure 3-10, the courses do not vary much. A normal distribution fits the histogram of the courses with a mean value of 123 degrees and a standard deviation of 1.8 degrees. This means that the courses of the ships do not change much when the ships are sailing in the waterway. There are three reasons for this phenomenon. Firstly, the location of the case study is a straight channel where the ships normally do not need to change their course during passage. Secondly, the channel we studied is relatively narrow (about 270 m navigable width), and there is no room to change course significantly. Thirdly, the only reason for changing course is an encountering situation. With the limited width of the waterway, ships may opt for speed change to make a safe maneuver and avoid collision, as what is shown in the speed variation in Figure 3-9.

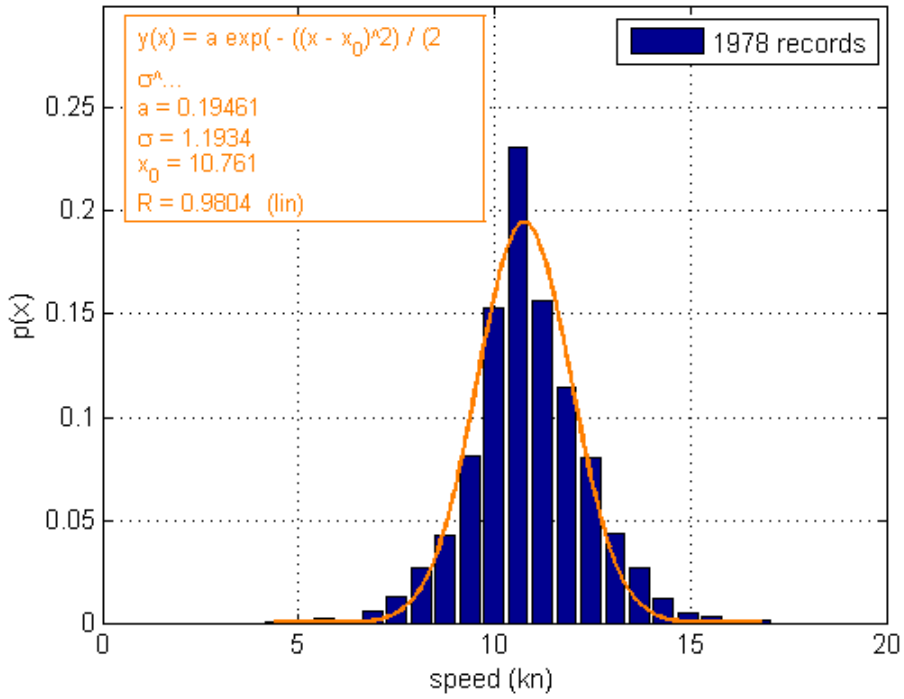

Figure 3-9 Speed distribution of incoming containerships (less than 5100t, 1978 passages)

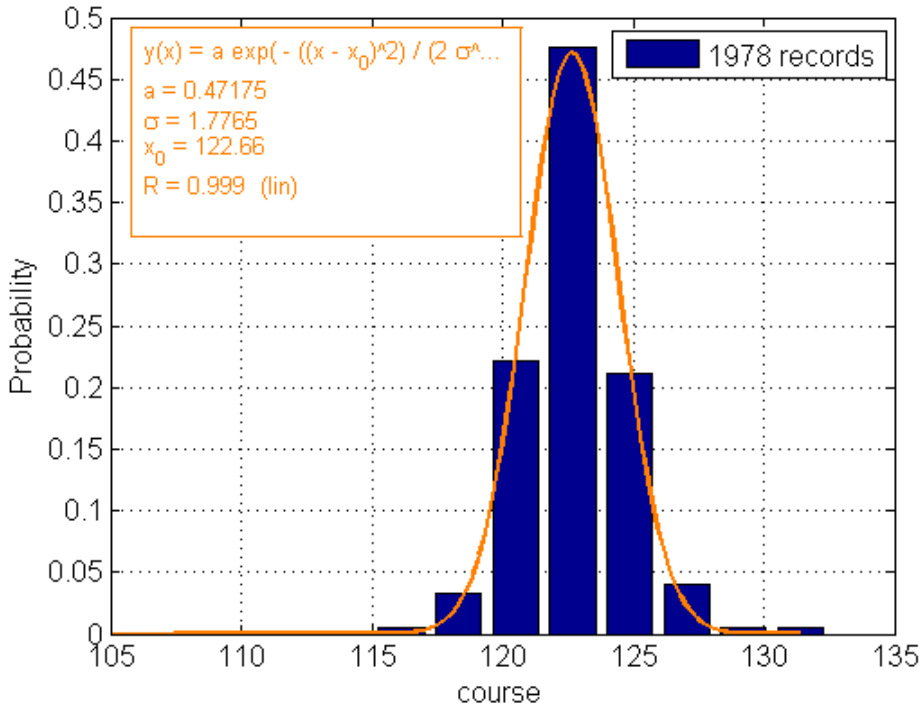

Figure 3-10 Course distribution of the ships (incoming containerships less than 5100t, 1978 passages)

3.3.3.5 Comparing the position changes along the channel

The container ships keep a straight average path in the straight channel. The lateral position does not change much (Table 3-6). However, the standard deviation gets larger when the ships come to the 9th crossingline, where the channel gets wider.

Table 3-6 Positions change of Incoming vessel for containers 0-5100 GT

crossingline number	Average deviation from the center	δ
crossingline1	0.185	0.076
crossingline5	0.188	0.076
crossingline9	0.181	0.093

3.4 Discussion and conclusion

This research presents AIS data analysis to deepen our understanding about the ship traffic in the waterway. This understanding is important for realistic ship traffic simulations to be performed later on in this work for maritime risk analysis. Some dynamic values (position, speed, course, time interval) of ship AIS information are analyzed, and the values are presented in a statistical way to describe the characteristics of the ship traffic behavior. The statistical characteristics indicate that it is reasonable to use statistical methods to describe the behavior of the ship traffic. These statistical distributions can provide a sound basis for simulation in the next stage of research. The statistics at the boundary of the study area are used as input in ANTS model. The different characteristics of ship traffic need to be reflected in the ANTS model.

The data analysis at this stage only concerns the direct information. There is other indirect information beyond this analysis that is also important to describe the ship traffic, including ship interaction, human factor, and ship response to navigational environment. For the ship interaction part, it concerns head-on situation, overtaking situation, and ship avoidance of objects and grounding. Those interactions are influenced by individual behavior as a result of human factors and regulations, and will be further investigated in Chapter 6.

4. INFLUENCE OF VISIBILITY, WIND, AND CURRENTS

4.1 Introduction

This chapter examines whether the influences of visibility and wind, and currents are sufficient to be reflected in the simulation. Visibility and wind, and currents are external conditions that may affect navigational safety of ships. Low visibility obstructs the visual lookout of ship Officers on Watch (OOW). Collisions would happen if a vessel on collision course is not observed. Wind, on the other hand, exerts forces on the ship. The influence of currents is another external factor, which not only affects the maneuverability of the ship, but also may lead to change of speed over ground. A good experienced OOW may be able to compensate the effects by appropriate ship maneuvering. The analysis aims to check whether the visibility and wind significantly affects the behavior of ships. If there are any significant differences, visibility and wind should be incorporated in the simulation. The influence of currents are not examined in this study, but the conclusions of another recent study are adopted (Shu et al., 2013b). However, a simplified description of the current in the study area has been derived to be included in the simulation of a drifting ship.

Shu et al. (2013b) examined the external influences of visibility and wind for ship traffic in another part of the Botlek area of the Port of Rotterdam. Small influences are found of the visibility on vessel speed (less than 1 kn of speed) and vessel path (less than 20 m of channel width), and there is a small influence of crosswind on vessel speed (less than 1 kn). Shen (2012) also concludes that there are small influences of wind on vessel path. But, the differences are very small (less than 5% of channel width). Shu et al. (2013a) further investigated the influence of currents and concluded that only ship speed is influenced a little.

In addition to the above studies, we will examine the influences for the studied area. Average ship behavior on lateral position and speed in each extreme external condition are compared with the same in the general situation to examine the differences. If the differences are small enough, it is not necessary to reflect the influences in the traffic

simulation. Ship behavior in the general situation means the general ship traffic behavior elaborated in Chapter 3, which includes the ship traffic behavior in all kind of conditions.

4.2 Visibility

This section discusses ship traffic behavior in low visibility. Visibility was considered an important element for safe navigation: 21 ship collisions out of 92 cases happened in bad visibility in the Netherlands (van Manen, 2001). According to COLREGs (International Regulations for Preventing Collisions at Sea), “safe speed” based on experience should be maintained in conditions of low visibility. In order to know the behavioral differences in low visibility, this thesis examines the differences by comparing ship traffic behavior in the condition of low visibility to ship traffic behavior in the general situation.

The comparison consists of three steps. Firstly, the frequencies of different visibility levels and the time a certain visibility level lasts are studied. Secondly, the time periods with low visibility are singled out to select ship passages in the AIS database within the same period. Thirdly, the differences in average position and average speed for each size category of container ships in extreme low visibility are compared with the same in general condition.

4.2.1 Visibility conditions in the studied area

Normally, the visibility in the Port of Rotterdam is quite good. We have got historical visibility data for a period from 1/1/2008 to 19/10/2011 in the Port of Rotterdam, nearly 2 million records in total. The visibility data is recorded with a time interval of one minute. The measurement point is located at “Geulhaven” in the Port of Rotterdam (Figure 4-1), which is located at the end of the waterway studied.

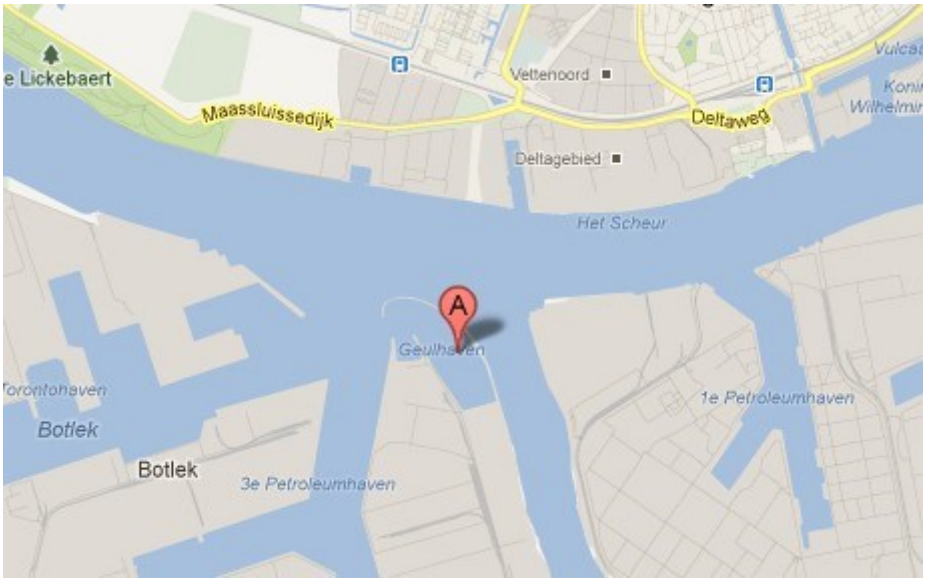

Figure 4-1 The location of the visibility is recorded for wind and visibility

The time period with poor visibility is limited in the Port of Rotterdam. The histogram of visibility less than 5,000 m (Figure 4-2) is shown to get a visibility distribution based on visibility records in the years of 2009 and 2010. There are about 10,000 records with visibility less than 1,000 m. As the record of visibility was updated each minute, the time periods with visibility less than 1,000 m amounts to about 166 hours only.

The time periods with visibility less than 1,000 m are singled out for selecting ship passages to analyze ship traffic behavior in low visibility in 2009 and 2010. Although visibility is constantly changing over time, poor visibility can be regarded as a continuous phenomenon with visibility around 1,000 m for hours. In other words, in several hours of low visibility, the measurements of visibility are sometimes larger than 1,000 m and sometimes lower than 1,000 m. In data selection, this study treats the whole period (with visibility around 1,000 m) as a time period of the rather poor visibility. Most of the periods of low visibility (less than 1,000 m) last less than 5 hours (Figure 4-3). Furthermore, the ship passages during the low visibility periods are selected from the AIS database for analysis.

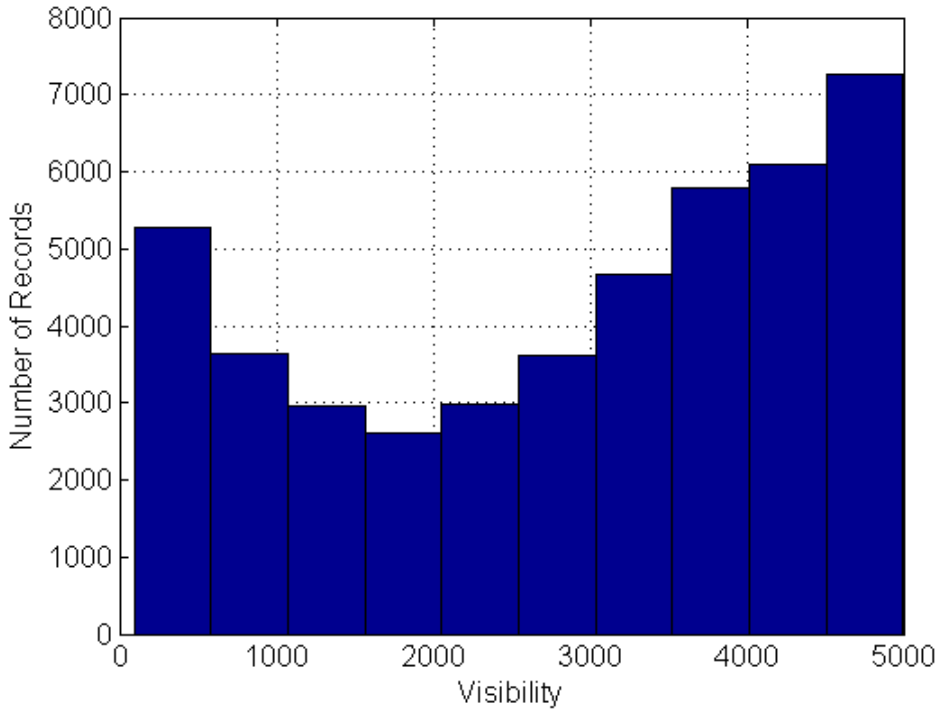

Figure 4-2 Histogram of visibility less than 5000m (44912 records in 2009 and 2010)

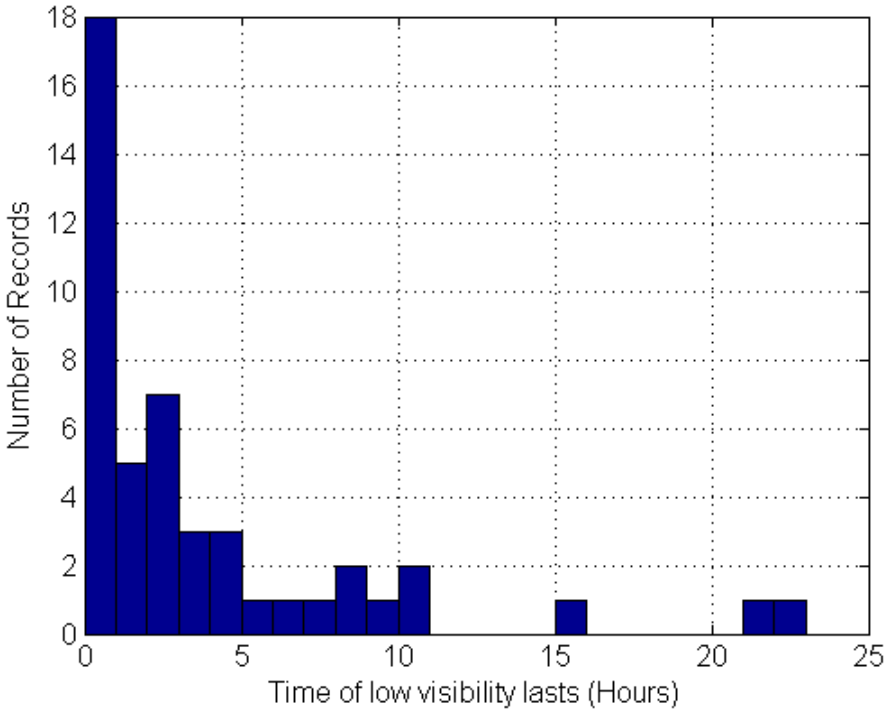

Figure 4-3 Histogram of the time periods that the low visibility lasts (47 records in 2009 and 2010)

4.2.2 Influence on ship traffic behavior from low visibility

This section compares the ship traffic behavior in low visibility with the same in the general situation. Average vessel path and average speed are presented to show the differences. In order to statistically examine the influence on ship passages in low visibility, the average position deviation from the centerline for each vessel category (Table 4-1 and Table 4-2) and the average speed for each vessel category (Table 4-3 and Table 4-4) are calculated. These characteristics are compared with the same in the general situation.

The average position deviations for different categories of container ships in low visibility are similar to those in the general situation. For incoming container ships, the average deviations from the centerline are identical to the general situation (Table 4-1). However, we can observe that incoming container ships tend to navigate slightly closer to the channel bank in low visibility. A similar phenomenon occurs for outgoing container ships (Table 4-2), whereby the ships navigate even slightly closer to the waterway bank. However, most of the differences are within the 5% range.

The speed change in low visibility is small (less than 1 kn). For incoming vessels, a larger speed difference (about 0.7 kn less) is observed for small ships compared to the average speed in the general situation (Table 4-3). However, the speed of larger ships shows little difference in low visibility. A similar phenomenon is found for the outgoing vessels (Table 4-4). In any case, the speed differences are within 1 kn, although we can find observable

speed differences for both incoming vessels and outgoing vessels. As a whole, it can be concluded that extreme low visibility does not affect the speed choices much compared to the general situation. The slight differences do not need to be reflected in the simulation.

Table 4-1 Visibility influence on (non-dimensional) average ship path for incoming container ships

	Ship behavior in The general situation		**Ship behavior in low visibility**		**Difference**
Ship categories	Lateral deviations from the centerline	Number of ship passages analyzed	Lateral deviations from the centerline	Number of ship passages analyzed	Difference on lateral deviations
Less than 5100 GT	0.18	1978	0.15	20	-0.02
5101 GT to 12000 GT	0.15	6652	0.16	59	0.01
12000 GT to 20000 GT	0.14	854	0.15	8	0.01
20000 GT to 38000	0.13	1448	0.13	9	0.00
Larger than 38001 GT	0.10	421	0.15	5	0.05

Table 4-2 Visibility influence on (non-dimensional) average ship path for outgoing container ships

	Ship behavior in The general situation		**Ship behavior in low visibility**		**Difference**
Ship categories	Lateral deviations from the centerline	Number of ship passages analyzed	Lateral deviations from the centerline	Number of ship passages analyzed	Difference on lateral deviations
Less than 5100 GT	0.17	2110	0.19	15	0.02
5101 GT to 12000 GT	0.15	6808	0.17	56	0.02
12000 GT to 20000 GT	0.13	845	0.22	9	0.09
20000 GT to 38000	0.11	1459	0.14	17	0.03
Larger than 38001 GT	0.08	432	0.08	2	-0.01

Table 4-3 Visibility influence on average ship speed for incoming container ships

	Ship behavior in The general situation		**Ship behavior in low visibility**		**Difference**
Ship categories	Average speed (kn)	Number of ship passages analyzed	Average speed (kn)	Number of ship passages analyzed	Difference on average speed (kn)
less than 5100 GT	10.83	1978	10.10	20	-0.74
5101 GT to 12000 GT	10.35	6652	10.02	59	-0.34
12000 GT to 20000 GT	9.27	854	9.49	8	0.22
20000 GT to 38000	8.20	1448	8.33	9	0.13
Larger than 38001 GT	7.71	421	8.38	5	0.67

Table 4-4 Visibility influence on average ship speed for outgoing container ships

	Ship behavior in The general situation		Ship behavior in low visibility		Difference
Ship categories	Average speed (kn)	Number of ship passages analyzed	Average speed (kn)	Number of ship passages analyzed	Difference on average speed (kn)
Less than 5100 GT	11.85	2110	11.19	15	-0.65
5101 GT to 12000 GT	10.95	6808	10.28	56	-0.68
12000 GT to 20000 GT	10.12	845	9.89	9	-0.23
20000 GT to 38000	9.35	1459	9.38	17	0.03
Larger than 38001 GT	8.81	432	8.70	2	-0.11

4.2.3 Discussion

In this section, we analyzed the behavior of container ships in the situation of low visibility (visibility less than 1000 m). It is found that the ship behavior is similar to the behavior in the general situation. In this way, we can conclude that the traffic behavior of container ships is not significantly influenced by low visibility. However, the extent of the influence on ship traffic behavior should be examined by comparing the detailed behavior for each category of ships.

The similarities of the traffic behavior show that the navigational equipment and additional lookout on board are quite reliable during periods of low visibility. Also the VTS center in the Port of Rotterdam may contribute to the relatively small influence. Finally, the slight differences of traffic behavior may be caused by a higher level of safety awareness on board. There are two possible reasons for explaining that the ships tend to navigate closer to the channel bank. The OOW may not visually observe other ships with head-on situations in low visibility, and the TCPA (Time to Closest Point of Approach) becomes very short which constrains possible collision avoidance maneuvering. In order to avoid possible unforeseen encounter from the other side of the waterway, ships tend to navigate closer to the channel bank. Another possible reason is that the navigational aid and geographical signs (waterway bank or other structures on the bank) are more visible to the OOW, when the ships come closer to the bank. It's easier for the ship officers to confirm the ship positions and courses provided by the electrical equipment on board.

The differences of ship traffic behavior for other types of ships are assumed to be not significantly influenced by low visibility. Firstly, the spatial distribution and speed distribution of ship passages in low visibility are "bell shaped", which are similar to the same in the general situation. Secondly, no significant position differences (on 5% range) and speed differences (1 kn) are found when comparing the ship traffic behavior in low visibility to the general situation. Thirdly, the behavioral differences for different types of ships are small in the general situation. So we do not expect significant differences in low visibility.

4.3 Wind

Wind is another external factor that affects navigational safety of ships. Wind exerts forces on ships. With this effect, wind can either enlarge the swept path of a ship (crosswind), or change the speed of a ship (fore wind or stern wind). If a ship loses propelling power (e.g. due to an engine problem), the ship will drift on the water under the influence of wind, which is a dangerous situation. On the contrary, navigating ships are able to compensate the wind force. In the case of crosswind, a ship is able to adjust its heading to maintain the intended course. In the case of fore wind (or stern wind), the ships can adjust the vessel speed to overcome the force of the wind. In this section, we statistically analyze the ship behavior in rather strong wind conditions to examine the wind influence on the ship behavior.

4.3.1 Wind condition in the studied area

The wind directions are shown in compass degrees. 0 and 360 degrees stand for wind coming from the north, 90 degrees stand for wind coming from the east, 180 degrees is southern wind and 270 degrees is western wind. The strength of wind is recorded in meters per second. The time interval for the records is 5 minutes. The measurement point is also located at “Geulhaven” in the Port of Rotterdam (Figure 4-1).

The wind is constantly changing throughout the year. There are 104,059 valid records in the year 2009. This study uses a “wind rose” to represent the frequency of wind for each direction (Figure 4-4). The wind rose is equally spaced into 24 bins. Wind speeds in the area vary from 0 to 18.2 m/s (Figure 4-5). The most frequent wind speed is around 4.5 m/s, and the frequencies get less towards zero and higher wind speed.

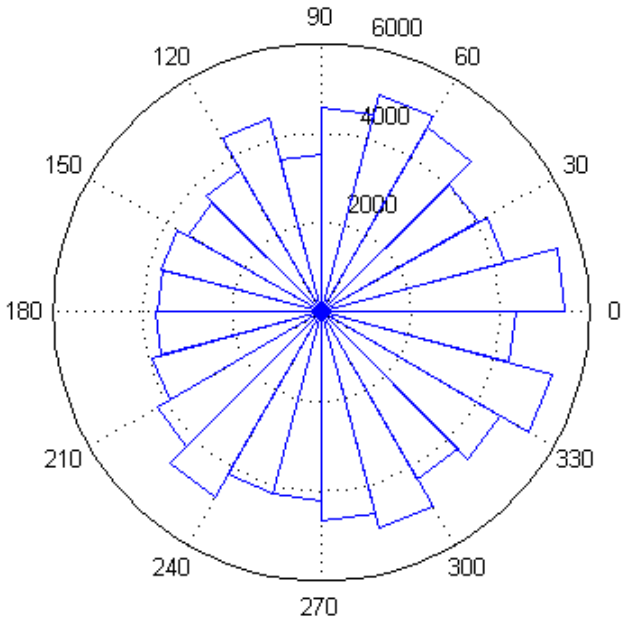

Figure 4-4 Wind rose of the year 2009 (104059 valid records)

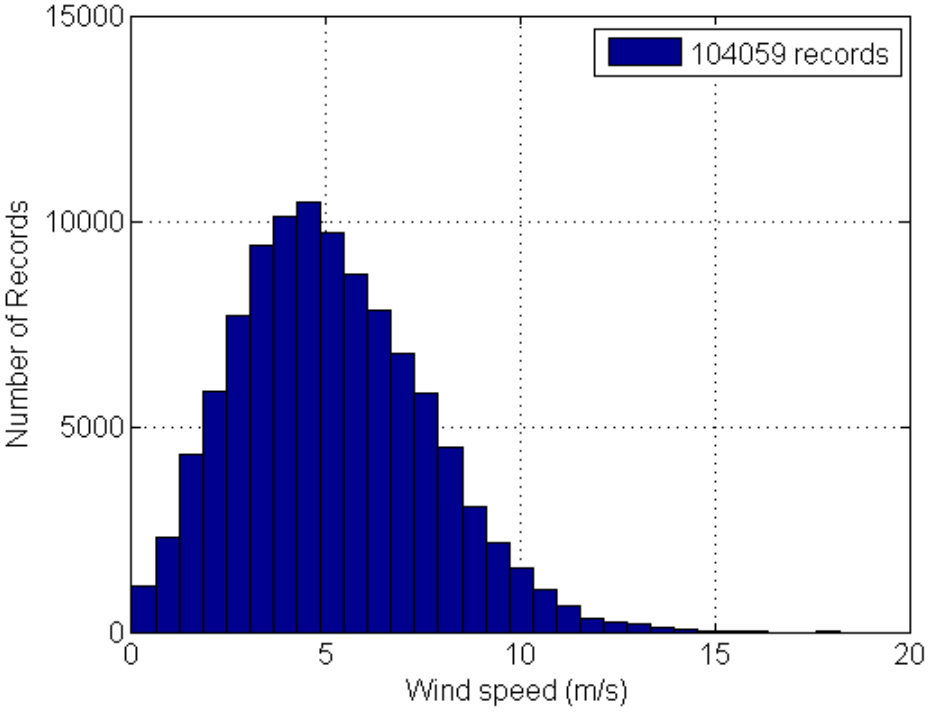

Figure 4-5 Speed distribution of wind in the whole year 2009

4.3.2 Influence on ship traffic behavior from rather strong wind

The wind with a speed larger than 10 m/s is considered as rather strong wind in the analysis to collect a sufficient number of ship passages for statistical analysis. We compare the ship traffic behavior in rather strong wind with the same in the general situation. Average vessel paths and average speeds are compared for the differences. The situations with crosswind and fore (stern) wind are studied separately.

It can be seen that the average positions under crosswind for different categories of container ships are very similar to the same in the general situation. For incoming container ships, the average position deviation from the centerline is identical to the general situation (Table 4-5). There is only one exceptional case that is 12% left to the general situation. But, that single case cannot change the conclusion that the influences of rather strong wind are not significant (within 5% of difference) for most of the cases. Similarly, for outgoing vessels, we can conclude that the average position deviations for each category of container ships are also similar to those in the general situations (Table 4-6). Although it is observed that some ships have significant position shifts which are larger than 5% range to either side, the number of ship passages with significant position shifts is small (9 passages altogether). The average position of the dominant 15 passages with tonnage between 5101 GT to 12000 GT do not shift much. Finally, we can conclude that the wind does not significantly affect the position choices. In other words, the ships are able to compensate the force from the crosswind.

The speed differences in the crosswind are relatively small (less than 1 kn). For incoming vessels, all the ships choose to navigate faster in crosswind than in the general situation (Table 4-7). For outgoing vessels, small ships tend to navigate with smaller speed than in the general situation (Table 4-8). However, larger ships choose a little bit larger speed in crosswind than in the general situation. In any case, the speed differences are within 1 kn. It seems that most of ships increase speed in rather strong crosswind. The reason might be that increasing speed can enhance maneuverability and stability of ships.

Table 4-5 Influence on (non-dimensional) average ship path for incoming containers of each category from crosswind

	Ship behavior in the general situation		**Ship behavior in wind**		**Difference**
Ship categories	Lateral deviations from the centerline	Number of ship passages analyzed	Lateral deviations from the centerline	Number of ship passages analyzed	Difference on lateral deviations
Less than 5100 GT	0.18	1978	0.14	5	-0.04
5101 GT to 12000 GT	0.15	6652	0.16	28	0.01
12000 GT to 20000 GT	0.14	854	0.03	1	-0.12
20000 GT to 38000 GT	0.13	1448	0.14	6	0.01
Larger than 38001 GT	0.10	421	0.04	1	-0.05

Table 4-6 Influence on (non-dimensional) average ship path for outgoing containers of each category from crosswind

	Ship behavior in the general situation		**Ship behavior in wind**		**Difference**
Ship categories	Lateral deviations from the centerline	Number of ship passages analyzed	Lateral deviations from the centerline	Number of ship passages analyzed	Difference on lateral deviations
Less than 5100 GT	0.17	2110	0.10	5	-0.07
5101 GT to 12000 GT	0.15	6808	0.15	15	0.01
12000 GT to 20000 GT	0.13	845	0.19	1	0.06
20000 GT to 38000 GT	0.11	1459	0.17	2	0.06
Larger than 38001 GT	0.08	432	-0.01	1	-0.09

Table 4-7 Influence on average ship speed for incoming containers of each category from crosswind

	Ship behavior in the general situation		**Ship behavior in wind**		**Difference**
Ship categories	Average speed (kn)	Number of ship passages analyzed	Average speed (kn)	Number of ship passages analyzed	Difference on average speed (kn)
less than 5100 GT	10.83	1978	11.36	5	0.53
5101 GT to 12000 GT	10.35	6652	10.55	28	0.19
12000 GT to 20000 GT	9.27	854	11.10	1	1.83
20000 GT to 38000 GT	8.20	1448	8.72	6	0.51
Larger than 38001 GT	7.71	421	7.80	1	0.09

Table 4-8 Influence on average ship speed for outgoing containers of each category from crosswind

	Ship behavior in the general situation		**Ship behavior in wind**		**Difference**
Ship categories	Average speed (kn)	Number of ship passages analyzed	Average speed (kn)	Number of ship passages analyzed	Difference on average speed (kn)
Less than 5100 GT	11.85	2110	11.34	5	-0.51
5101 GT to 12000 GT	10.95	6808	10.53	15	-0.42
12000 GT to 20000 GT	10.12	845	10.70	1	0.58
20000 GT to 38000 GT	9.35	1459	9.95	2	0.60
Larger than 38001 GT	8.81	432	9.70	1	0.89

The average deviations under fore (stern) wind for each category of container ships are very similar to those in the general situation. For incoming container ships (under the force of stern wind), the average deviations from the centerline are identical to the general situation (Table 4-9). We can still find that the average ship positions shift a little bit to the centerline of the waterway compared with the average position in the general situation, except that

the average position of the largest ships (only 7 passages) shifts to the starboard channel bank. Nevertheless, the differences are within the 5% range. Similarly, for outgoing vessels (under the force of fore wind), we can conclude that the average deviations for each category of container ships are also identical to the general situations (Table 4-10). We find that the ships shift a little bit to the channel bank compared with the average positions in the general situation. However, the differences are also within the 5% range. In conclusion, the fore and stern winds do not affect the position choice in the waterway. In other words, the ships are able to compensate the force from the wind, and the ships do not change their positions under the influence of fore and stern wind.

The speed differences in the fore and stern wind are relative small (less than 1kn/s). For incoming vessels (under wind from stern), small ships have very similar average speeds compared with the average speed in the general situation (Table 4-11). Larger ships choose a little bit smaller speed in stern wind condition than in the general situation. For outgoing vessels (under the fore wind), the speed differences are also small (Table 4-12). In any case, the speed differences are within 1 kn. In conclusion the fore and stern winds do not affect the speed choices much.

Table 4-9 Influence on (non-dimensional) average ship path for incoming containers of each category from stern wind

	Ship behavior in the general situation		**Ship behavior in wind**		**Difference**
Ship categories	Lateral deviations from the centerline	Number of ship passages analyzed	Lateral deviations from the centerline	Number of ship passages analyzed	Difference on lateral deviations
Less than 5100 GT	0.18	1978	0.17	41	-0.01
5101 GT to 12000 GT	0.15	6652	0.12	103	-0.03
12000 GT to 20000 GT	0.14	854	0.11	12	-0.03
20000 GT to 38000 GT	0.13	1448	0.11	20	-0.01
Larger than 38001 GT	0.10	421	0.14	7	0.05

Table 4-10 Influence on (non-dimensional) average ship path for outgoing containers of each category from fore wind

	Ship behavior in the general situation		**Ship behavior in wind**		**Difference**
Ship categories	Lateral deviations from the centerline	Number of ship passages analyzed	Lateral deviations from the centerline	Number of ship passages analyzed	Difference on lateral deviations
Less than 5100 GT	0.17	2110	0.22	31	0.04
5101 GT to 12000 GT	0.15	6808	0.18	98	0.03
12000 GT to 20000 GT	0.13	845	0.13	13	0.00
20000 GT to 38000 GT	0.11	1459	0.11	23	0.01
Larger than 38001 GT	0.08	432	0.12	4	0.04

Table 4-11 Influence on average ship speed for incoming containers of each category from stern wind

	Ship behavior in the general situation		Ship behavior in wind		Difference
Ship categories	Average speed (kn)	Number of ship passages analyzed	Average speed (kn)	Number of ship passages analyzed	Difference on average speed (kn)
less than 5100 GT	10.83	1978	10.90	41	0.07
5101 GT to 12000 GT	10.35	6652	10.41	103	0.06
12000 GT to 20000 GT	9.27	854	8.88	12	-0.39
20000 GT to 38000 GT	8.20	1448	8.02	20	-0.19
Larger than 38001 GT	7.71	421	7.10	7	-0.61

Table 4-12 Influence on average ship speed for incoming containers of each category from fore wind

	Ship behavior in the general situation		Ship behavior in wind		
Ship categories	Average speed (kn)	Number of ship passages analyzed	Average speed (kn)	Number of ship passages analyzed	Difference on average speed (kn)
Less than 5100 GT	11.85	2110	12.12	31	0.27
5101 GT to 12000 GT	10.95	6808	11.14	98	0.19
12000 GT to 20000 GT	10.12	845	10.07	13	-0.05
20000 GT to 38000	9.35	1459	9.23	23	-0.12
Larger than 38001 GT	8.81	432	9.28	4	0.46

4.3.3 Discussion

In this section, we observed ship behavior in rather strong wind condition (wind speed larger than 10 m/s). We analyzed average ship behavior on average position and average speed for ships in crosswind and fore (stern) wind. The “bell shaped” distributions for traffic behavior are not significantly different from the general situations. It is concluded that the ship traffic is not significantly influenced by the wind condition.

We compared ship traffic behavior differences on average position and average speed for each size category of container ships. The similarity in average values indicates that rather strong wind does not significantly affect the behavior of container ships. The analysis shows that the container ships are able to compensate the external influence from wind. In the crosswind situation, ships are able to compensate the wind force to maintain the desired courses. In the fore (stern) wind situation, the wind influence is even less.

However, slight differences on speed choices can be observed from the data analysis, which reflects the fact that the ships have to constantly adjust the vessel speed (speed relative to water) to compensate the influence from wind. The angle between ship and wind is

constantly changing throughout the waterway. It is reasonable that a slight speed difference is caused by difficulty in ship maneuvering.

The ship behavior influences for other ship types can be assumed to the same as for containerships. First of all, the spatial distributions and speed distributions of ship passages in strong wind are “bell shaped”, which are similar to the same in the general situation. Secondly, no significant difference (on 5% range) can be found comparing the passages of most of the ships in rather strong wind to the general situations.

The ship behavior in wind needs further study. In this section, we have only observed wind influence on ship passages in a straight waterway. The ship passages in a waterway bend and the ships behavior in the bend with strong wind are not studied yet. Especially when the ships are changing course at relatively low speeds, the wind influence can be much larger. The ship maneuvering behavior should be analyzed considering the size and maneuverability of the ships.

4.4 Currents

4.4.1 Currents in the studied area

As stated, the AIS data analysis for the influence of currents on ship behavior is left for future research. However, a simplified description of the currents is developed in this section to allow reproduction of the current effects in case of a drifting ship in the ship traffic simulation. Based on the results from Shu et al. (2013a), a ship is able to change ship speed to compensate possible current influence on the speed over ground, and the currents do not affect the position choices of ships.

The currents are affected by two factors, which are water discharge from the river origin and tide from the sea. So, the currents are constantly changing with time in terms of velocity and direction.

Tide is reflected by water level changes. The water level (with respect to Amsterdam Ordnance Datum) changes throughout time (Figure 4-6). It can be observed that the semi-diurnal tide comprises two high tides and two low tides in approximately 25 hours. Other than tide, a factor for change of currents (in terms of direction and velocity) is river discharge (one record per day) (Figure 4-7). The measurement point for river discharge is located at Lobith, far upstream of the studied area. The discharge can vary from less than 1,000 m^3/s to above 8,000 m^3/s.

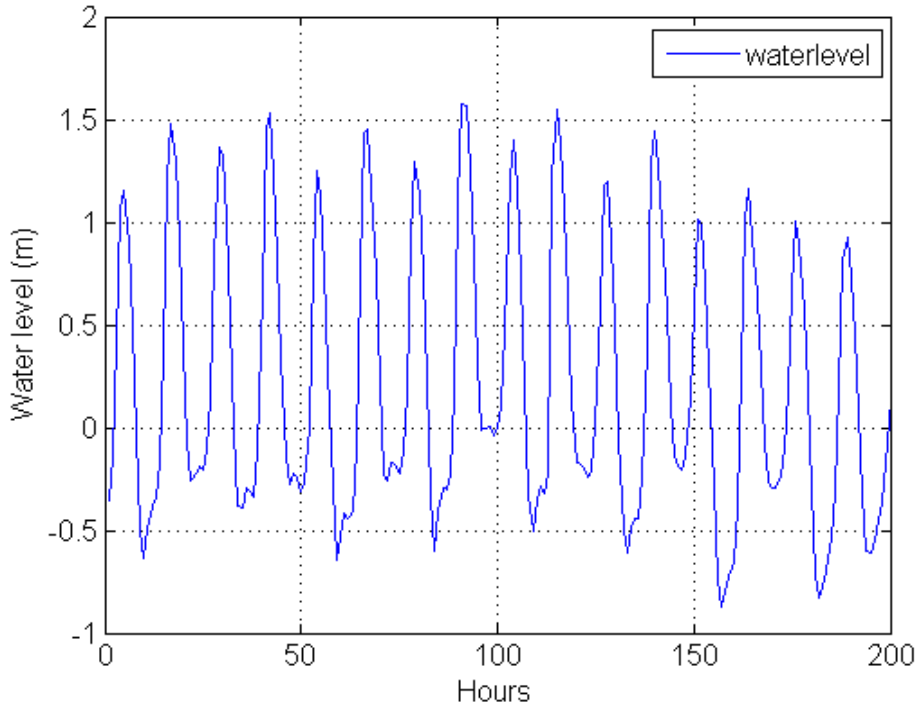

Figure 4-6 Records of Water level in 200 hours (200 records from 00:00 01/01/2010 to 07:00 09/01/2010)

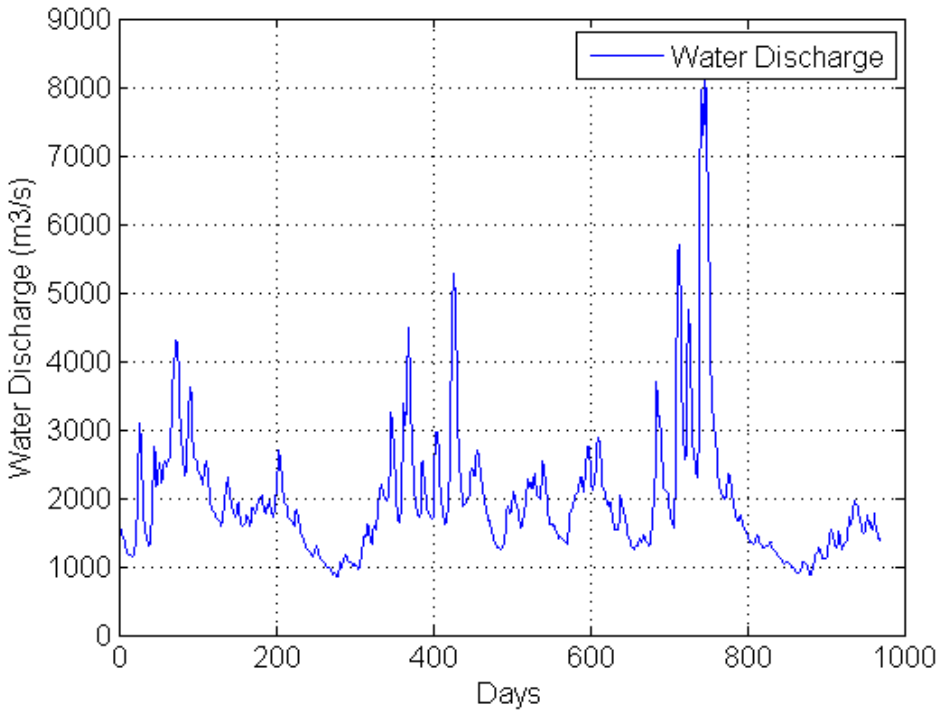

Figure 4-7 Records of water discharge at Lobith (969 records from 01/01/2009 to 27/08/2011)

4.4.2 Hydrodynamics simulation results in terms of water level and currents

The Port of Rotterdam provided the hydrodynamic simulation results for currents in the studied area by using the software Delft3D®. Specific tide conditions and river discharge are treated as inputs in the simulation. Neap tide and spring tide are the tide conditions. Average water discharge (2300 m^3/s) is chosen for the river discharge. The date of 23/09/2011 is selected for neap tide and 31/08/2011 is selected for spring tide. As a result, different current fields are derived from the hydrodynamic simulation results. With respect to current velocity, we get horizontal currents with velocities and directions in 3D geographical space (latitude, longitude and water depth).

The horizontal current velocity is different at different water depths (Figure 4-8). This is explained by the difference in density between the salt sea water and the fresh river discharge. We selected the current fields at -5 m of water depth to present the results, because the currents at this level represent the waterway currents that influence the ships. The draughts of ships in the waterway vary between 4 m and 10 m. The hypothesis is that the currents at -5 m can represent the cumulative current effect on the ships. The current speed does not change much for water depth from -2 m to -6 m (Figure 4-8), which represent the current influence on ships with a draught from 4 m to 12 m. Therefore, we treat large ships and small ships in the same way. Another reason for choosing this value is that the Port of Rotterdam also provides real-time current velocity at -5 m water depth for ship navigation. As an example, the change of current velocity at the measuring location is shown in Figure 4-9.

A simulated current field shows that the horizontal currents differ in different locations of the channel (Figure 4-10). The vectors stand for the currents in the local area, the length shows current velocity, and the direction shows the direction of the water flow. The current velocity is larger in the center of the waterway, and it gets smaller close to the bank.

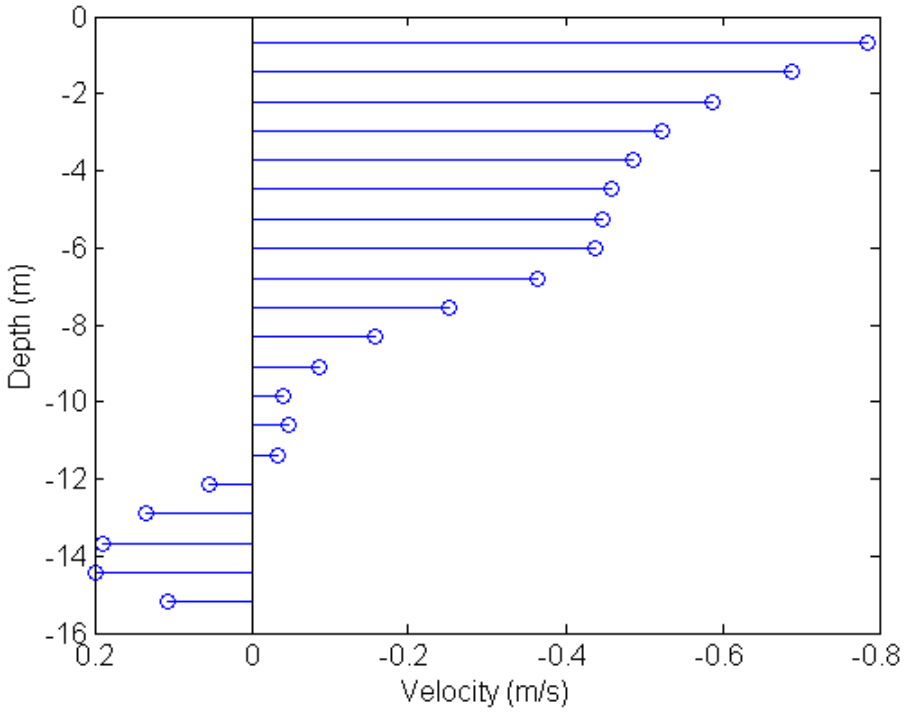

Figure 4-8 The x component of velocity in different water depth, where 0 m depth stands for water surface (the data comes from hydrodynamic simulations of currents fields at point (4.263927 E, 51.906354 N)

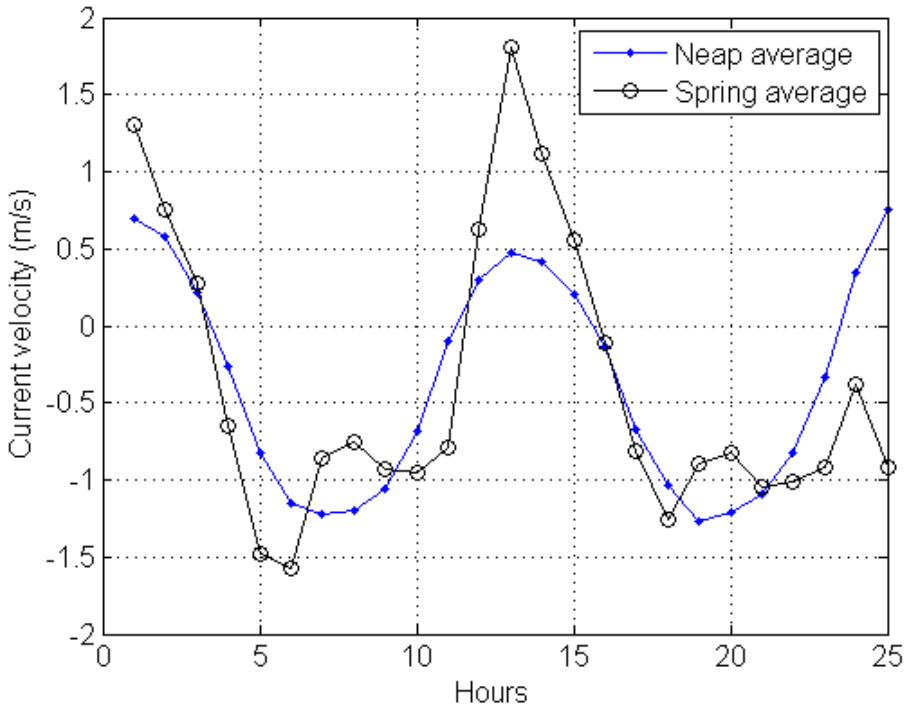

Figure 4-9 Current velocity in neap tide and spring time with average river discharge at location (4.263927 E, 51.906354 N, - 5 m)

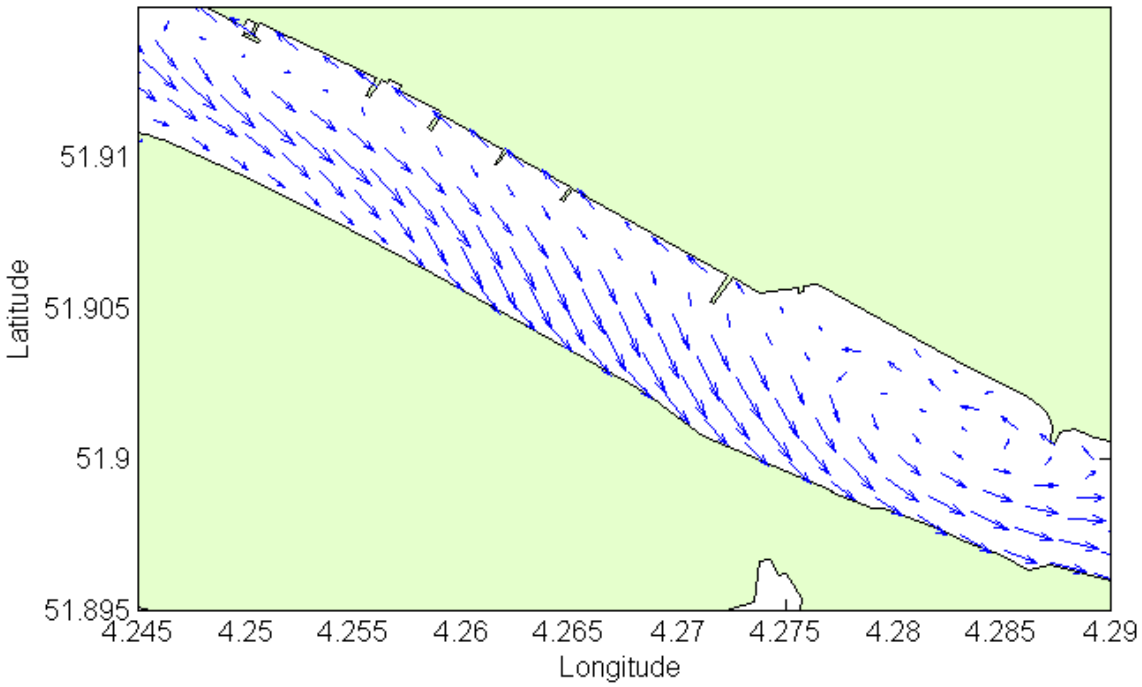

Figure 4-10 Currents field of 6th hour (condition: spring tide, river discharge 800m^3/s)

4.4.3 Discussion

The influence of the currents on ship behavior is very complex. First of all, the currents differ in 3D geographical space. Different sizes (especially draughts) of ships are influenced by different currents as the current velocity differs significantly with water depth. Secondly, the current changes with time. Hence the method introduced for reproducing currents is very coarse. It is better to get hydrodynamic simulation results for the whole time period to know the currents in the studied area, to determine the influence of currents on the ships behavior more precisely.

Further studies are needed for the current effects in simulation. This involves AIS data analysis of the ship behavior in extreme currents and sudden changes of currents, especially when there is a cross current.

4.5 Conclusions

In the above sections, it is concluded that the external effects of visibility and wind do not influence on the normal traffic behavior very much. It is assumed that wind and currents only influence the movement of ships with malfunction. Therefore, this study will treat the ship traffic behavior in the same way as in the general situations in the simulation. For drifting ships 24 hours of current fields at -5 m will be included in the simulation for spring tide and neap tide. The ship movements under the influence of wind or currents will be discussed in Chapter 6.

5. MULTI-AGENT CONCEPT FOR SIMULATION

5.1 Introduction

In Chapter 2, it is concluded that simulation method show advantages in providing sufficient ship (traffic) details, realistic representation of ship traffic behavior and environment, and evolving sufficient factors listed in Section 2.3.7. Chapter 3 and 4 studied the ship traffic behavior in normal situation and the situations with environmental influences. It is observed that the ships try to adapt to the geometry of the channel according to their characteristics. Moreover, the regulations and common practices play important roles in ship behavior. However, the simulation method and framework that involves the ship (traffic) details, behavior, regulations, common practices, and the effects from wind and currents is unknown yet.

This chapter describes the framework and key elements for a realistic nautical traffic simulation model based on multi-agent simulation and artificial force field. Taking advantage of the multi-agent concept, the autonomous ships are able to perceive their local circumstances (encountering situations, waterway geometry), and make decisions to maneuver the ship based on regulations and common practices in ship navigation. The structure of agent-based simulation design will be introduced. In this design, several crucial elements are presented: (i) the existing nautical traffic simulations and advantages of multi-agent simulations; (ii) the strategy for development of the current model; (iii) model description based on the ODD (Overview, Design concepts, Details) protocol; (iv) introduction of artificial force field theory that simulates the interactions and collision avoidances among ships; and (v) steering behavior of the individual ship. Chapter 6 will describe the details of the submodels in the ODD protocol.

5.2 Nautical Traffic Simulation with Multi-agent system

The simulation models for ships have been developing over three decades. Following the first simulation approach by Davis et al. (1980), in recent years two different types of

simulation models were developed, one for ship traffic simulation and the other one for individual ship simulation.

For ship traffic, Hasegawa et al. (2000) developed SMARTS (Marine Traffic Simulation System) for ship traffic in a port. However the routes and waypoints are predetermined and dynamic collision avoidance behavior was not the focus. A different simulation model with dynamic ship movements with different ship types and ship sizes has been developed for the Gulf of Finland (Goerlandt et al., 2011). However, the behavior of individual ships is simplified to implement the collision avoidance behavior. This is because the hydrodynamic behavior of the individual ships and the human influences are very complex.

For individual ships, the interaction with other ships and the role of human interventions are important. Dynamic ship movements can be simulated with manned ship-handling simulators (e.g. the Mermaid 500 at MARIN). One of the drawbacks is that normally only scenarios with certain extreme circumstances are simulated using the system. Another disadvantage is that the interactions between ships are based on expert judgment. And different traffic patterns and uncertainties in the waterway are difficult to be reflected by this system, because the simulations are time consuming and the equipment is expensive (Webster, 1992). Other cheaper options are simulation of ship movements based on Fuzzy Logic (Priadi et al., 2012), Bayesian Networks (Szwed et al., 2006), and Neural Networks (Łącki et al., 2012). But these methods remain dependent on expert opinions or other human interventions.

The use of agent-based models is a logical step for realistic nautical traffic simulations, because ship traffic is a complex self-organizing system with autonomous entities. Firstly, the approach has been applied to other traffic modes such as road traffic (Zhang et al., 2005) and pedestrians (Murakami et al., 2002). Those models showed advantages on both the individual agent level and the traffic level. On the agent level, the individual behavior is realistic and reflects the proper characteristics of the agent, e.g. the mathematical equations make the car agent behave as a car does in real life. On the traffic level, the simulation showed the statistical characteristics of the traffic. Secondly, the multi-agent system has the potential to reflect interactions (e.g. evasive behavior), emergent behavior (e.g. collision avoidance in different situations), and uncertainties (a number of random variables to describe uncertainties), which are lacking in most of the existing ship traffic simulation models. The concept design of the multi-agent simulation for ship traffic is described in (Vaněk et al., 2012, Xiao et al., 2009, Zhang et al., 2009). However, the details of models and how good these represent the reality are not clearly stated.

Multi-agent simulation is a suitable candidate for representing ship traffic for several reasons: (i) the behavior of a ship is based on cognitive decision making by ship officers on board; (ii) the behavior changes of a ship are based on dynamic navigational circumstances including behavior of other ships; (iii) the behavior of a ship will affect the local

circumstances of other ships, and vice versa; (iv) ship behavior conforms to rules including regulations and common practices; (v) ship traffic is a complex self-organizing system, which is difficult to describe by simple mathematical equations. The individual ship behavior shows stochastic characteristics.

5.3 Strategy for agent based modeling of ship traffic

5.3.1 The NetLogo Platform for Multi-agent Simulation

The NetLogo platform is selected for the current simulations. The advantage is that it provides an open source software platform for multi-agent simulations (Wilensky, 1999) with efficient output subroutines such as a graphical interface. It is designed to be suitable for modeling "complex systems developing over time". Railsback et al. (2006) studied the advantages and disadvantages in more detail. NetLogo works as follows.

There are 4 types of built-in agents in the NetLogo, viz., Turtles, Patches, Links, and the Observer (Figure 5-1). Turtles are agents moving around within the environment (ships in this case). Patches are agents that provide the environment with coordinate systems and maps (the waterway). Links connect two agents together. We use these agents to calculate the bearings and distances between two agents in the simulation for the variables in the artificial forces. The Observer agent represents a person who is supervising the simulation.

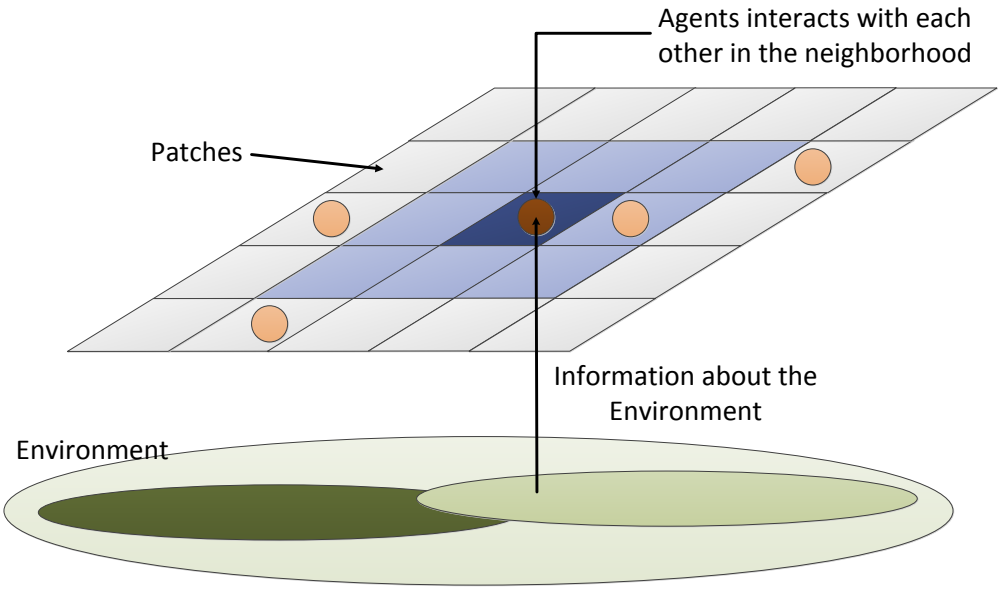

Figure 5-1 The structure of NetLogo model, based on (Macal et al., 2010)

5.3.2 Use of AIS Data

The AIS (Automatic Identification System) provides field data for boundary inputs, model verification and validation for simulations. After interpretation of ship tracks provided by AIS data, we derived information of ship traffic behavior that is characterized by the mean values and statistical distributions of position, speed, heading, and time interval for different types and sizes of ships (introduced in Chapter 3 and 4). The details for obtaining statistical characteristics are also available in the literature (Xiao et al., 2012). Then the continuous distribution function is used to generate random numbers for input of the model. Moreover, the AIS tracks and statistical properties can be used to verify mathematical models built in simulation to get more accurate and realistic results.

5.3.3 ODD protocol for Describing Agent Based Nautical Traffic Model

The model description follows the ODD protocol (Grimm et al., 2006, Grimm et al., 2010). The application of this protocol is necessary because the content is complex. The ODD protocol provides a standardized method to record several inputs and equations, which are integrated into a complex structure. The ODD protocol divides the model into three blocks (Overview, Design concepts, and Details), which are subdivided into seven elements: Purpose, State variables and scales, Process overview and scheduling, Design concepts, Initialization, Input, and Submodels. These elements are addressed separately below.

5.4 ODD protocol for detailed description of the model

5.4.1 ODD element 1: Purpose

The purpose is to design a nautical traffic model based on a multi-agent system that can be used for safety studies. The model specifically explores the interactions between ships and the emergence of different encountering situations in a straight waterway. The influence of wind and currents can be taken into consideration when needed to reproduce reality.

Other than risk analysis of current situations, the model is able to predict future situations. When ship traffic intensifies with time, safety standards become increasingly important for ships and infrastructures (e.g. bridges and berths). The additional information needed to be known is the future traffic density. Then the regulation of ship arrivals will be changed for the future situations. If larger ships are going to appear more in the future, this also can be reflected.

5.4.2 ODD element 2: State Variables and Scales

The dimension of the geographical space is less than 10 kilometers. The critical state variables are listed in Table 5-1. The listed variables treat geographical positions of ships, moving status, and ship maneuverability.

Table 5-1 State variables used to describe model entities

State variable	Variable description
xcor	x coordinate in coordinate system
ycor	y coordinate in coordinate system
heading	heading of a ship
shipspeed	speed of a ship
rotation speed	the rate of turning
K&T	maneuverability indices

5.4.3 ODD element 3: Process Overview and Scheduling

This element describes the crucial processes in the simulation. The sequence of events and the function of events are shown in Figure 5-2. Additional processes that are part of NetLogo and therefore not mentioned here are setup procedure for maps, navigational aids, procedures for additional information (e.g. generating graphs) and additional functions (e.g. report function for monitoring outcome and statistics). Key processes in the Figure are described below:

- Creating a ship at the boundary of the simulation area: the ships are created at each boundary of the waterway. Each ship is assigned with a size, ship type, speed, heading, and initial position at the boundaries.

- Generating time interval for the next ship: the time interval between the passages of two ships reflects the traffic density in the simulation. We can expect more interactions between ships if the time intervals are small. Therefore, more collision avoidance behavior can be observed. The time interval is generated as a random number of statistical distributions of ship arrivals either from field study (AIS data analysis) or based on predictions made.

- Collision candidates and interactions among ships: this process includes collision avoidance behavior, change in heading, change in position, and change in speed. (i) Ship collision avoidance behavior guarantees the moving ships to stay in the waterway and to avoid grounding (path following). When they encounter with ("sense") other ships, they try to avoid collision with one another based on regulations and common practices. The avoidance behavior is reflected by rudder angle (the extent of the turning). (ii) Change in heading involves a simple ship maneuvering model to reflect the response of course change to rudder angles. (iii) Change in position makes the ship move ahead based on the speeds and courses, together with the velocities of currents on patches. (iv) Change in speed functions to change the speed of the ships based on AIS data observations.

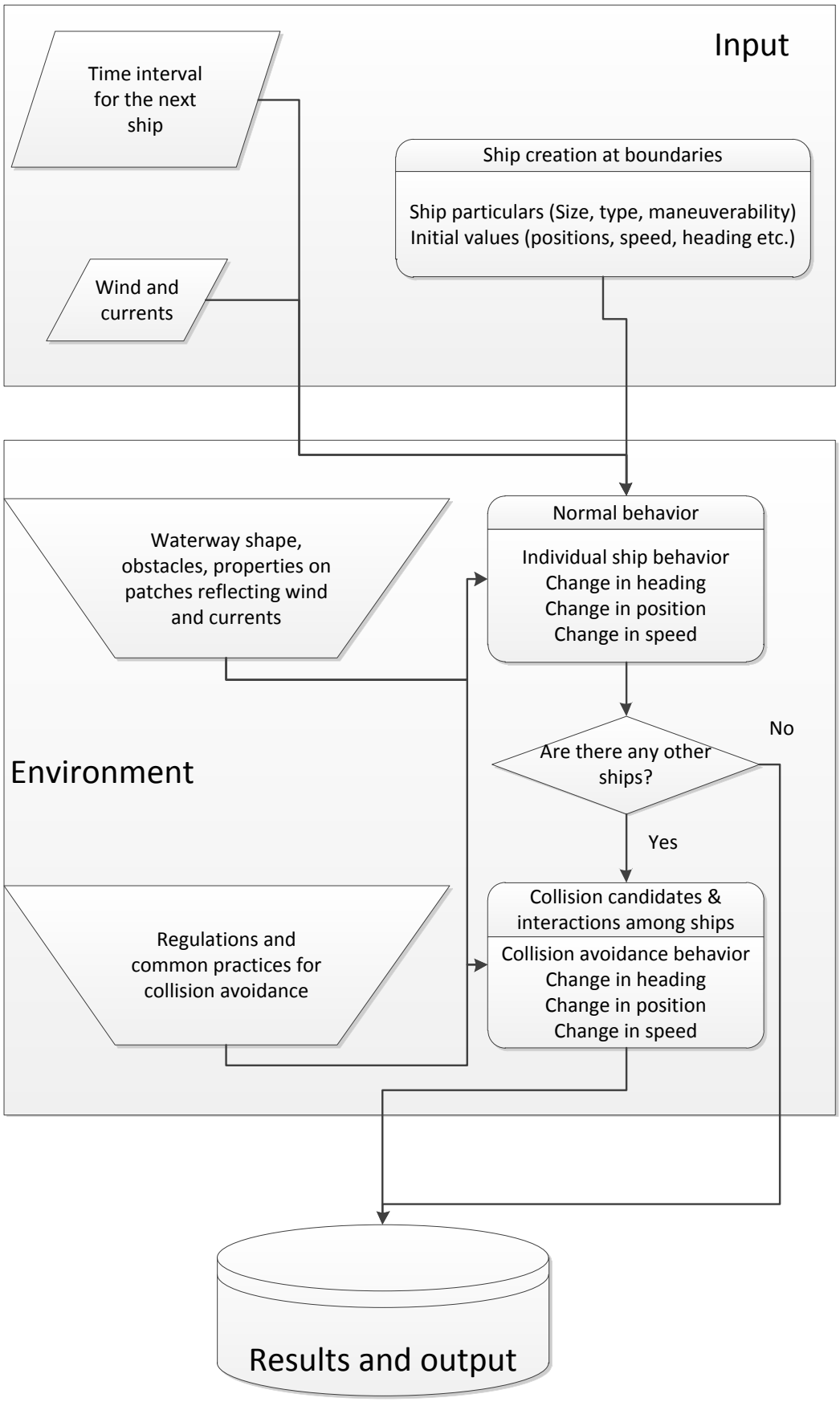

Figure 5-2 The relationships and processes of events during each time step

5.4.4 ODD element 4: Design Concepts

5.4.4.1 Basic principles

The individual ships navigate safely based on regulations, ship conditions, and local environment perceived. In order to avoid collision, the ships are able to constantly adapt to the local environment and change navigational strategy proactively based on regulations and common practices. On the other hand, the behavior of the ships affects the local environment of the other ships. As an agent based system, a simple principle design of nautical traffic simulation using a multi-agent concept is shown in Figure 5-3.

5.4.4.2 Sensing

The ships are able to identify the navigational aids along the waterway. And they are also able to sense the obstacles and other ships in the waterway for collision avoidance. The assumption is that the obstacles and the other ships are always observed by sharp lookout on board. The way to represent sensing is using links to connect the ships and the objects observed by the ships. In the program, the link lengths can be observed by each ship connected by the links, and the ship avoidance behavior is based on the distances and bearings of the objects connected by the links.

Other than the obstacles, the ships are able to observe the environmental conditions like wind and currents (with direction and velocities), e.g. the ship can sense the currents within certain geographical area without creating links. The ship behavior can be influenced by the environmental conditions.

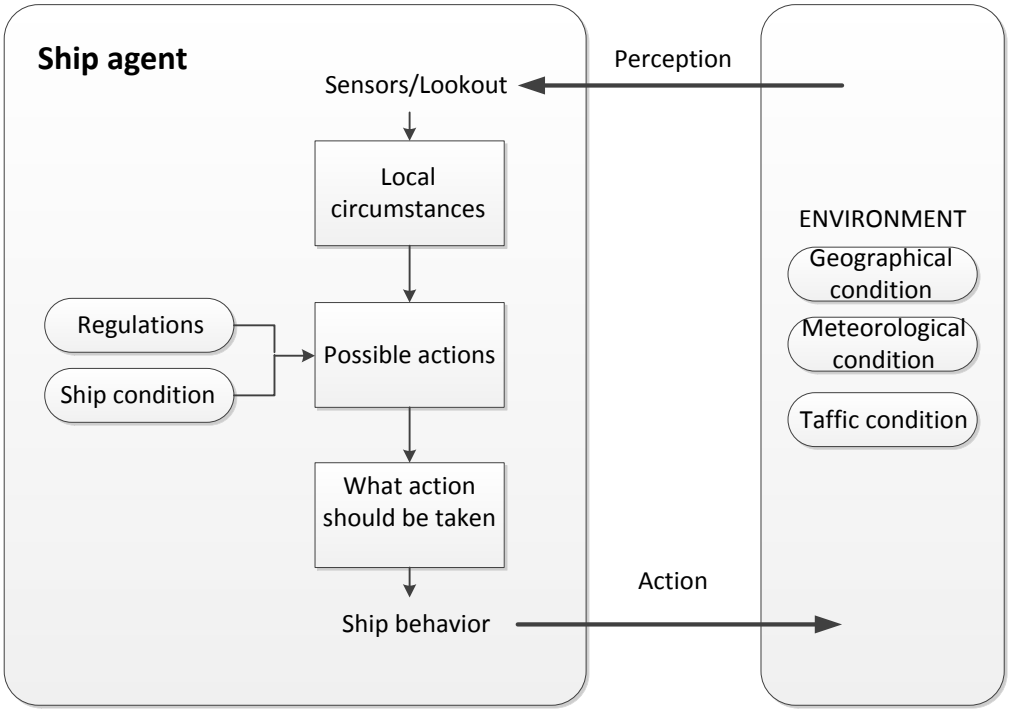

Figure 5-3 Concept model of autonomous intelligent ship agent

5.4.4.3 Adaptation

A simple adaptive behavior built in the simulation is that the ship can always adapt its heading according to the geometrical shape of the waterway. In other words, the ships should be able to maintain the relative position to the starboard side to keep on navigating without grounding. This function includes calculating the geometrical shape of the waterway defined by navigational aids and adapting to the shape by calculating the necessary change of ship heading and direction based on two adjacent local navigational aids in the waterway.

5.4.4.4 Emergence

The interactions and behavior in different encountering situations are the emergent behavior which results in position change and speed change of ships throughout the waterway. Especially, when multiple encounters happen at the same time, we are looking at the whole collision avoidance process, the reaction of the ships, and the deviation from the original path. The multiple ship encounters involve ships with different types, sizes, speeds, and bearings.

5.4.4.5 Stochasticity

There are many variables in the model, and some of those variables result in stochastic emergent events in the simulation. Firstly, when we create a ship at the boundary of the simulation, the positions, headings, and speeds are generated by random numbers from (normal) distributions with different means and variances. Secondly, the sizes and types are also randomly generated from predefined categories and classes. Thirdly, the time differences between two consecutive ships are generated by random numbers from an (exponential) distribution. In the collision avoidance behavior, we also use random choices of critical distances to take action and of extent of the deviations from the original positions. All those stochastic variables and ship behavior provide different situations which could happen in practice. These further evolve different encountering situations involving two different ships (or multi-encountering situations with more than two ships) with different positions, dimensions, types, speeds, behavior, human factors.

5.4.4.6 Interactions

There are two different kinds of interactions. One is the ships' evasive behavior from the fixed objects and waterway banks. The other one is the ship avoidance behavior with respect to other ships in different encounters based on COLREGs (International Regulations for Preventing Collisions at Sea) and common practices (Figure 5-4).

The evasive behavior from the fixed objects is very simple. The ships always keep a certain distance (calculated with the help of links) from the channel bank. The default critical distance in the program for the evasive behavior is 20 m. This default value is set irrespective of ship dimensions and types. However, larger ships keep farther away from the waterway banks in practice. Further AIS data analysis should be done to understand the critical values for evasive behavior.

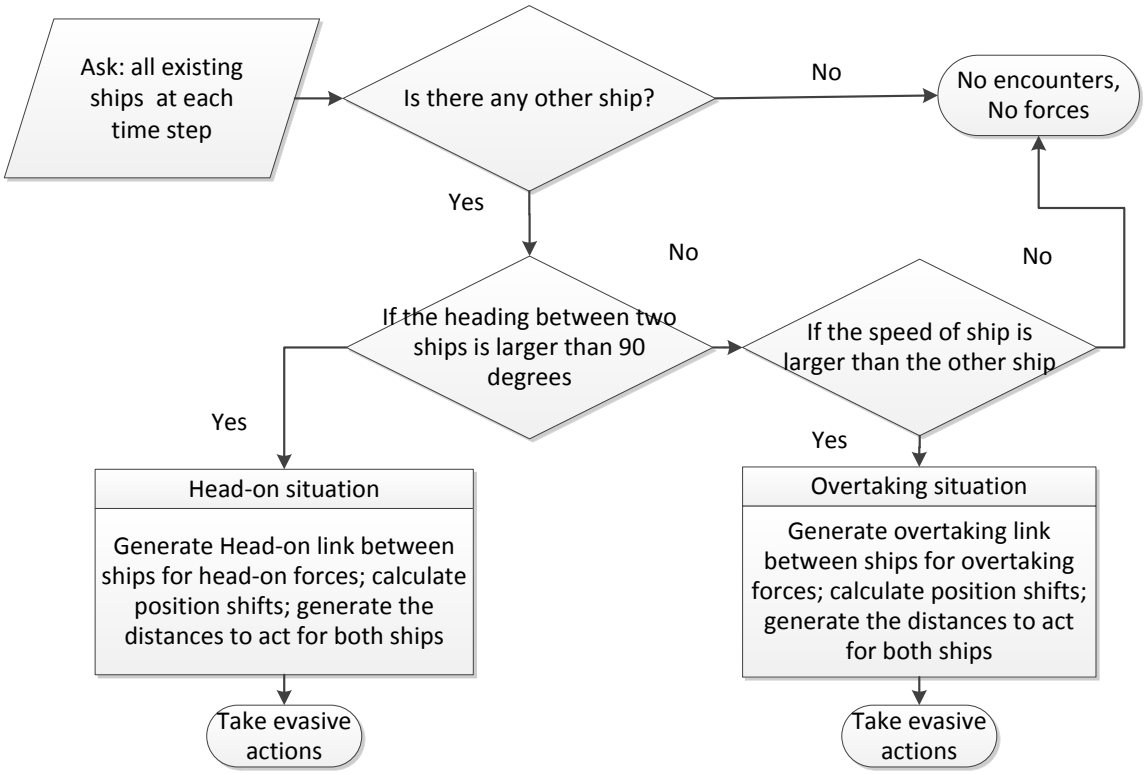

Figure 5-4 Algorithms for ship interactions

The ship avoidance behavior in the straight waterway applies to head-on encounter and overtaking encounter. Critical distant values (calculated with the help of links) for taking action are provided by random values from normal distributions, which are based on AIS data observations. The behavior taken by the ships conforms to COLREG's and common practices. The common practices like the magnitudes of deviations from the original lateral positions (position on an axis perpendicular to the current flow) and the rudder angles are determined by the artificial force field model, which is also based on AIS data analysis. The ODD element 7 and Section 6.2 introduce the artificial force field model in more detail.

The individual ship behavior is simulated with a dynamic ship maneuvering model, taking into account the movements in different local circumstances. The individual ship behavior is based on different internal conditions (vessel characteristics, maneuverability), external conditions (local environment and encounters). Mathematical models are built in the simulation to reflect the ship movements in wind and currents, when this is relevant.

5.4.4.7 Collectives

Different types and sizes of ships behave differently in the simulation. Those different characteristics are represented according to behavior that has been derived from statistical analysis of AIS data. An example is that the larger ships navigate closer to the center of the waterway, while the small ships make full use of the entire space in the waterway.

5.4.4.8 Observation

During the simulation, the spatial distribution of ship positions and speeds at selected places can be presented in a graph. We can also display the distributions for different categories of ships with different types and sizes to show differences. The distributions can be printed in a graph as well. Other than that, we can save the intermediate values and final results in a separate file, which can be further analyzed with statistical tools.

5.4.4.9 Prediction

In this stage of the model development, the ship is not able to predict the actions of the other ships, while appropriate prediction of the other ships in encounter is very important for ship navigation. However, as a straight waterway is a very simple geometrical condition, prediction of actions from other ships becomes less important. The reactive actions are sufficient for collision avoidance, as long as it is known beforehand that the ships follow the relatively straight path.

5.4.5 ODD element 5: Initialization

Sizes and the coordinate system are the initial setup values for the patches. The proportions of different ship types and sizes are the initial setup for the ships. The size of patch does not affect the result of the simulation. However, it affects observers' visual perception of the simulation interface during the simulation process. The coordinate system determines the number of patches, which affects the precision of the simulation. The proportions of ship types in this study are derived from statistical analysis of AIS data. This proportion can be adjusted when needed in the simulation process.

5.4.6 ODD element 6: Input

The inputs of ships during the simulation are created by random numbers from statistical AIS data analysis or from other real world data collected. The values include ship particulars, initial positions and speed, the time interval between two consecutive ships, wind and current.

5.4.7 ODD element 7: Submodel

Chapter 6 describes the mathematical submodels that are required to address some of the factors in the ODD description above. For each submodel, the following details if applicable are described: the mathematical equations; the conditions for invoking the equations; and statistical analysis that was used to optimize the models. There are two different kinds of submodels in this model. One is the artificial force field model that defines the navigational strategy for ship movement in different stages of encounters. The other kind of submodel directly determines the physical movements of the ships.

5.5 Steering Behavior of Individual Ship

A successful ship traffic simulation should represent individual ship behavior. On the individual ship level, the ship should navigate in the waterway, and the behavior is recognized as similar to the behavior in the real world. So, as the navigational steering strategy of individual ship is different from other means of transportation, the steering behavior specific for ship needs to be defined. Based on the simple steering behavior introduced by Reynolds (1999), steering behavior for ships is defined.

5.5.1 Seeking

The ship should be able to seek a specific position as a target to arrive at. In practice, waypoints are drawn on nautical chart before each voyage. One of the duties of the Officer on Watch is to guarantee punctual arrival at the waypoints which are marked on the nautical chart. So, in the simulation, the ship should also reflect this target seeking behavior, with "desired speed" and "desired course". We can treat the targets as the waypoints planned by the ship officers. Similarly, in some specific areas, leading marks and other special objects for navigation also can be treated as "targets" in the simulation.

5.5.2 Offset pursuit

Offset pursuit is very similar to the steering behavior of seeking (Figure 5-5). This behavior can be used in overtaking situations. The pursuing ship sets the other ship as target (which is moving). And the pursuing ship keeps a certain distance (free space) to the ship pursued. Further developments of this behavior require predictions of the target's future positions. Some researchers utilize DCPA (Distance to Closest Point of Approach) and TCPA (Time to Closest Point of Approach) as an indication of position prediction in simulations (Karmarkar et al., 1980).

In overtaking maneuvering, it is mentioned in COLREGs that "An overtaking vessel must keep out of the way of the vessel being overtaken". A certain free space can be defined as the extent of "out of the way". The magnitude and shape of the free space depends on the situation and the navigational environment. Some researchers refer to ship domain theory to explain the free space (Li et al., 2012a, Pietrzykowski et al.). However, the ship domain is not used in practice for ship navigation. Although the ship domain is beyond the scope of this research, the way of implementing free space in the simulation will be introduced in the next chapter.

When overtaking is not allowed by regulations or constrained by navigational conditions (e.g. overtaking is not allowed because of restricted navigational conditions, or restricted in vessel's ability to maneuver), offset pursuit is also useful to describe the ship following behavior, i.e. a ship constantly keeps a certain distance (free space) to other ships in front.

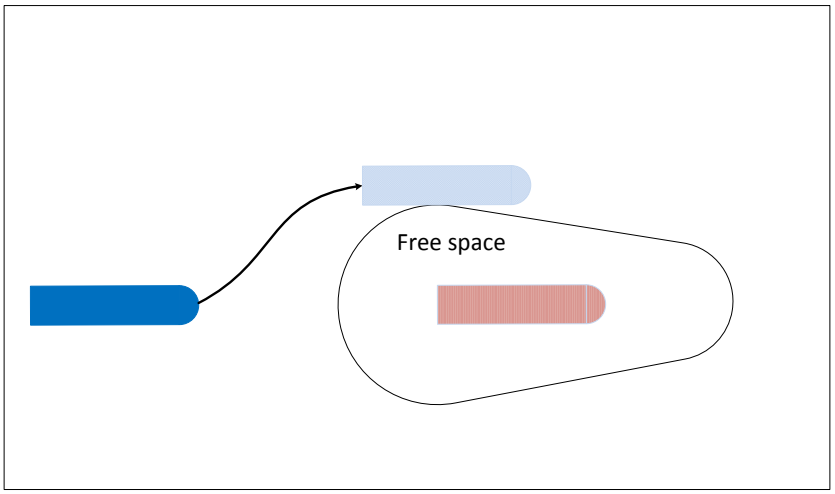

Figure 5-5 Illustration for offset pursuit behavior

5.5.3 Arrival

The arrival behavior is useful when a ship is approaching a specific location. It needs to slow down and make special maneuvering to adapt to another behavior like berthing, turning, or collision avoidance. We take an example of ship arriving at a waterway bend to show the use of arrival behavior (Figure 5-6).

Ships need to adapt to the local geographical conditions to proceed, as inland waterways are not always straight. In Section 3.5.2, we know from AIS data analysis that vessels increase speed in the straight waterway and decrease speed before waterway bend. Therefore, we set the waterway bend as a waypoint (target) to arrive at. In the simulation, when a ship is far away from the bend, the arrival behavior is identical to seeking behavior. However, when the ship gets a certain distance to the waypoint, it starts to decrease speed a little bit (especially for large ships) and make optimal maneuvering based on experience. As soon as the ship arrives at the waypoint, it can finish adapting the course according to the geographical shape of the waterway.

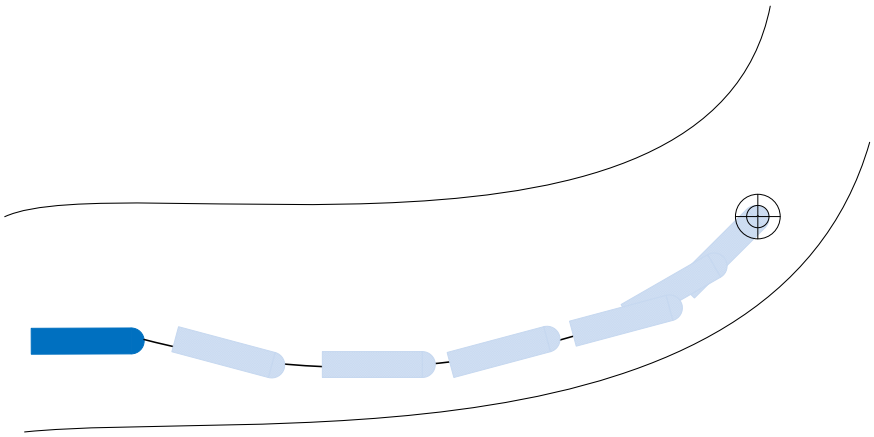

Figure 5-6 Illustration for arrival behavior before waterway bend

5.5.4 Obstacle avoidance

Successful obstacle avoidance behavior guarantees safe passages of ships in the channel. A ship constantly checks the coordinate positions of obstacles to assess the distances and relative directions to obstacles. Obstacles are ranked based on different levels of danger. The obstacle direct in front of the ship will be ranked as immediate danger, which should be treated in the first place. We take collision avoidance behavior from bridge piers as an example to show the use of obstacle avoidance behavior (Figure 5-7).

When a ship navigates in the waterway, it not only needs to avoid objects like waterway bank and shallow water area, but also needs to avoid other fixed objects like bridge piers and moored vessels. In Figure 5-7, the obstacles (bridge piers) are the imminent danger for ship navigation, so the ship adjusts its position to avoid them. We can determine a free space for the obstacle which guides the ship to take actions. However, if the ship navigates too close to the waterway banks, the risk of grounding becomes the first priority, and then the ship should take actions to keep a safe distance from the waterway banks.

5.5.5 Path following

Path following behavior determines the preferred ship passages in the waterway. It does not mean that the ships should follow a rigid predetermined path without any deviation. This behavior allows a ship to deviate from the ideal path. But as soon as the deviation is large enough, the ship should be able to correct its position and resume to a limited distance from the ideal path (Figure 5-8). It seems that the ship is safer when it is navigating in a “comfortable zone”. But when the ship is in the vicinity of an obstacle or another ship, the path following behavior does not work anymore. In this case, the ship deviates substantially from the ideal path to avoid collision.

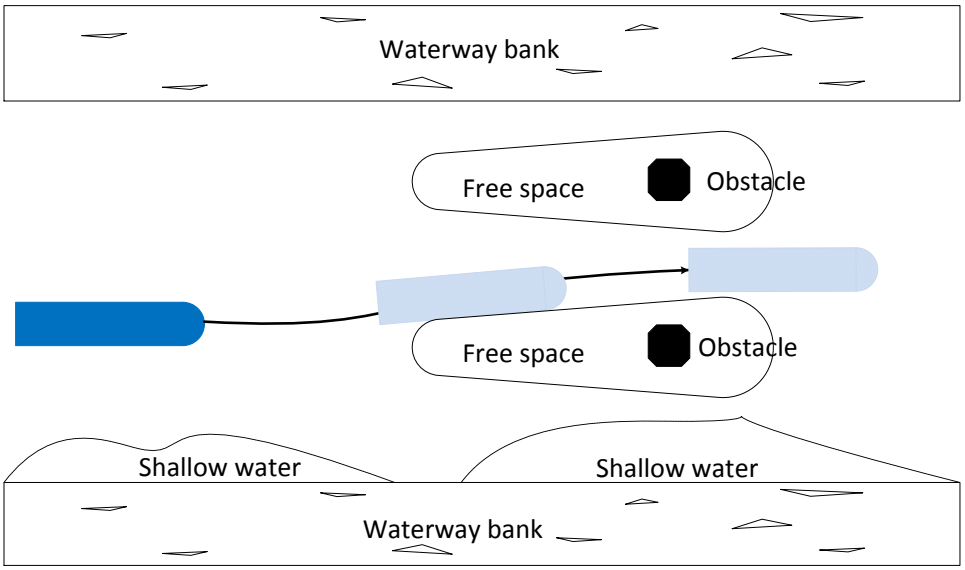

Figure 5-7 Illustration of obstacle avoidance behavior for obstacles

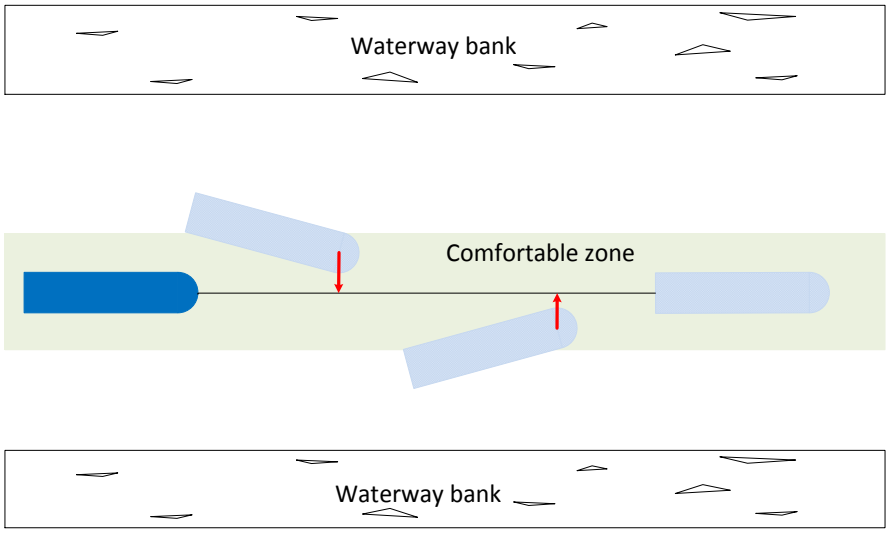

Figure 5-8 Illustration of path following behavior

According to the AIS data analysis in Figure 3-7, larger ships prefer to stay close to the centerline of the waterway, and smaller ships navigate closer to the waterway banks. Although the lateral spatial distributions show that the ship position deviations from the mean position are large, we can still find the ships' preferences of tracks in the waterway. If the deviation exceeds a certain limit, the ship officers will correct the ship positions. As is shown in Figure 5-8, when a ship goes to the other side of the waterway, or it goes too close to the waterway banks, the ship will return to its "comfortable zone".

5.5.6 Wall following

Wall following behavior makes the ships to follow the direction of a waterway bank. The ships always keep a certain offset from the "wall" (waterway bank), no matter whether it is navigating in a straight waterway or it is navigating at an intersection (Figure 5-9).

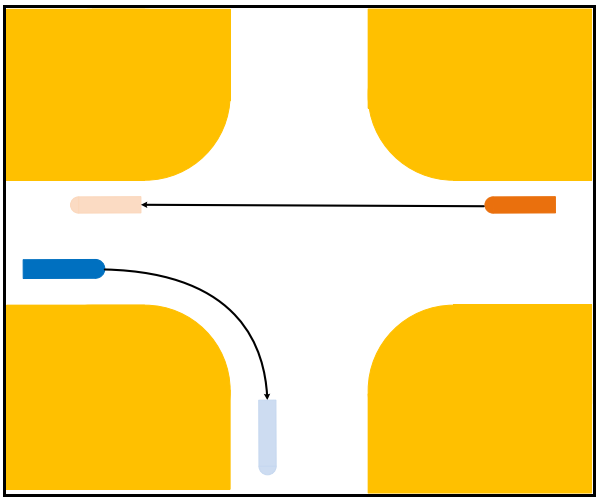

Figure 5-9 Illustration of wall following behavior

5.5.7 Flow field following

Flow field following behavior represents the influence of local currents or wind. For instance, rather than actively steering of the ship, a ship can be passively steered by the current flow. The current field is simulated at several points in the coordinate system. Then the algorithm constantly checks the relative position with respect to the points that represent the currents in the neighborhood of the ship, and the current values (current velocity and current direction) at the location of ships are derived (Figure 5-10). The speed over ground of a ship is calculated by ship speed and local current speed. The effects of wind can be represented in a similar way. Moreover, the flow field following behavior dominates the movement of a ship when malfunctions happen to the ship (e.g. simulating engine failure).

5.5.8 Unaligned collision avoidance

Unaligned collision avoidance behavior tries to prevent two or more ships from moving in arbitrary directions with arbitrary velocities. It involves predicting the future positions of all the ships. If the "free space" is invaded, actions should be taken to avoid collision. The actions should conform to regulations like COLREGs and common practices.

In order to conform to the regulations, a ship should be able to ascertain the relative bearing of other ships and distance to other ships (Figure 5-11). The built in criteria in the algorithm should constantly check the responsibilities between ships by bearings and distances. The ships take actions according to the responsibilities described in the regulations.

Figure 5-12 shows an example of unaligned collision avoidance behavior. The future positions of "ship A" and "ship B" are very close if the speeds of both ships are maintained. Actions must be taken to avoid a collision. Then "the ship A" finds that it is responsible to give way, and "ship B" is recognized as the stand-on vessel. So, "ship A" takes actions to "give way" before it goes to the "future position". Meanwhile, the "ship B" should maintain its course and speed to "stand on".

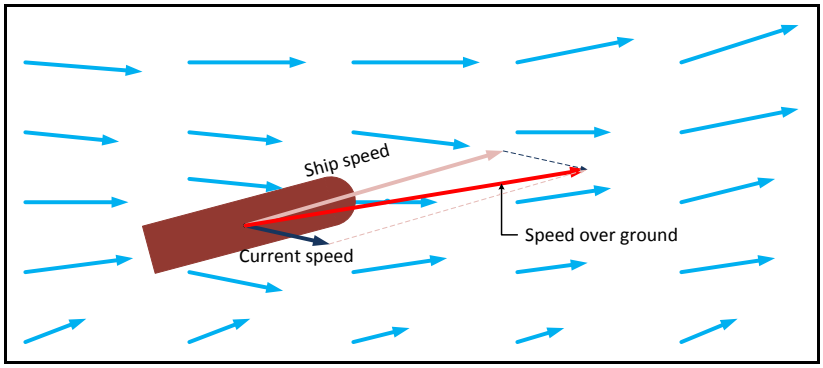

Figure 5-10 Illustration of flow field following behavior (The blue arrow stands for current direction and velocity)

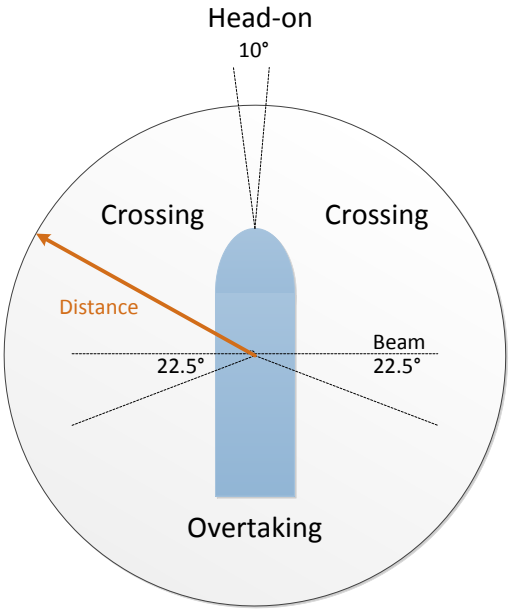

Figure 5-11 Encounter types according to COLREGs (Based on (Goerlandt et al., 2011))

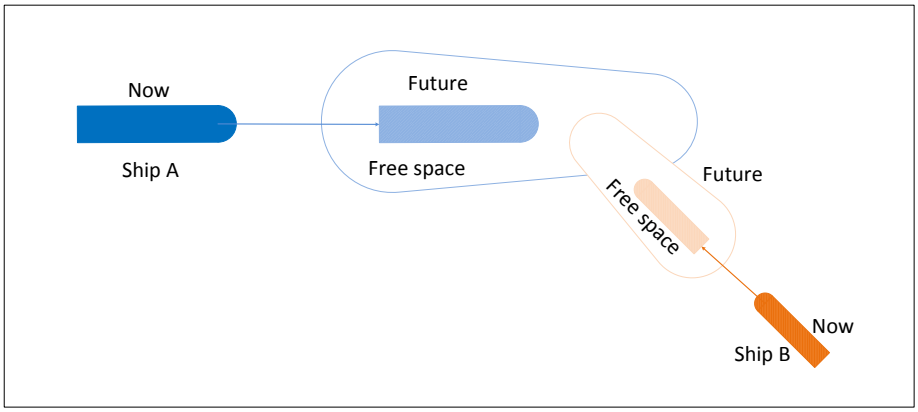

Figure 5-12 Illustration of unaligned collision avoidance behavior

5.5.9 Leader following

Leader following behavior describes the ships' tendency to maintain the same speed as the leader. Meanwhile, it keeps a relative fixed position to the leader. When the leader changes speed and course, the followers also change the speeds and courses to maintain the relative position. Moreover, the followers need to avoid collision with each other.

Leader following behavior is very relevant to represent the escorting behavior of tugs (Figure 5-13). The ship with constrained maneuverability can be treated as the leader. The tugs around the leader maintain the same speed and course to the ship with constrained maneuverability. The relative position can be shifted a little bit when a tug is attached to the ship.

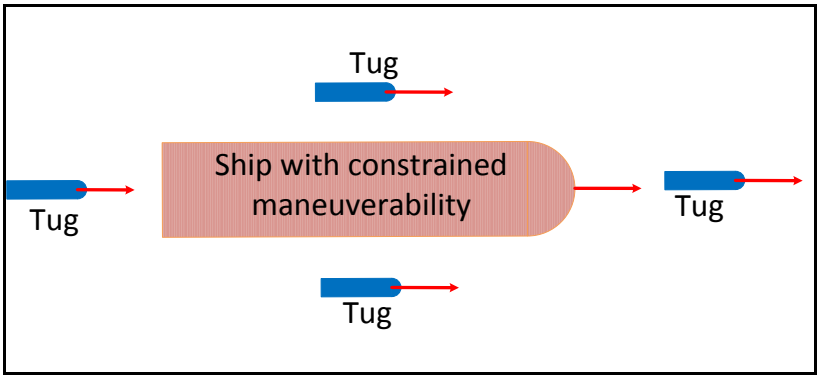

Figure 5-13 Illustration of leader following behavior

5.6 Conclusion

This chapter demonstrates that an agent-based model is a realistic modeling option. The Netlogo platform has been chosen for the multi-agent system. However, setting the model up is not a simple task. It requires a systematic description of relevant elements in the simulation. The ODD protocol supports this effort effectively.

6. SUBMODELS IN A MULTI-AGENT SIMULATION

6.1 Introduction

This chapter describes the submodels in the ANTS model. For each submodel, the following details (if applicable) are described: the mathematical equations; the conditions for invoking the equations; and the statistical analyses that are used to create the models. The submodels are aiming to reproduce each part of the real world processes, including collision avoidance and physical movements that are similar to Figure 5-2. For collision avoidance, this thesis includes normal situation and situation with head-on encounter and overtaking encounter. In normal situation, the ships are not disturbed by the other ships. Therefore the lateral positions will not deviate from the original lateral positions during the passages. For head-on encounter, the ships will deviate a little bit from the original lateral position to respond to the situation. For overtaking encounter, the overtaking ship deviates to the port to avoid collisions, while the overtaken ship may deviate to the starboard to guarantee the safe passage of the overtaken ship. For each encounter involving two ships, the processes include original positions of the two ships, positions at the closest point of approach, positions after encounter (which is not necessarily resuming to the original position). The behavior at each step is based on the judgment of OOW (Officer on Watch). In the data analysis described in this chapter, the different processes are based on distances. The details of the processes during encounters can be found in Figure 6-5 and Figure 6-9.

There are two different types of submodels. One is the artificial force field model that defines the navigational strategy for the ship movement in different stages of encounters. In Chapter 5, we introduced the artificial force field theory and its use in Artificial Intelligence (AI) field. In this chapter, we adopt the concept of artificial force field and implement it into ship encounters. This model has an indirect impact on ship movement. That is to say, the artificial forces determine the rudder angles that subsequently determine the movement of ships including change in ship heading and lateral position. The data analysis provides encounters and individual ship tracks that are used for the development of an artificial force field model. The second type of submodel directly determines physical movements of the

ships; the Nomoto model determines the ship's turning and movement with certain speed. The ship speed change model determines accelerations in different sections of the waterway. Finally, the remaining models determine the effects of wind and currents in different situations.

6.2 Artificial force field model

6.2.1 Artificial force field theory

The multi-agent simulation provides a platform for the interactions among ships and the environment. The artificial force field represents the modeling of the decision making process and collision avoidance behavior based on different situations in encounters. Different artificial forces are needed to implement the steering behavior of individual ships. In this section, the obstacle avoidance model in the AI field is introduced, which is adopted for the nautical traffic simulation.

This section introduces the development of three artificial forces for encountering situations: head-on force, overtaking force, and force from the waterway bank. The parameters are identified and the equations are developed for artificial forces. The dynamic movements of the other ships are treated as a potential threat of the safety. After perception of the dynamic threat from the other ships by the ship officer, the artificial force mimics the decision making for collision avoidance. The decision making is based on a combination of factors that include regulations, common practice, and dynamic local navigational circumstances around the ship.

6.2.1.1 Methods for obstacle avoidance

Ribeiro (2005) introduced three methods for obstacle avoidance, the bug algorithm, potential field, and the vector field histogram for robots. The robots are able to avoid collision and achieve a goal when they are provided with the knowledge of the surrounding environment. Moreover, the robots are able to partially detect the surroundings and couple this to the prior knowledge of environment to update the situation and make evasive decisions.

- The bug algorithms

  In the model, the robot follows a direct route towards a goal until an obstacle is sensed, in which case the robot goes around the obstacle to achieve the goal (Figure 6-1). It is supposed that a robot is moving from point s to point g, and it has a sensor to detect the obstacles. The robot will follow a direct path from point s to point g if no obstacle ahead. However, O1 and O2 are in the way of the direct path, and the robot sensed O1 at H1, it goes around O1 towards L1 to resume the direct path. In the same way, the robot goes

around all the objects till the goal is reached. This is a very simple way for simulating collision avoidances, and the objects are fixed and sensible for the robot.

- Potential field methods

The robot is considered as a charged particle which is navigating around charged obstacles, and the obstacles therefore exert a certain force on the robot in a force field. Obstacles are either static or moving, so that the robot in the force field has to constantly observe the obstacle and senses the forces to avoid collision. The potential field can be seen as a force gradient at specific points.

If a robot is treated as a positively charged particle, the obstacles to be avoided are also positively charged, and then the robot has the potential to avoid collision under the repulsive forces from the obstacles. Let q represent the positively charged robot, the repulsive force gets larger when the robot approaches the obstacle, and the force is zero when the robot is far away from the obstacle. Then the repulsive potential is written as:

$$U_{rep_i}(q) = \begin{cases} \frac{1}{2} k_{obst_i} \left(\frac{1}{d_{obst_i}(q)} - \frac{1}{d_0}\right)^2, & \text{if } d_{obst_i}(q) < d_0 \\ 0, & \text{if } d_{obst_i}(q) \geq d_0 \end{cases} \quad (6 - 1)$$

Where $d_{obst_i}(q)$ is the minimal distance from q to the obstacle i, k_{obst_i} is a scaling constant and d_0 is the obstacle influence threshold.

- The Vector Field Histogram

The Vector Field Histogram (VFH) is a real-time obstacle avoidance method that is able to detect the obstacles in the local surroundings and simultaneously steer to the desired direction with a controlled speed. The collision avoidance behavior is implemented in 3 steps:

Step 1 generating a 2D Cartesian histogram grid map which is constituted by cells with a certain value. The value can be detected by the local sensor of the robot.

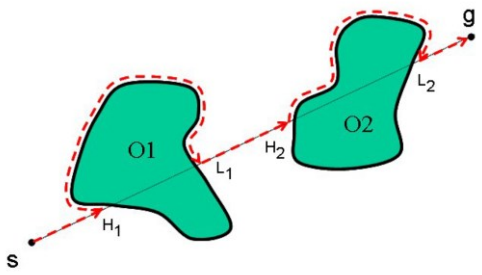

Figure 6-1 Obstacle avoidance with Bug 2 algorithm (Ribeiro, 2005)

Step 2 the robot is detecting local environment and transferring the surrounding into a histogram.

Step 3 robot is corresponding to the histogram and adapting the velocity and course according to the obstacle.

6.2.1.2 Predictive collision avoidance model

In predictive collision avoidance model (Karamouzas et al., 2009), the artificial force field is adopted to obtain collision avoidance for pedestrians. There are two different forces, one is for speed change, and the other one is for collision avoidance. The magnitude of the force for speed change is a function of velocity and relative direction, and the speed change is associated with a preferred speed of the individual pedestrian. The goal force F_g is defined as:

$$F_g = \frac{1}{\tau}(\mu_i^{pref} n_{gi} - V) \quad (6 - 2)$$

Where, $n_{gi} = \frac{g_i - x_i}{\|g_i - x_i\|}$, g_i is goal position, μ_i^{pref} is speed, τ is the time spent that a pedestrian reaches the speed μ_i^{pref}.

On the other hand, the force for collision avoidance behavior is a function of distance to the object. The repulsive force F_ω is defined as:

$$\begin{cases} F_\omega = n_\omega \frac{d_s + r_i - d_{iw}}{(d_{iw} - r)^k}, \text{if } d_{iw} - r_i < d_s \\ 0 \qquad \text{otherwise,} \end{cases} \quad (6 - 3)$$

Where the constant k indicates the steepness of the repulsive potential, n_ω is the normal vector of the wall, r_i is the radius of the disc that is assumed to be the terrain of a pedestrian, d_{iw} defines the shortest distance between the pedestrian and the wall and d_s denotes the safe distance that the pedestrian prefers to keep from the building.

What is innovative in the predictive collision avoidance model is that the magnitude of the avoidance force is defined with four intervals. The force gets smaller as the distance gets larger. However, there are thresholds d_{max} and d_{min} that defines both thresholds of an "impenetrable barrier", which regulates the two boundaries of constant part of the function for force. The force is constant within the boundaries.

The result of this model showed a smooth avoidance behavior by applying forces iteratively which are calibrated and optimized by statistical analysis. The advantages were apparent by comparing the results of the calibrated model to the Helbing's social force model (Helbing et al., 1995) and the Reciprocal Velocity Obstacle (RVO) approach (Van den Berg et al., 2008) visually and quantitatively. In visual comparison to the Helbing's model, the result of the model showed less curvature and small movement; Compared to the RVO, the model

showed a smooth flow and more energy efficient motions by less frequent speed change of simulated pedestrians, especially in crowded environment. Quantitative comparison to the aforementioned two models also showed advantages. Compared to the Helbing's model in the hallway scenario, the analysis showed that the proposed approach leads to shorter path, time-efficient motions, less interaction, and lower acceleration for the pedestrians. Compared to the RVO in the hallway scenario, the proposed approach led to less-curved paths, lower movement effort and turning effort. All the comparisons were significant by t-test with $p < 0.01$.

6.2.1.3 Discussion

The bug algorithm for collision avoidance behavior is the simplest one. The robot can avoid collision with the obstacles. However it is not a cost efficient way with the shortest route. The real ship tracks do not take this approach for collision avoidance. But it gives a clue on "Wall following" behavior introduced in Section 5.5.6.

The vector field histogram method is not an ideal example of the force field concept. One comment is that the extent of turning in obstacle avoidance needs to be defined in another way. The other remark is that constantly sensing the local histograms costs large computational capacity for a computer. The simulation process can be slow if the number of robots gets large, or if the cells for the world in which the robot can move are too many.

Potential field methods and predictive collision avoidance models have the same characteristics, involving an artificial force that is related to the distance between robot (pedestrian) and obstacles. The extent of turning is based on the artificial forces. These models are the preferred method for the ship traffic models. However, the functions need to be derived based on AIS data analysis, regulations, and common practices.

One thing to notice for the force field is that the force field in the literature is purely based on assumptions. It is assumed that the robots or pedestrians are able to avoid collision with each other. However, for nautical traffic simulation, the collision avoidance behavior should conform to regulations and common practices. Therefore, in order to reflect the common practices, AIS ship tracks should be analyzed to derive the parameters in the force field for realistic ship movements.

6.2.2 Relevant regulations in COLREGs for encountering situations

Relevant regulations in COLREGs (International Regulations for Preventing Collisions at Sea) are provided and interpreted to understand ship behavior in the waterway. For collision avoidance, regulations determine the strategy for ship collision avoidances. However, this thesis only addresses the important regulations that relevant for the specific straight channel, rather than all the regulations in the COLREGs. Interpreting regulations helps to build the artificial force in the simulation that reflects the behavior required by the

regulations. The common practices that are not specifically provided by regulations are also reflected in the artificial forces. These common practices are reflected in several ways. First of all, ships should sail with a reasonable distance to the bank that neither endangers the ship to groundings nor endangers the ship to collisions with other ships. Secondly, ships should keep a reasonable distance from the other ships. Thirdly, ships should navigate at a safe speed. A safe speed is defined in the COLREGs as "every vessel shall at all times proceed at a safe speed so that she can take proper and effective action to avoid collision and be stopped within a distance appropriate to the prevailing circumstances and conditions." The safe speed is determined by vessel conditions and navigational circumstances. There is no specific speed provided, so the common practice of safe speed and distances to channel banks should be obtained from AIS data analysis. The interpretations of the regulations are the following:

- "Every vessel shall at all times maintain a proper look-out by sight and hearing as well as by all available means appropriate in the prevailing circumstances and conditions so as to make a full appraisal of the situation and or the risk of collision." (Article 5 in COLREGs)
  Interpretation: In the simulation, ships are able to observe each other within the capability limit of radar or other forms of look-out, as what is happening in reality. However, extreme weather conditions, human error, mechanical failure, or intervention of another ship may result in accidents.

- "(a) Any action taken to avoid collision shall be taken in accordance with the Rules of this Part and shall, if the circumstances of the case admit, be positive, made in ample time and with due regard to the observance of good seamanship. (b) Any alteration of course and/or speed to avoid collision shall, if the circumstances of the case admit, be large enough to be readily apparent to another vessel observing visually or by radar; a succession of small alterations of course and/or speed should be avoided." (Article 8 in COLREGs)
  Interpretation: The action taken should be positive means that the action should be active and effective so that the collision can be avoided even without cooperation from the other ship. Small changes of ship course or speed should be avoided, because these small changes might not be observed by the other ship. Made in ample time means the actions taken should be at a proper distance, neither too late nor too early. However, the actions should be restricted in the confined waterways.

- "A vessel proceeding along the course of a narrow channel or fairway shall keep as near to the outer limit of the channel or fairway which lies on her starboard side as is safe and practicable." (Article 9 in COLREGs)

Interpretation: Ships in the simulation must keep at the starboard side. However, from observations of overtaking situations, the overtaking ship may navigate to the port side to avoid collisions. This normal practice should be reflected in the simulation.

- "Any subsequent alteration of bearing between the two vessels shall not make the overtaking vessel a crossing vessel within the meaning of these rules or relieve her of the duty of keeping clear of the overtaken vessel until she is finally past and clear." (Article 13 in COLREGs)
  Interpretation: "Keeping clear of" should be implemented in the simulation. The regulation does not define the exact distance for " Keeping clear of" in overtaking. However, the AIS data analysis manifests common practices in this situation. So, we can analyze the AIS ship tracks and make use of artificial forces to implement the overtaking behavior.

- "When two power-driven vessels are meeting on reciprocal or nearly reciprocal courses so as to involve risk of collision each shall alter her course to starboard so as to each shall pass on the port side of the other." (Article 14 in COLREGs)
  Interpretation: Similar to actions for overtaking, this should be observed from the AIS ship tracks for the following: the extent of course altering, the extent of lateral position shift, and the distances between the two ships for the evasive behavior to begin.

6.2.3 Different artificial forces and their functions

In the multi-agent simulation, after ship agents are generated at the boundaries of the environment, the artificial forces apply to the ships. The function of the artificial force is to determine the tendency to shift the own-ship to starboard or port for certain lateral distances for safe passage. The potential of interactions among ships takes effect when critical distances between the ships are reached. The artificial forces apply throughout different stages of encounters.

In order to implement regulations in the simulation, we have to distinguish different forces based on different situations (Figure 6-2). The artificial forces are represented by vectors. There are three types of forces, which apply in a similar way. The first force comes from the channel bank ($\mathrm{F}_{\mathrm{bank}}$). This force works on the ship to balance the force from the other ship in a head-on situation or an overtaking situation. The second force comes from another ship within a head-on situation ($\mathrm{F}_{\mathrm{head-on}}$). This force makes the ship shift to starboard as required in Article 14 in COLREGs. The last force comes from another ship within an overtaking situation. This force makes the overtaking ship shift to port ($\mathrm{F}_{\mathrm{overtaking}}$), and at the same time makes the overtaken ship shift to starboard to cooperate ($\mathrm{F}_{\mathrm{overtaken}}$), as

normally observed in the AIS ship tracks. Overtaking on the starboard side could happen, but in reality this rarely occurs in the studied area. After the two ships are clear of each other, the force will be dismissed. These forces are developed to model ship collision avoidances realistically.

Based on the pedestrian model (Karamouzas et al., 2009), the assumption of the repulsive force is defined as:

$$\boldsymbol{F} = \begin{cases} \frac{\mathbf{k_{obst}}}{\mathbf{R^n}}, & \mathbf{if\ R < R_s} \\ \mathbf{0}, & \mathbf{otherwise} \end{cases} \quad (6 - 4)$$

F represents the force. The constant n indicates the steepness of the repulsive potential. $\mathrm{k_{obst}}$ is a scaling constant which could be a function of ship type, size, and speed. This function will be determined by statistical analysis of the AIS ship tracks. R defines the shortest distance between the ship and channel bank. $\mathrm{R_s}$ denotes the threshold for the forces. The forces for distances larger than $\mathrm{R_s}$ will be considered zero. If there are multiple ships around within a short distance, only one force will be applied based on distances. That is reasonable because the ships solve the encountering situation one by one in the restricted waters.

In this simulation, we use navigational waterway boundaries indicated by navigational aids instead of channel banks (although in the text we refer to channel banks). One reason is that the irregular shape of the channel banks will affect the measurement of distances for forces from the channel bank. Another reason is that the ships are actually following the guide of navigational aids although the purpose is avoiding grounding to the channel banks.

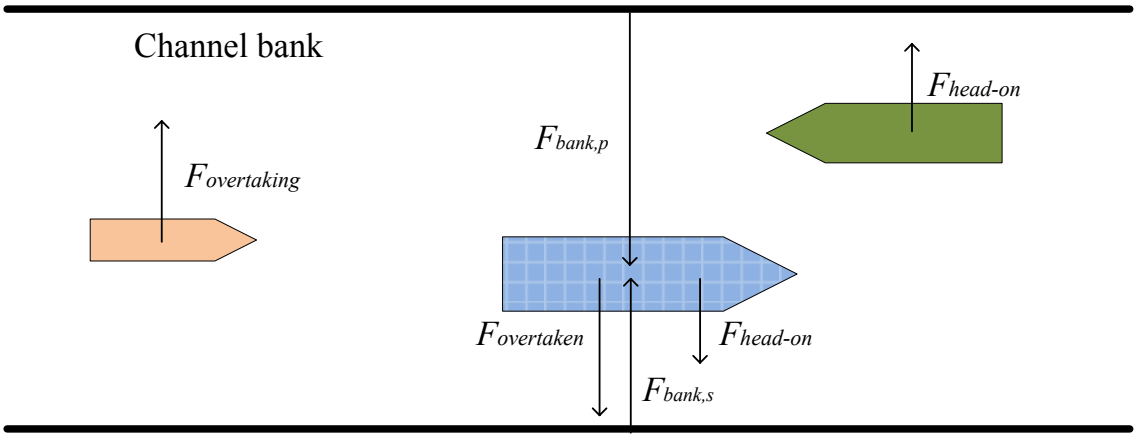

Figure 6-2 Forces in the simulation model

6.2.4 Assumptions for the shape of the artificial force field

The first priority is to analyze the ship behavior and make assumptions for the forces. The assumptions made should be consistent with real practices in ship navigation. Therefore, questions are raised for applicable assumptions for the forces. Based on the questions, at least four choices are made that are applicable for the artificial forces, and there is evidence provided in the following analysis to make the best choice. As the first step, ship encounters are selected from the AIS ship tracks. The parameters in the encounters are measured and recorded. The second step is determining the parameters in the equations for the artificial forces. Then this thesis makes use of the correlation coefficient between variables to find the critical factors which actually affect the artificial forces. We also statistically analyzed the distances from the AIS ship tracks when "positive" and "obvious" actions are taken on board. Consequently, the shape of the force field is finalized.

6.2.4.1 Assumptions for the force field from channel banks

There are at least four choices for the shape of the force field from channel banks, see Figure 6-3. This subsection answers the three following questions that determine which kind of force field is more applicable in the channel.

a. Do the ships always seek the safest point where the threats from the channel banks are the lowest? If so, the force field should be continuous as shown in Figure 6-3 (a). Otherwise, there should be a "vacant area" in the force field, in which no threat is perceived by Officers on Watch from the channel banks, as is shown in Figure 6-3 (b).
b. What are the factors that contribute to the parameters in the equations? Do the threats increase with distances to the channel banks, LOA, Gross Tonnage, or speed?
c. How does the perceived threat increase as the ship gets closer to the channel bank? Figure 6-3 (b), (c) and (d) show the different sensitiveness of the threat to the distance between the ship and waterway bank. This is relevant for the exponent n in Equation (6 - 4).

According to observations of the AIS ship tracks (42 cases of head-on encounters altogether), there should be a place of "vacant area" in the force field. Also, it is hypothesized that when a ship is navigating in the "vacant area", the forces from the channel banks are the lowest. Firstly, it is observed that the ship positions shift to starboard or port throughout the encounters. Differences are observed by comparing the lateral positions at the beginning of the encounters and at the end of the encounters, when no other ships affect the choices of the lateral positions in the situations. Secondly, the spatial distributions of ship positions which were introduced in Chapter 3 suggest that the ships pass the crossing-line with normally distributed positions rather than looking for a single optimum position. In this sense, the assumption in Figure 6-3 (a) is not considered applicable. Therefore which one should be chosen from the other options in Figure 6-3 depends on the way the force

changes with the distance. The type of force field will be finalized after the factors for the forces are found.

6.2.4.2 Shape of the force field from other ships

There are also four choices for the shape of the force field from the other ships, see Figure 6-4. This subsection answers the following three questions that determine which kind of force field is more applicable in the channel:

a. What is the area covered by the force field from the other ships? Is that similar to the ship domain or the collision diameter that is mentioned in Chapter 2, with predetermined size of the force field? If so, the force field of the other ships should be similar to Figure 6-4 (a). Otherwise, the size of the force field will be flexible.
b. What are the factors that contribute to the forces? Does the threat increase with distances to channel banks, LOA, Gross Tonnage, or speed?
c. How does the perceived threat increase as the ships get closer? The Figure 6-4 (b), (c) and (d) shows different sensitiveness of the threat to the distance between ships.

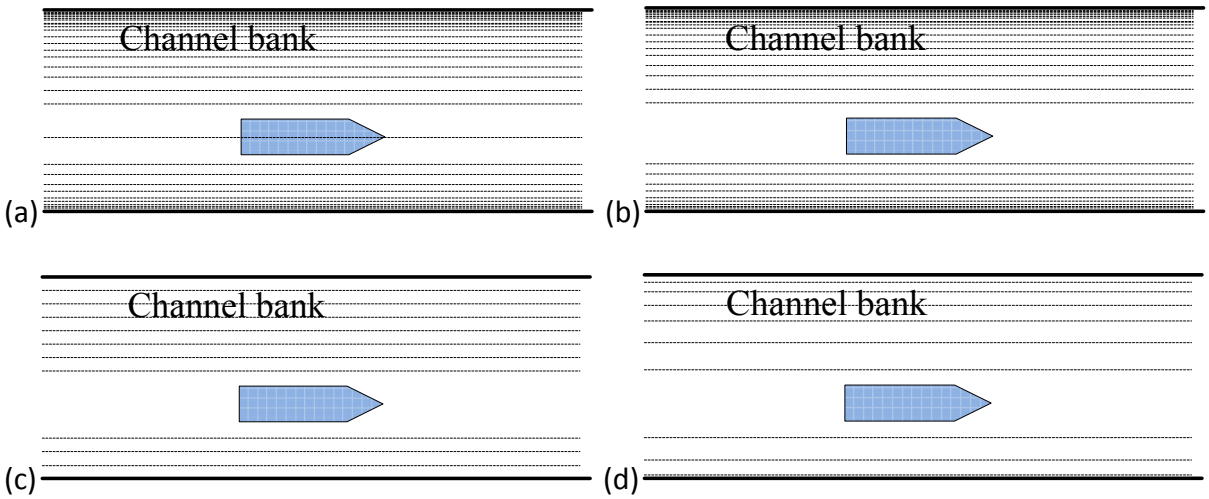

Figure 6-3 Different types of force fields assumed for shape of force field from channel banks

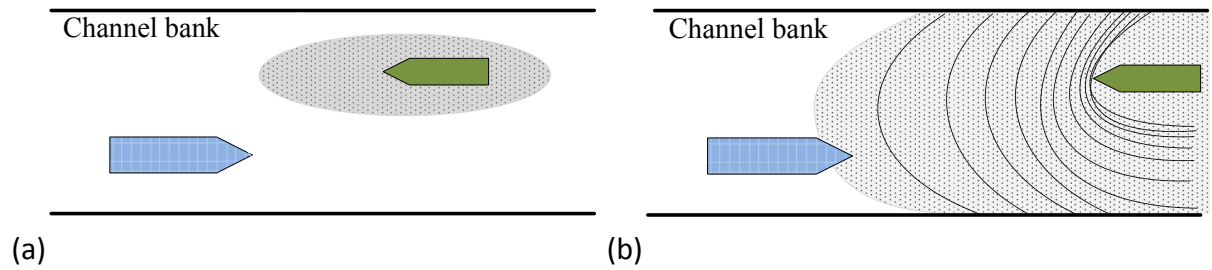

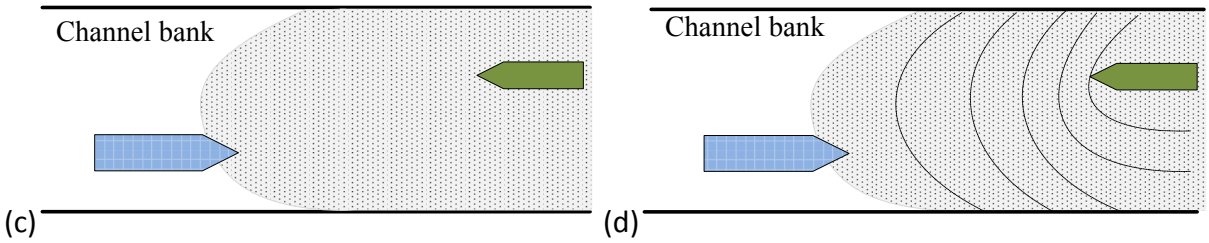

Figure 6-4 Different types of force fields assumed for shape of force field from other ships

According to observations of the AIS ship tracks, it is not possible to define the shape of the force field, because the ships take actions from a large distance in a head-on encounter. Then, the option in Figure 6-4 (a) is not applicable. According to the regulations "Actions taken to avoid collision should be: positive; obvious; made in good time", and therefore the magnitude of the force should be determined at the time when a ship starts to deviate from its course. Also the ships keep steady at the Closest Point of Approach (CPA), and forces are balanced at the same time. Further, small changes in ship position in an encounter are not good seamanship behavior. So the force will not change with the distances between the ships. Therefore we can assume that the force does not depend on the distance between the ships. Then the options in Figure 6-4 (b) and (d) are considered not applicable and option (c) remains. However, what factors do contribute to the forces will be identified in Section 6.2.5.

6.2.5 Parameters in the artificial forces based on statistical analysis

6.2.5.1 Statistical method for finding reasonable parameters

The procedure to determine $\mathrm{k_{obst}}$ and exponent (n) in Equation (6 - 4) is more complicated, and this will be described in the following section. Correlation coefficient analysis is used to identify the factors that contribute to the magnitude of the force and the force changes. Subsequently, the results of the correlation coefficients are interpreted to determine $\mathrm{k_{obst}}$ and exponent (n). The formula to calculate the correlation coefficient between two variables is as follows:

$$r = \frac{\sum_{i=1}^{n}(x_i-\bar{x})(y_i-\bar{y})}{\sqrt{\sum_{i=1}^{n}(x_i-\bar{x})^2}\sqrt{\sum_{i=1}^{n}(y_i-\bar{y})^2}} \qquad (6 - 5)$$

where, $\bar{x}$ and $\bar{y}$ are the sample means. n is sample size, and r is a value between -1 and 1. A r value closer to zero means a weaker correlation between the two variables.

There are several factors that may contribute to Equation (6 - 4). There is a list of samples observed in the AIS ship tracks for each factor, while the sample size for each factor depends on the number of ship encounters that we studied. 72 ship passages in head-on encounters and 13 overtaking encounters are used in the analysis, so the sample size for each parameter is 72 and 13 respectively. The sample size of overtaking encounters is small, because it is more difficult to find perfect overtaking encounters in the area. It takes a long time for one

ship to overtake another. So in most of the cases, only half of the overtaking process happened in the studied area. Therefore, the AIS information for overtaking encounters always catches a proportion of the overtaking process, either the beginning or the end. The analysis was done with the proportion of ship tracks in which the Closest Point of Approach lies in the studied area.

Correlation coefficient results for different pairs of factors are calculated and shown in a matrix, using the Matlab® function "correoef()".We use a matrix of correlation coefficients analysis to select the parameters for Equation (6 - 4). This matrix is used so that each pair of factors is calculated with Equation (6 - 5) at least once. The factors in the first row and first column in the matrix are the factors that can be observed from the AIS ship tracks. The matrix of the results is presented in two different ways, a matrix with valued cells and a matrix with colored cells (Appendix VI). The colored cells are transformed from the valued cells and this makes the analysis easier. The red and blue cells stand for strong correlations between two variables in the matrix. The lighter colors in the middle of the "color map" denote low correlations.

6.2.5.2 Parameter identification for force from channel bank

The AIS ship tracks are plotted using Autodesk® AutoCAD® Civil 3D® software, and different distances are measured in the plot for a further matrix of correlation coefficient analysis. Figure 6-5 illustrates the distances that are measured in head-on encounters. The factors that are selected in the correlation coefficient analysis are listed in Table 6-1, in which introductions and abbreviations for each factor are provided. "Dh" is the distance between the two ships when a ship starts to take action. The behavior is observed by checking if there is an obvious change in heading from observing the AIS ship tracks. Distances to either side of the waterway are recorded to know the lateral position shift of a ship to manifest the extent of influence by the other ship that she encounters. The distances are measured in three phases of an encountering situation: at the beginning of an encounter, at the Closest Point of Approach (during an encounter), and after an encounter. The numbers "1", "2", and "3" in different factors indicate the three phases in the encounters. There are different forms of non-dimensional ship positions that are included in the analysis, which are "RO", "P (Position)", and "Δ(1/Dr)". This helps to identify the way that the artificial force changes with distances, and whether the ships take both distances from the port side and the starboard side into account for collision avoidances.

Table 6-1 Factors in the matrix of correlation coefficient analysis in head-on encounters

Parameters	Introductions
Dh	Distance to the other ship when the own-ship starts to take action
Dl1	Distance to the port boundary of the channel when the own-ship starts to take action
Dl2	Distance to the port boundary of the channel at the closest point of approach
Dl3	Distance to the port boundary of the channel after the encounter
Dr1	Distance to the starboard boundary of the channel when the own-ship starts to take action
Dr2	Distance to the starboard boundary of the channel at the closest point of approach
Dr3	Distance to the starboard boundary of the channel after the encounter
RO1	Ratio for distances (Dl1/Dr1)
RO2	Ratio for distances (Dl2/Dr2)
RO3	Ratio for distances (Dl3/Dr3)
V1	Ship speed when the own-ship starts to take action
V2	Ship speed at the closest point of approach
V3	Ship speed after the encounter
GT	Gross tonnage of the own-ship
GT_O	Gross tonnage of the other ship in the encounter
LOA	LOA (Length Overall) of the own-ship
LOA_O	LOA (Length Overall) of the other ship in the encounter
ΔRO1	Difference for the ratios (RO2 - RO1)
ΔRO2	Difference for the ratios (RO3 - RO2)
P1	Non-dimensional ship position when the own-ship start to take action (Dr1/(Dl1 + Dr1))
P2	Non-dimensional ship position at the closest point of approach (Dr2/(Dl2 + Dr2))
P3	Non-dimensional ship position after the closest point of approach (Dr3/(Dl3 + Dr4))
Δ(1/Dr1)	Another form of position change (1/Dr2 - 1/Dr1)
Δ(1/Dr2)	Another form of position change (1/Dr3 - 1/Dr2)

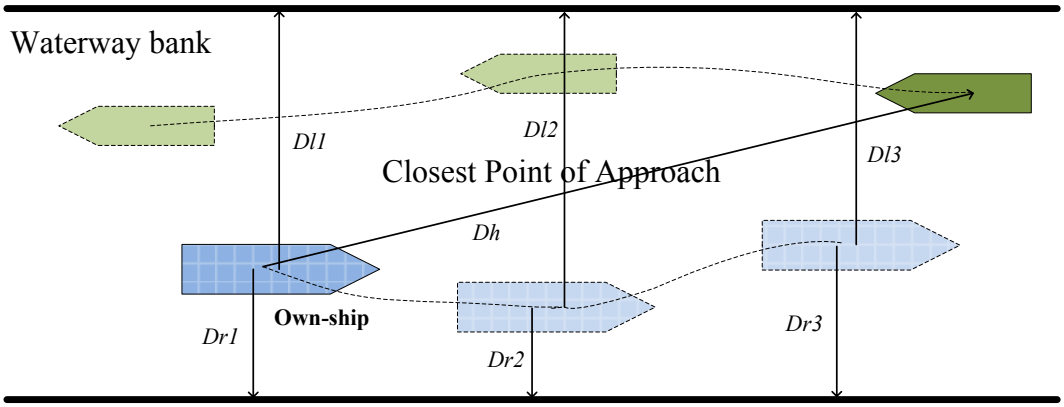

Figure 6-5 Illustration for distances in the correlation coefficient analysis in a head-on encounter

After the encounter analysis and measurement, the matrixes are shown in Appendix VI, Figure VI-1 and Table VI-1. After looking at the matrix, at least the following results can be found. The relevant item numbers are indicated with an ellipse in Figure VI-1 as well.

a. The speeds (V1, V2, V3) do not show a strong correlation with any other factors.
b. LOA shows a stronger correlation with other factors than Gross Tonnage.
c. LOA shows a strong correlation with some of the distances to the channel banks. Strong correlations are found between LOA and the distances to the starboard boundary of the channel (0.45, 0.49, and 0.37 respectively). Also the LOA is not significantly correlated with position changes.
d. "Δ(1/Dr1)" is correlated with "Dr1" (-0.66). The correlation between "Δ(1/Dr1)" and "Δ(1/Dr2)" is very weak (0.08). The correlation between "Δ(1/Dr2)" and "Dr1" is relatively weak (-0.2).
e. The correlation between "Dr2" and "Dr3" (0.75) is stronger than "Dr1" and "Dr2" (0.57). Also, the correlation between "Dr1" and "Dr3" is the weakest (0.37).

The correlation coefficient results need interpretation to find the causational relationship between the factors. The following points about the factors for parameters of artificial forces can be made as interpretation of the results:

a. The ship speed is not related to the force, because speed appears to have a weak correlation with any other factors. However, the Gross Tonnage and LOA have much larger values of correlation coefficient. It is reasonable that the ship size affects the collision avoidance behavior in restricted waters.
b. LOA is a stronger indicator than Gross Tonnage. Therefore, LOA can be used as a parameter in force formulas instead of Gross Tonnage.
c. LOA affects ship positions, because a larger LOA results in larger distances to the channel bank, as the correlation between LOA and distances to the starboard boundary of the channel (Dr1, Dr2, and Dr3) is positive. We can anticipate a larger force for a larger ship. Moreover, LOA is not directly correlated with lateral position changes (change of forces), because there may be several other factors that contribute to the lateral position changes.
d. The strong correlation between "Δ(1/Dr1)" and "Dr1" manifests that ships in the middle of the channel are subject to a larger lateral position shift during an encounter, while a ship with a very close position to the starboard boundary of the channel is subject to a smaller position change. The weak correlation between "Δ(1/Dr1)" and "Δ(1/Dr2)" implies that ships do not necessarily resume their original lateral positions after encounters. This further confirms that the position change in the "vacant area" does not experience much force from the channel banks, because the lateral positions are not the same comparing before and after encountering. If the "vacant area" does not exist, the force before the encounters and the force after the encounters will be the same.
e. The correlations for different forms of "distance to the starboard boundary of the channel (Dr1, Dr2, and Dr3)" show further evidence of inconsistency of the positions. Also it further confirms the "vacant area" assumption for the force field.

Based on this analysis, we can confirm that there should be a “vacant area” in the force field, and it can be assumed that “Dr3” could be the threshold of the force from the channel bank. The assumption for Officer on Watch is that the force from the bank is bearable when the ship position is in the “vacant area”. As “Dr1” is normally larger than “Dr3” from data observation, the ship with “Dr1” is in the “vacant area” if we treat “Dr3” as the threshold. So the ships do not need to shift further to the port side to avoid threat of grounding at the threshold after encounters. Based on data observations, the ships normally do shift a little bit away from the starboard side of the channel bank after passing the Closest Point of Approach. This shows that the force from the channel bank exists. Subsequently, the LOA should be included in Equation (6 - 4), as different LOAs affect the positions of the ships. Therefore, the formula for the force from the channel bank is derived as:

$$\mathrm{F_{bank}(R)} = \mu * \frac{\mathrm{LOA}}{\mathrm{R^n}} \qquad (6 - 6)$$

where μ is a constant and R is the distance to the starboard boundary of the channel.

6.2.5.3 Determining constants in the formula

This subsection studies the constants in the equations. The force difference with or without the influence from the other ship can be observed by the position changes during encounters and after encounters. So, based on Equation (6 - 6), the change in force from the channel bank (caused by force from the other ship) is:

$$\Delta \mathrm{F}_{bank} = \mathrm{F}_{bank}(\mathrm{R_3}) - \mathrm{F_{bank}(R_2)} = \mu * \mathrm{LOA} * (\frac{1}{\mathrm{R_3^n}} - \frac{1}{\mathrm{R_2^n}}) \qquad (6 - 7)$$

In which $\mathrm{R_2}$ is the distance to the starboard boundary of the channel at CPA (Dr2 in Figure 6-5), $\mathrm{R_3}$ is the distance to the starboard boundary of the channel after encounters (Dr3 in Figure 6-5), μ and n are the constants. For determining the constants, this study further examines the correlations between the selected factors and the distance derivatives that are $\left(\frac{1}{\mathrm{R_2^n}} - \frac{1}{\mathrm{R_1^n}}\right)$ and $\left(\frac{1}{\mathrm{R_3^n}} - \frac{1}{\mathrm{R_2^n}}\right)$, in which n = 0.5, n = 1, n = 2, n = 3, n = 4, and n = 7 are shown in the matrixes to show the differences. n = 0.5, n = 1, n = 2, n = 3, n = 4, and n = 7 are selected values that are involved in a number of experiments of the analysis. Other than 0.5, integer numbers are selected because this makes the model simpler. Table 6-2 lists these different distance derivatives. Other factors that are included in the matrix calculation are LOA, LOA of the other ships, Gross Tonnage, and Gross Tonnage of the other ships.

The matrixes are shown in Figure VI-2 and Table VI-2. After looking at the matrix, the following results can be found. Based on the matrix of correlation coefficient analysis, n = 3 is the most appropriate value for the formula. When n = 3, the correlation between LOA and the distance derivative “DD2_3” is 0.27. The correlation does not increase much when n gets even larger (indicated with an ellipse in Figure VI-2). Therefore, n = 3 is the most proper

number for Equation (6 - 6). Further, this means that the assumed shape of the force field should be type (b) in Figure 6-3. Then, Equation (6 - 6) turns out to be:

$$F_{bank}(R) = \mu * \frac{LOA}{R^3} \quad (6 - 8)$$

It is observed from Figure VI-2 that LOA appears to have a stronger correlation with the different derivatives of "DD2" $\left(\frac{1}{R_3^n} - \frac{1}{R_2^n}\right)$ than with different derivatives of "DD1" $\left(\frac{1}{R_2^n} - \frac{1}{R_1^n}\right)$. Also, the different derivatives of "DD2" $\left(\frac{1}{R_3^n} - \frac{1}{R_2^n}\right)$ show stronger correlations with themselves than "DD1" $\left(\frac{1}{R_2^n} - \frac{1}{R_1^n}\right)$. This further proves that it is better to assume R_3 as the threshold of force from the channel bank, because the lateral position shifts from R_2 to R_3 indicate more about the force change to get rid of the effects of the "vacant area". Therefore, the force difference from the channel bank during and after an encounter is:

$$\Delta F_{bank} = F_{bank}(R_3) - F_{bank}(R_2) = \mu * LOA * \left(\frac{1}{R_3^3} - \frac{1}{R_2^3}\right) \quad (6 - 9)$$

The force difference is ultimately reflected by a lateral position shift. So, after regression analysis between the position change $(R_2 - R_3)$ and ΔF_{bank} (Figure 6-6), we can derive the constant μ = 168260. Then the residuals between the forces and the position change can be approximated by the normal distribution (Figure 6-7).

Table 6-2 Different distance derivatives as factors in matrix of the correlation coefficient analysis

Parameters	Introductions
DD1_7	Distance derivative $\left(\frac{1}{R_2^7} - \frac{1}{R_1^7}\right)$
DD1_4	Distance derivative $\left(\frac{1}{R_2^4} - \frac{1}{R_1^4}\right)$
DD1_3	Distance derivative $\left(\frac{1}{R_2^3} - \frac{1}{R_1^3}\right)$
DD1_2	Distance derivative $\left(\frac{1}{R_2^2} - \frac{1}{R_1^2}\right)$
DD1_1	Distance derivative $\left(\frac{1}{R_2} - \frac{1}{R_1}\right)$
DD1_h	Distance derivative $\left(\frac{1}{R_2^{0.5}} - \frac{1}{R_1^{0.5}}\right)$
DD2_7	Distance derivative $\left(\frac{1}{R_3^7} - \frac{1}{R_2^7}\right)$
DD2_4	Distance derivative $\left(\frac{1}{R_3^4} - \frac{1}{R_2^4}\right)$
DD2_3	Distance derivative $\left(\frac{1}{R_3^3} - \frac{1}{R_2^3}\right)$
DD2_2	Distance derivative $\left(\frac{1}{R_3^2} - \frac{1}{R_2^2}\right)$
DD2_1	Distance derivative $\left(\frac{1}{R_3^1} - \frac{1}{R_2^1}\right)$
DD2_h	Distance derivative $\left(\frac{1}{R_3^{0.5}} - \frac{1}{R_2^{0.5}}\right)$

Therefore, the real position change is determined by two factors. One is the perceived artificial force from other ships in encountering; the ship position shifts closer to the starboard channel bank to compensate for the force. The other is a random residual (the discrepancy between theory and practice for head-on force). Thus, the real lateral position shift is defined as:

$$R_2' = R_2 + \Delta R \tag{6 - 10}$$

where ΔR is a random number from normal distribution $\Delta R \sim \aleph(1.44, 7.2^2)$.

6.2.5.4 Artificial force from a ship in a head-on situation

$F_{head-on}$ comes from the other ship in a head-on situation, which should balance the force from the channel bank ΔF_{bank}, so ΔF_{bank} is used as a substitute for $F_{head-on}$. Correlation coefficient analysis is also used here to analyze the factors that contribute to $F_{head-on}$. Table 6-3 lists the factors other than those listed in the Table 6-1 for a matrix of correlation coefficient analysis. In this case, we separated the outgoing ships and incoming ships. For each head-on encounter, we treat the outgoing ship as the own-ship and the incoming ship as the other ship. The matrixes of results are shown in Figure VI-3 and Table VI-3.

Table 6-3 Factors other than those listed in Table 6-1 in a matrix of correlation coefficient analysis for the artificial force from head-on ships

Parameters	Introductions
Dl1_O	Distance to the port boundary of the channel when the other ship starts to take action
Dr1_O	Distance to the starboard boundary of the channel when the other ship starts to take action
RO1_O	Ratio for distances (Dl1/Dr1) for the other ship
V1_O	Speed of the other ship when the other ship starts to take action
Dl2_O	Distance to the port boundary of the channel at the closest point of approach for the other ship
Dr2_O	Distance to the starboard boundary of the channel at the closest point of approach for the other ship
RO2_O	Ratio for distances (Dl2/Dr2) for the other ship
V2_O	Ship speed at the closest point of approach for the other ship
Dl3_O	Distance to the port boundary of the channel after encounter for the other ship
Dr3_O	Distance to the starboard boundary of the channel after encounter for the other ship
RO3_O	Ratio for distances (Dl3/Dr3) for the other ship
V3_O	Ship speed after encounter for the other ship
dF	The force difference (ΔF_{bank}) from the channel bank during encountering and after encountering based on Equation (6 - 9) for the own-ship
dF_O	The force difference (ΔF_{bank}) from the channel bank during encountering and after encountering based on Equation (6 - 9) for the other ship

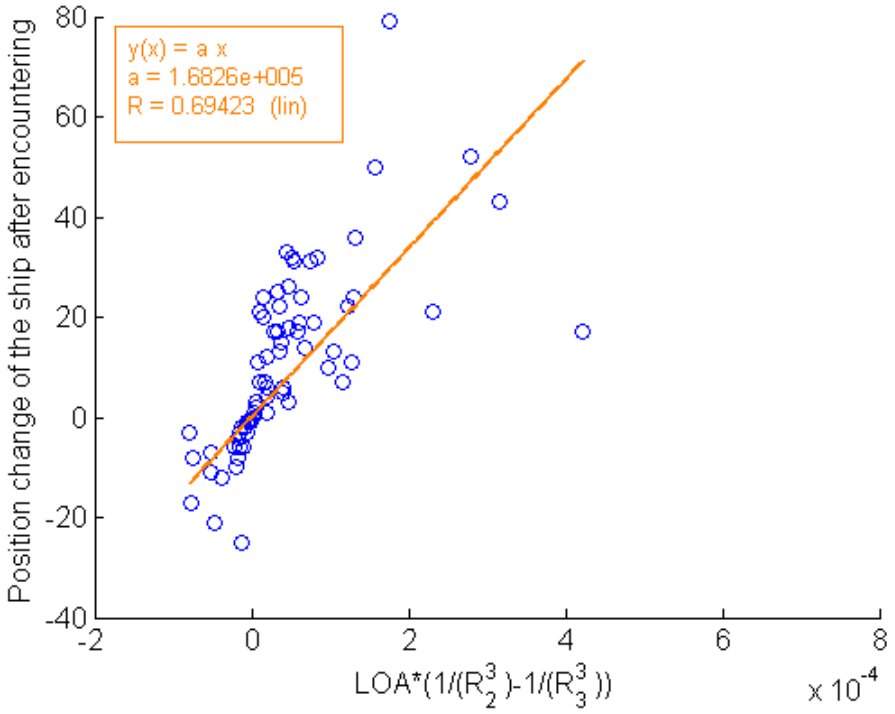

Figure 6-6 Regression analysis between the position change and Δf_{bank}

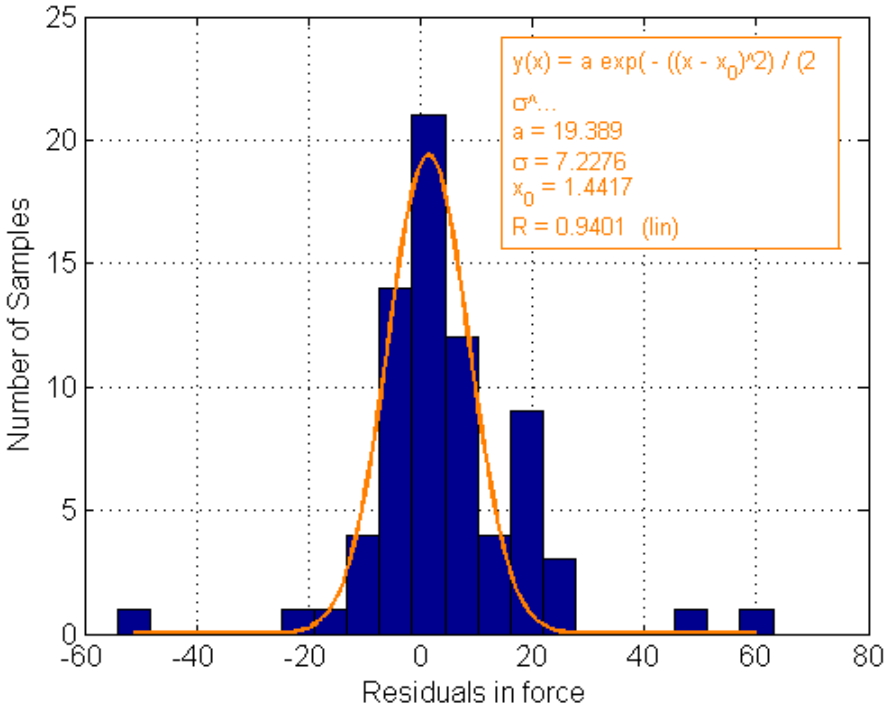

Figure 6-7 Normal distribution for residuals in Figure 6-6

In the analysis, we mainly examine the force difference (ΔF_{bank}) of both incoming ships and outgoing ships in head-on encounters and the factors that may contribute to $F_{head-on}$. The

results in the ellipse area of Figure VI-3 indicate that the force is not correlated with the characteristics of counterpart ships (LOA or speed) in a head-on situation. Moreover, the correlation between forces and distances does not show the same pattern when comparing incoming ships and outgoing ships. Therefore, the perception of the force $F_{head-on}$ is not a function of the characteristics of other ships. This is contrary to the common understanding that the characteristics of ships count as factors.

Although we cannot find any factors that contribute to an equation, the force is reflected by ΔF_{bank} from counterpart ships in encounters, as $F_{head-on}$ should be balanced with ΔF_{bank}. We can treat the force difference from the channel bank (ΔF_{bank}) as a substitute for force from the ship in a head-on situation ($F_{head-on}$). Figure 6-8 shows the artificial forces calculated by Equation (6 - 9). The random perceived artificial force when the other ship appears in a head-on encounter can be:

$$F_{head-on} = \Delta F_{bank} \sim \aleph(2.27, 6.8^2) \quad (6 - 11)$$

6.2.5.5 Artificial force from a ship in an overtaking situation

For overtaking situations, the AIS ship tracks are also plotted using Autodesk® AutoCAD® Civil 3D® software, and different distances are measured in the plot for a further matrix of correlation coefficient analysis. Figure 6-9 illustrates the distances that are measured in overtaking encounters.

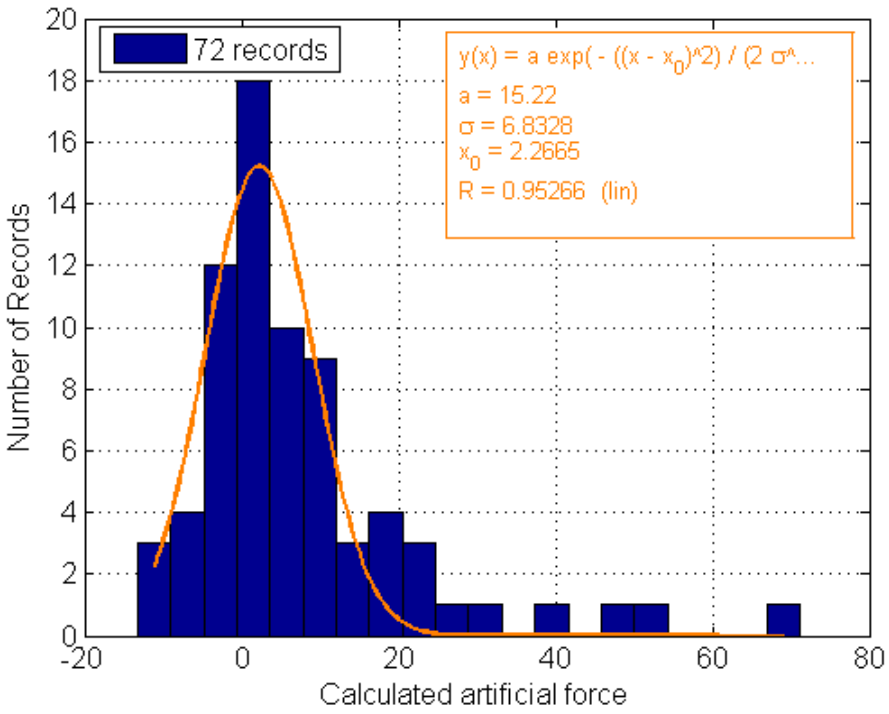

Figure 6-8 Normal distribution for force in head-on situations

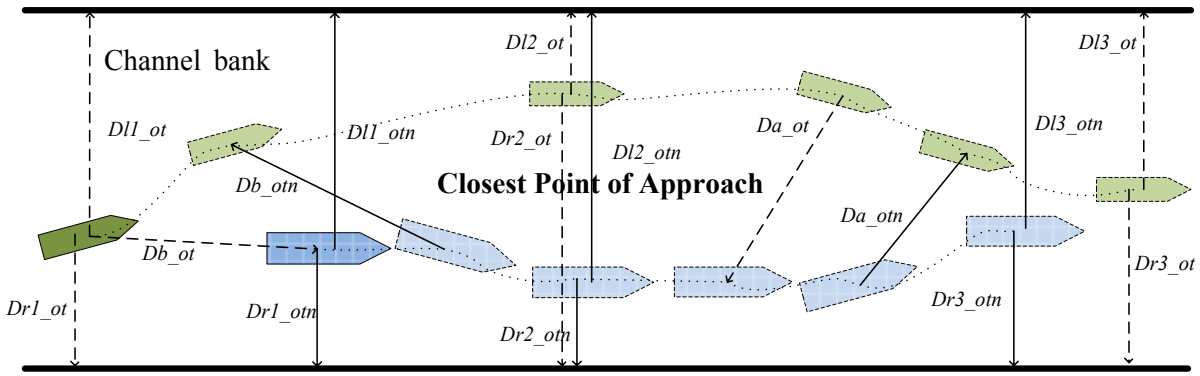

Figure 6-9 Illustration for distances in en overtaking encounter

The numbers of collected overtaking encounters are small, so assumptions need to be made for the overtaking process based on previous results for developing artificial forces. 13 overtaking cases (two with the complete process, 11 with half of the process) are found. There is one case in which a tug overtakes on the starboard side of another ship. This case was not taken into the statistical analysis, because that behavior is completely different. It is expected that only very small ships overtake on the starboard side in that section of the channel, although more evidence from the AIS ship tracks is needed to draw a firm conclusion.

First of all, it is assumed that the force from the channel banks in an overtaking situation works in the same way as in head-on situations. $\mathrm{F}_{\mathrm{overtaken}}$ from port and $\Delta\mathrm{F}_{\mathrm{bank}}$ should be balanced at the closest point of approach. The force perceived by the overtaken ship is calculated in the same way as force in the head-on situation, because the behavior of the ship is very similar to the behavior in the head-on encounter. Then,

$$\mathrm{F}_{\mathrm{overtaken}} = \Delta\mathrm{F}_{\mathrm{bank}} \sim \aleph(2.27, 6.8^2) \qquad (6 - 12)$$

Secondly, the overtaken ships normally shift to starboard in the encounter and the lateral position in the encounter is calculated by Equation (6 - 9). The difference is that the threshold distances are smaller, when the overtaken ships start to take action to shift before and after the overtaking process ("Db_otn" and "Da_otn" in Figure 6-9).

Thirdly, the overtaking ship navigates to the port side of the overtaken ship, and it is subjected to the force from the port bank of the channel $\mathrm{F}_{\mathrm{bank,p}}(\mathrm{L})$ and the force from the overtaken vessel $\mathrm{F}_{\mathrm{overtaking}}$ from starboard. Those two forces should be balanced at the Closest Point of Approach.

Fourthly, what is unique for the force from the port bank in overtaking is that the overtaking ships initially are subjected to a force from the starboard side at the early stage of the overtaking process. When it navigates to the port side of the overtaken ship, the threat from the port bank of the channel starts to take effect. When we calculate the force change for

the port channel bank, it is assumed that the ship comes from "far away" from the port bank (where the force changes from zero to $F_{bank,p}(L_2)$). Thus the force difference is defined as:

$$\Delta F_{bank,p} = F_{bank,p}(L_2) - 0 = 168260 * \frac{LOA_{overtaking}}{L_2^3} \quad (6 - 13)$$

In which L_2 (Dl2_ot in Table 6-4) is the distance to the port bank at the Closest Point of Approach.

The final assumption is similar to $F_{head-on}$. $F_{overtaking}$ is not correlated with the characteristics of the other ships in encounters, and L_2 is calculated by $\Delta F_{bank,p}$ 12 cases of overtaking encounters are used to develop an equation for the artificial force $F_{overtaking}$. With $\Delta F_{bank,p}$ calculated in Equation (6 - 13), $F_{overtaking}$ can be defined as:

$$F_{overtaking} = \Delta F_{bank,p} \sim \aleph(6.87, 6.3^2) \quad (6 - 14)$$

In this equation, only a positive random number generated will be used in the simulation, because it is assumed that the ships only navigate to the port side in the overtaking process.

As the number of overtaking encounters is very small, the matrix of correlation coefficient analysis is used in a different way from the previous analysis. Rather than directly finding the parameters, the matrix of correlation coefficient analysis is used to check whether the assumptions of the artificial force for an overtaking ship are applicable in this case. Table 6-4 lists the factors that are selected in the correlation coefficient analysis. The matrixes of results are shown in Figure VI-4 and Table VI-4.

Table 6-4 Factors in the matrix of correlation coefficient analysis for the artificial force for overtaking ships

Parameters	Introductions
Dl2_ot	Distance to the port boundary of the channel at the closest point of approach for the overtaking ship
Dr2_ot	Distance to the starboard boundary of the channel at the closest point of approach for the overtaking ship
V2_ot	Ship speed at the closest point of approach for the overtaking ship
GROSS_ot	Gross tonnage of the overtaking ship
LOA_ot	LOA (Length Overall) of the overtaking ship
Dl2_otn	Distance to the port boundary of the channel at the closest point of approach for the overtaken ship
Dr2_otn	Distance to the starboard boundary of the channel at the closest point of approach for the overtaken ship
V2_otn	Ship speed at the closest point of approach for the overtaken ship
GROSS_otn	Gross tonnage of the overtaken ship
LOA_otn	LOA (Length Overall) of the overtaken ship
D_cpa	Distance between the two ships at the closest point of approach
F_ot	The force for the overtaking ship that comes from the overtaken ship

The results of the matrix of correlation coefficient analysis are consistent with most of the assumptions. The results indicated in the ellipse area of Figure VI-4 show that the force on the overtaking ship ("F_ot") has a weak correlation with the speed of the own-ship and LOA of the overtaken ship. The force appears to have a strong correlation with the distance to the port boundary of the channel ("Dl2_ot") and the LOA of the own-ship. These results are in line with the assumptions for the force of the overtaking ship.

However, results also show an unexpected correlation. There appears to be a strong correlation between the force on the overtaking ship and the speed of the overtaken ship ("V2_otn"). This is not assumed, as this is not consistent with the previous analysis that ship speed is not a factor of force. However, theoretically the speed of the ships is also an important factor in the overtaking process. The overtaking ships are supposed to increase their speed and the overtaken ships are supposed to decrease their speed, if the situation gets difficult. Since the sample size is small (12 samples), it is not possible to answer now whether speed should be taken into consideration for overtaking forces. Therefore, ship speed is not taken into account in this study. The speed change in the overtaking encounters should be further studied in the future.

6.2.6 Thresholds of distances for artificial forces

Thresholds of distances for artificial forces are introduced in this subsection. The forces from channel banks and forces from ships take effect within certain distances. Also different ships respond to the forces at different distances. Therefore, statistical analysis is needed for the thresholds of distances at which the artificial forces start to take effect in a simulation.

6.2.6.1 Thresholds of distances for forces from the channel bank

As was mentioned in Section 6.2.4.2, the threshold for artificial force from the channel bank is the distance to the right bank of the channel after encounters ("Dr3" in Figure 6-5, or R_3 in Equation (6 - 9)). From Figure VI-1, it is observed that "Dr3" is correlated with the LOA. After the regression analysis between the LOA and "Dr3" (Figure 6-10), the threshold for artificial force from the channel bank can be expressed as:

$$\mathrm{R}_3 = 0.21 * LOA + 85.39 + \Delta\mathrm{R}_3 \qquad (6 - 15)$$

Where $\Delta\mathrm{R}_3$ is a random number from the normal distribution $\Delta\mathrm{R}_3 \sim \aleph(-4.2, 23.1^2)$.

6.2.6.2 Thresholds of distances for forces from head-on ships

From the AIS ship tracks (as illustrated in Figure 6-5), we can observe the "distance to act" ("Dh" in Table 6-1) for ships in an head-on encounter. "Distance to act" is the distance between the two ships when a ship starts to take action, and the $\mathrm{F}_{head-on}$ starts to take effect. After the correlation coefficient analysis, it is found that "Distance to act" is not significantly correlated with the LOA, Gross Tonnage or speed. Therefore, we statistically

analyze the numbers observed in the ship tracks. Then, we use a random normal process to generate the "Distance to act" for a head-on encounter:

$$D_{head-on} \sim \aleph(1548, 706^2) \quad (6 - 16)$$

6.2.6.3 Thresholds of distances for forces from overtaking ships

In overtaking encounters, there are two distances for thresholds for $F_{overtaking}$ and $F_{overtaken}$. One is the distance to act at the beginning of overtaking maneuvering when the force starts to take effect. The other one is the distance to act after the Closest Point of Approach when the forces are reduced. Then the overtaking ship starts to resume its position to the starboard side and the overtaken ship starts to shift to port. $D_{overtaking}$ and $D_{overtaking\_after}$ are adopted for both the overtaking ships and the overtaken ships, as the number of overtaking encounters is small and the distances for both ships are very similar. In other words, $D_{overtaking}$ is for "Db_ot" and "Db_otn" in Figure 6-9 and $D_{overtaking\_after}$ is for "Da_ot" and "Da_otn" in Figure 6-9. With statistical analysis, the "distances to act" in both situations are:

$$D_{overtaking} \sim \aleph(384, 358^2) \quad (6 - 17)$$

$$D_{overtaking\_after} \sim \aleph(308, 182^2) \quad (6 - 18)$$

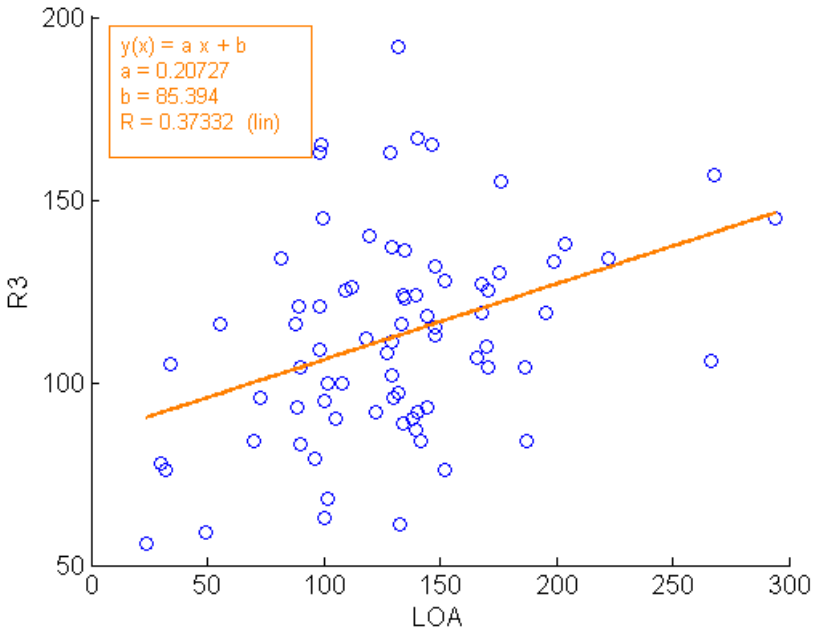

Figure 6-10 Regression analysis between the LOA and R_3

6.2.7 Algorithms for artificial forces and ship interactions

Figure 6-11 shows the algorithm for the application of artificial forces. The first priority is determining the encountering situations (overtaking or head-on). The ships with opposite courses should be in a head-on situation. Overtaking situations apply only when the ship behind is faster.

In head-on situations, R_2 is calculated based on $F_{head-on}$ and R_3, then $D_{head-on}$ is generated. As soon as the distance between two ships is less than $D_{head-on}$, the ship starts to turn starboard to shift its position to the position with the distance to starboard bank at R_2. After the Closest Point of Approach, the ship shifts to a lateral position with the distance to the starboard bank at R_3.

In overtaking situations, the overtaking ship and overtaken ship behave differently. For an overtaken ship, the behavior is the same as in a head-on situation. R_2 is calculated based on $F_{overtaken}$ and R_3, then $D_{overtaking}$ is generated for the distance to act. Then the ship position shifts to R_2 during the encounter and then to R_3 after the encounter with $D_{overtaking\_after}$ to the overtaking ship. For the overtaking ship, $F_{overtaking}$ is generated for L_2, then with $D_{overtaking}$, the ship shift position to the port side at a distance to the port bank at L_2. Then after arriving at a distance to the overtaken ship with $D_{overtaking\_after}$, the ship starts to resume its original lateral position before the encounter.

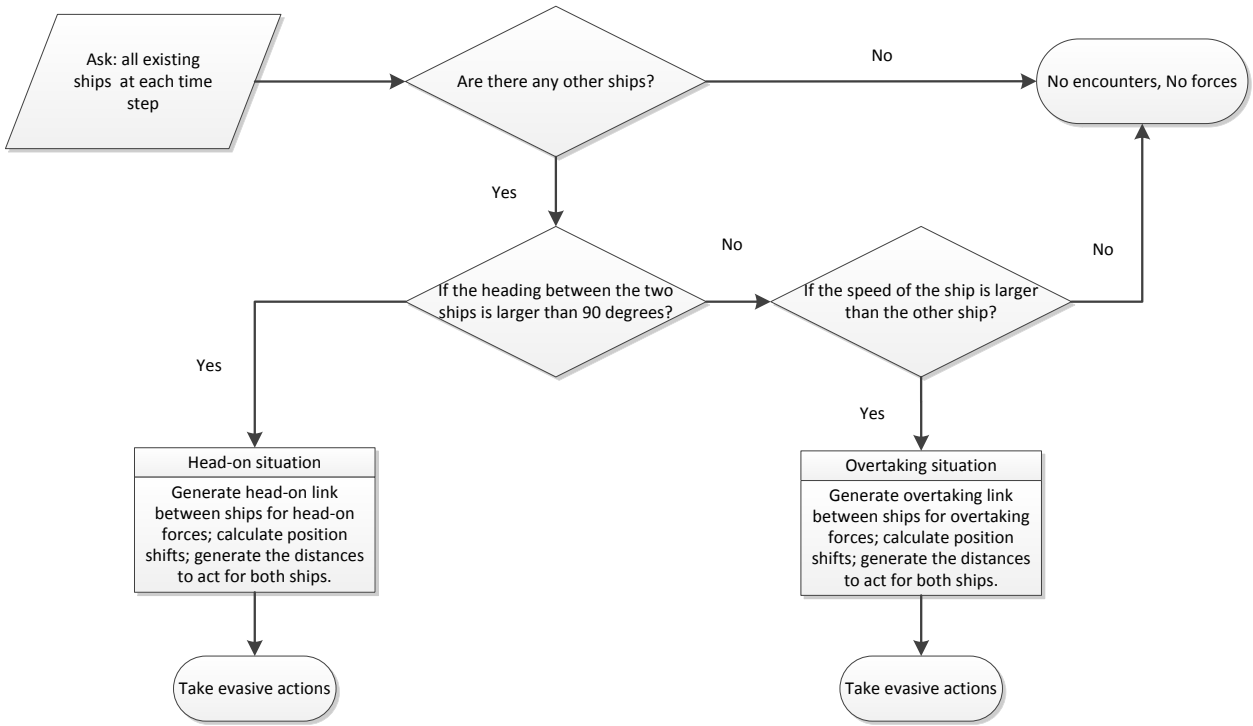

Figure 6-11 Algorithms for the application of artificial forces and ship interactions

6.2.8 Discussion

In this section, the development of the artificial forces has been described. Three different types of artificial forces are introduced, which are forces from the channel banks, forces from head-on ships, and forces in overtaking situations. Those forces guide the ships to shift to port or starboard side to avoid collisions as required by regulations and common practices. The method of correlation coefficient analysis is used to find the factors that contribute to the artificial forces. Based on this analysis, we have developed formulas for different artificial forces. The parameters and constants in the formulas are derived from the matrix of correlation coefficient analysis of relevant factors in encounters.

Several relevant articles in COLREGs are provided and interpreted. This allows the requirements of regulations and common practices to be built into the artificial forces in the virtual environment. This also allows the behavior of ships, especially ship interactions in encounters, to be reproduced realistically in the simulation.

The matrix of correlation coefficient analysis is used to find the factors that contribute to the formulas for the artificial forces. This method is innovative in finding the relationships between different factors, and it can also be used to compare and find the most relevant factor from factors with similar characteristics. For instance, both the LOA and Gross Tonnage are characteristics for ship dimensions. However, it is found that the LOA is a better indicator for the artificial force than Gross Tonnage because the correlation coefficient results for the LOA are larger. Therefore, the LOA is selected for formulas of the artificial forces. Other than that, when the sample size is small, the matrix of correlation coefficient analysis is used to check whether the assumptions for the artificial forces are applicable.

Artificial force from the channel bank increases with the LOA, and it decreases with the distance to the channel bank. The developed artificial force helps to reflect reality in at least four aspects. Firstly, it is more dangerous for larger ships to navigate in a confined channel. Secondly, it reflects that the smaller the distance to the bank, the more dangerous for the ships. Thirdly, it is safer to shift to starboard in the middle of the channel, and it is much more dangerous for the same distance of lateral position shift when a ship is navigating very close to the starboard bank. In addition, it tells us that the “vacant areas” for different ships are different, and the larger ships have smaller “vacant areas”, as R_3 is correlated with the LOA. This is consistent with the reality that larger ships prefer to stay closer to the center of the channel. Finally, for the formulas of forces, μ is a constant. In this thesis, only μ in a straight waterway is relevant, because the ship tracks are collected from a straight waterway. It is expected that this constant is different for different shape of waterways.

The artificial forces ($\mathrm{F}_{head-on}$, $\mathrm{F}_{overtaking}$and $\mathrm{F}_{overtaken}$) are randomly generated numbers that are not dependent on the characteristics of the other ships in encounters. This is reasonable in real practice. Different Officer on Watch perceive the threat of the other ship

differently in navigation. From observations of the ship tracks, most of the ships take action in encounters. However, there is a small proportion of ships which do not take action or even shift to the opposite direction during encounters. This further proves that random choices of forces are practical, and it is also a contribution to the stochastic characteristic of the multi-agent simulation.

Overtaking on the starboard side is not included in the analysis. This is because the overtaken ships shift to the port side to avoid collision, and the behavior is opposite from overtaking on the left. More data of ship tracks are needed to study this behavior.

For the artificial forces, the parameters and some regression analysis need further study. We statistically analyzed 39 cases of head-on encounters and 13 cases of overtaking encounters. These encounters are found from 3 months of AIS data. However, it is very time consuming to select and analyze the encounters, and many encounters in the AIS data were found to have problems (missing information in most cases), which were therefore not taken into account in the analysis. Hence, the study was based on a limited number of ship tracks of good quality. It is believed that the parameters in the formula can be more accurate and better reflect the reality if more ship tracks are analyzed. Behavior difference for different ship types is not included in the analysis due to the insufficient number of ship tracks processed.

Random normal processes were used to reflect the parameters for simplicity, as the distributions were fitted with normal curves, although the dataset that was tested was rejected by normal distribution. The random normal process is the way we approximate the ship behavior. However, ship interactions and human decisions are far more complicated than random normal processes. This is an area that needs further study and analysis. Especially concerning overtaking situations, more cases are needed for statistical analysis to improve the formulas and the “distances to act”. The “distance to act” at the beginning of the process is normally larger than the distance to act at the end when the ship starts to resume the position during the overtaking encounters.

We made several assumptions in this section to apply artificial forces to ship interactions in the simulation. These assumptions are useful at this stage of research. Nevertheless, the assumptions need further validation for future applications. For example, especially for an overtaking situation, speed may be taken into account.

In this research, we implemented the artificial forces for ships in a straight waterway. This lays the basis for artificial forces in waterways with intersections and waterway with bends. The equations for different artificial forces are subject to modifications to apply in more complicated waterways. More rules and navigational strategies for ship movement need to be taken into account. However the method introduced in this study forms good basis for further research.

6.3 Models for realistic movement of ships

The artificial forces dominate the navigational strategy for ship movements in the channel. This section introduces the models that carry out the navigational strategy for ship movements and make the ships move forward realistically in the simulation.

6.3.1 The Nomoto model for ship movement

6.3.1.1 Formula for the Nomoto model

The Nomoto model that originates from Kawaguchi's research provides the basis for the maneuvering simulation of each ship with maneuverability indices of K and T (Kawaguchi et al., 2004). This model uses time steps. The parameters include: ship maneuverability, rudder position, ship heading, and speed.

$$x_{i+1} = x_i + S_p * \cos\Phi_i * \Delta t \quad (6 - 19)$$

$$y_{i+1} = y_i + S_p * \sin\Phi_i * \Delta t \quad (6 - 20)$$

$$\Phi_{i+1} = \Phi_i + \gamma_i * \Delta t \quad (6 - 21)$$

$$\gamma_{i+1} = \gamma_i + (K\delta - \gamma_i) * \Delta t / T \quad (6 - 22)$$

In ship navigation, a larger K means a good ability to change the course of the ship, while a larger T indicates the ship has a better ability to keep its course. The value of K and T depends on rudder angle, ship dimensions, and ship type. Δt is the time step in the simulation, S_p (m/s) stands for the speed of the ship, Φ (degree) is the heading of the ship and γ (degree/second) indicates the rate of turning. δ (degree) means rudder angle. Therefore, in every time step Δt (second), the equations above will be applied to determine the new ship position and course.

For indices of K and T, there are non-dimensional forms:

$$K' = K(L/V) \quad (6 - 23)$$

$$T' = T(V/L) \quad (6 - 24)$$

In which L is length of a ship, V is speed of the ship.

6.3.1.2 Statistical analysis of the maneuverability indices with different ships

In order to generate maneuverability indices of K and T for different ships, we must predict K and T for different types and lengths of vessels that are included in the AIS data. In this section, we statistically analyze 47 ships from literature with non-dimensional K and T (K' and T'), ship types, loading conditions and dimensions (Table VII-1). The table come from

the research by Li et al. (2007) and Li (2008). Then we derive the formula for K and T indices for simulation.

The correlation coefficient analysis is used to find the factors that contribute to equations to derive K' and T'. The results show that K' and T' have a strong correlation with LOA, B (Beam), d (Draught), C_b (Block Coefficient) and Ld/A_R (rudder area ratio). Also there is a strong correlation between K' and T', as shown in Figure 6-12. As in those parameters only length is reliable in the AIS data, after regression analysis we have:

$$\mathrm{K}' = 0.31 * \mathrm{T}' + 0.99 + \Delta T_1' \qquad (6 - 25)$$

Where $\Delta \mathrm{T}_1'$ is a random number from normal distribution $\Delta \mathrm{T}_1' \sim \aleph(-0.16, 0.26^2)$.

The best way to derive K' and T' is using Length as a parameter. Both Length and Beam are reliable data in AIS signals. However, Length is strongly correlated with Beam, so either Length or Beam can be used as a parameter for K' and T'. Length is chosen because it is already used as a parameter in the force field. The information of draught is available in the signal, but the information is not reliable as the values are not always well recorded. It is observed from Table VII-1 that oil tankers have larger values on C_b and Ld/AR. For the other ships, the length and type is not closely correlated with C_b or Ld/AR. Therefore, the 47 ships can be divided into two groups to take the C_b into consideration. One group is oil tankers, while the other group is ships other than oil tankers. Ld/AR is not provided by the AIS data, so we omit this parameter.

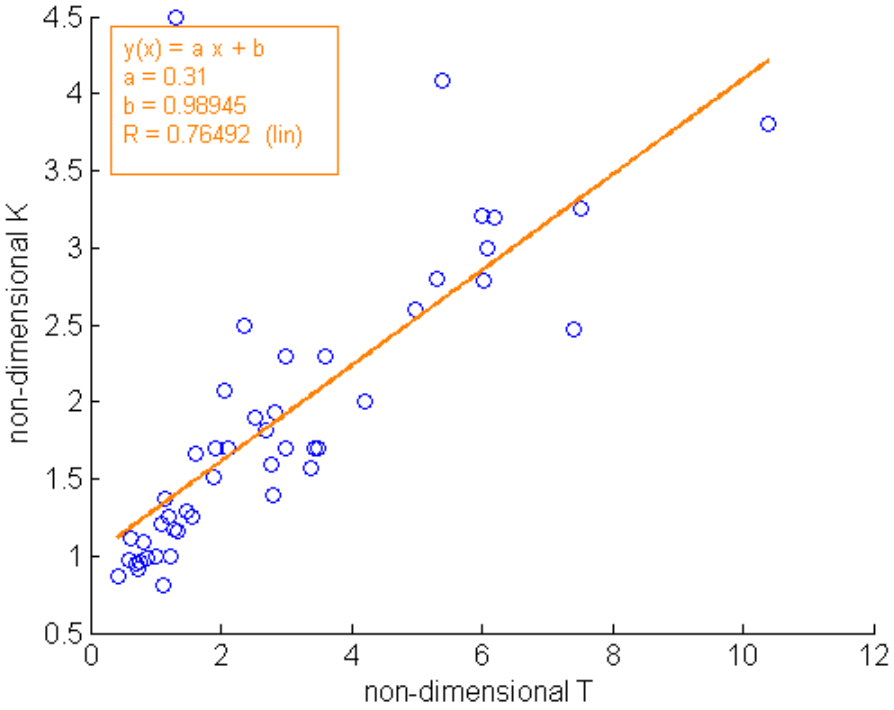

Figure 6-12 Regression analysis between K' and T'

For oil tankers, after regression analysis between T' and ship length L (Figure 6-13):

$$T' = 0.0165 * LOA + 0.54 + X \quad (6 - 26)$$

Where X is a random number from the normal distribution $X \sim \aleph(-0.03, 2.12^2)$.

For ships other than oil tankers, the correlation between T' and ship length is weak. Therefore, for any ship length, T' is generated by a random exponential distribution (Figure 6-14):

$$T' \sim \mathrm{Exp}(1.74),\ T' > 0.5 \quad (6 - 27)$$

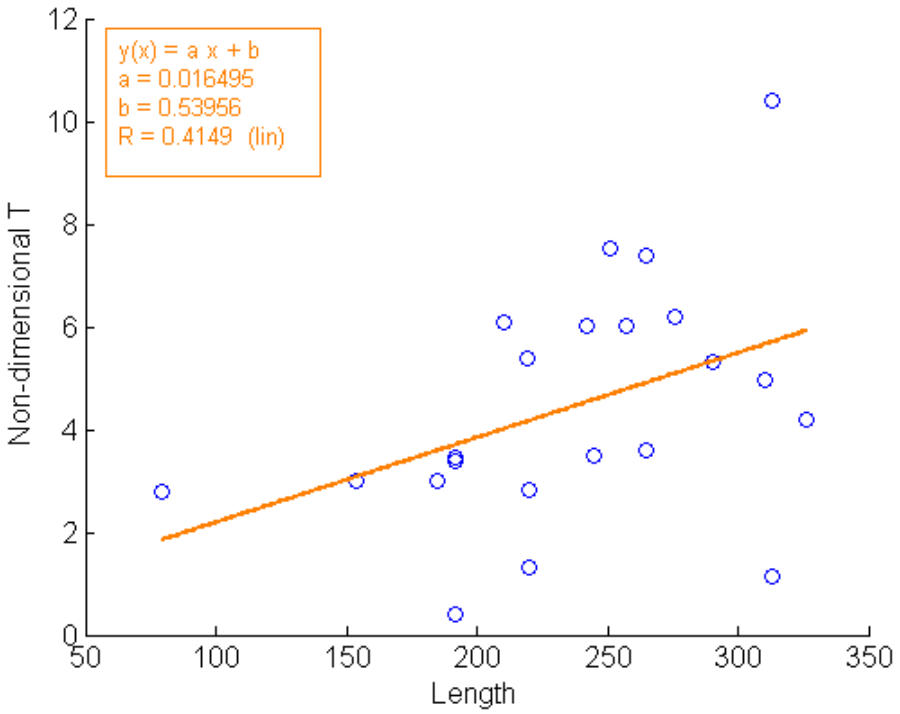

Figure 6-13 Regression analysis between T' and Length for oil tankers

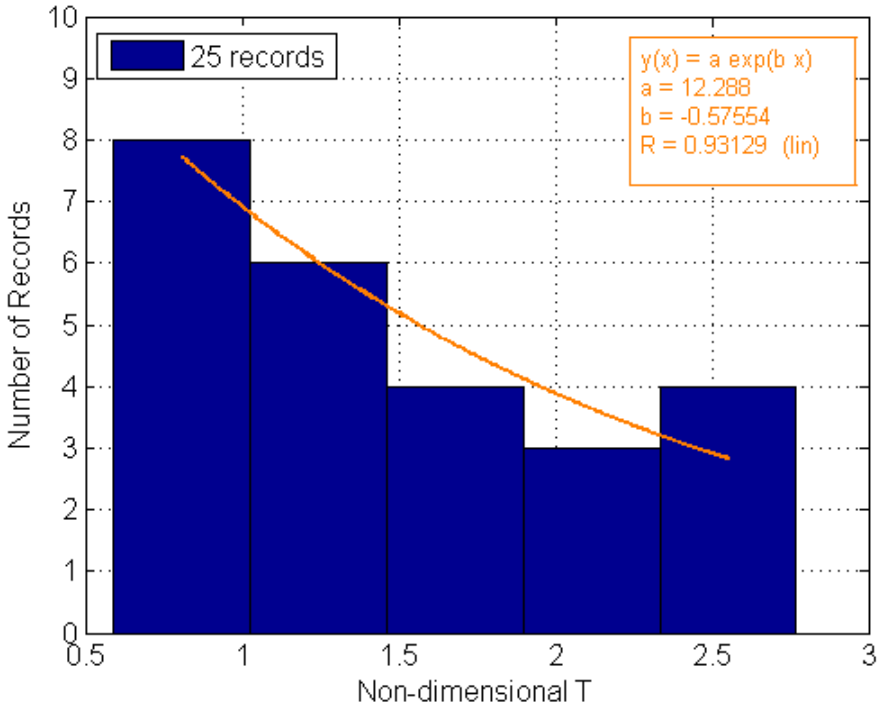

Figure 6-14 Distribution of T′ for ships other than oil tankers

6.3.1.3 Discussion

This section provides the method to generate stochastic maneuverability indices of K and T for ships with different length, speed and type. With the maneuverability indices, the ship movements in simulation are more realistic. However, the Nomoto model is a simplified dynamic ship maneuvering model. More accurate ship maneuvering models can be further studied and implemented to reproduce more realistic ship movements. One thing to notice is that a more accurate ship maneuvering model does not help with the navigational strategy for the lateral position shifts in encounters. However, it does help with a realistic reproduction of the ship movements determined by rudder angle, for instance drift angle at different times.

There are several factors that contribute to better maneuverability of ships in reality, but these factors are not implemented in the simulation. Firstly, the formulas for indices of K and T are derived from the 47 ships available. It is the maximum optimization of ship maneuverability that this research can provide. More samples for statistical analysis can result in better predictions. Secondly, inland barges and newly built ships have much better maneuverability than old ships, so the maneuverability of ships in a simulation may be lower than in reality. Thirdly, the effect of side thrusters is not implemented, as a side thruster increases ship maneuverability in reality. Finally, it is assumed that the maneuverability indices of K and T are not affected by the shallow water effect. However, the fact is that the

water depth affects maneuverability. The effect of shallow water is beyond the focus of this research, so it can be referred for future research.

6.3.2 Ship speed change model

6.3.2.1 Acceleration for ships at each time step in the simulation

Proper accelerations for ship speed should be implemented in the simulation. Ships increase speed in a straight channel (Figure 6-15), and decrease speed at the end of the channel. Therefore, accelerations are needed for different types and gross tonnages of ships. It is assumed that ships in the same category change speed in the same way as the average speed, and the acceleration is constant between two adjacent crossing-lines. Then different ships with different original speeds have different accelerations in the same section of channel. The speed change for different ship categories can be calculated by:

$$\Delta v_n = v_n - v_{n-1} \tag{6 - 28}$$

In which $\mathrm{v_n}$ and $\mathrm{v_{n-1}}$ are average ship speeds between two adjacent crossing-lines. Therefore, the accelerations of ships for different original speeds can be derived using the equations below:

$$\int_{\mathrm{t_1}}^{\mathrm{t_2}} (\mathrm{v_0} + a\mathrm{t})\mathrm{dt} = \mathrm{S_n} \tag{6 - 29}$$

$$\int_{\mathrm{t_{n-1}}}^{\mathrm{t_n}} (a\mathrm{t})\mathrm{dt} = \Delta \mathrm{v_n} \tag{6 - 30}$$

In which S_n is the distance between the two adjacent crossing-lines, v_0 is the original speed at crossing-line number $(n-1)$, a is acceleration, $t_{\mathrm{n-1}}$ is time at crossing-line number $(n-1)$ and t_n is time at crossing-line number n. Then, the acceleration at each time step can be calculated.

6.3.2.2 Discussion

The model for acceleration is a very much simplified reflection of reality. The ship's response to a thruster is a very complicated process. Also, different officers choose different speeds and engine orders, and this further makes the acceleration process more complicated. However, the speeds of ships are constrained by the local navigational environment. Reasonable speeds are chosen for ships in the same area. In this research, the speed and acceleration affects the number of overtaking encounters. In this sense, the statistical speed and speed change are good enough for traffic simulation and risk analysis.

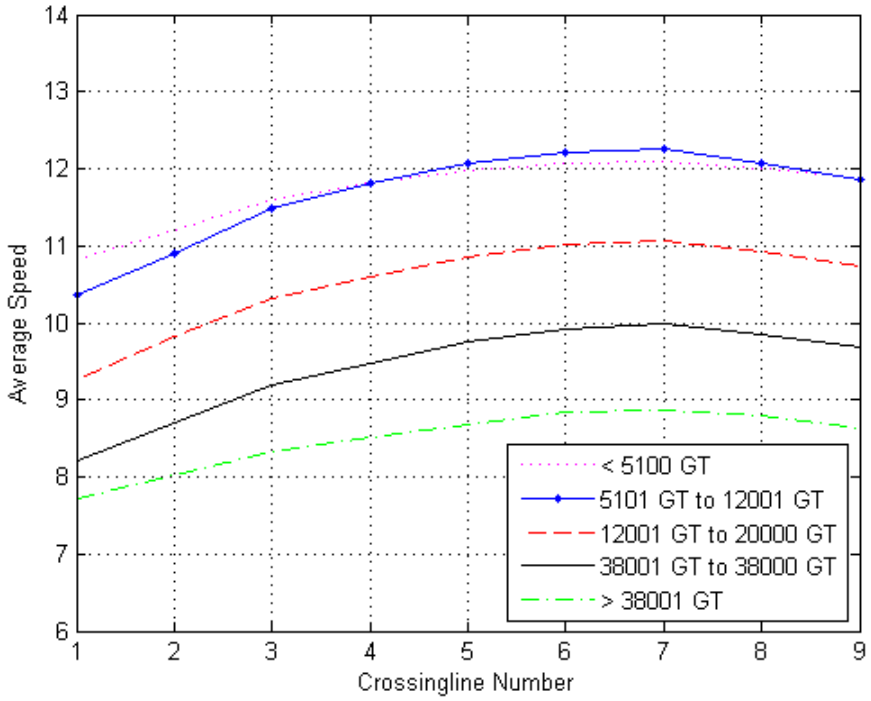

Figure 6-15 Average speed of containers in incoming direction

6.3.3 Ship movement in wind

6.3.3.1 Drift velocity of a ship to the leeside by wind

It is assumed that the ship speed can compensate for parallel wind. However, for wind from the side, the drift velocity of the ship to the leeside can be calculated by (Fang et al., 2009):

$$V_T = K * K' * \sqrt{\frac{B_a}{B_w}} * e^{-0.14V_s} * V_a \qquad (6 - 31)$$

where $K \in (0.038, 0.041)$; K' is the correction modulus for shallow water, which is indexed in Table 6-5; B_a is the hull area above the waterline (m^2), while B_w is the hull area below the waterline (m^2); V_s is the ship velocity in wind (kn); and V_a is the wind velocity relative to the ship (m/s). The wind speed relative to the ship can be calculated by:

$$\overrightarrow{V_a} = \overrightarrow{V_s} + \overrightarrow{V_w} \qquad (6 - 32)$$

In which $\overrightarrow{V_s}$ is the ship speed, and $\overrightarrow{V_w}$ is the wind speed.

Table 6-5 Correction modulus for ships in shallow water K' (based on (Fang et al., 2009))

Water depth (H)/real draught (d)	1.1	1.5	2.0
K' for ordinary cargo ships	0.6	0.7	0.8
K' for very large ships (C_b >0.8)	0.5	0.6	0.7

6.3.3.2 Discussion

This model provides the drift velocity of a ship to the leeside by wind, which can be implemented in the simulation with time steps. The shallow water effect in the river is considered by the correction modulus. In the simulation, the course of the ship should be calculated so that the ship can correct the course to navigate in the restricted channel in wind. As B_a/B_w is not available in the simulation, this is assumed to be constant and equal to 1.

6.3.4 Ship movement in currents

6.3.4.1 Ship speed in a current field

The currents in the channel are significant. Nevertheless, the effect of the current is compensated for normal navigating ships. However, for ships with rudder failure or engine failure, ship movements in currents need to be implemented in the simulation. In the multi-agent simulation, the current field is indicated by “current agents”. Each “current agent” is located at a fixed geographical point with current velocity in different hours. At each time step, the current velocity at the location of the “ship agent” is set as the current velocity of the closest “current agent” around the “ship agent” (Figure 6-16). Then, the ship speed over ground can be calculated by:

$$\overrightarrow{V_g} = \overrightarrow{V_s} + \overrightarrow{V_c} \tag{6 - 33}$$

In which $\overrightarrow{V_s}$ is the ship speed and $\overrightarrow{V_c}$ is the current velocity.

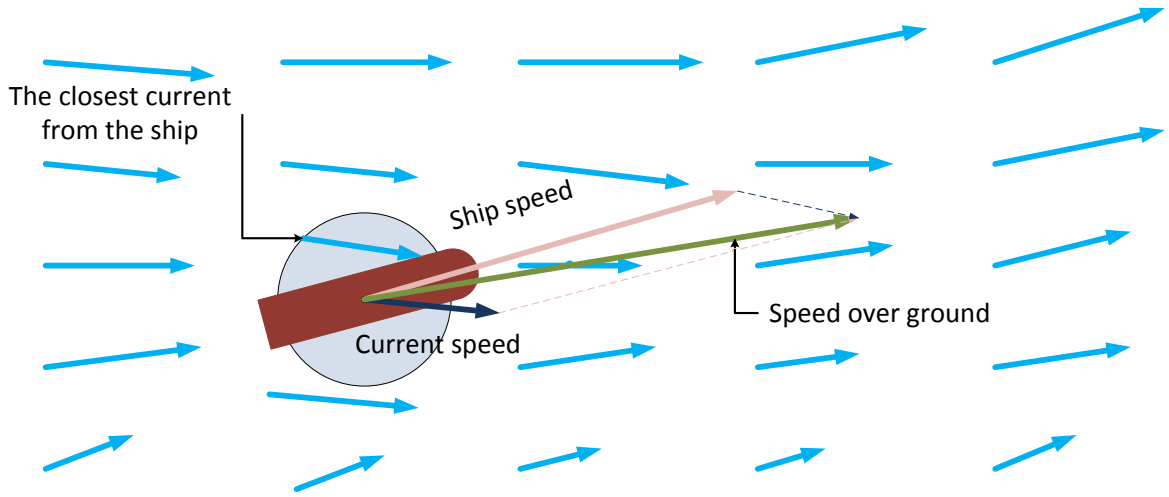

Figure 6-16 Ship speed in the current field

6.3.5 Ship movement with engine failure without emergency anchoring

6.3.5.1 Introduction

As was introduced in the Drift Model (Fang et al., 2009), the movement of a ship after engine failure can be divided into two parts. One part is the ship movement caused by inertia, and the other part is the ship movement with no inertia, caused by wind and current. In this submodel, the inertia, current velocity, and wind are the main causes of ship movement.

6.3.5.2 Ship speed with inertia

Based on Fang et al. (2009), the instantaneous speed after engine failure can be calculated by:

$$\mathrm{V}_s = \mathrm{V}_0 * e^{-t/T_{st}} \quad (6 - 34)$$

$$T_{st} = c/ln2 \quad (6 - 35)$$

Where V_0 is the ship speed at the beginning of the engine failure; T_{st} is the time constant of the ship deceleration; the constant c can be found by ship displacement from Table 6-6; and t is time spent after engine failure. The influences from the wind and currents can be referred to Section 6.3.3 and Section 6.3.4. In addition, current velocity is taken into account, because the current effect can no longer be compensated for by rudder. Wind velocity relative to the ship is calculated by:

$$\overrightarrow{V_a} = \overrightarrow{V_s} + \overrightarrow{V_c} + \overrightarrow{V_w} \quad (6 - 36)$$

In which $\overrightarrow{V_s}$ is ship speed, $\overrightarrow{V_c}$ is current velocity, and $\overrightarrow{V_w}$ is wind speed.

Table 6-6 Time constant for different displacements (disp.) (based on (Fang et al., 2009))

Disp. (t)	C (min)	Disp. (t)	c (min)	Disp. (t)	c (min)	Disp. (t)	c (min)
1000	1	~21000	6	~66000	11	~136000	16
~3000	2	~28000	7	~78000	12	~152000	17
~6000	3	~36000	8	~91000	13	~171000	18
10000	4	~45000	9	~105000	14	~190000	19
~15000	5	~55000	10	~120000	15	~210000	20

6.3.5.3 Ship speed without inertia

At this stage, the ship speed is driven by wind and current. The current influence is referred to in Section 6.3.4. Based on (Fang et al., 2009), the drift velocity of the ship by wind is:

$$V_T' = K * K' * \sqrt{\frac{B_a}{B_w}} * V_a \quad (6 - 37)$$

$$\overrightarrow{V_a} = \overrightarrow{V_c} + \overrightarrow{V_w} \quad (6 - 38)$$

6.3.5.4 Discussion

The ship may drop anchor to stop the ship, when the ship speed is slow enough. However, anchoring is not included in this research. This could be a topic for further research.

6.4 Conclusions

The submodels of the ANTS model have been described, which is the last part of the ODD protocol. For ship interactions, we implement the artificial forces for different encountering situations based on the AIS ship tracks. There are several types of forces for head-on and overtaking encounters. The ship can avoid collisions in a realistic way. The ship avoidance behavior conforms to the regulations and common practice in the waterway. A dynamic ship maneuvering model and a model for speed change are provided to guarantee more realistic ship movements in ship avoidance behavior. Models for influences from wind and currents are also provided to reflect these external influences.

7. MODEL SETUP, CALIBRATION AND VALIDATION

7.1 Introduction

This chapter treats the initial setup, model calibration, and model validation. The initial setup procedure provides specific conditions and environment for the Dutch case, as described in the previous chapters. The calibration tries to assess the performance of the algorithm and tune the parameters to better represent reality. In the validation process, this study compares the output from the simulation to AIS data.

In the initial setup, the coordinate system, proportions of different types of ships, and initial time for the default setting are introduced. The geographical area was defined by the procedure of the initial setup of the coordinate system. The initial setup also provides a way of transferring coordinates between the coordinate system in NetLogo and the geographical coordinate system (latitude and longitude) in the real world.

The calibration procedure in this study involves calibrating parameters for the traffic simulation to reproduce realistic outputs. The calibration has been carried out in the coding process. Different scenarios with different input and emergent situations are checked to find whether the simulation program produces the desired output. Finally, tables of values for the parameters and their ranges are provided as a result of the calibration.

In the model validation, two years (2009 and 2010) of simulation output has been compared with the AIS data. The same two years of AIS data was used for the calibration of the model, which is not ideal for validation. This was accepted taking into account the additional validation for the Chinese case. Ship behavior at both ship traffic level and individual ship level resulting from the simulation is checked with the corresponding AIS data. Differences are shown between statistical results of the simulation output and the results of the AIS data analyses. A number of outputs or intermediate outputs for the traffic are checked, which include the proportions of different types of ships, the weekly number of ship arrivals, daily number of ship arrivals, hourly number of ship arrivals, distribution of time intervals

between two consecutive ships, overall image of the trajectories of ship traffic, distributions to describe ship behavior and the ship interactions in encounters.

7.2 Simulation Setup

7.2.1 Setup for coordinate systems

As the coordinate system in the NetLogo environment is different from the geographical coordinate system of the Earth's surface, the ship positions from GPS (positions with latitude and longitude) must be transferred into the NetLogo environment. The studied area covers a rectangular shaped geographical area with about 3,200 meters of channel. The area is determined by two geographical points (Table 7-1). Other points are transferred with reference to these two geographical points. After configuration of the map in NetLogo, each patch in the NetLogo environment stands for 4 m^2 of geographical area in reality. In other words, each unit in the NetLogo coordinate system stands for 2 m of length in reality.

The positions of navigational aids, the -10.0 m depth contour, as well as channel banks are transferred into the NetLogo environment. Those objects include the channel banks, navigational aids, crossing-lines, geographical locations for currents, and initial positions of ships setup at the boundaries of the channel. The ships will be generated at both boundaries of the simulation, with a random number for y-coordinate. Details of the random numbers for initial variables of different categories of ships are shown in Appendix IX. In this way, the ship positions in the simulation results can be transferred back into the geographical coordinate system to compare with the AIS data. The comparison can be used in calibration and validation of the simulation model.

7.2.2 Setup for the different types of ships

The initial setting of the different types of ships can be found in Table 7-2. There are 8 different types of ships in the data analysis, which are reflected by different colors in the simulation. The proportion of each type of ship is set based on the proportion in the AIS data. This setting allows the numbers of ships for different types of ships to be similar to reality. The initial setting makes sure that the number of ships in each type is generated exactly the same way as the numbers in the setting. In the program, a set of agents (with variables) is used to control the ship generation for different types of ships. In the simulation, a monitor function is used to count the number of ships generated to make sure the setting works. This initial setting also reproduces the reality that each couple of consecutive ships can be either the same type or different from each other. The algorithm is based on the Cars Guessing Game model that is standard in NetLogo (Teahan, 2010). The way that traffic density is reproduced refers to section 3.3.

Table 7-1 Different coordinate systems for the boundary points of the map in simulation

Coordinate systems	Latitude and longitude	Universal Transverse Mercator (UTM)	NetLogo coordinate system (ycor, xcor)
Northwest	51.915620 N, 4.246833 E	5752388 N, 585755 E	524.5, -704.5
Southeast	51.896337 N, 4.28725 E	5750292 N, 588573 E	-524.5, 704.5

Table 7-2 Initial setting of proportions for different types of ships in the simulation based on 28 months of AIS data from 01/01/2009 to 01/05/2011

Type code	Type	Number of passages in 28 months of AIS data	Color	Setting for Numbers
I	**General dry cargo ships**	12474	Magenta	125
II	**Container ships**	11353	Blue	114
III	**Chemical ships, LPG, LNG, Oil tanker**	11512	Red	115
IV	**Tugs**	3119	Lime	31
V	**RoRo**	3089	Orange	31
VI	**Dredging ships**	2339	Pink	23
VII	**Others**	2220	Green	22
VIII	**Unknown type**	7836	White	78
-	**Total**	53942	-	539

7.2.3 Setup for the initial time

The initial time partially determines the number of ship passages in each week, as the number of ship passages increases in time. The default setting of the initial time is the first day in 2009. This number can be modified. The number of passages in each week will increase in the simulation process. Another default setting for time is that each time step in the simulation represents 1 second of time.

7.3 Model calibration

The calibration procedure helps to tune the parameters in the simulation from default values to reproduce more realistic results. The parameters in the artificial force field model were already determined in the model development. At this stage, calibration involves a lot of work in running the simulation, and checking the results on both the ship traffic level and individual ship level. Firstly, simulations with different variables need to be checked to make sure that the behavior of the ship traffic is correct. Secondly, in case of any unexpected results, the input parameters or algorithm are adjusted to make sure that correct outputs are produced. For example, the extreme values generated by the random normal process should be kept within a certain range. Otherwise, unexpected or unrealistic ship behavior

can be generated. There were many problems solved by calibrating the model again and again. The details of essential calibrations are elaborated in the following paragraphs.

Many default parameters as derived from the AIS data, and were designed for the best were applied in the initial runs. It was found that adjustments were needed. After calibration, the following parameters are tuned to better represent the reality.

- Coordinates of ships at the boundary of the simulation
  Each category of the ship has a random number from a normal distribution for the y-coordinate. The x-coordinate would be either the maximum or minimum value of the system, depending on the direction of the ship. The details of calibration for each category of the ships can be found in tables in Appendix IX (Table IX-1 to Table IX-8).

- Gross tonnage
  The tonnages of ships are based on the AIS data observations. Every type of ship has a specific limit of tonnages. The ships cannot be larger than the maximum tonnage in the real world. The details of calibrations for ship tonnages and the distributions can be found in tables in Appendix. The details of calibrations for ship tonnages and the distributions can be found in tables in Appendix IX (Table IX-1 to Table IX-8).

- LOA
  The minimum LOA is defined at 2 m. There are different lengths of ships in the simulation. Also we use random numbers generated from statistical distributions for lengths. The numbers generated can be less than 2 m, but no ship can be less than 2 m in length in the real world. Therefore, an LOA that is less than 2 m in the simulation will not be accepted.

- Ship speed
  The minimum speed is defined at 2 kn. In practice, a ship should maintain a certain speed to keep its maneuverability. Otherwise it is neither able to avoid collision, nor able to compensate the effects from wind and currents. To successfully reflect that, the speed of the ships should be higher than 2 kn. If the generated random number is less than 2 kn, a new random number will be generated until the number is higher than 2 kn. This is executed with a “while loop” in the algorithm. More details on speed can be found in the tables of Appendix IX (Table IX-1 to Table IX-8).

- Acceleration for speed of ships in different sections
  A ship changes its speed based on the geographical position in the channel. Accelerations are calibrated for different types and tonnages of ships at different sections of the channel. The details of calibration for container ships with Gross Tonnages less than 5100 t are chosen as an example. The accelerations between two

adjacent crossing-lines are calculated, so for each ship passage, there are 8 values for accelerations. These values will determine the speed change of ships. The details of calibration on this matter are also given in Table IX-9 in Appendix IX.

- Maneuverability indices of K and T
  The ships should have a minimum maneuverability. Therefore, based on statistics about non-dimensional maneuvering indices K' and T', Table VII-1 shows that 0.59 is the minimum value for T'.

- Artificial forces
  The parameters in the artificial forces are based on statistical analysis of the data derived from individual AIS ship tracks in encountering situations. Therefore part of the determined for the artificial forces is already introduced in Chapter 6. The next paragraph describes further calibration of the parameters based on the performance of the artificial forces in the simulation.

  The artificial forces are special variables that determine the lateral position shifts in ship encounters. The forces should be limited to certain ranges, so that the ship avoidance behavior is neither exaggerated nor unnoticeable. For head-on forces ($\mathrm{F}_{head-on}$), it cannot be less than -14. Otherwise, the ship goes too much to the port side in a head-on situation. This is not realistic, although a deviation to the port is possible. For overtaking forces ($\mathrm{F}_{overtaking}$), the force is not less than 3, so that the overtaking ship can keep enough distance to the overtaken ship. This range makes the overtaking behavior to conform to the regulation that the avoidance actions should be obvious. The details of calibration on this matter are found in Table IX-10 of Appendix IX.

- Thresholds of distances for artificial forces
  Distances at which the artificial forces start to take effect should be limited to certain ranges, so that the ships take actions neither too early nor too late to avoid collision. Based on the statistical analysis of ship encounters, the critical thresholds for these distances were determined. For a head-on encounter, the distances ($\mathrm{D}_{\mathrm{head-on}}$) should be in a range between 500 m and 3,500 m. For an overtaking encounter, the distance before CPA ($\mathrm{D}_{\mathrm{overtaking}}$) should be in a range between 150 m and 1,000 m, while the distance after CPA ($\mathrm{D}_{\mathrm{overtaking\_after}}$) should be in a range between 100 m and 900 m. The details of calibration on this matter are presented in Table 10 of Appendix IX.

- Number of ships in each week/day
  Based on the AIS data observations, for most of the cases, the number of ship arrivals per week is no less than 300. This also guarantees at least 10 ship arrivals per day.

7.4 Model validation

After calibration, validation of the simulation model is achieved. It has been argued that the uncertainties hidden in the background knowledge and lacking some key features of the ship encountering process may undermine the validity of maritime quantitative risk analysis (QRA) (Goerlandt et al., 2014). This thesis performs a validation by comparing the model output and field data (AIS data) on a traffic level and individual ship level. The uncertainties that are reproduced by stochastic characteristics of the model are compared with the field data (AIS data) on a traffic level in statistical way, while the ship encountering process is compared with individual ship level of AIS ship tracks.

For the ship traffic level of model validation, we examine whether the model properly reproduces the critical traffic characteristics and traffic behavior. Also the outputs at ship traffic level are evaluated on several aspects. Firstly, it is checked that whether the ship density in a certain period of time is the same as the AIS data. Secondly, there is evidence to check whether the variations of ship density in different weeks, different days, and different hours are properly reproduced. Thirdly, for ship arrivals, the distribution of time intervals between ships is checked. Fourthly, a face validation is produced to compare the ship tracks with the AIS data overall. This is an empirical comparison of the simulation and reality. Finally, the ship traffic behavior is compared, i.e., the spatial distribution, speed distribution, and course distribution to check whether the characteristics of the ship behavior are represented properly.

For the individual ship level of model validation, it is examined whether the model is able to reproduce the individual ship behavior in different situations. Also the outputs on individual ship level are evaluated, including head-on encounters, overtaking encounters, and accident scenarios with the effects of currents and winds.

The simulation has been performed for only once, therefore the confidence interval for the stochastic variables and results are wide. Several runs of the same simulation are needed to reduce the confidence interval of the variables.

7.4.1 Ship traffic level of model validation

7.4.1.1 Validation for variation of traffic density

Variation of traffic density in time is reflected by variance of ship arrivals. There are several random processes mentioned in Section 3.3.2 that are used to reproduce realistic variations

over the year, the month, the week, the day, and the hour in the simulation. The following paragraphs indicate that the simulation can reproduce those variations.

The numbers of ships of different types are similar to the AIS data. Statistics are provided for the numbers of ships of different types. The overall number of ship passages in the simulation is 48,821, which is 5.8% more than the 46,141 passages in reality. The details can be found in Table 7-3. The results from the simulation are very similar to the AIS data in general. The differences are considered acceptable because the differences will not significantly affect the safety level of ship traffic. Due to the stochastic nature of the variables, there are always small differences.

The histograms compare the numbers of ship arrivals in different weeks between the AIS data and simulation results (Figure 7-1), and differences can be found. The histogram shows that the weekly variation in ship arrivals generated from the simulation is larger than reality. The discrepancy can be explained by the variations used in the simulation that was introduced in Section 3.3.2. Firstly, a normal random process is used to generate the expected number of ships for each week in the simulation. This results in discrepancy from the real data. Secondly, several random processes mentioned in section 3.3.2 are used to reproduce realistic variations over the year, the month, the week, the day, and the hour in the simulation. When these variations are coupled with the random process of the time intervals between ships, the variations get amplified. The details of the differences recorded in the simulation process can be found in Appendix X.

The histograms also compare the AIS data and simulation results for the number of ship arrivals on different days, see Figure 7-2. The daily numbers of passages show smaller differences compared with the weekly numbers. The reasons for the discrepancy are the same as for the weekly variations. The details of the differences recorded in the simulation process can be found in Appendix X.

Table 7-3 Numbers for different ships types from simulation results and AIS data for two years (2009 and 2010) of traffic simulation

Type code	Setting for numbers	Percentage in setting	Number of passages in simulation results	Percentage in simulation	Difference in percentage
I	125	23.19%	11437	23.43%	0.2%
II	114	21.15%	10438	21.38%	0.2%
III	115	21.34%	10066	20.62%	-0.7%
IV	31	5.75%	2836	5.81%	0.1%
V	31	5.75%	2835	5.81%	0.1%
VI	23	4.27%	2101	4.30%	0.0%
VII	22	4.08%	2007	4.11%	0.0%
VIII	78	14.47%	7101	14.54%	0.1%
-	539	100.00%	48821	100.00%	0.0%

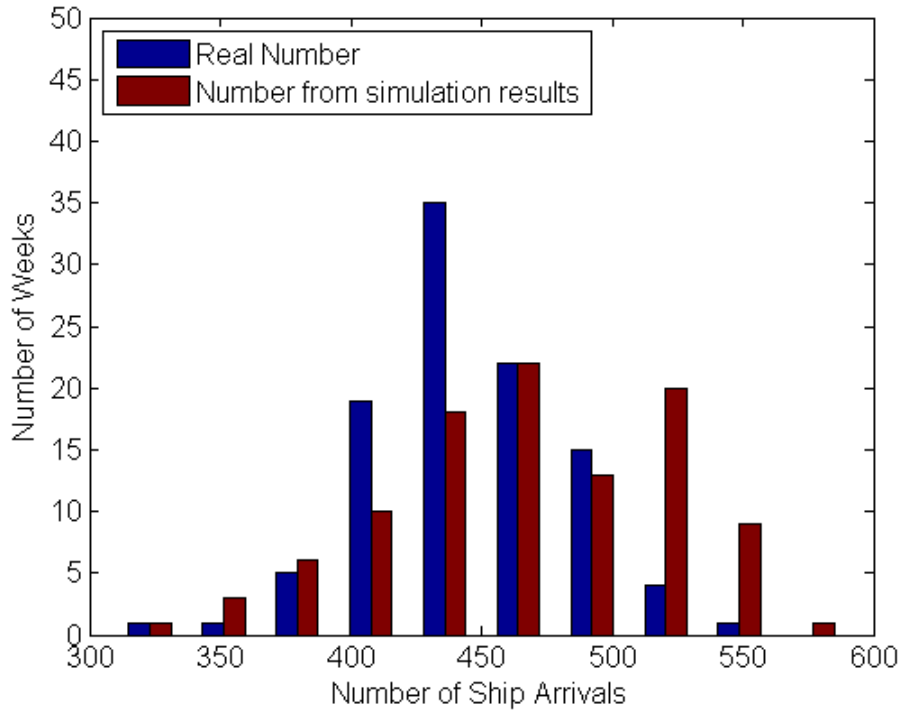

Figure 7-1 Histogram of the weekly number of passages in simulation results and AIS data (103 weeks)

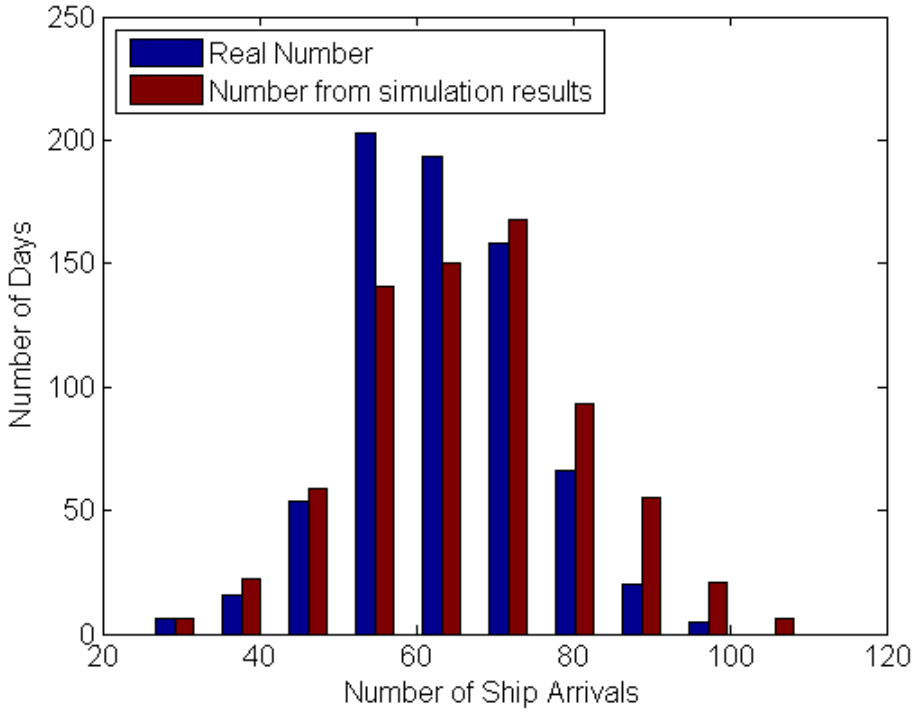

Figure 7-2 Histogram of the daily number of passages in simulation results and AIS data (720 days)

Further proportions of ship arrivals in different hours throughout the day for the two years of output are compared (Figure 7-3). The simulation results are quite similar to the AIS data. Two peaks can be found in both histograms. Successfully reflecting these proportions is important, because the traffic density largely influences the number of encounters, which finally influences the safety level.

It is interesting to analyze the differences between the simulation results and the AIS data. The differences come from the algorithm of ship generation. Ideally, there should be no differences between simulation and reality, if the time intervals are short enough. However, in this simulation a random exponential process is used to generate time intervals for the next ship at the time when the previous ship appears at the boundary of the model. Therefore, the new ship could arrive in an hour that is different from the hour that the time interval is generated, especially when the time interval is generated at the end of the hour. That means that the time interval generated in one hour can be counted in ship arrivals of the following hours (the time interval can be hours long). This is the reason that there are small differences in the hourly proportion of ship arrivals.

The distribution of time intervals between ships in the simulation results are also compared (Figure 7-4). The parameter (b = -0.000783) for the probability density function of the exponential distribution is only slightly larger than the same from the AIS data (b = -0.000808), as the number of ships generated in the simulation is only slightly higher than reality. The simulation output is not exactly the same as reality. One reason is that the random exponential process generates small differences. Another reason is that the random exponential process is combined with variances in different weeks, different days and different hours. It is important to reflect time intervals properly, because the time intervals also affect the number of ship encounters.

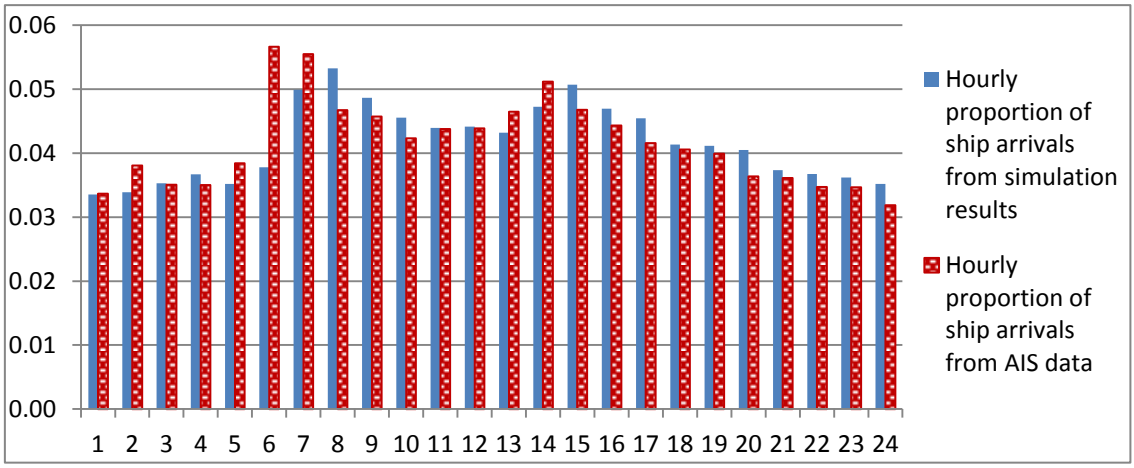

Figure 7-3 Hourly proportion of ship arrivals in 24 hours

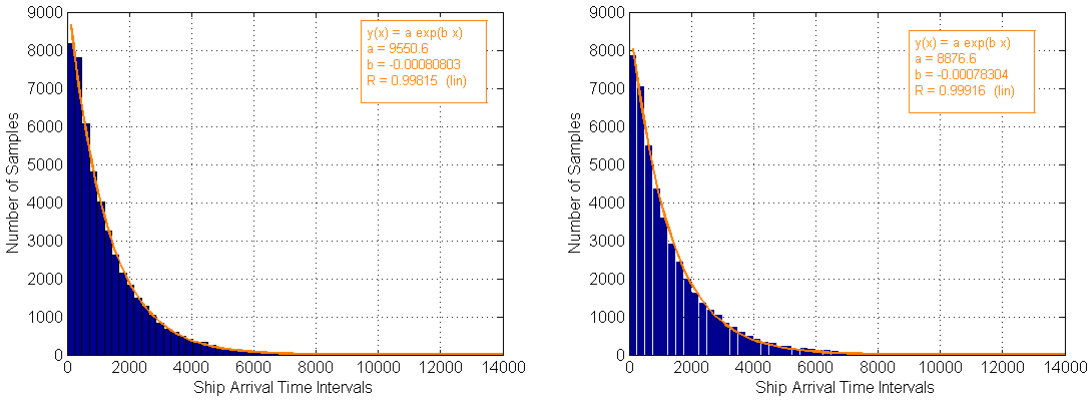

Figure 7-4 Ship arrival distribution of time intervals from the simulation results (left) and the AIS data (right)

7.4.1.2 Face validity for the overall ship trajectories

The following face validity of ship trajectories shows that the ship traffic is similar to the real world and the algorithms of the program are valid. Firstly, it can be observed that the ships normally navigate in the starboard side of the channel. Also, the algorithm for ship avoidance behavior is functioning. Secondly, the ship trajectories from the simulation (Figure VIII-1) are very similar to the ship trajectories from the AIS data (Figure VIII-2). From the trajectories, it can also be observed that the ship positions are spread out in the channel, which shows the feature of the spatial distributions of their positions. Finally, ships with different speeds and sizes are also reflected.

7.4.1.3 Spatial distributions of ship traffic

Different types and dimensions of ships behave differently, as described in Chapter 3. The parameters are characterized by normal distributions with different means and standard deviations. As the algorithms for ship behavior are the same for different types and dimensions of ships, instead of evaluating all the types of ships, evaluating a single category of ships can reflect the correct reproduction of all other ships with different types and tonnages. Therefore, incoming container ships with Gross Tonnage less than 5100 t are chosen for the ship traffic level of validation.

Spatial distributions from the simulation results show that the ship positions are reproduced. The detailed differences for means and standard deviations are given in Table 7-4. Only small differences can be found between the simulation results and the reality. The largest difference is 3.7% of channel width, which is only about 10 m. The deviations are not considered significant.

Table 7-4 Comparison of (non-dimensional) spatial distributions on different crossing-lines between the simulation results and the AIS data

	Mean position in simulation	Mean position from AIS data (with 95% confidence intervals)	Difference in mean positions	Standard deviation in simulation	Standard deviation from AIS data (with 95% confidence intervals)	Difference in standard deviations
crossing-lines 1	0.169	0.185 (0.181, 0.189)	-0.016	0.076	0.076 (0.072, 0.080)	0.000
crossing-lines 5	0.183	0.188 (0.184, 0.193)	-0.005	0.086	0.076 (0.072, 0.081)	0.009
crossing-lines 9	0.218	0.181 (0.176, 0.186)	0.037	0.082	0.093 (0.088, 0.098)	-0.011

What is especially interesting is that the small proportion of ships which navigate on the port side of the channel are properly reproduced (a small proportion of the distribution with a negative x-coordinate in Figure 7-5 that is beyond the curve fitting of normal distribution). This proportion of ships is not included in the input of the simulation, because the random normal processes are used for the input. However, the proportion of ships comes out from the simulation process with ship interactions. This further shows the advantage of an agent-based model and realistic representation of the reality.

For risk analysis, reproducing this characteristic is relatively important. The ships that navigate on the port side are more dangerous than those navigating on the starboard side. It is observed from the simulation that the reason the ships navigate on the port side is that they are overtaking other ships (as can be seen in Figure 7-10), which again increases the risks.

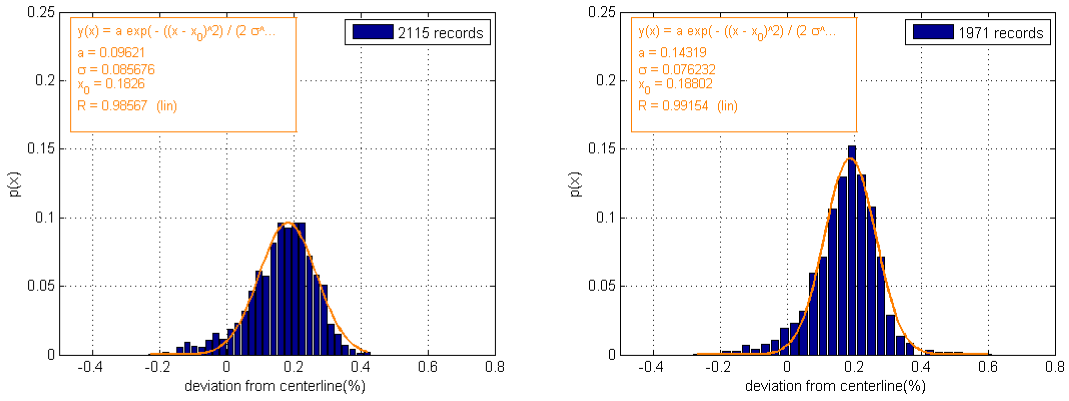

Figure 7-5 Spatial distribution for Incoming containers ships from the simulation results (left) and the AIS data (right) (less than 5100 GT, Crossing-line 5)

7.4.1.4 Speed distributions of ship traffic

Speed distributions from the simulation results show that the ship speed and speed change are reproduced in the simulation. The detailed differences for mean positions and standard deviations can be found in Table 7-5. Only small differences (less than 0.6 kn) can be found between the simulation results and the reality.

7.4.1.5 Heading distributions of ship traffic

Heading distributions from the simulation results show that the ship headings are reproduced in the simulation. Only small differences can be found between the simulation results and the reality (Table 7-6). The standard deviations are normally smaller than the reality, because there is very rigid course following behavior in the simulation, which tries to make the ship headings exactly the same as the curve of the channel. However, in reality ships may take a less rigid course following maneuvering strategy for navigation.

Table 7-5 Comparing speed distributions on different crossing-lines between the simulation results and the AIS data

	Mean speed in simulation (kn)	**Mean speed from AIS data (with 95% confidence intervals) (kn)**	**Difference in mean speed(kn)**	**Standard deviation in simulation (kn)**	**Standard deviation from AIS data (with 95% confidence intervals) (kn)**	**Difference in standard deviations (kn)**
crossing-lines 1	10.8	10.8 (10.62, 10.9)	0.0	1.2	1.2 (1.06, 1.33)	0.0
crossing-lines 5	11.4	11.9 (11.73, 12.03)	-0.5	1.2	1.5 (1.33, 1.62)	-0.3
crossing-lines 9	11.3	11.9 (11.72, 12.05)	-0.6	1.2	1.5 (1.28, 1.62)	-0.3

Table 7-6 Comparing heading distributions on different crossing-lines between the simulation results and the AIS data

	Mean heading in simulation (degrees)	**Mean heading from AIS data (with 95% confidence intervals) (degrees)**	**Difference in mean heading (degrees)**	**Standard deviation in simulation (degrees)**	**Standard deviation from AIS data (with 95% confidence intervals) (degrees)**	**Difference in standard deviations (degrees)**
crossing-lines 1	121.5	122.5 (122.5, 122.6)	-1.0	0.2	1.7 (1.63, 1.76)	-1.5
crossing-lines 5	121.7	122.2 (122.1, 122.2)	-0.4	0.3	1.3 (1.21, 1.35)	-1.0
crossing-lines 9	114.4	115.7 (115.6, 115.9)	-1.3	2.2	2.8 (2.61, 2.89)	-0.6

7.4.2 Individual ship level of the model validation

The ship avoidance behavior in encounters is the most important part in this research, as the appropriate representation of the ship avoidance behavior largely affects the success of the simulation model, and consequently the risk analysis. For validation on the individual ship level, scenarios for ship encounters and scenarios with accidents are provided to check whether the algorithms get the movements in these situations right. For encounters, the trajectories of two ships in the corresponding encountering situation are compared between the simulation results and the AIS data. For validation, the program is set up to reproduce only two ships with encountering situations, taking into account the effects of wind and currents (Appendix XI provides additional cases). For the scenario with an accident, movements of a single ship without influence of other ships are presented.

Other than encounters involving only two ships, there are different emergent situations with different encounters involving different numbers of ships. The collision avoidance behavior for multiple ship encounters is based on the ship encountering behavior of two ships (head-on encountering and overtaking encountering). The multiple encounters involving more than two ships at the same time is important for risks, because the ships get closer and maneuvering becomes difficult. It involves complex collision avoidance based on regulations and common practices, with both speed changes and position shifts in a practical order. However, considering that multiple encounters happen very rarely and there is not enough data available for analysis, the performance of multiple encounters is not evaluated, but this is subject of further research.

7.4.2.1 Validation for head-on encounters

A head-on encounter from the AIS data is selected as a case to reproduce in the simulation. The initial values of the AIS data are transferred into the NetLogo environment. The details of the initial parameters of the two ships (a container ship with incoming direction and a tug with outgoing direction) are shown in Table 7-7. The following paragraphs introduce detailed descriptions for this case.

It is found that the result for a head-on encounter in the simulation is similar to the AIS ship tracks. Figure 7-6 is produced from the simulation, while Figure 7-7 compares the ship tracks from the AIS data and ship tracks derived from the simulation outputs. Both the simulated ship tracks and the AIS ship tracks show the shifts of the positions. In the encountering situation, the outgoing ship navigates as close as possible to the starboard side of the channel bank as the size of the ship is very small. Meanwhile, the incoming ship (large in size) originally navigating at the center of the channel shifts its position to the starboard side of the channel during the encountering, and then it shifts the position to the center of the channel after the encountering.

Table 7-7 Initial parameters for ships in a head-on encounter scenario (case 1)

Parameters	Container ship (Incoming)	Tug (Outgoing)
xcor	-693.13	174.54
ycor	366.07	-87.70
LOA (m)	168.11	24
Gross Tonnage (t)	17488	127
Speed (kn)	7.8	7.80
Heading (°)	126	300
Dr1 (m)	132	82
Dr2 (m)	112	45
Dr3 (m)	127	56
d_{head} (m)	1969	545

Ideally, both the ship tracks are exactly the same. However, the tracks are not exactly the same as shown in Figure 7-7. For the incoming container ship, the simulated ship track is subject to oscillations. Also the largest discrepancy (about 41 m) happens at the bottom right corner of the Figure 7-7. However, in the encountering process, the largest discrepancy of the tracks for the container ship is 24 m, which happens after the Closest Point of Approach. The lateral position shift in the simulation appears larger than in reality. For the tug, the largest aberrancy (27 m) happens before the Closest Point of Approach. A sudden course change happened on the tug in reality, which is not supposed to happen in the simulation. It is found that the simulation cannot reflect this.

The rudder angle is also presented as an output of the simulation (Figure 7-8). The rudder angle changes in a range between -5 and 5 degrees, and these angles are acceptable in the straight channel. This further proves that the simulation can provide realistic results, although we do not have real records of rudder angles to verify the results. However, we can observe oscillations in the rudder angles, and this probably causes the oscillations in the ship tracks. This is partly because the ships follow a very rigorous rule of artificial force, that strictly calculates the rudder angle, but it is not so good for course keeping. An advanced pilot system is needed in the future development that provides different styles of ship navigation that achieve similar navigational strategy. For instance, an experienced helmsman may order rudder angles beyond the range of (-5, 5) degrees and keep the ship steady after maneuvering according to the ship maneuverability. If a new pilot system can reflect this in a simulation, the ship turning can respond faster. As a result, the same navigational strategy will be applied and the avoidance behavior will be more obvious, as required by the COLREGs.

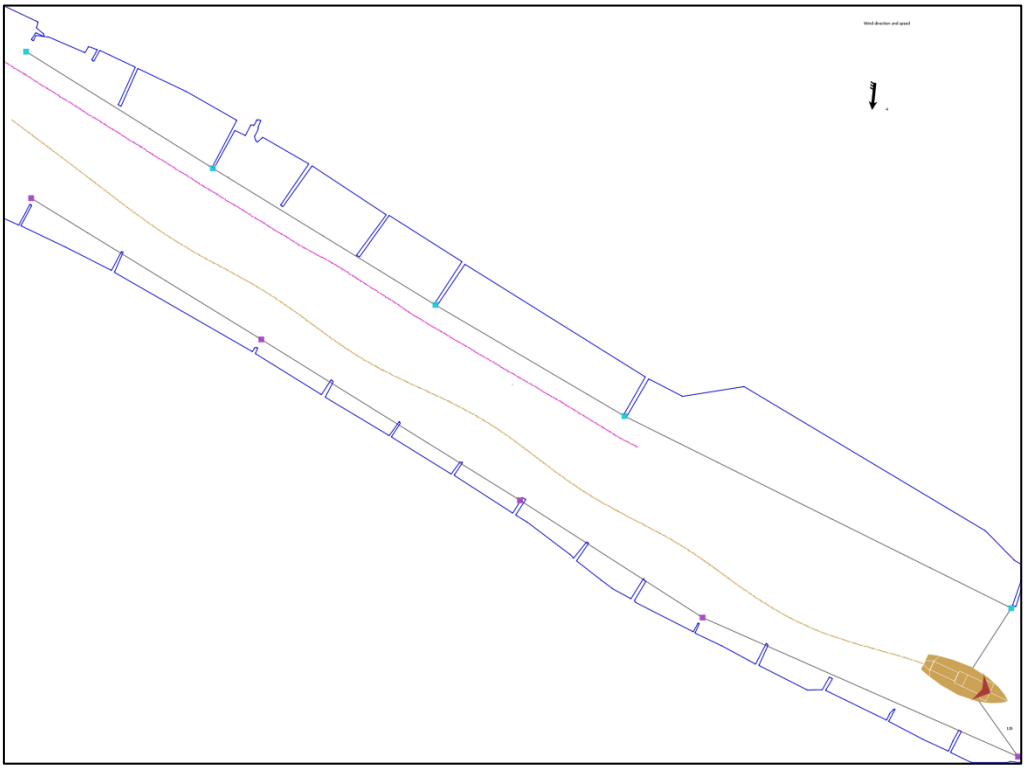

Figure 7-6 Ship tracks of a head-on encounter from simulation interface (case 1)

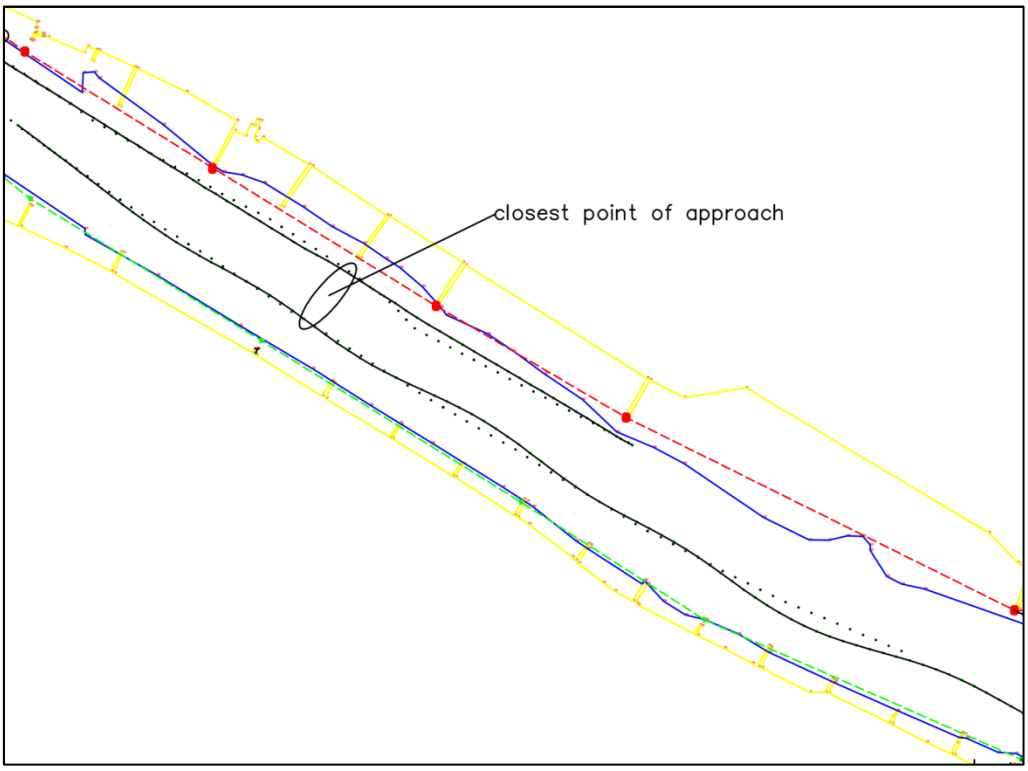

Figure 7-7 Comparing ship tracks of a head-on encounter between the AIS data (black dots) and results from the simulation (black lines) (case 1)

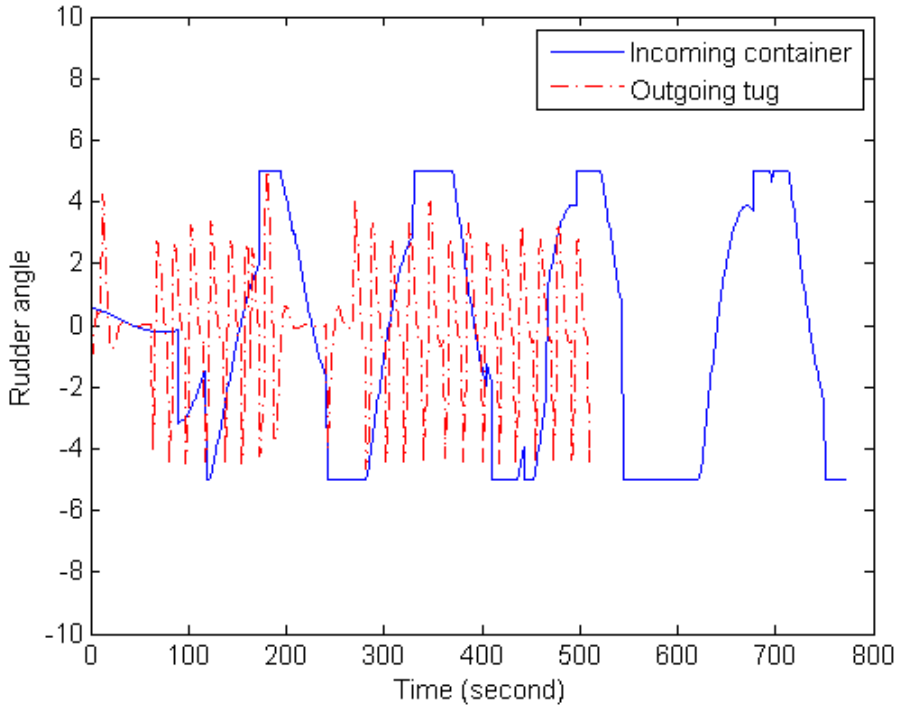

Figure 7-8 Rudder angles in a head-on encounter (a positive value means rudder angle to starboard) (case 1)

7.4.2.2 Validation for overtaking encounters

An overtaking encounter is selected as a case to reproduce a similar scenario in the simulation. The initial values of the AIS data are transferred into the NetLogo environment. The details of the initial values of the two ships are shown in Table 7-8.

Table 7-8 Initial parameters for ships with an overtaking encounter scenario (case 1)

Parameters	Chemical ship (overtaken)	Container ship (overtaking)
xcor	-326.97	-697.22
ycor	102.879	350.04
LOA (m)	79.88	113.76
Gross Tonnage (t)	1640	3999
Speed (kn)	7.8	10
Heading (°)	121	125
Dr2 (m)	69	N/A
Dr3 (m)	96	214
Dl2 (m)	N/A	172.25
$D_{overtaking}$ (m)	740	693
$D_{overtaking\_after}$ (m)	343	436

In general, the simulated ship track and the AIS ship track are very similar. Figure 7-9 is produced from a simulation, while Figure 7-10 is produced from the AIS data. In this scenario, a container ship is overtaking a chemical ship. At first, the two ships are far away from each other, and they are both navigating on the starboard side of the channel. At a critical point in the middle of the Figure 7-9, the chemical ship starts to maneuver even closer to the starboard side. This is a signal for the container ship to start the overtaking maneuver. Then the container ship navigates to the port side of the channel to avoid collision with the chemical ship. Finally, both of the ships move to the positions shown at the bottom right of Figure 7-9. Although there is AIS information missing in Figure 7-10, the trend of the positions in the figure shows that the simulated ship tracks and the AIS ship tracks are very similar.

The tracks are not exactly the same comparing the simulation results and the AIS ship tracks, as is shown in Figure 7-10. For the overtaking ship, the largest discrepancy (47m) happened when the ship started to alter its course for overtaking. That is because the overtaking process happened slightly earlier in reality than in the simulation. The ship tracks in reality also seem smoother than in the simulation. However, when it comes to the Closest Point of Approach, the ship tracks are almost the same. The overtaken ship shifted slightly more to the starboard side in the encountering. There were small oscillations in the simulated ship tracks, and consequently 16 m of discrepancy at most from the AIS ship track can be observed.

The rudder angle is also reflected as an output for the overtaking encounter (Figure 7-11). The rudder angle changes in a range between -5 and 5 degrees, and these angles are acceptable in a straight channel. In particular, the rudder angles for the overtaking container ship are reflected very well. It is obvious and neat (with just a few orders and obvious turning). This also proves that the simulation can provide realistic results.

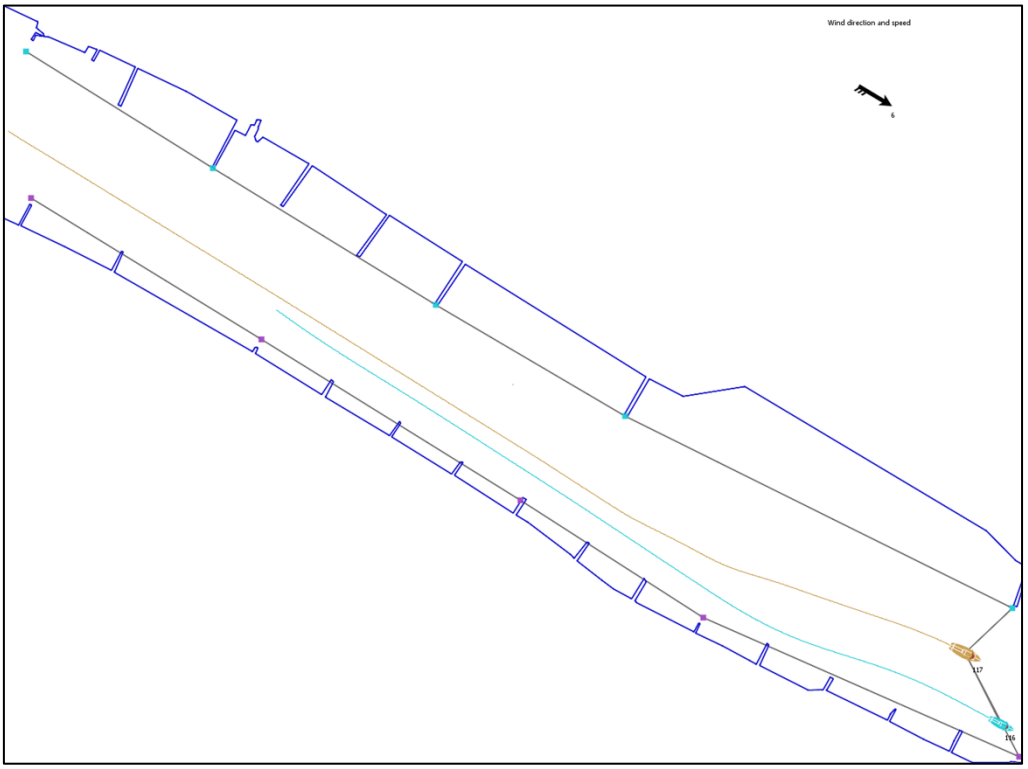

Figure 7-9 Ship tracks of an overtaking encounter from a simulation interface (case 1)

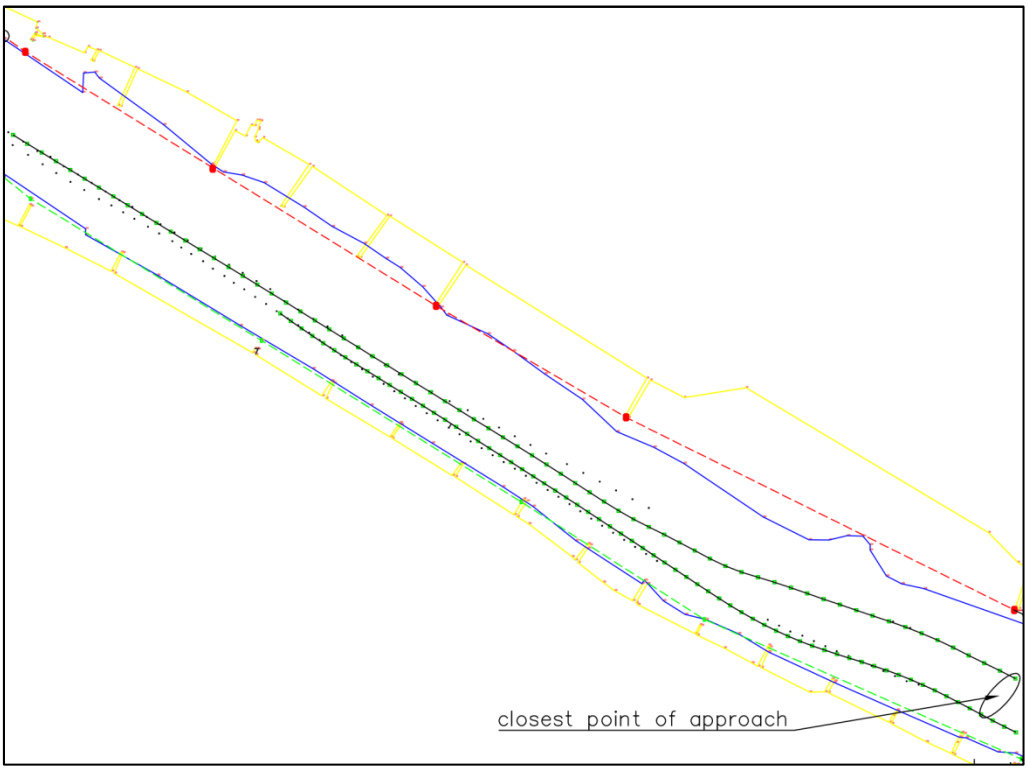

Figure 7-10 Comparing ship tracks of an overtaking encounter between the AIS data (black dots) and results from the simulation (black lines) (case 1)

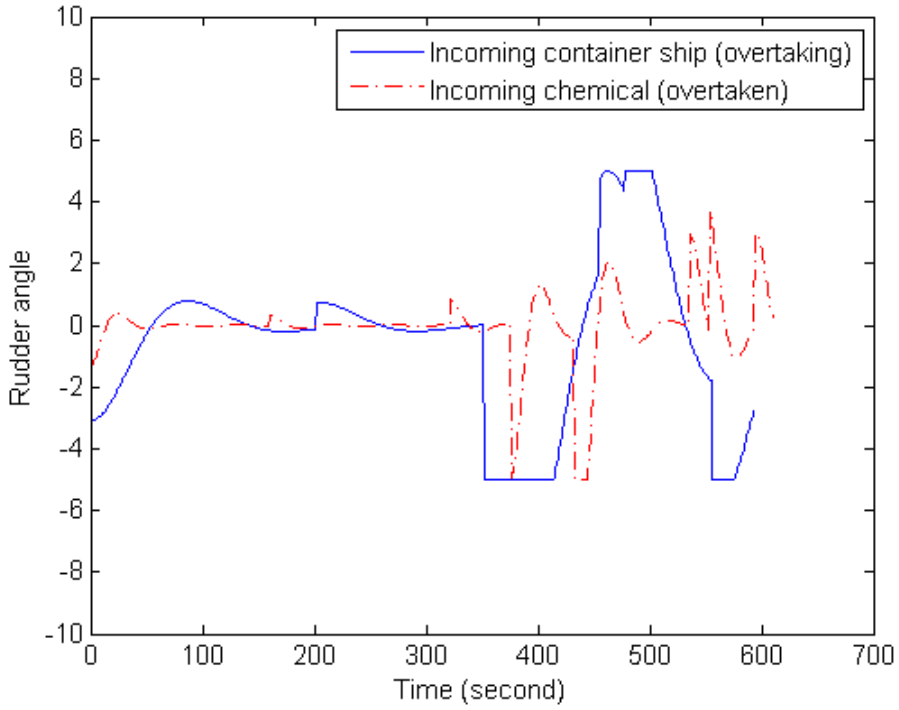

Figure 7-11 Rudder angles in an overtaking encounter (a positive value means rudder angle to starboard) (case 1)

7.4.2.3 Validation of ship behavior with a malfunction

A scenario with engine failure on board is shown in the simulation. The scenario starts with engine failure on board. The currents and wind are taken into account for the movement of the ship, with setup details in Table 7-9. The whole process of the movements is divided into two parts. At first, the ship speed decreases while the inertia of the ship dominates the movements of the ship. After the speed has decreased to a certain point, the currents and the wind effects dominate the movements of the ship.

Table 7-9 Initial parameters for ships in engine failure

Parameters	Ship
xcor	-402.3
ycor	188.5
LOA (m)	201.2
Gross Tonnage	34625.2
Wind speed (m/s)	10.0
Wind direction (degrees)	180.0
Main currents (m/s)	0.6
Speed (kn)	7.2
Time-constant (minute)	8.0
Drift speed by wind (m/s)	0.3

Figure 7-12 shows the process of ship movements with engine failure. The relative positions in the whole process are shown, with the ship shapes in the figure. The small arrows in the figure stand for the current field, while the arrow at the upper right corner stands for the wind (with direction and magnitude). In the figure, a 201 m incoming ship navigating with a speed of 7.2 kn is suffering from engine failure (positioned with the ship shape at the upper left corner of the figure). Then, the ship is not able to change its course anymore. With the force from wind, the position shifts to the starboard bank of the channel very slowly. After 8 minutes of time, the ship speed decreases dramatically. The force of wind and currents dominate the movements of the ship, and the ship exposes her abeam to the wind (with 90 degrees of heading). Finally, the ship drifts with the effect of wind and currents, and then collides with the starboard bank of the channel (positioned with the ship shape in the bottom right). The crosswind showed its effects in the ship track. The currents are also reproduced in the simulated environment.

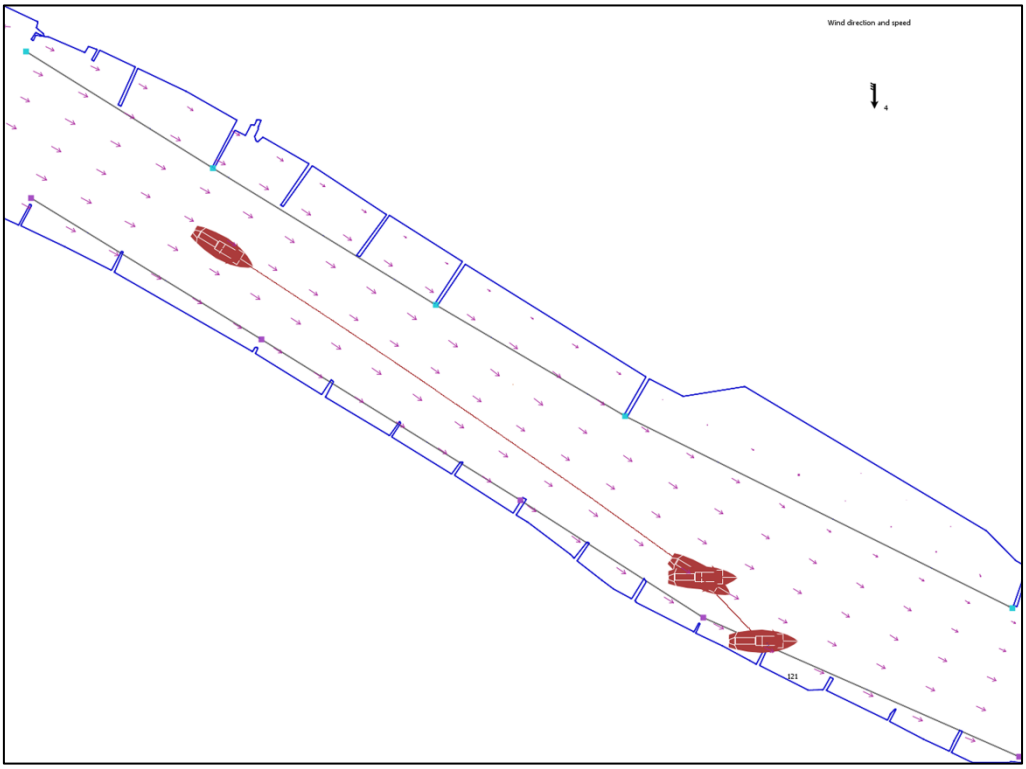

Figure 7-12 Ship tracks of an engine failure scenario from a simulation interface with the current field (indicated by vectors in the waterway) and the wind from the north (indicated by a vector) in the upper right corner

7.5 Discussion

Calibration and validation of the model are presented in this chapter to show how much we have achieved to simulate the ship traffic. In general, this is the highest accuracy that has been achieved for simulating ship traffic on both a traffic level and individual ship level so far. Further study could be developing a standard procedure for calibrating maritime traffic simulation.

In the model validation, this study evaluated the reproduction of ship behavior on both a ship traffic level and individual ship level. Firstly, on a ship traffic level, differences in the number of ship arrivals are found between the simulation and the AIS data. Further understanding of ship arrivals in time was needed, which included the weekly fluctuation of number of arrivals and daily fluctuation of the numbers of arrivals, taking into account the hourly differences of arrivals and time intervals. Secondly, on an individual ship level, different scenarios of ship encounters and accidents are reproduced. The effect of currents and wind are also included in the scenarios with accidents. Ship tracks in the simulation results are compared with the ship tracks derived from the AIS data. This thesis focused on encounters with two ships. Encounters that involve multiple ships are divided into several head-on and overtaking encounters in the simulation. However, in reality, the evasive actions involving multiple ships are not so straightforward. Encounters that involve multiple ships need further research and implementation in the simulation to achieve the maximum capacity of the multi-agent simulation. Effects from wind and currents are proved to be successfully implemented in the model by means of the submodels, although these effects could not yet be compared with any real data. Finally, more advanced hydrodynamic models for ship maneuvering, current effects, and wind effects may need to be implemented in the future to make the simulation more accurate and realistic.

7.6 Conclusions

This chapter checked that the required elements, inputs, and equations introduced in the previous chapters are correctly implemented in the simulation model. In the calibration, the ranges of the inputs and parameters were determined to ensure correct reproduction of reality. In the model validation, statistics and illustrations are provided to compare the output from the simulation with the AIS data analysis. The simulation output show similarity with the AIS data. It is concluded that the simulation model can reproduce realistic ship traffic in a straight waterway. The achieved level of precision for ship movement has not been found in existing literature. Further research will be needed to develop the ANTS model to a curved waterway and situations with crossing traffic.

8. CASE STUDY OF THE CHINESE WATERWAY

8.1 Introduction

This chapter presents a case study of a Chinese waterway, including the AIS data analysis (excluding the development of the artificial forces), simulation results and validation. This case study demonstrates that the artificial force field concept and multi-agent simulation developed for the Dutch waterways is applicable to the Chinese waterways. This further proves that the agent-based artificial force model has potential to be applicable worldwide for nautical traffic simulations. This chapter shows the similarities and differences in the AIS data analysis of ship traffic behavior and characteristics of the waterway between the Dutch case and the Chinese case, and the effects of the differences. Finally, the results of the model validation for this case are presented.

In this case, a nearly straight waterway at the Su-Tong Bridge is chosen (31° 46' 39.54" N, 120° 59' 41.49" E). The Su-Tong Bridge is located in Nantong city of Jiangsu Province, China, 108 kilometers from the mouth of the Yangtze River. The river is 8,146 meters wide and the main waterway passes under the Su-Tong Bridge. The bridge has a main span of 1,088 meters (890 m navigable) and 62 meters clearance in height. It was designed for passage of 50,000 t container ships and 48,000 t convoys. The characteristics of the waterway and the position of the bridge are shown in Figure 8-1.

The ship traffic under the Su-tong Bridge is quite busy. So it is an interesting test case for applying the artificial force field theory. Relevant local ordinances include the following. According to the separation scheme of the Jiangsu Waterway, the 890 m navigable waterway is separated into 4 traffic lanes, 2 traffic lanes for incoming ships and 2 traffic lanes for outgoing ships. The 500 m wide “Deep-Draft channel” is in the middle, marked by navigational aids, with a 100 m wide traffic separation zone in the middle. The two 200 m wide (if available) “suggested channels” for incoming “small ships” and outgoing “small ships” are located at both sides of the “deep-draft channel”. The “deep-draft channel” is specifically navigable for “very large ships” and “large ships”, and the “suggested channels” are specific for “small ships”. According to the local regulations, “very large ships” are ships

(convoys) which have a fresh water draught of more than 9.7m or a length of more than 205m, or ships (convoys) with a maximum height above water which is close to the span clearance of the bridge and overhead cables, or ships (convoys) with a restricted maneuverability. Also “large ships” are ships (convoys), which have a fresh water draught of between 4.5m and 9.7m or a length between 50m and 205m in the regulation. “Small ships”, also defined in the regulations, are ships (convoys) with dimensions smaller than “very large ships” and “large ships”. An important ordinance factor is that overtaking is not allowed in the waterway near the bridge area. These regulations should be reflected in the simulation.

Figure 8-2 shows a map that provides all the geographical information that is needed in the simulation. The “Deep-Draft channel” is indicated by boundaries of the “Deep-Draft channel”, that is indicated by the navigational aids. The “suggested channel” is outside the boundaries of the “Deep-Draft channel”. The Su-Tong Bridge is perpendicular to the “Deep-Draft channel”. The 7 crossing-lines for data analysis are also shown on the map.

The positions of the navigational aids are not correct in Figure 8-2. Therefore some ship positions are plotted outside the channel at both ends of the waterway in Figure XII-1. Normally, the ships do not navigate outside the traffic lanes, which are marked by the navigational aids. However, the positions for the navigational aids come from a map made in the year 2001, which is 10 years before the year that the AIS data was collected. The positions of the navigational aids might have been adapted to the new geographical shape of the waterway, as sediment transportation can result in shifts of the waterway shape. With incorrect navigational aids, the traffic lanes on the map are no longer correct. Therefore, when the ship positions are plotted on the map, they are shown outside of the traffic lanes. Nevertheless, the positions of the navigational aids in the neighborhood of the bridge are correct, as the bridge piers are always fixed.

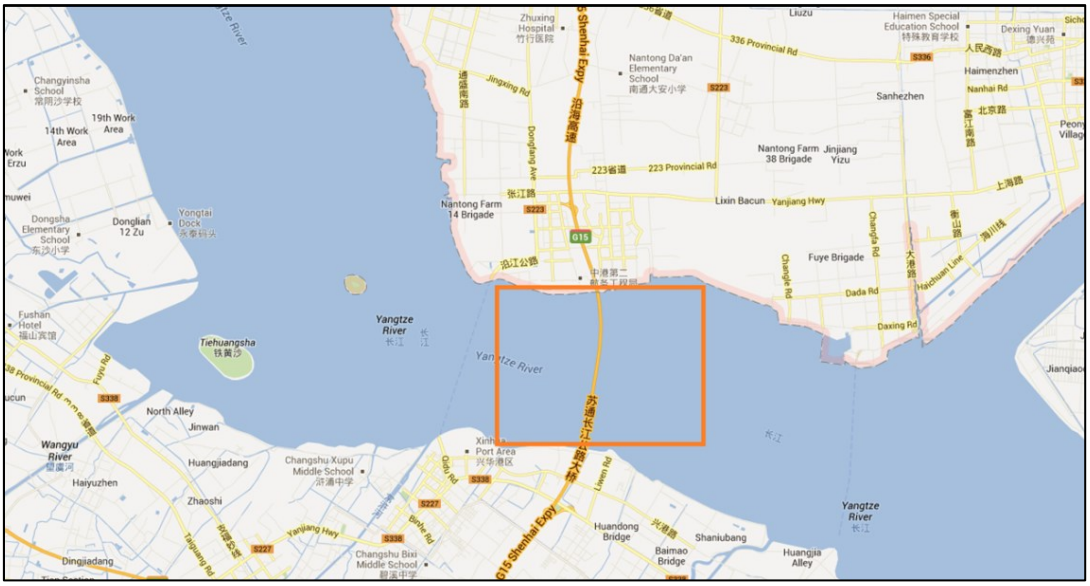

Figure 8-1 The characteristics of the waterway and the simulated area with the bridge (in the rectangle)

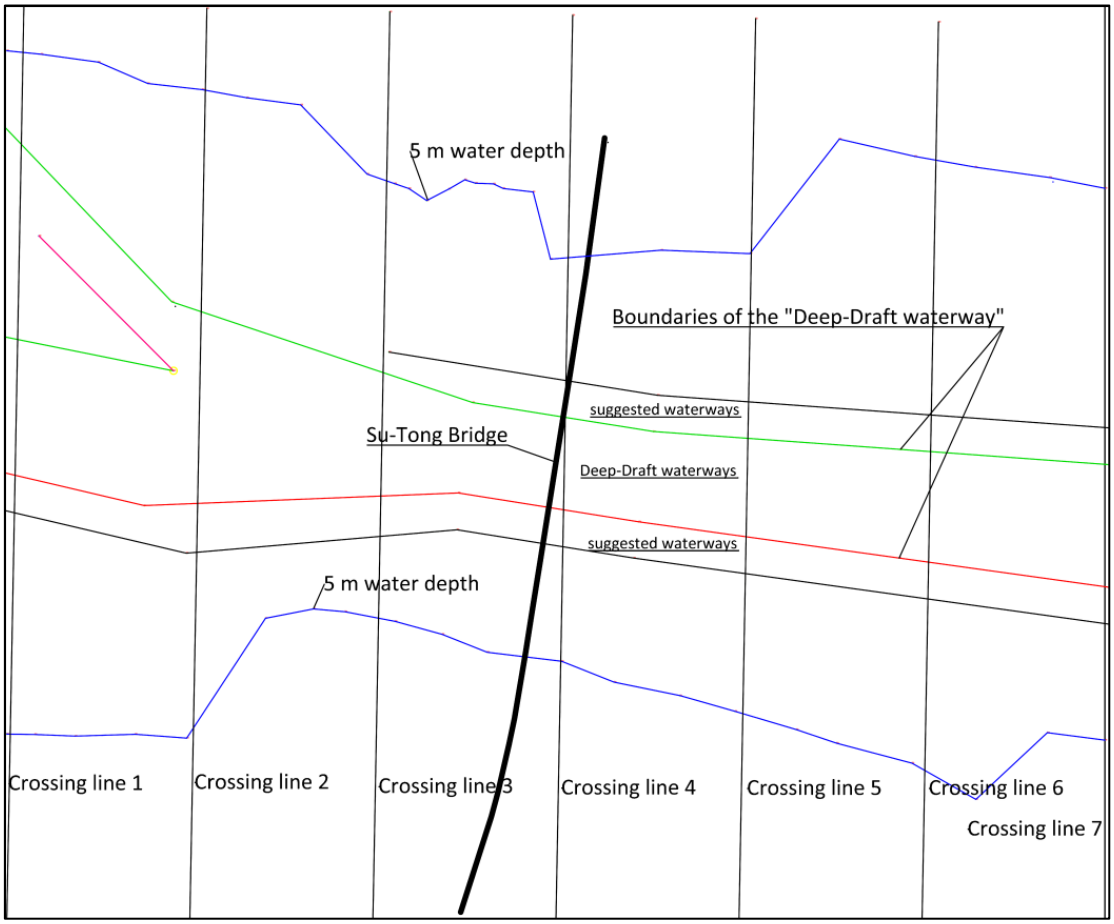

Figure 8-2 The studied area of the waterway and positions of the waterway boundaries and crossing-lines

8.2 Preprocessing AIS data for the Chinese case

8.2.1 Introduction of the Chinese AIS data studied

The China MSA (Maritime Safety Administration of the People's Republic of China) provided three months of AIS data for the case study and was kind enough to provide other related information such as records of wind and visibility. The AIS data was not very well maintained, as most of the information on the ship types and LOA (Length overall) is missing. Positions of the GPS antenna were deleted in the data collected. Another problem of the data is that many ships were not equipped with an AIS system onboard, and therefore those ships could not be observed in the data.

Crossing-lines which are perpendicular to the waterway are made to derive the data for ship traffic behavior. The crossing-lines are 1,000 m apart from each other, with the fourth crossing-line lying at the same geographical location of the Su-Tong Bridge. Then the ship behavior in an area of 3,000 m on each side of the bridge is analyzed. The parameters analyzed are the same as in the Dutch case.

8.2.2 Ship arrivals for traffic density for the Chinese case

8.2.2.1 Daily ship arrivals

Based on the AIS data analysis of October 2010, the daily number of incoming ship passages is 208 on average, while the daily number of outgoing ship passages is 205 on average. However, in reality the daily number of ship passages is much larger than this number, and the next chapter (Chapter 9) will demonstrate that the simulation is able to compensate for the number of ships that is missing in the AIS data, and reproduce the real number of ship passages. This chapter however demonstrates and evaluates the simulation model that reflects the daily ship arrivals based on the AIS data analysis.

8.2.2.2 Hourly ship arrivals

The number of ship arrivals in different hours throughout the day varies. The proportions of ship arrivals throughout 24 hours are observed from the AIS data, see Figure 8-3. The proportions of ships for each hour are aggregated from 12 days of the AIS data. The proportions of ships in different hours are very different. The peak hours happened in the afternoon, while there are much fewer ships during the night.

8.2.2.3 The time intervals between ships

With Equation (8 - 1), the time intervals (TI) can be obtained from the database. Also the histogram of the time intervals with exponential curve fitting (similar to the Dutch case) is shown in Figure 8-4.

$$\mathrm{TI_n} = \mathrm{TA_n} - \mathrm{TA_{n-1}} \qquad (8 - 1)$$

The exponential distribution function can be derived for the time intervals of outgoing ship arrivals:

$$\mathrm{f(x)} = \frac{1}{377} e^{-\frac{1}{377}x} \qquad (8 - 2)$$

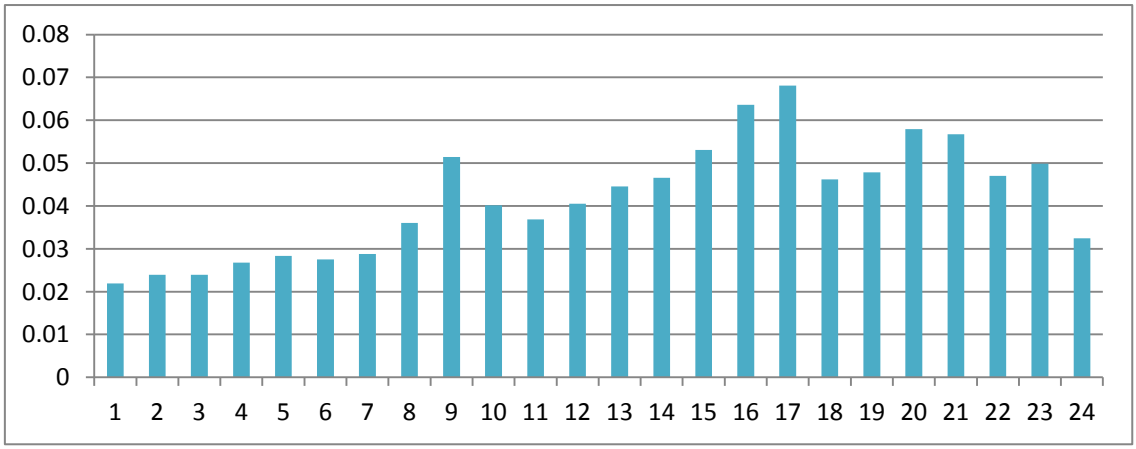

Figure 8-3 Hourly proportion of outgoing ships in 24 hours in China (the x-axis is the hours and the y-axis is the proportions)

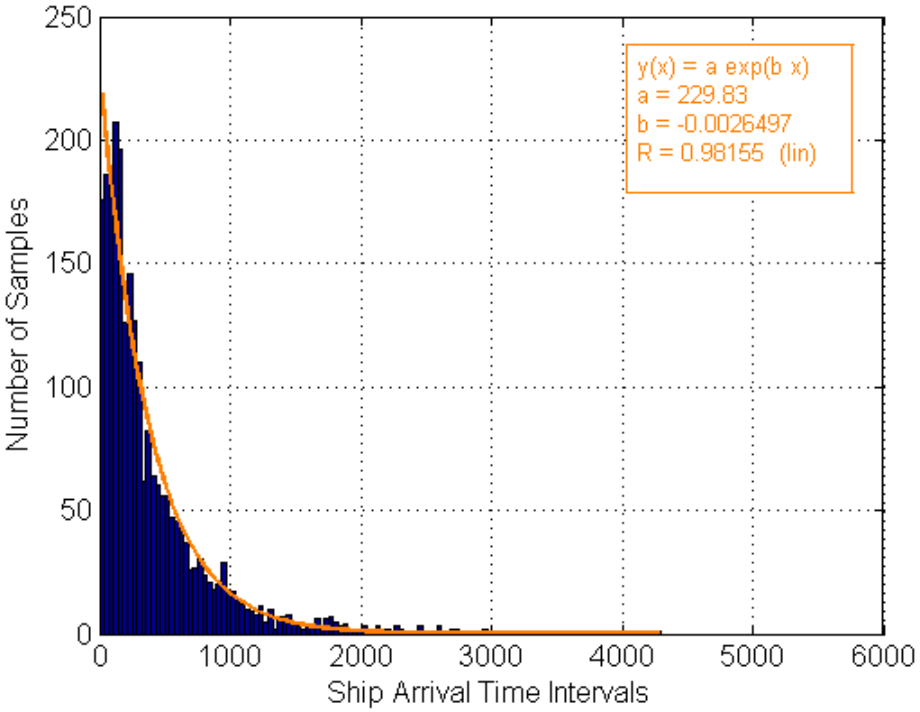

Figure 8-4 Ship arrival distribution of time interval in China (2,490 samples)

8.2.3 Ship traffic behavior for the Chinese case

8.2.3.1 Vessel classification based on the LOA

The dimensions of ships navigating in the Su-Tong Bridge area are smaller than the Dutch case. Figure 8-5 shows the histogram of the observed ship lengths that are available in the AIS data. According to the local regulations on the traffic separation scheme, the ships are further divided into two groups according to the LOA, as the information on draught is not available. Thus, in this analysis, “small ships” are ships with a LOA of less than 50 m, and “large ships” are ships with a LOA larger than 50m.

8.2.3.2 Spatial distribution of ships

The lateral spatial distribution on the crossing-lines is an important input at the boundaries of the simulation model. The distributions provide the statistical properties of ship traffic behavior. Figure 8-6 shows an example of the lateral spatial distribution for incoming “large ships” at the location of the Su-Tong Bridge. In the Chinese case, we set the width of “deep-draft channel” as the unit of waterway width for non-dimensional spatial distributions. On crossing-line number 4, the channel width of the “deep-draft channel” is 500 m. Therefore, in Figure 8-6, the value 0.5 on the axis is the point for the starboard boundary of the traffic lane for “large ships”. The mean position for the ship traffic is 0.31, with a standard deviation of 0.07. We can observe that the ship positions lie in the 0.1 to 0.5 range of the non-

dimensional waterway width. This means almost all the incoming ships are navigating in the 200 m of traffic lane specific for the incoming “large ships” under the bridge.

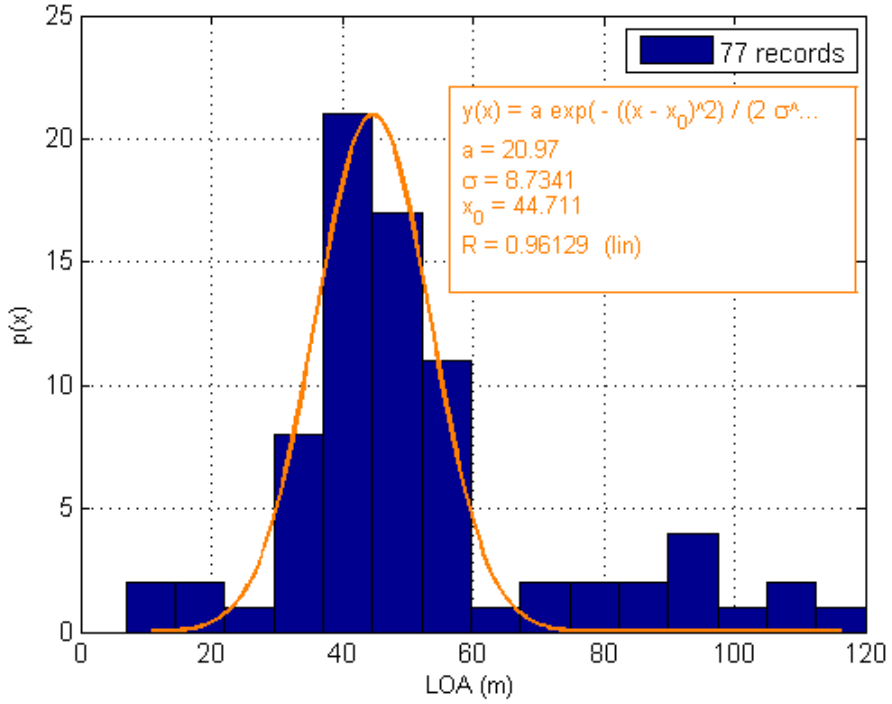

Figure 8-5 Histogram of the ships with the LOA in Su-Tong Bridge area for the Chinese case

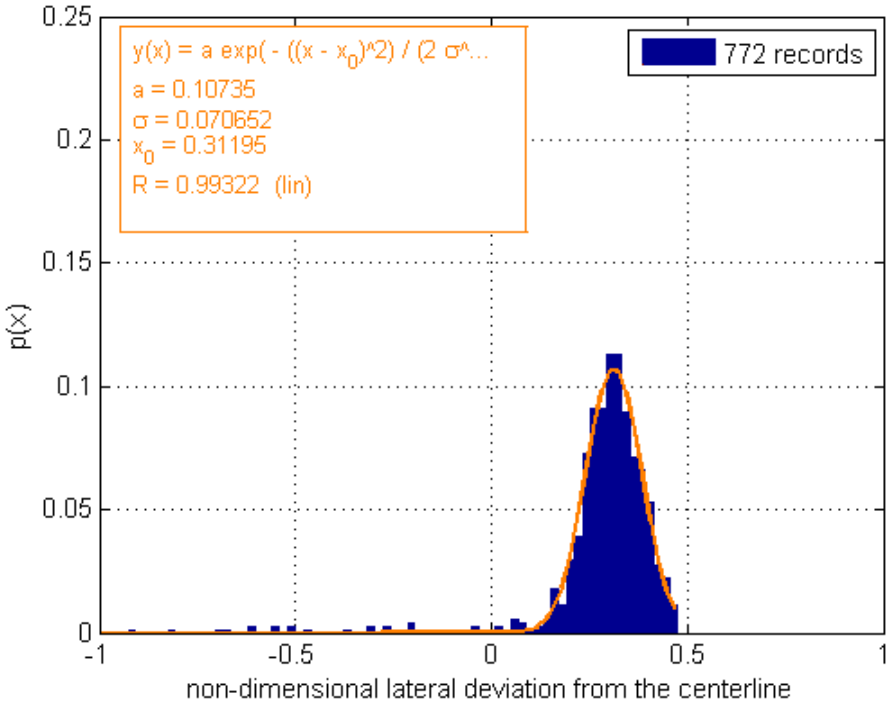

Figure 8-6 Spatial distribution for incoming “large ships” at the crossing-line number 4 for the Chinese case

Other than Figure 8-6, Table 8-1 lists the different means and standard deviations of the normal distributions for “large ships” and “small ships” for selected crossing-lines. From the table, it is found that the non-dimensional mean positions are changing, especially at the boundaries of the waterway, and the ships do not strictly conform to the rules of the traffic separation scheme. It is also found that the standard deviations are also changing. The standard deviations for ship spatial distributions are getting smaller from west to east. That means the ships spread over a larger space at the west boundary of the area.

8.2.3.3 Speed distributions of the ships

Ships sail with different speeds in the bridge area on different crossing-lines (Figure 8-7). The following observations can be made. (i) The “large ships” navigate with a relatively higher speed than “small ships” in general. (ii) The outgoing “large ships” navigate faster than the incoming ships. This shows the influence of the river currents on the ship speeds. However, for “small ships”, the speeds for both incoming ships and outgoing ships are very similar. (iii) The ships do not change speed much in the area, which is different from the Dutch case.

A normal distribution is used to describe the speed distribution for the ships in Figure 8-8. In the simulation, the parameters of mean values and standard deviations are used to generate random ship speeds at the boundaries of the simulation model. Other than Figure 8-8, Table 8-2 shows the different parameters from normal distributions for ship speeds of “large ships” and “small ships” on both the incoming and outgoing direction on selected crossing-lines.

Table 8-1 Parameters of non-dimensional mean lateral positions and standard deviations for “large ships” and “small ships” on selected crossing-lines for the Chinese case

Crossing-line number	Ship category	Direction	Mean deviation from the center	Standard deviation
1	Large ships	Incoming	0.778	0.159
1	Large ships	Outgoing	0.633	0.220
1	Small ships	Incoming	0.867	0.341
1	Small ships	Outgoing	0.574	0.138
4	Large ships	Incoming	0.312	0.071
4	Large ships	Outgoing	0.249	0.070
4	Small ships	Incoming	0.679	0.094
4	Small ships	Outgoing	0.643	0.088
7	Large ships	Incoming	-0.049	0.068
7	Large ships	Outgoing	0.731	0.081
7	Small ships	Incoming	0.731	0.081
7	Small ships	Outgoing	1.151	0.078

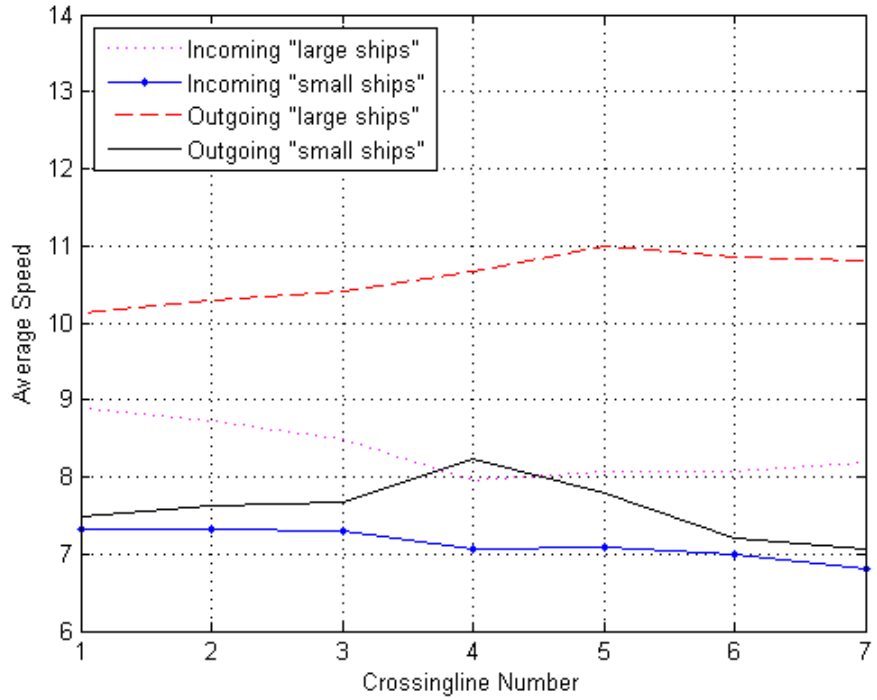

Figure 8-7 Average speed of ships in both incoming and outgoing directions throughout the waterway from crossing-line number 1 to crossing-line number 7 for the Chinese case (6 km of waterway)

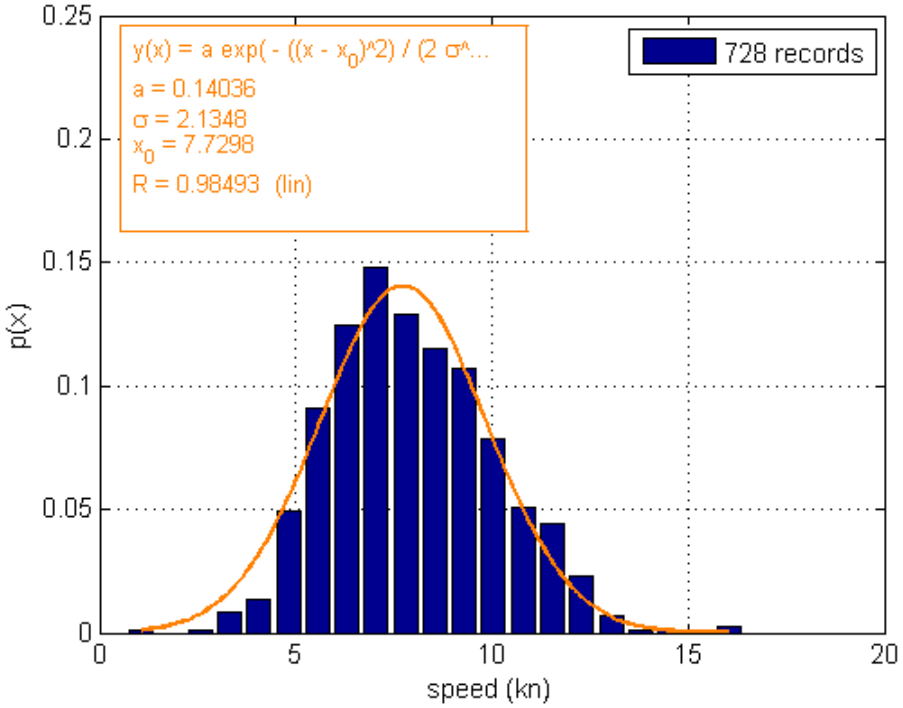

Figure 8-8 Speed distribution for incoming “large ships” at crossing-line number 4 for the Chinese case (location of bridge)

Table 8-2 Parameters of mean speeds and standard deviations for “large ships” and “small ships” on selected crossing-lines for the Chinese case

Crossing-line number	Ship category	Direction	Mean speed (kn)	Standard deviation (kn)
1	Large ships	Incoming	8.75	1.78
1	Large ships	Outgoing	10.57	1.97
1	Small ships	Incoming	7.18	1.43
1	Small ships	Outgoing	7.17	2.01
4	Large ships	Incoming	7.73	2.13
4	Large ships	Outgoing	11.11	2.07
4	Small ships	Incoming	6.98	1.85
4	Small ships	Outgoing	8.14	2.13
7	Large ships	Incoming	7.96	1.92
7	Large ships	Outgoing	11.37	2.30
7	Small ships	Incoming	6.73	1.51
7	Small ships	Outgoing	7.00	1.93

8.2.3.4 Course distributions of ships

A normal distribution is fitted to the course histogram (Figure 8-9). The parameters of mean values and standard deviations are used for generating random ship courses at the boundaries of the simulation model. Table 8-3 shows the different parameters from normal distributions of ship courses for “large ships” and “small ships” on both incoming direction and outgoing direction for selected crossing-lines.

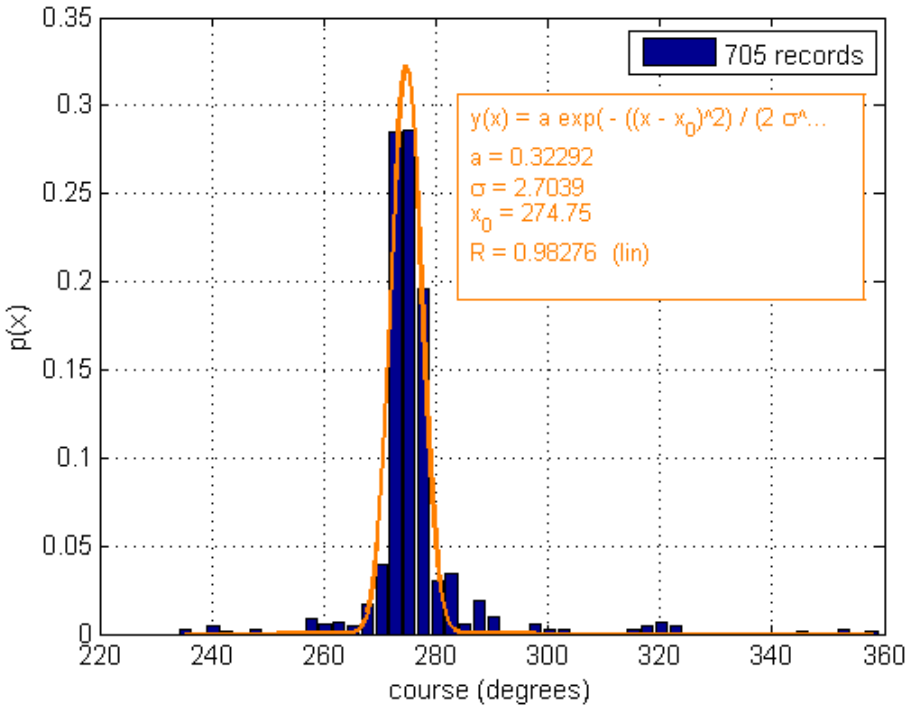

Figure 8-9 Course distribution for Incoming “large ships” at crossing-line number 1 (location of bridge) for the Chinese case

Table 8-3 Parameters of mean courses and standard deviations for “large ships” and “small ships” on selected crossing-lines for the Chinese case

Crossing-line number	Ship category	Direction	Mean course (degrees)	Standard deviation (degrees)
1	Large ships	Incoming	275	2.7
1	Large ships	Outgoing	99	3.3
1	Small ships	Incoming	285	10.4
1	Small ships	Outgoing	99	4.5
7	Large ships	Incoming	278	2.4
7	Large ships	Outgoing	106	2.2
7	Small ships	Incoming	278	3.5
7	Small ships	Outgoing	108	3.7

8.3 Environmental conditions as input for the Chinese case

8.3.1 Introduction

Environmental conditions are analyzed to know their impact on ship behavior. As was discussed in Chapter 4, the relatively low speed of wind and currents in the hinterland has very little effect on the ship behavior, when the ships are under control. However, if any malfunction happens onboard, the ship behavior is considerably influenced by wind and currents. Therefore the local environmental conditions also need to be reflected in the simulation.

8.3.2 Wind influence

As in the Dutch case, the wind directions are shown in compass degrees. 0 and 360 degrees stand for wind coming from the north, 90 degrees stand for wind coming from the east, 180 degrees is southern wind and 270 degrees is western wind. The speed of wind is recorded at an interval of 1 min. The measurement point is located at the “Hai-Tai Ferry Jetty”, which is located about 10 km downstream from the Su-Tong Bridge.

Two months of wind records were collected for the analysis. We also use a “wind rose” to represent the frequency of wind for all directions (Figure 8-10). For wind speed, normal distribution is used to fit the wind speed data (Figure 8-11). It turns out that the wind speeds are very low, as most of the wind records are less than 10 m/s.

From the analysis, it is obvious that the influence of wind is very small, so wind influence is neglected for simulating ships which are under control, as the influence can be easily compensated with maneuvering. For the ships that are out of control, the wind influences are taken into account for ship drifting.

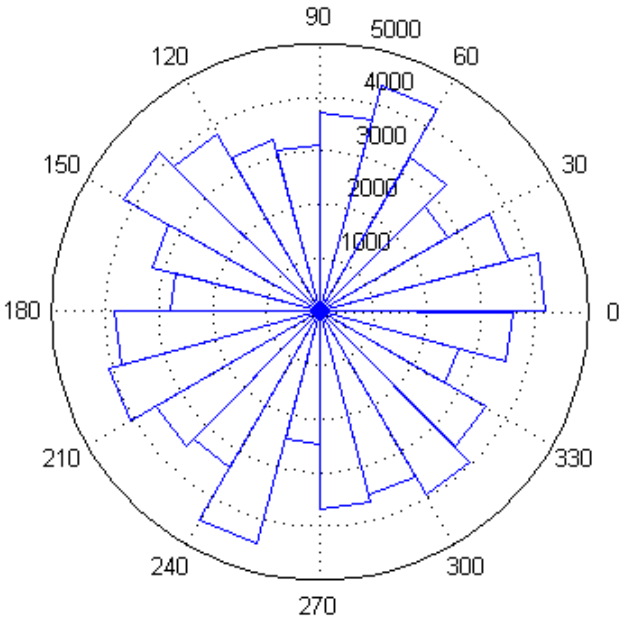

Figure 8-10 Wind rose of October and November in 2010 for the Chinese case (85,336 valid records)

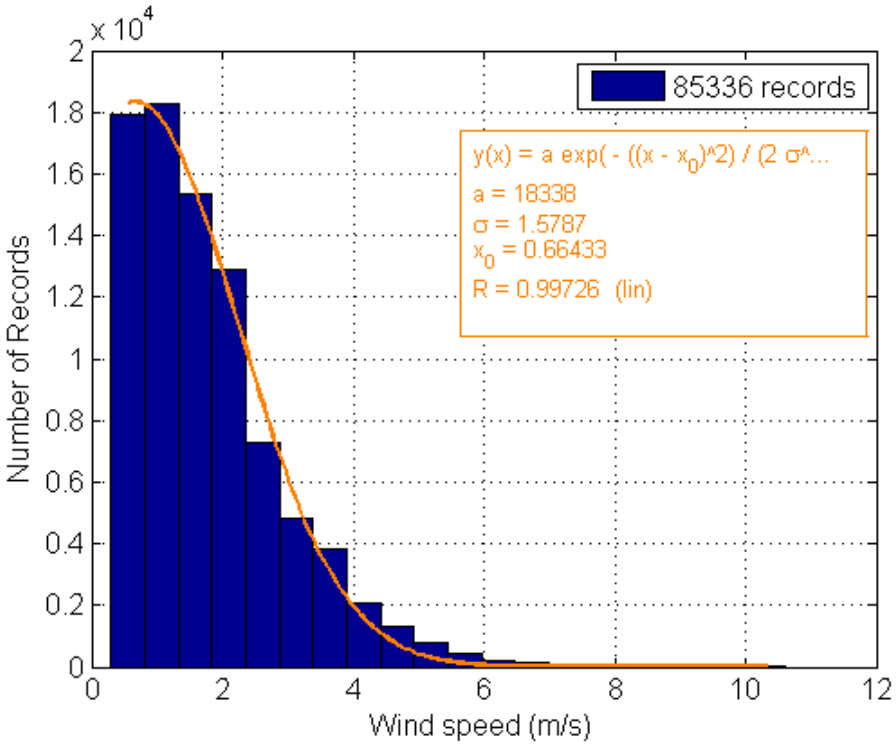

Figure 8-11 Wind speed distribution for October and November in 2010 for the Chinese case

8.3.3 Currents influence

3D simulation results of the current field are not available for the Yangtze River. Thus, only measured data at selected locations is available. In order to reflect the current influence in the traffic simulation, the maximum currents in both upstream and downstream are selected to approximate the currents. The approximation may not be accurate, but it is based on the data we were able to get for this project. This case demonstrates that the currents are included, although the data is not sufficient compared to the Dutch case in the previous chapter. The input data for currents can be modified if more data is available for the model application in the future.

Based on 20 days of measured currents from 19/09/1999 to 28/9/1999 (a period with high water discharge) and 21/2/2000 to 01/03/2000 (a period with low water discharge), the maximum incoming current speed is 2.44 m/s, with a flow direction of 269 degrees. The maximum outgoing current speed in is 3.86 m/s, with a flow direction of 091 degrees. Based on the tidal cycle in the Dutch case, the current speed is approximated as:

$$V_c = -0.71 + 3.15 * \cos\Theta \qquad (8 - 3)$$

where V_c is current speed (m/s), and a positive value means outflowing direction (091 degrees). Θ is phase position (0 to 360 degrees) in a tidal cycle. It is assumed that a full tidal cycle is 12 hours. Then, the phase difference for two adjacent hours ($\Delta\Theta$) is 30 degrees.

8.3.4 Visibility influence

The records of visibility are maintained in the same way as the wind. The visibility is recorded in a unit of meters, at an interval of 1 min per record. The measurement point is also located at the “Hai-Tai Ferry Jetty”, which is about 10 km downstream from the Su-Tong Bridge.

Two months of visibility records were collected for the analysis. We also use the histogram distribution to represent the frequency of visibilities (Figure 8-12). Normally the visibility is quite good, as most of the records are larger than 1,000 m. Influence on the visibility for the ships is very small, and therefore the influence of visibility is neglected in the simulation.

8.4 Simulation Setup for the Chinese case

8.4.1 Setup for coordinate systems

Similar to the Dutch case, the map for the Chinese case (Figure 8-2) is also transferred into the NetLogo coordinate system (Table 8-4). Each patch in the NetLogo environment stands for 100 m^2 of geographical area in reality. In other words, each unit of the NetLogo coordinate system stands for 10 m of length.

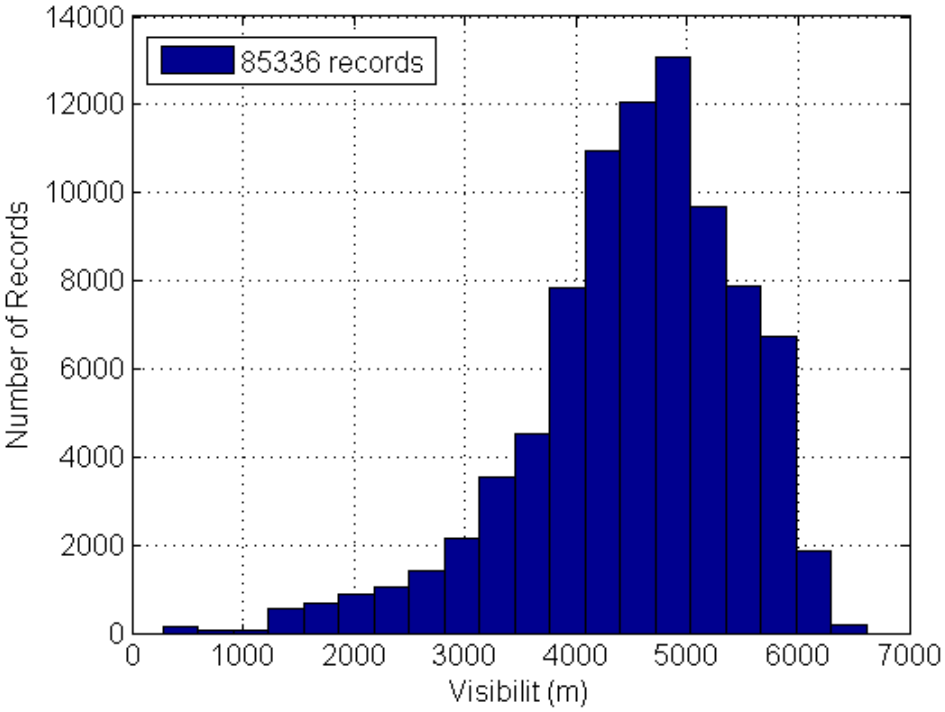

Figure 8-12 Visibility distribution from October and November in 2010 for the Chinese case

Table 8-4 Different coordinate systems for the boundary points of area in the simulation

Coordinate systems	Latitude and Longitude	Universal Transverse Mercator (UTM)	Netlogo coordinate system (ycor, xcor)
Northwest	31.799695 N, 120.962699E	3520041 N, 307131 E	250, -300
Southeast	31.75561 N, 121.027002 E	3515041 N, 313130 E	-250, 300

8.4.2 Setup for proportion of ships in different lanes for the Chinese case

As the LOA of ships are missing from the AIS data, we can only categorize the ships by the traffic lane they were navigating from the AIS data observation. Based on statistical analysis, there were 2,373 ships examined, of which 1,593 ships were navigating in the “Deep-Draft channel” and 780 ships were navigating in the “suggested channel”. The “large ships” are supposed to be navigating in the “Deep-Draft channel” and the “small ships” are supposed to be navigating in the “suggested channel”. Therefore, the statistical values are used in the proportions of “large ships” and “small ships” in the simulation.

8.5 Model calibration for the Chinese case

The program for the Chinese case is only slightly modified from the program for the Dutch case. The algorithms in the program are very similar, except for small modifications of ship behavior adapting to the local regulations and common practices. Most of the values for the

parameters and ranges are default values from the Dutch case as well. However, some of the parameters are calibrated for different geographical conditions and characteristics of the ship traffic in this case.

As the AIS information for many parameters is missing, this case takes many default values from the Dutch case. Firstly, parameters for gross tonnage are the same as the Dutch case, and gross tonnage is calculated based on the LOA. Secondly, the maneuverability indices of K and T are based on the default values. Thirdly, the artificial forces, thresholds of distances and the ranges are based on the Dutch case. Finally, head-on situations only apply in the "Deep Draft channel", because of the separation scheme.

However, there are also several parameters that are specific for the Chinese case. Firstly, lateral positions (Table 8-1) and speeds (Table 8-2) from different categories of ships at the boundary of the simulation are derived from the local AIS data analysis. Secondly, speed acceleration is not considered, because we did not observe much speed change in this case. Thirdly, the weekly number of ships and monthly differences are ignored, as we did not collect a whole year of AIS data for this case. Fourthly, there are specific rules in the simulation for the Chinese case, as separation scheme and specific rules are applied in this area. Therefore, the following rules are implemented into the program specifically for the Chinese case. (i) The ship traffic is separated into four traffic lanes based on the LOA. (ii) The overtaking encounters in different traffic lanes are not treated as encounters in the simulation, as they are navigating in separated lanes. (iii) The ships will not overtake each other in bridge area, as overtaking is not allowed in the bridge area. (iv) The boundaries of the "bridge area" are not defined in the regulation. In this thesis the "bridge area" is defined as the area around the bridge that is inside the boundary indicated by the closest navigational aids to the main bridge towers. As the closest navigational aids are 500 m away from the main bridge towers, the length of the "bridge area" is 500 m on either side of the bridge. Overtaking is halted in the simulation when the ships are at a distance of less than 500 m to the bridge.

8.6 Simulation output and validation of the model for the Chinese case

Validation of the outputs from the model should be made to prove that the simulation is realistic. This is demonstrated by comparing the model output and field data (AIS data). Three months of simulation output is analyzed to compare with the results from the AIS data analysis. This process is similar to the model validation introduced in Section 7.4.

8.6.1 Validation of the traffic density

Variance of traffic density in time is reflected by the variance of ship arrivals. There are several random processes mentioned in Section 8.2.2 that are used to reproduce realistic

variations for different days and different hours in the simulation. The following paragraphs indicate that the simulation is able to reproduce those variations.

This study compares the proportions of ship arrivals in different hours throughout the day. The simulation results are similar to the AIS data (Figure 8-13). The time intervals between ships in the simulation results are also reflected. The parameter (b = -0.0029) for the probability density function of the exponential distribution is only slightly larger than the same from the AIS data (b = -0.0027), so the number of ships generated in the simulation is slightly higher than in reality Figure 8-14.

The following results of ship movements in general show that the algorithms of the program are correct. Firstly, it is observed that most of the ships are navigating in the specific traffic lanes, especially when the ships are navigating in the bridge area. Secondly, the ship trajectories from the simulation (Figure XII-1) are very similar to the ship trajectories from the AIS data (Figure XII-2). From the trajectories, it is also observed that the ship positions are spread out in the waterway. Thirdly, ships with different speed and sizes are also reflected. Finally, the wind influences are included.

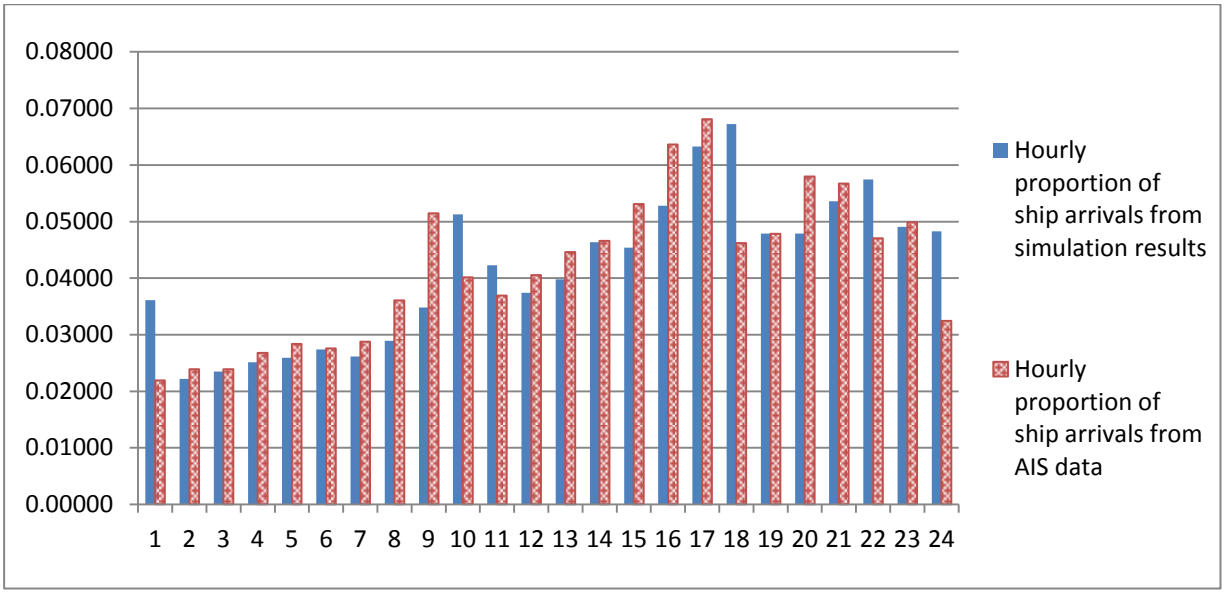

Figure 8-13 Hourly proportions of ship arrivals for outgoing ships in 24 hours

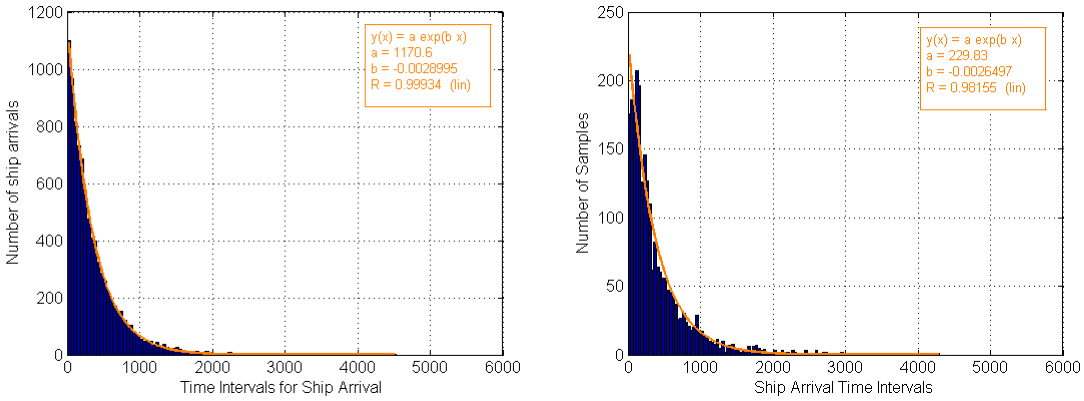

Figure 8-14 Ship arrival distribution of time intervals from the simulation results (left) and the AIS data (right)

However, there are differences when we compare the ship tracks from the simulation to that of reality. Firstly, only the ships that navigate under the main span are included in the simulation. In real practice, there are many jetties on both riverbanks (north and south). Also there are specific routes for these ships to berth, and these ships are not taken into account in the simulation because the numbers are very small and their behavior is unpredictable. This is the reason that we can see ships navigate far away from the designated traffic lanes in the AIS data observations. Secondly, the ships that navigate towards the river branches are not included in the simulation, as the numbers are very small. The ships that navigate to the river branches sail in a different direction after they navigate through the bridge area. This explains why the AIS ship tracks deviate from the traffic lanes to the north at both boundaries.

8.6.2 Spatial distribution

In the Chinese case, the parameters are also characterized by normal distributions with different means and standard deviations. Also the parameters from simulation results and the parameters from the AIS data are compared to evaluate the outcome of the simulation.

Non-dimensional spatial distributions from the simulation results show that the ship positions on crossing-line number 4 (located at the bridge) are well reproduced. However, the ship positions on both boundaries of the area are not (Table 8-5). For “small ships” on crossing-line number 4, the mean positions and standard deviations are reproduced very well. However, for “large ships” the differences are larger than for the “small ships”. The largest difference on crossing-line number 4 is for incoming “large ships”, with 7.8% of difference of the waterway width (500 m) which is 39 m. This means the incoming “large ships” in the simulation navigate 39 m closer to the center of the waterway than in the real world. For the traffic positions at both boundaries, the differences are even bigger. The largest difference is found to be 33.1 %. This means that most of the ships were navigating beyond the specific traffic lanes and the simulation cannot reproduce the deviations.

Table 8-5 Comparison of (non-dimensional) spatial distributions on the different crossing-lines between the simulation results and the AIS data

Crossing-line number	Ship category	Direction	Mean lateral position in simulation	Mean lateral position from AIS data	Difference in mean positions	Standard deviation of position in simulation	Standard deviation of position from AIS data	Difference in standard deviations
1	Large ships	Incoming	0.643	0.778	-0.135	0.088	0.159	-0.071
1	Small ships	Incoming	1.198	0.867	0.331	0.095	0.341	-0.246
4	Large ships	Incoming	0.234	0.312	-0.078	0.099	0.071	0.028
4	Large ships	Outgoing	0.284	0.249	0.035	0.086	0.07	0.016
4	Small ships	Incoming	0.679	0.679	-0.001	0.099	0.094	0.005
4	Small ships	Outgoing	0.641	0.643	-0.003	0.091	0.088	0.003
7	Large ships	Outgoing	0.464	0.731	-0.267	0.124	0.081	0.081
7	Small ships	Outgoing	0.867	1.151	-0.284	0.080	0.078	0.002

However, there are reasons for the differences in positions for the ship tracks at both boundaries of the simulation (outgoing ships on crossing-line number 7 and incoming ships on crossing-line number 1). The outgoing ships navigate on the outside of the traffic lanes as shown in the AIS ship tracks (see the eastern boundary of Figure XII-2). This is also reflected in the position differences (around 30% of waterway width) in the statistical analysis (Table 8-5). However, the simulation did not reflect it well. The reason is that the positions of the navigational aids are not correct, although we tried to calibrate the parameters to enable the ships to navigate outside of the traffic lanes at the end of the voyage. The positions at both ends of the voyages will be corrected if the updated correct map is at hand. However, the simulation results are much better at crossing-line number 4, because the positions of navigational aids in the neighborhood of the bridge are correct.

8.6.3 Speed distribution

Speed distributions from the simulation results show much better results than the spatial distributions. The detailed differences for mean positions and standard deviations can be found in Table 8-6. The differences of the mean speeds are less than 1 kn, when comparing the simulation results to the reality.

Table 8-6 Comparison of speed distributions on different crossing-lines between the simulation results and the AIS data

Crossing-line number	Ship category	Direction	Mean speed in simulation (kn)	Mean speed from AIS data (kn)	Difference in mean speed (kn)	Standard deviation of position in simulation (kn)	Standard deviation of speed from AIS data (kn)	Difference in standard deviations (kn)
1	Large ships	Incoming	7.97	8.75	-0.78	1.90	1.78	0.12
1	Small ships	Incoming	6.77	7.18	-0.41	1.51	1.43	0.08
4	Large ships	Incoming	7.97	7.73	0.24	1.90	2.13	-0.23
4	Large ships	Outgoing	10.57	11.11	-0.54	2.00	2.07	-0.07
4	Small ships	Incoming	6.77	6.98	-0.21	1.51	1.85	-0.34
4	Small ships	Outgoing	7.20	8.14	-0.94	2.00	2.13	-0.13
7	Large ships	Outgoing	10.57	11.37	-0.80	2.00	2.3	-0.30
7	Small ships	Outgoing	7.21	7	0.21	2.00	1.93	0.07

There are two reasons for the speed differences. Firstly, we assumed that the ships do not change speed in the simulation, except when the ships must slow down to stop overtaking other ships in the bridge area. The assumption is based on the AIS data analysis, in which minor speed change was observed. However, this is not the case in reality. The ships are always able to change speed for safe navigation and ship avoidance. Secondly, in the simulation the currents are neglected, but the currents may influence the traffic speed in reality. There are quite significant currents in the Yangtze, as the velocity of the currents can be 3.86 m/s as mentioned in Section 8.2.3.3. The fact is that some small inland barges do not have the capacity to compensate for the influence of the currents.

8.7 Discussion

In the Chinese case, the environmental conditions and regulations are different from the Dutch case. Therefore there are small modifications for local regulations and common practices for ship behavior. Values of important parameters and ranges are calibrated. First of all, the geographical shape of the waterway is very different. The navigable waterway is much wider than the waterway in Rotterdam. Secondly, the local regulations are different. A traffic separation scheme applies in the Chinese waterway and it separates different ships by sizes and directions. It also makes the ship navigation much safer. However, due to the complexity of the routes, different berths on the waterway bank, and traffic density, a

realistic reproduction of all the ship behavior is difficult. Therefore only the traffic in the major traffic lanes is reproduced. Thirdly, the traffic density is different. The traffic density in the Chinese case is much larger than the Dutch case. Finally, the quality of the AIS data is different. Much information such as ship dimensions and ship types is missing. Therefore, for further improvement of the simulation output, the data needs to be better maintained, and other sources of information are needed.

In the model validation, we evaluated the reproduction of ship traffic on a macroscopic level. The hourly differences of arrivals and time intervals are reflected well. However, we also tried to compare the ship tracks in the simulation results and ship tracks derived from the AIS data. The incorrect positions of the navigational aids make it difficult to reproduce correct ship behavior, especially towards the boundaries. An updated correct map is crucial for realistic results. Many ships navigating in the Yangtze are not equipped with the AIS system, which makes the data analysis more difficult. The individual ship encounters are not evaluated for this case due to the quality of the AIS data.

8.8 Conclusions

This chapter demonstrated that the multi-agent simulation and artificial force field model can be applied in the Chinese waterway. Although there are many differences between the Chinese case and the Dutch case, the program can be slightly modified and the parameters can be calibrated for new situations. The model and the concepts are the same. This chapter also demonstrated that correct simulation output depends on correct information, including the geometry of the waterway, map, AIS data, wind and currents.

The Chinese case is also a second validation of the agent-based model developed in the Dutch case. The results showed that the agent-based model performs well and hence it is widely applicable in different waterways around the globe, provided there is sufficient AIS data and other local information.

9. UTILIZING THE SIMULATION FOR PROBABILISTIC RISK ANALYSIS

9.1 Introduction

Gucma (2009) introduced the definition for risk (R) of maritime traffic that is a multiplication of accident probability and loss:

$$\mathbf{R} = \sum_{i=1}^{n} P_i C_i \qquad (9 - 1)$$

Where: P_i is the probability of i-th accident in a given time (i = 1, 2, …, n); C_i is the consequence of i-th accident in a given time; and n = number of possible accidents.

This chapter demonstrates several cases to study the probabilities that can be used in probabilistic risk analysis that is the probability component of Equation (9 - 1). This is achieved by utilizing the simulation model to get results that can be used for further applications, especially for risk analysis.

Goerlandt et al. (2011) categorized the existing models for collision probabilities into static probability models and dynamic probability models. However, Chapter 2 differentiates the two categories as models based on the analytical methods and models based on simulation methods. Chapter 2 also introduced a model based on the statistical method and a model based on networks. P_i can be derived either by any of the four methods introduced in Chapter 2, or by using a combination of several methods.

Several case studies are presented in this chapter that utilize the agent based simulation model developed in this study to either derive a parameter that can be used in the static probability model (based on the analytical method) to calculate P_i, or to derive P_i directly from simulation as a dynamic probability model (based on the simulation method). These case studies show the way that this simulation model can be used for a number of other purposes.

After running the program for a predetermined period of time for each case study, the selected simulation output appears in the "Command Center" of the NetLogo interface and this can be saved in a separate text file. The output information for each ship at each time step is similar to the AIS information, which includes position, heading, speed, gross tonnage, LOA, and ship type. Other intermediate variables can also be included in the output file if needed. With the output, statistical analysis can be conducted to derive probabilities of incidents.

There are different unique characteristics for the cases shown in this chapter. Firstly, with sufficient statistics of the input parameters, the simulation model can simulate traffic and help to count the number of encounters. A similar function is possible for most of the existing ship traffic simulation models. However, the ANTS model is able to simulate simple collision avoidance behavior, and it is also able to count the number of ships involved in close encounters that are not able to avoid collision after simple evasive behavior. Secondly, the simulation model can generate output based on insufficient statistics of input parameters. An example of an application for insufficient data is the Chinese case that is presented in Section 9.6. If a lot of information is missing because many ships are not installed with AIS equipment on board, like in China, a reasonable estimation of what is missing in the AIS data is needed, and parameters can be calibrated by the anticipated input values. Finally, probabilistic risks can be studied as well.

9.2 Theories for probabilistic risk analysis

9.2.1 Probability of ship collisions

The number of collision occurrences in a period of time is calculated as follows (Goerlandt et al., 2011):

$$\mathrm{N_C} = \mathrm{N_A} * \mathrm{P_C} \tag{9 - 2}$$

Where $\mathrm{N_A}$ is the number of collision candidates, which is the number of ships that are involved in close encounters, provided that no further evasive action is taken other than simple evasive action. The simple evasive actions are the actions taken for encounters (head-on or overtaking between two ships), when collision can be prevented by lateral position change by either one of the ships in the encounter. $\mathrm{P_C}$ is the probability that further evasive action by any means has failed, with a magnitude between 10^{-5} and 10^{-4} (Goerlandt et al., 2011, Nyman et al., 2010).

9.2.2 Probability of groundings with engine failure

The number of grounding occurrences in a period of time can be calculated with the method similar to probability of ship collision.

$$N_E = N * T_E * R_{EF} * R_E \quad (9 - 3)$$

where N is the number of ship passages in a certain period of time. T_E is the average time for each ship passage in the studied area. R_{EF} is the failure rate of main engine. R_E is the average accident rate for each occurrence of engine failure. Based on statistical analysis by Kiriya (2001), the failure rate of the main engine (R_{EF}) is 0.857 case/1000Hr.

9.2.3 Probability of groundings with rudder failure

The number of grounding occurrences in a period of time can be calculated, with a method similar to the probability of ship collision.

$$N_R = N * T_R * R_{RF} * R_G \quad (9 - 4)$$

where N is number of ship passages in a certain period of time. T_R is the average time for each ship passage in the studied area. R_{RF} is the failure rate of the rudder system. R_G is the accident rate for each occurrence of rudder failure. Based on statistical analysis by (Kiriya, 2001), the failure rate of Navigation and Communication Equipment (R_{RF}) is 0.735 case/1000Hr.

9.3 Dutch case studies for probabilities from the simulation model

This section discusses utilizing the nautical traffic simulation model to derive different probabilities for near misses or accidents that can be further applied in risk analysis. For ship to ship collisions, the simulation helps to count the number of ships that are involved in close encounters after simple evasive action provided in the simulation, or ships with engine failure or rudder failure on board that are unable to take evasive actions.

9.3.1 Number of ships that are involved in close encounters (N_A)

The collision candidates are determined by simulation. N_A is dependent on the time period and the year selected for the simulation. In the simulation, a distance of 20 m is selected as criteria for a close encounter, as 20 m is about half of the width of two ships that result in collision. The criterion of a close encounter is selected, because in most of the cases, the ships are not on a colliding course. Even if they are on a colliding course, a simple shift of lateral ship position allows deviation from the colliding course. With the criterion, the selected collision candidates involves the ships that are shown to be very close to each other, and the situations are considered to be dangerous even after the effect of simple evasive action. The close encounters may be caused by multiple encountering of ships, malfunction on board (engine failure and steering failure) or an error in simple evasive behavior.

After running the traffic simulation for a time period of three years (2009, 2010, and 2011), the output shows that the number of collision candidates amounts to 6,159. Therefore, the number of collision candidates per year in the period is (N_A) is 2,053.

9.3.2 Average incident rate for each occurrence of engine failure (R_E)

For deriving R_E from simulation, 1,000 cases of engine failures onboard are generated at random times with random positions for ships that are navigating in the simulation. In order to represent reality, only one ship will suffer from engine failure at each time period. The ship tracks with engine failures are shown in Figure XIII-1. When a ship track is shown outside the waterway, the ship will be recognized as grounded. After observations, there are 228 ships grounded as a result of 1,000 engine failures. Thus, the grounding rate (R_E) after engine failure is 0.228.

9.3.3 Average incident rate for each occurrence of rudder failure (R_G)

For deriving R_G from the simulation, 1,000 cases of rudder failures onboard are generated at a random time with random positions for each ship that is navigating in the simulation. In order to represent the reality, the ship tracks with rudder failures are shown in Figure XIII-2. When a ship track is shown outside of the waterway, the ship will be recognized as grounded. After observations, there are 257 ships grounded with 1,000 occurrences of rudder failure. Thus, the grounding rate (R_G) after rudder failure is 0.257.

9.4 Probabilistic risk analysis (P_i) for the Dutch case

This section discusses utilizing the probabilities derived from the simulation (N_A, R_E, R_G) for further application in deriving probabilistic risks (P_i) using the theories introduced in Section 9.2. In this section, the probability of collision, the probability of grounding with engine failure, and the probability of grounding with rudder failure are calculated. The groundings are assumed to be caused by mechanical failure (engine failure or rudder failure), while the ship collisions are assumed to be caused by human error.

9.4.1 Dutch case study of probability of ship collisions per year (N_C)

In Section 9.3.1, the number of collision candidates (N_A) is derived from the simulation. The probability that further evasive action by any means has failed (P_C) for a port area is unknown yet. However, based on the estimation provided in the literature for open sea, the P_C will have a magnitude between 10^{-5} and 10^{-4} (Goerlandt et al., 2011, Nyman et al., 2010). Therefore, the results of the probability of ship collisions per year can be calculated with Equation (9 - 2) for different magnitudes of P_C. This is just a demonstration of the application. More studies are needed for deriving P_C for each specific case.

Table 9-1 Probability of ship collisions per year for different magnitudes of P_C

Cases	N_A	P_C	N_C
1	2053	0.00001	0.02053
2	2053	0.0005	0.10265
3	2053	0.0001	0.2053

9.4.2 Dutch case study of the probability of groundings with engine failure (N_E)

Probability of groundings with engine failure (N_E) can be calculated with Equation (9 - 3). In Section 9.3.2, the grounding rate ($R_E = 0.228$) after engine failure is derived from the simulation. The number of ship passages ($N = 46141$) in a certain time period (the years 2009 and 2010) can be derived from statistical analysis of the AIS data. T_E (0.12125 h) is calculated from the waterway length (2800 m) and the average ship speed (11.88 kn). Then for the studied area, the average grounding rate per year for a time period of 2009 and 2010 by Equation (9 - 3) is calculated as $N_E = 0.558$.

9.4.3 Dutch case study of the probability of groundings with rudder failure (N_R)

Probability of groundings with rudder failure (N_R) can be calculated with Equation (9 - 4). In Section 9.3.3, the grounding rate ($R_G = 0.257$) after rudder failure is derived from the simulation. The number of ship passages ($N = 46141$) in a certain time period (the years 2009 and 2010) can be derived from the statistical analysis of the AIS data. T_R (0.12125 h) is calculated from the waterway length (2,800 m) and the average ship speed (11.88 kn). Then for the studied area, the average grounding rate per year for a time period of 2009 and 2010 by Equation (9 - 4) is calculated as $N_R = 0.528$.

The simulated grounding rate is very similar to the real data. In the case studies, the probability of groundings with rudder failure ($N_R = 0.528$) and engine failure ($N_E = 0.558$) per year is 1.086 altogether. If the probability of groundings is divided for each kilometer of waterway length, the grounding rate for each kilometer of waterway length in one year is 0.39. In the Eurocode model (Vrouwenvelder, 1998), an example was provided for the grounding rates: 28 ships were observed to hit the river bank in a period of 8 years and over a distance of 10 km, with a ship density of 8,000 ships per year in the waterway of the Nieuwe Waterweg near Rotterdam in the Netherlands. That is to say, the grounding rate for each kilometer of waterway length in one year is 0.35. This probability is very similar to the result calculated from the simulation output (0.39). However, the number of ship passages in real data comes from the years 2010 and 2011, in which the traffic density is much higher than the real data.

9.5 Accident rate directly derived from the simulation for the Dutch case

The previous section shows the way that the simulation model helps to derive intermediate probabilities as part of risk analysis. This section introduces the way the simulation generates the final probabilities of accidents. The only difference is that all the processes are included in the simulation program in this case. Therefore, there should be a process for generating accident candidates. First of all, failure rates are calculated. Based on statistical analysis by Kiriya (2001), the failure rate of the main engine (R_{EF}) is 0.857 case/1000h, and the failure rate of the Navigation and Communication Equipment (R_{RF}) is 0.735 case/1000h. In other words, it takes 1,167 hours of Accumulated Operation Time for each failure of the main engine in the simulation. For each failure of the navigational equipment (rudder failure), it takes 1,361 hours of Accumulated Operation Time in the simulation. Secondly, a parameter in the simulation is used to calculate the Accumulated Operation Time for the ships. Once the Accumulated Operation Time is higher than the failure rate of the main engine or navigation equipment, malfunction of engine failure or rudder failure will happen on a random ship in the simulation. Thirdly, if a ship has a problem with the rudder or engine, it will navigate without rudder effect and drift with the effect from wind and current, and finally it will run into another ship or aground on the waterway banks. The detailed ship behavior and ship characteristics will be recorded in a separate file of the NetLogo interface. We can then find the number of accidents and calculate the accident rates from the data in the file. In this section, only mechanical failures are simulated for accidents. Human errors in different circumstances are not addressed although they are more important.

In the simulation, a period of 10 years from the years of 2020 to 2029 is selected for the demonstration. The number of ship passages per week has increased at a rate of 0.68 per week on average based on the data from the years 2009 and 2010 in Chapter 3. Thus, in this case, the anticipated traffic density is taken into consideration to derive the accident rates for the selected years in the future.

After simulation, there are 538,533 outgoing ship passages and 539,333 incoming ship passages that are generated in the simulation. The average number of ship passages per year is 2.3 times as large as in the years 2009 and 2010.

The numbers of accidents are derived, which are 38 for groundings with engine failure, 38 groundings with rudder failure, and 74 close encounters for collisions with engine failure or rudder failure. That is to say, the larger traffic density results in increased probability of grounding (3.8 cases per year), after failure of the main engine or navigational equipment. For close encounters, 74 close encounters for 10 years is a very low rate, and therefore the probability of ship to ship collision that is caused by malfunction on board is very low in the simulated period.

9.6 Traffic simulation and risk analysis with insufficient data for the Chinese case

9.6.1 Traffic simulation with insufficient data for the Chinese case

For the Chinese case, the simulation output was statistically analyzed and validated with reference to the AIS data analysis results. However, the AIS data did not fully reflect the real situation in the waterway, as there are a lot of ships that did not carry the AIS system and they were not included in the AIS data. According to the observations from the China MSA (Maritime Safety Administration of the People's Republic of China)[2], the number of ship passages (Table 9-2) is very different from the number of passages observed in the AIS (e.g. 208 passages per day on average for incoming ships). Therefore, the number of missing ships should be reflected in the simulation.

In the simulation, the missing number of ship passages is compensated by increasing the frequency of ship arrivals at the boundaries of the simulation. The input parameters derived from the AIS data can be treated as samples that are randomly selected from the real traffic, and therefore the values for the parameters do not necessary need to be modified. As the real traffic density observed by China MSA is much larger than the AIS data analysis, the traffic density in simulation is multiplied by a factor of 2 to see whether we can generate realistic results as well.

When the ships without an AIS system onboard are taken into account in the simulation, it is assumed that the proportions of "large ships" and "small ships" that are missing in the AIS data are the same. This assumption may not be true, as it is very possible that a larger proportion of ships without the AIS system are "small ships". Since we did not investigate the proportions, it is assumed that the proportions remain the same for simulation.

After simulation, the spatial distributions and the speed distributions are compared to the statistical results of the AIS data to see whether the output is similar to the reality (Table 9-3 and Table 9-4). The process is the same as in Chapter 8. The results of comparisons are similar to the results introduced in Chapter 8. The parameters on the crossing-lines are reproduced well, but the parameters on both boundaries still need improvement. A correct map is needed for further improvement.

Table 9-2 Number of ship passages from both directions for selected days observed by the China MSA

Date	Number of incoming ship passages	Number of outgoing ship passages	Number of ship passages (incoming and outgoing)
18/11/2012	875	599	1474
15/06/2012	735	915	1650
18/03/2013	870	680	1550

[2] Number of ship passages of the Nan-Tong Cross-section, provided by the China MSA, http://www.ntmsa.gov.cn

Table 9-3 Comparing (non-dimensional) spatial distributions on the different crossing-lines between the simulation results and the AIS data

Crossing-line number	Ship class	Direction	Mean position in simulation	Mean position from AIS data	Difference in mean positions	Standard deviation of position in simulation	Standard deviation of position from AIS data	Difference in standard deviations
1	Large ships	Incoming	0.486	0.778	-0.293	0.267	0.159	0.108
1	Small ships	Incoming	1.041	0.867	0.174	0.212	0.341	-0.129
4	Large ships	Incoming	0.199	0.312	-0.114	0.092	0.071	0.021
4	Large ships	Outgoing	0.295	0.249	0.046	0.091	0.070	0.021
4	Small ships	Incoming	0.661	0.679	-0.018	0.105	0.094	0.011
4	Small ships	Outgoing	0.639	0.643	-0.004	0.094	0.088	0.006
7	Large ships	Outgoing	0.417	0.731	-0.315	0.105	0.081	0.024
7	Small ships	Outgoing	0.945	1.151	-0.206	0.126	0.078	0.048

Table 9-4 Comparing speed distributions on the different crossing-lines between the simulation results and the AIS data

Crossing-line number	Ship class	Direction	Mean speed from simulation	Mean speed from AIS data	Difference in mean speed	Standard deviation of speed from simulation	Standard deviation of speed from AIS data	Difference in standard deviations
1	Large ships	Incoming	7.96	8.75	-0.79	1.95	1.78	0.17
1	Small ships	Incoming	6.71	7.18	-0.47	1.51	1.43	0.08
4	Large ships	Incoming	7.96	7.73	0.23	1.95	2.13	-0.18
4	Large ships	Outgoing	10.56	11.11	-0.55	1.98	2.07	-0.09
4	Small ships	Incoming	6.71	6.98	-0.27	1.51	1.85	-0.34
4	Small ships	Outgoing	7.21	8.14	-0.93	2.01	2.13	-0.12
7	Large ships	Outgoing	10.56	11.37	-0.81	1.98	2.30	-0.32
7	Small ships	Outgoing	7.21	7.00	0.21	2.01	1.93	0.08

9.6.2 Risk analysis with updated traffic density for the Chinese case

After knowing that the simulation output is realistic with doubled traffic density, we can estimate the accidents directly. In the simulation, the year 2010 is selected for demonstration. In this simulation, the collision probability with the bridge piers is calculated. The collision accidents are identified as follows: if a ship passes a main bridge tower at a distance of 30 m or less, the ship tracks will be recorded as an accident case, while if a ship passes a bridge pier of the side span at a distance of 20 m or less, the ship tracks will also be recorded. The distance criteria are roughly half of the average ship width and half of the pier width added together. It is assumed that collision will happen if the distance criteria are met. The distance for the main bridge tower is larger because the dimensions are larger. The behavior of the ship will be recorded in a separate file for further analysis.

After running the simulation for a whole year, 395,228 ship passages were generated, in which there were 112 cases of engine failure and 96 cases of rudder failure that occurred during the simulation process. 7 cases of collision accidents between ships and the bridge were observed. This is not realistic as no collision accident happened to the Su-Tong Bridge since July of 2010. However, this is a demonstration of how the model works. The details of the accidents can be found in Table 9-5. We can find that three ships collided with the main towers of the bridge, and four ships collided with the side piers. In these collisions, the speeds of the ships are very low, except one case with powered collision (4.1 kn). However, the tonnage of ship (250.9 t) is very small in the case of the powered collision, and it probably will not cause serious damage to the bridge.

Table 9-5 The details for the 7 incidents of collisions between the ship and the bridge for the Chinese case

ID	xcor	ycor	Course	Speed (kn)	Tonnage (t)	LOA (m)	Bridge pier	Failure type
1	-14.5	-103.7	162.0	0.5	449.8	44.4	side pier	engine failure
2	-13.3	-92.1	102.9	4.1	250.9	35.7	side pier	rudder failure
3	-7.2	-51.3	179.0	1.0	892.0	57.2	main tower	engine failure
4	-12.7	-85.4	97.0	0.7	413.5	43.0	side pier	engine failure
5	-6.5	-52.0	14.0	1.3	833.6	55.8	main tower	engine failure
6	-11.9	-84.9	55.0	0.3	398.0	42.4	side pier	engine failure
7	-6.7	-54.3	187.0	0.6	171.1	31.0	main tower	engine failure

9.7 Discussion

Various simulation output and further risk analysis were provided for the Dutch case or the Chinese case. Different output can be generated according to different purposes. Different simulation results are used to derive the probability of accidents. As the simulation is a realistic way of representing ship traffic, taking into account the many variables and effects, the results are much more reliable than the analytical methods. In this way, the advantage of the simulation is that the ship behavior is recorded, and the way that the ships are involved in accidents, is also known from the simulations. The records can be used to analyze the accident scenarios for further analysis, design of mitigation measures. It also provides information for the consequence assessment of accidents.

With the help of the simulation, a number of probabilities can be estimated. First of all, the number of close encounters can be derived. Also, the number of collisions can be calculated using the analytical method for the next step, provided with a failure rate that the ships are unable to avoid collision in a close encounter. However, we cannot derive the exact number of accidents directly by the simulation because the nautical traffic simulation is unable to reflect the ship behavior in a close encounter, as the seafarers are suffering from great psychological pressure, and therefore the actions are unpredictable in this research. Lacking scenarios of close encounters and a lack of study on ship behavior in close encounters are the main reasons for this inability. Further study is needed to represent the details for close encounters. Second, the probability of groundings with engine failure or rudder failure can be derived indirectly or directly from simulation, with additional information of failure rate of engine or rudder. For indirect anticipation, we can easily generate 1,000 cases of mechanical failures on board, and the behavior of the ships with mechanical failures can be simulated. An independent file will record the tracks, and finally the grounding rate can be checked with the information of geographical shape of the waterway. For direct anticipation, the rate of mechanical failures is built in the program. However, the process of simulation takes longer than an indirect approach, because we have to wait a long time for each single case of mechanical failure, as in reality. Independent files for the ship tracks from the simulation process can also be made available.

The accident rates derived from the simulation is relatively high. There are several reasons for this. Firstly, the failure rate of the rudder and engine are very high. The failure rates are from the statistics of sea going ships, which could be larger than the case in the Dutch inland waterway. Secondly, anchoring is not considered in the simulation. However, in real practice, the ships should avoid collision by any means. The common way, other than to reverse the engine to decrease the speed of the ship, is anchoring. The grounding rates may become lower if proper anchoring happens.

The future situations can be anticipated. When the traffic volume increases in the future, the self-organized individual ships can adapt their behavior based on increased ship avoidances and dynamic change of local situations, and constitute a new traffic pattern. This has been demonstrated by a Chinese case.

Further development for risk analysis is needed. Firstly, more accident reports need to be studied to determine the factors that cause the accidents. Secondly, the failure rates of the main engine or rudder also need further study. Thirdly, and especially important, further study will be needed for ship behavior in close encounters and immediate dangers, and the response of other ships in these situations also needs to be reflected. Finally, the ship behavior in the waterway bend and in case of crossing lanes need further study to improve the risk analysis.

9.8 Conclusions

This chapter presents the ways that the simulation models can be used for further applications, especially for risk analysis. The output information is similar to the AIS information, which includes position, heading, speed, gross tonnage, LOA, and ship type of each ship at each time step. With the output, statistical analysis is conducted to derive the details of the ship behavior from the simulation. It can be also used to estimate different probabilistic risks.

An advantage of the simulation is that the model can simulate the situations of interest. Some cases are provided as examples. Firstly, the ship density can be compensated for the same situation in reality. Secondly, the situations in the future can be anticipated. And finally, the situations can be reproduced again and again to derive more accurate probabilities.

Other than the applications for risk analysis, the model can be applied for other purposes that need knowledge of realistic traffic status. For instance, it can be used for arranging tug assistance, the application of new regulation, optimizing waterway width for port design etc.

10. CONCLUSIONS AND RECOMMENDATIONS

This thesis seeks better methods for Probabilistic Risk Analysis (PRA) of maritime accidents. A number of steps have been taken to achieve the goal, including literature review, data analysis, theory build up, programming, calibration, and case studies. There are fruitful results in developing artificial forces, innovative application of multi-agent simulation in nautical traffic, and statistical analysis and graphical representation of the AIS (Automatic Identification System) data. Section 10.1 presents the answers to the research questions and the experience from the work. Recommendations for further research are presented in Section 10.2.

10.1 Research findings

The main objective of this research is developing a simulation tool that provides information of detailed ship behavior in specific navigational environment on both the ship traffic level and the individual ship level, for safety analysis, decision making, planning of ports and waterways, and design of mitigation measures. In order to achieve the main objective of this research, the following research questions have been composed:

- What are the limitations in the existing methods for maritime risk analyses? What are the advantages of using a simulation method? (RQ1)
- How can we derive the information from AIS data and further utilize the information for simulating realistic ship behavior? (RQ2)
- How can we develop a realistic nautical traffic simulation model with detailed description of its methodology, concept, structure, calibration, and validation? (RQ3)
- How can we utilize the simulation in probabilistic risk analyses and further applications? (RQ4)

The ANTS model is the simulation tool that has been developed to achieve the main objective of this research. The conclusions with respect to the research questions are presented below.

Research Question 1 It is concluded from Chapter 2 that the most desirable model should take into consideration all risk elements that are mentioned in the existing models. The ships should be categorized into more detailed groups. The encountering situations and collision avoidance behavior should be taken into account with the effects of wind, current and visibility. The models based on networks produce results based on existing probabilities and expert opinions. However, those models cannot provide many details for improving the safety level of the ship traffic.

Simulations are considered to be an indispensable part of maritime risk analysis. Different simulations catch different elements of reality. However, the existing simulation methods are either weak in reproducing realistic collision avoidances on traffic level or weak in reproducing realistic individual ship movements. Simulation method showed its advantages in providing sufficient of ship (traffic) details, realistic representation of ship behavior and environment, and evolving sufficient factors that need to be taken into consideration. Reproduction of the complex system of ship traffic can't be achieved by the other methods. It is concluded that the simulation method is the best way to execute PRA with realistic detailed behavior on both ship traffic level and individual ship level, taking into account the influence of wind and currents.

Research Question 2 The AIS data on selected crossing-lines that are perpendicular to the channel is statistical analyzed for the characteristics of the ship traffic. The tracks of the ships involved in encounters are plotted for detailed analysis of individual ship behavior.

The AIS provides field data for boundary inputs, model verification and validation for simulations. After interpretation of the ship tracks provided by the AIS data, we derive information of ship traffic behavior that are characterized by the mean values and statistical distributions of position, speed, heading, and time interval for different types and sizes of ships. These characteristics are compared between normal conditions and conditions with extreme wind, currents and visibility to identify the influences of visibility, wind and currents. As a result, the influences are very small that do not need to be reflected in the simulation. On the individual ship level, this thesis studies a number of ship encounters for developing an artificial force field and the mathematical expressions for the artificial forces. Moreover, the AIS tracks and statistical properties can be used to verify mathematical models built in the simulation to get more accurate and realistic results.

Artificial forces are developed based on the AIS data with ship encounters. This thesis has developed statistical analyses of ship encounters and involved a matrix of the correlation coefficient analysis for the development of the artificial force field model for collision avoidances. The matrix of the correlation coefficient analysis was used to choose the parameters and eventually to develop the equations of artificial forces. The parameters in the forces include distances to the waterway boundary, distances to the other ship in the different stages of an encountering situation, and other characteristics such as the LOA,

speed and gross tonnage of the ship. As far as we know, this is the first time that an artificial force field model is developed based on field data (the AIS data in this study).

Research Question 3 The ANTS model is an agent-based model. It has been demonstrated that the model can be effectively developed with the ODD protocol. The ODD protocol is used in this thesis for detailed model description of the complex system in a structured way. The multi-agent simulation has many advantages for realistic nautical traffic simulation. The submodels also have critical contributions to reproduce reality.

The ODD protocol provides a framework that tries to incorporate the elements that need to be considered in real practice into the nautical traffic simulation. With the help of the ODD protocol, the multi-agent concept is applied in the ANTS model in several innovative ways. Firstly, many variables were defined that are important for the agent-based model to capture the most important features for the ship traffic. Secondly, the relationships and processes of events during each time step of the simulation are provided. Thirdly, the inputs, initialization, and sub-models for the simulation are also included in the protocol for ship behavior in the ANTS model. A number of sub-models have been created to describe the behavior of the ships. Other than the artificial forces, the dynamic ship maneuvering model and the model for speed change are provided for realistic ship movements in ship avoidance behavior. The model for influences of wind and currents are also provided to reflect the external influences.

A multi-agent system is applied to the nautical traffic simulation in the ANTS model. The use of agent-based models is a logical step for realistic nautical traffic simulations, because ship traffic is a complex self-organizing system with autonomous entities. In this system, the individual ships are autonomous active agents that are able to interact with each other within a virtual navigational environment. The navigational environment includes the geographical environment, ship encountering situations, and meteorological environment. The ship agents can sense the local environment and determine the strategy for its behavior on its own. Every individual ship behavior affects the traffic environment. On the other hand, the traffic environment also affects the decision making of individual ships. The situations are constantly changing, and the individual ship is constantly responding to the change. The interactions of ships are mainly collision avoidances and common practice that are required by regulations (e.g. COLREGs), based on perceptions of the local navigational environment.

The development of the artificial force field model is another innovative achievement for realistic reproduction of ship behavior. This thesis developed artificial forces based on the AIS data with ship encounters. The model development includes finding parameters, determining constants, and finally coming to mathematical equations for the forces. The decision making process for ship maneuvering is mimicked using artificial forces for the evasive behavior and collision avoidance behavior of ship interactions. Decisions are made based on the assessment of the ship's own situation, allowing random path choices within

the safety margin. The behavior also conforms to regulations and common practice of the waterway. Therefore, the behavior of the ships is consistent with reality. The decision making process based on artificial forces is considered to be better than the existing method based on fuzzy logic and neural networks. For one thing, the decision making for a navigational strategy based on artificial forces is more realistic and rational. Second, the artificial force model is easier to implement in the simulation by adding several parameters and simple mathematical models. Therefore the artificial force field model is more suitable for a complex traffic simulation.

The Dutch and Chinese case has been studied to apply the agent-based artificial force model. For model calibration, the parameters are tuned and ranges are provided for the variables in the models. For validation, this thesis compares the simulation outputs with the AIS data on both the ship traffic and the individual ship traffic level. On a ship traffic level, a number of characteristics have been validated. Those characteristics include the proportions of different ship types, variation of traffic density in time, overall image of trajectories of the ship traffic, and statistical distributions to describe the characteristics of ship behavior. On an individual ship level, ship interactions in encounters are included, and the ship tracks are compared with the AIS data. Rudder angles for individual ships are also an output from the simulation. However, no field data is available for validating the rudder angles.

Research Question 4 Case studies have been provided for probabilistic risk analysis of accidents. The probabilities of accidents can be derived for accidents with ship to ship collision, collisions between ship with bridge piers, and groundings with rudder failure or engine failure. Those applications demonstrate the advantages of the simulation model.

The simulation also provides detailed traffic behavior, such as the process leading to the accidents and the reasons for the accidents. Therefore mitigation measures can be studied. Other than that, the model is able to predict ship traffic in the future. Traffic behavior in the future can be further used for port and waterway design.

10.2 Recommendations for future research

The artificial force model has been applied in a relatively straight waterway for both the Dutch case and Chinese case. However, there are still several places need improvements. The waterway shape and different types of ships are not taken into account for collision avoidance behavior in this study. Thus, the AIS ship tracks at waterway intersections and bends need to be studied for developing artificial forces in those geometries. Further, more encounter situations involving different types of ships need to be collected to analyze the effect of ship types on the artificial forces.

A ship maneuvering model is provided to reproduce the movements of ships. However, the hydrodynamic model is very simple compared to a ship handling simulator. We speculate

that in the future a more complex hydrodynamic model can be implemented which takes into account the effects of shallow water, the banks of the channel, etc. This will also help to describe the ship behavior in close encounters (with the effect of ship suction) and behavior after collisions, taking into account all the hydrodynamic effects. However, the limited computational capacity may be a problem for implementing a complex hydrodynamic model for ship movements.

Human reaction in a close encounter is not sufficiently developed in this model. When a collision is not avoidable by any means, the behavior of the ships is not easy to predict. In this situation, the “stand-on vessel” defined by COLREGs have to take proper action. However, the actions are not so easy to predict because either the decision making process in the emergent situation is unpredictable or the action taken is beneficial for the own-ship and leaves more risks for the other. Therefore, sufficient collision avoidance behavior should be further studied to correctly reflect the behavior in the emergent dangers.

In the model, ships are treated as autonomous agents. In the navigational environment, a ship is able to perceive the waterway shape, the distances and bearings to the other ships, and the characteristics of the other ships. Active collision avoidances are based on regulations. In addition, the effects of the wind and currents are passively exerted on the ships. The future model should include cognitive agents that can predict the behavior of the other ships in collision avoidances, especially in encounters involving more than two ships. Also, the ships can communicate with each other and finally reach an optimal strategy for collision avoidances. This is relevant for developing artificial forces for collision avoidance at busy cross sections.

I. STATISTICAL TOOLS USED

I.1 Normal probability plot in data analysis

Normal probability plot is a graphical method to assess normality of a sample vector data. A straight line is drawn on the plot. Data plotted close to the straight line indicates the sample vector conform to normal distribution. On the contrary, departures from the straight line reject the normal hypothesis. The Normal probability plots are performed by using MATLAB® function “normplot ()” throughout this thesis.

I.2 The Lilliefors test

The Lilliefors test is two-sided goodness-of-fit test modified from the Kolmogorov-Smirnov test of vector normality, which is comprised by several steps (Razali et al., 2011). Firstly, the mean and variance of the sample vector data is estimated. Secondly, what is calculated is the maximum discrepancy between the empirical cumulative distribution function and the cumulative distribution function (CDF) with mean and standard deviation equal to the mean and standard deviation of the sample vector, also see Equation (I - 1). Finally, the maximum discrepancy is assessed to determine whether the null hypothesis of normality is rejected.

$$D = \max_x |F^*(X) - S_n(X)| \qquad \text{(I - 1)}$$

Where $S_n(X)$ is the cumulative distribution function of the sample vector, and $F^*(X)$ is cumulative normal distribution function with mean and variance of the vector data.

The Lilliefors tests are performed by using MATLAB® function “lillietest ()” throughout this thesis.

I.3 Jarque-Bera test

The Jarque-Bera test is a two-sided goodness-of-fit test for whether a sample vector has the skewness and kurtosis matching a normal distribution with unknown mean and variance. The test statistic is (Jarque et al., 1987):

$$\mathrm{JB} = \frac{\mathrm{N}}{6}\left(\mathrm{S}^2 + \frac{(\mathrm{K}-3)^2}{4}\right) \quad \text{(I - 2)}$$

Where N is the number of samples in vector, S is the sample skewness, and K is the sample kurtosis.

$$\mathrm{S} = \frac{\hat{\mu}_3}{\hat{\sigma}^3} = \frac{\frac{1}{\mathrm{n}}\sum_{\mathrm{i}=1}^{\mathrm{n}}(\mathrm{x_i}-\bar{\mathrm{x}})^3}{\left(\frac{1}{\mathrm{n}}\sum_{\mathrm{i}=1}^{\mathrm{n}}(\mathrm{x_i}-\bar{\mathrm{x}})^2\right)^{\frac{3}{2}}} \quad \text{(I - 3)}$$

$$\mathrm{K} = \frac{\hat{\mu}_4}{\hat{\sigma}^4} = \frac{\frac{1}{\mathrm{n}}\sum_{\mathrm{i}=1}^{\mathrm{n}}(\mathrm{x_i}-\bar{\mathrm{x}})^4}{\left(\frac{1}{\mathrm{n}}\sum_{\mathrm{i}=1}^{\mathrm{n}}(\mathrm{x_i}-\bar{\mathrm{x}})^2\right)^2} \quad \text{(I - 4)}$$

Where $\hat{\mu}_3$ and $\hat{\mu}_4$are the estimates of third and fourth central moments, $\bar{\mathrm{x}}$ is the sample mean, and $\hat{\sigma}^2$ is the variance.

The Jarque-Bera tests are performed by using MATLAB® function “jbtest ()” throughout this thesis.

I.4 Kolmogorov-Smirnov test

Kolmogorov-Smirnov test is a nonparametric statistical test to check whether a vector data belong to hypothesized empirical distribution. The test statistic is (Lopes et al., 2007):

$$\mathrm{D_{KS}} = \max|\mathrm{F(x)} - \mathrm{P(x)}| \quad \text{(I - 5)}$$

Where $\mathrm{F(x)}$ is the empirical CDF, and $\mathrm{P(x)}$ is a known CDF. When comparing two samples with cumulative distribution functions $\mathrm{F(x)}$ and $\mathrm{G(x)}$, the test statistic is defined as:

$$\mathrm{D_{KS}} = \max|\mathrm{F(x)} - \mathrm{G(x)}| \quad \text{(I - 6)}$$

The Kolmogorov-Smirnov tests are performed by using MATLAB® function “kstest ()” and “kstest2 ()” throughout this thesis. “kstest ()” performs a Kolmogorov-Smirnov test to compare the values to a standard normal distribution, whereas “kstest2 ()”performs a two-sample Kolmogorov-Smirnov test to compare the distributions of the values in the two data vectors.

I.5 Chi-squared (χ2) goodness-of-fit test

Chi-square tests the goodness-of-fit between the sample distribution histogram and the continuous distribution histogram. The test is practiced in the following steps throughout the thesis. The first step is dividing the sample vector into n number of bins. The hypothesis is that the values in each bin will have equal frequency between the sample and the theoretical density. The second step is calculating the value of the test statistic is:

$$\chi^2 = \sum_{i=1}^{n} \frac{(O_i - E_i)^2}{E_i} \quad \text{(I - 7)}$$

Where χ^2 is Pearson's cumulative test statistic, which asymptotically approaches a Chi-square distribution. $\mathrm{O_i}$ is an observed number of observations, $\mathrm{E_i}$ is an expected number of observations. The expected number of observations $\mathrm{E_i}$ in each bin provided sample size N can be calculated by：

$$E_i = \mathrm{p}_i \times N \quad \text{(I - 8)}$$

$\mathrm{p_i}$ is cumulative probability density within the bin width. The final step is to verify whether the value of the test reject the null hypothesis of theoretical continuous distribution on certain significance level. A failure of rejection shows that the continuous distribution can be used in the simulation to produce similar histogram.

There is no optimal choice for the number of bins (n). And χ^2 also allow flexible choice of Bin boundary. A required bin width would result in at least 5 counts for each bin. Rule of thumb for the number of bins is used:

Table I-1 Number of Bins needed for a sample size in Chi-squared (χ2) goodness-of-fit test

Sample Size N	Number of Bins
20	Do not use χ^2 test
50	5 to 10
100	10 to 20
>100	$\sqrt{N}$ to $N/5$

I.6 Coefficient of determination

Coefficient of determination (R^2) is used to describe how well a regression line fits a set of data. The value of R^2 is between 0 and 1, and a closer to 1 indicates a regression line fit the data well. the definition of the R^2 is:

$$R^2 = 1 - \frac{ss_{err}}{ss_{tot}} \quad \text{(I - 9)}$$

$$ss_{err} = \sum_i (y_i - f_i)^2 \quad \text{(I - 10)}$$

$$ss_{tot} = \sum_i (y_i - \bar{y})^2 \quad \text{(I - 11)}$$

Where y_i is value from sample vector, f_i is associated with modeled value, $\bar{y}$ is the mean of the sample vector.

II. ANALYSIS AND STATISTICAL TESTS FOR GENERATING WEEKLY VARIANCES OF SHIP ARRIVALS

In order to make sure that the suggested method can be used for generating random weekly variances of ship arrivals (section 3.3.2.2), this study provided two steps to test that the method for generating weekly ship arrivals is valid. Firstly, the residual from the linear regression of data from different years are from a continuous normal distribution with the same mean and variance. That makes sure that only one function is needed for generating random residuals for weekly variances. Secondly, the generated weekly variances of ship arrivals are similar to the real weekly variances. This further checks whether the function can generate similar results to reality. The following texts in the Appendix II introduce the two steps of tests in detail.

There are a number of vectors provided in the Table II-1 for the statistical tests and analysis. The residuals are calculated from the weekly ship arrivals and the linear regression. The table also provides the randomly generated numbers for the analysis.

The residual conforms to the normal distribution. The normal probability plot shows that the residuals of weekly ship arrivals and the linear regression (we use “residual vector” for short in the following texts) conform to normal distribution, see Figure II-1. The normal hypothesis of the “residual” is failed to be rejected by MATLAB® function “lillietest ()”at the 5% significance level. However, when it is tested with “jbtest ()”, the null hypothesis that the residual vector R in Table II-1 comes from a normal distribution is rejected. But we found an extreme number from week 52. If we left the number from week 52 out, the null hypothesis is not rejected. In the end, we still treat the residual vector R as normal distributed, as one sample is not considered to affect the results much.

Residual vectors in different years come from a normal distribution with the same mean and variance. It is found that the number of ship passages is increasing, we need to know whether the traffic density affect the mean and variance of the normal distributed residuals. The residual vector R in the Table II-1 is divided into two groups of vectors: one group

includes the 51 weeks of data from the year 2009, and the other group includes 51 weeks of data from the year 2010 (the week 52 is left out). The null hypothesis is that both the vectors come from a normal distribution of with the same mean and variance. After the normal probability plot, it is found that both scatters are following straight lines through the first and third quartiles, which indicates approximate normal distributions, see Figure II-2, in which "+" stands for scatter of vector from the year 2009 and "*" stands for scatter of vector from the year 2010. We also performed MATLAB® function "kstest2 ()", the null hypothesis at the 5% significance level is not rejected. This means that both residual vectors come from the same continuous distribution. Another evidence of similar normality is illustration of CDF (Cumulative Distribution Function) for both residual vectors. MATLAB® function "cdfplot ()" is used in this case, see Figure II-3. In conclusion, the analyses show that the residual vectors come from the same normal distribution, which is not affected by the increasing density of ship traffic.

Statistical analyses show that the generated number and the real number for weekly variances for ship arrivals come from the same continuous distribution. Firstly, the total number of passages in real data is 45804 in the two years. However, the generated total number of passages is 46421, which is similar to the real data. Secondly, MATLAB® function "kstest2 ()" fails to rejection of the null hypothesis that the weekly number of ship arrivals and the same vector generated by proposed method are from the same continuous distribution. Lastly, the histograms show that the real weekly numbers and the generated weekly numbers are similar (Figure II-4). In conclusion, the result also shows that the generated number can substitute the real number as data input for simulation.

Table II-1 Weekly variances, regression, residuals, and random numbers for incoming ship arrivals

Number of Week	Number of Ship Arrivals (N)	Calculated Number of Ship Arrivals by Regression line (CN)	Residual (R = N - CN)	Random Normal (RN) $\aleph(0, 32.9)$	Generated Number (GN = CN + RN)
1	362	410	-48	89.8	500
2	409	411	-2	-9.7	401
3	415	411	4	18.6	430
4	429	412	17	52.0	464
5	418	413	5	89.8	503
6	447	413	34	10.0	423
7	400	414	-14	-26.0	388
8	424	415	9	26.4	441
9	447	415	32	-43.4	372
10	450	416	34	-9.0	407
11	442	417	25	8.9	426
12	445	418	27	49.0	467
13	427	418	9	47.3	465
14	431	419	12	-0.9	418

15	392	420	-28	30.4	450
16	435	420	15	-10.6	409
17	437	421	16	21.7	443
18	410	422	-12	63.0	485
19	456	422	34	5.2	427
20	394	423	-29	-9.9	413
21	409	424	-15	-16.4	408
22	426	424	2	23.6	448
23	434	425	9	44.0	469
24	391	426	-35	69.9	496
25	437	426	11	1.8	428
26	414	427	-13	5.4	432
27	427	428	-1	-20.8	407
28	429	428	1	53.0	481
29	397	429	-32	-2.5	427
30	388	430	-42	-15.6	414
31	405	430	-25	71.8	502
32	425	431	-6	26.6	458
33	422	432	-10	23.6	456
34	446	432	14	-33.1	399
35	461	433	28	14.3	447
36	460	434	26	17.1	451
37	400	435	-35	-35.9	399
38	454	435	19	-7.4	428
39	461	436	25	-13.3	423
40	433	437	-4	17.4	454
41	412	437	-25	-33.1	404
42	399	438	-39	35.8	474
43	505	439	66	58.7	498
44	462	439	23	-10.0	429
45	453	440	13	-0.3	440
46	488	441	47	16.7	458
47	423	441	-18	39.6	481
48	442	442	0	17.2	459
49	434	443	-9	13.1	456
50	424	443	-19	-15.9	427
51	376	444	-68	-7.6	436
52	309	445	-136	20.2	465
53	372	445	-73	55.3	500
54	402	446	-44	18.7	465
55	457	447	10	-39.7	407
56	467	447	20	14.2	461
57	456	448	8	-3.0	445
58	468	449	19	-8.0	441
59	501	449	52	-7.2	442

60	433	450	-17	-28.9	421
61	455	451	4	-10.6	440
62	480	451	29	-25.8	425
63	493	452	41	-12.0	440
64	462	453	9	3.9	457
65	464	454	10	5.7	460
66	459	454	5	-7.1	447
67	504	455	49	-5.0	450
68	506	456	50	1.1	457
69	498	456	42	15.1	471
70	420	457	-37	42.1	499
71	437	458	-21	20.4	478
72	454	458	-4	-9.4	449
73	479	459	20	19.7	479
74	502	460	42	-8.1	452
75	419	460	-41	-58.6	401
76	422	461	-39	-77.2	384
77	515	462	53	-56.4	406
78	420	462	-42	-7.8	454
79	443	463	-20	-20.4	443
80	416	464	-48	-23.7	440
81	468	464	4	1.3	465
82	442	465	-23	-21.7	443
83	454	466	-12	-20.7	445
84	420	466	-46	20.0	486
85	429	467	-38	25.7	493
86	440	468	-28	80.1	548
87	448	468	-20	9.9	478
88	480	469	11	1.9	471
89	477	470	7	-18.9	451
90	438	471	-33	-6.4	465
91	495	471	24	-1.7	469
92	467	472	-5	-57.7	414
93	527	473	54	-8.5	465
94	476	473	3	24.7	498
95	509	474	35	-18.8	455
96	505	475	30	16.3	491
97	471	475	-4	32.6	508
98	526	476	50	35.4	511
99	486	477	9	25.5	503
100	543	477	66	-74.3	403
101	447	478	-31	-18.6	459
102	490	479	11	29.6	509
103	446	479	-33	13.0	492
Total	45804	-	-	-	46421

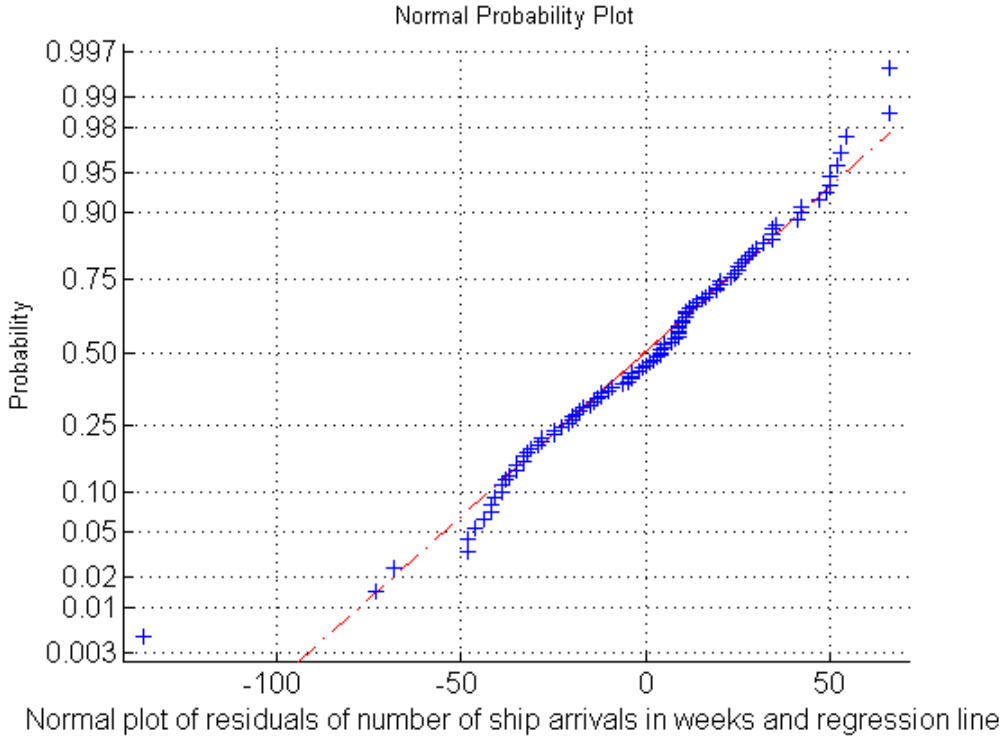

Figure II-1 Normal plot of residuals of number of ship arrivals in weeks and regression line (103 weeks)

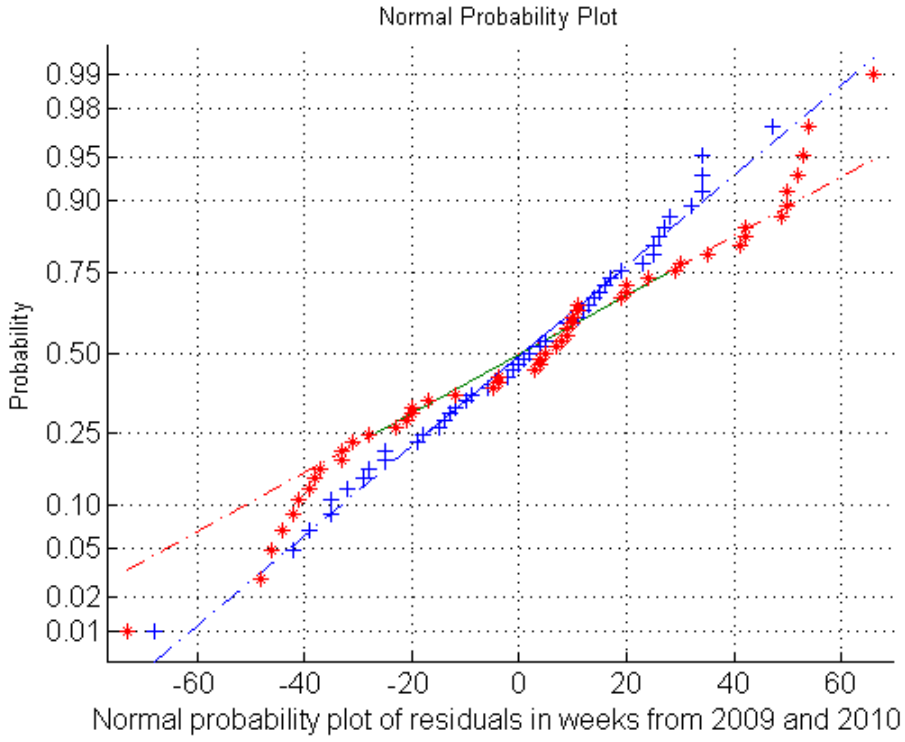

Figure II-2 Normal probability plot of residuals of number of ship arrivals in weeks and regression line for data from 2009 and 2010 (102 weeks)

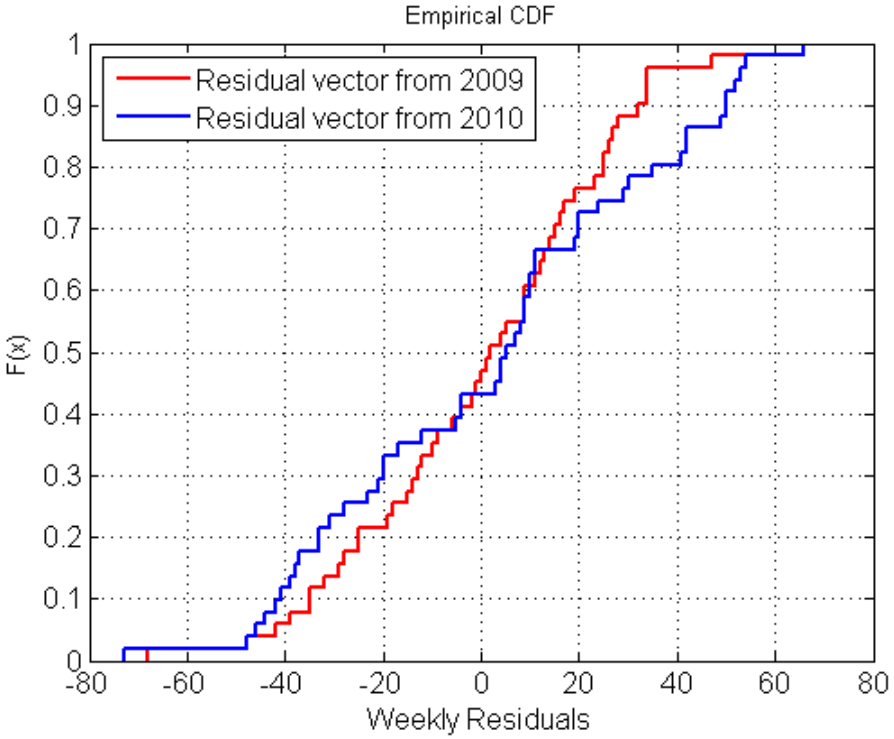

Figure II-3 CDF of residuals from number of ship arrivals in weeks and regression line for data from 2009 and 2010 (102 weeks)

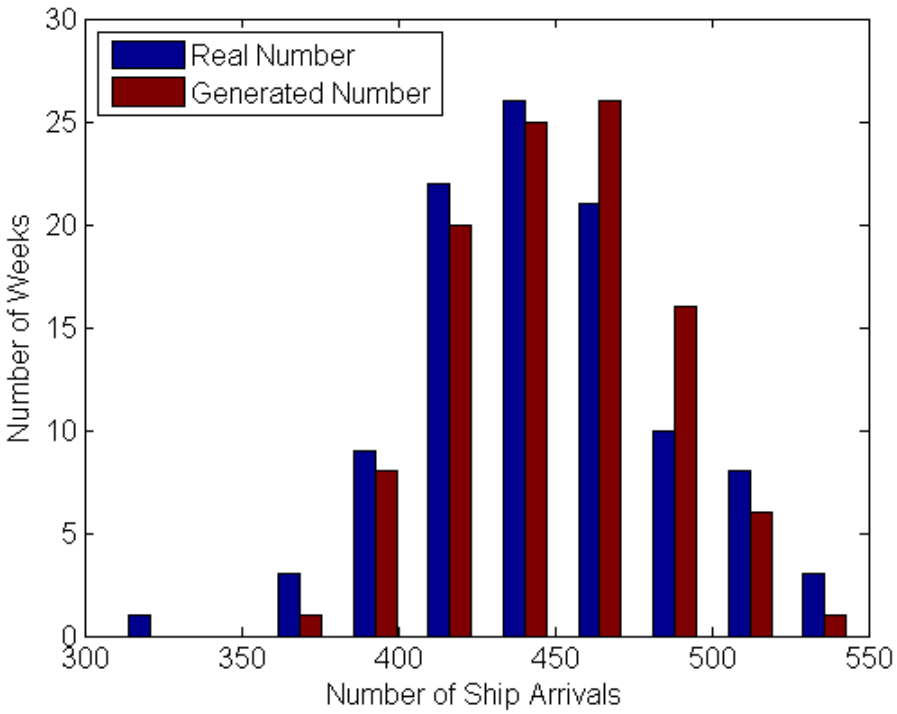

Figure II-4 Histograms of weekly number of passages and generated number (103 weeks)

III. ANALYSIS AND STATISTICAL TESTS FOR GENERATING DAILY VARIANCES OF SHIP ARRIVALS

In order to make sure that the suggested method can be used for generating random daily variances of ship arrivals (section 3.3.2.3), this study provided two steps to test that the method for generating daily ship arrivals is valid. The way for the test is the same as what have been done for the weekly variances.

The residual conforms to the normal distribution. We use normal probability plot to visualize the residuals for daily number of passages from the linear regression line (we use "residual vector" for short in the following texts). The "jbtest ()" does not reject the normal hypothesis of the residual, however the "lillietest ()" rejected the null hypothesis. Probably this is because the "lillietest ()" only good at testing small samples.

Residual vectors in different years come from a normal distribution with the same mean and variance. We divide the residual vector R into two groups of vectors, one group includes 360 days of data from the year 2009 (one data is left out to get the same sample size with the days in 2010), and the other group includes the 360 days of data from the year 2010. The null hypothesis is that both the vectors come from a normal distribution with the same mean and variance. After the normal probability plot, it is found that both the scatters are following straight lines through the first and third quartiles, which indicate approximate normal distributions, see Figure III-2. We also performed MATLAB® function "kstest2 ()", the null hypothesis at the 5% significance level is not rejected. This means that both residual vectors come from the same continuous distribution. Another evidence of similar normality is illustration of CDF for both residual vectors. MATLAB® function "cdfplot ()" is used in this case, see Figure III-3. In conclusion, the analyses show that the daily residual vector comes from the same normal distribution, which is not affected by the increasing density of ship traffic.

Statistical analyses show that the generated number and the real number for daily variances for ship arrivals come from the same continuous distribution. Firstly, the total number of passages in real data is 45804 in the two years. However, the generated total number of passages is 46562, which is similar to the real data. Secondly, MATLAB® function "kstest2 ()" fails rejection of the null hypothesis that the daily ship arrivals and the vector generated are from the same continuous distribution. Lastly, the histogram shows similarity between the real daily numbers and the generated daily numbers (Figure III-4). In conclusion, the generated number can substitute the real number as data input for simulation.

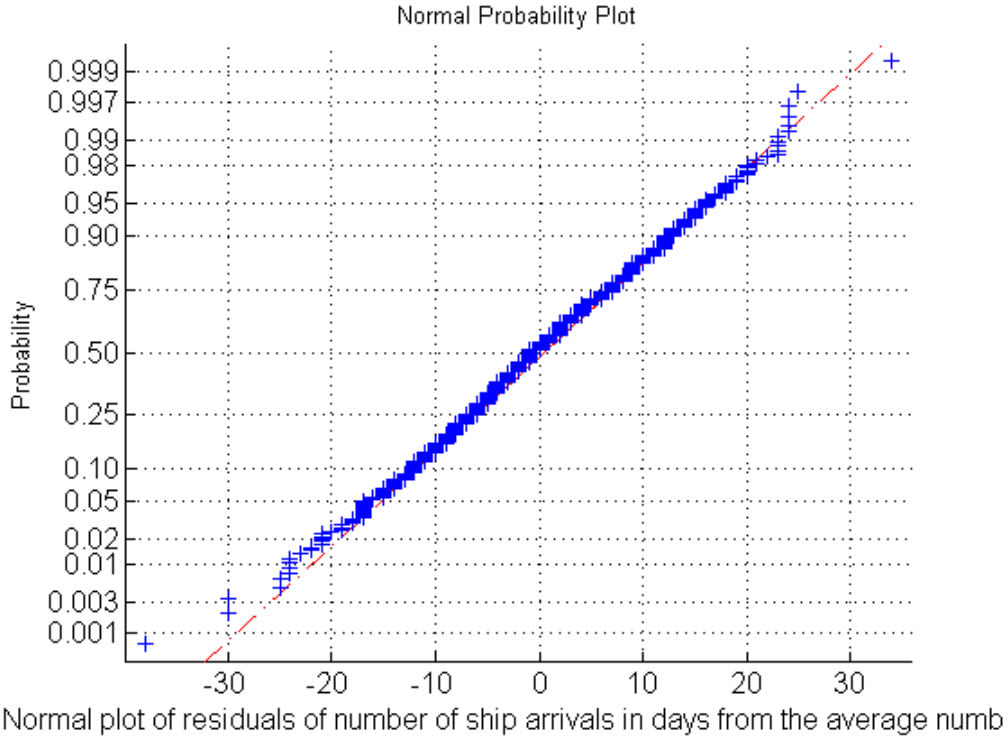

Figure III-1 Normal probability plot for daily residuals of ship passage from the average (720 days)

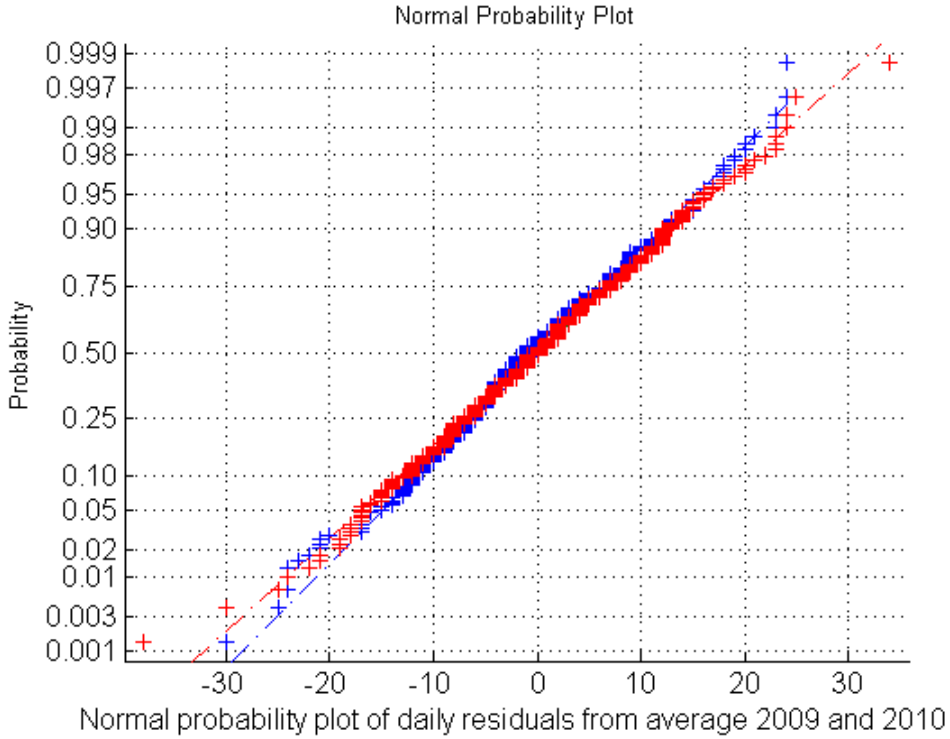

Figure III-2 Normal probability plot of daily ship arrivals residuals from average number dates from 2009 and 2010 (720 days altogether)

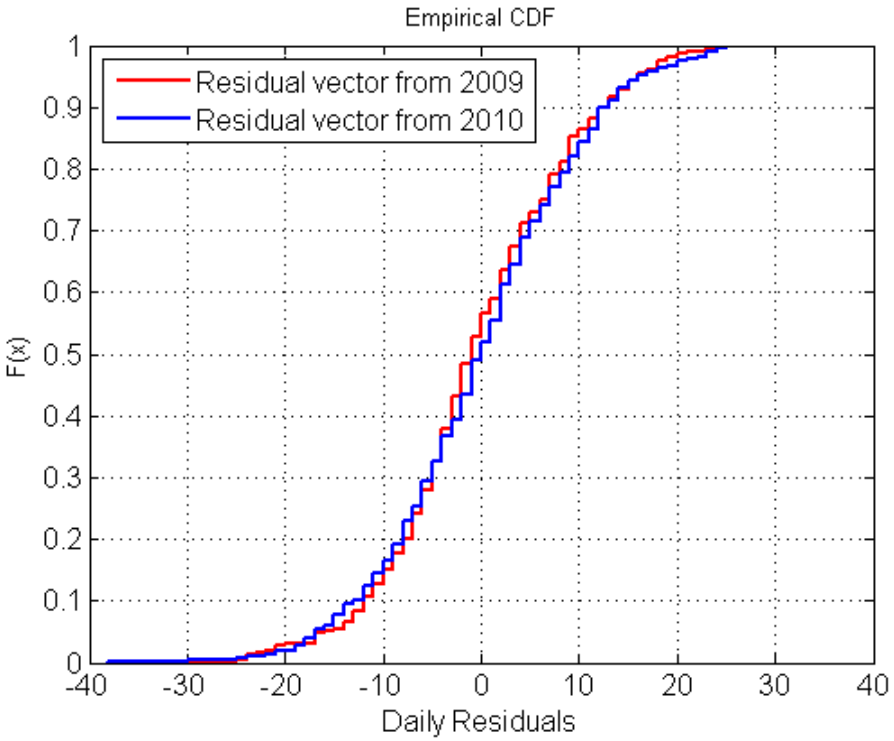

Figure III-3 CDF of residuals from number of daily ship arrivals and average number for data from 2009 and 2010 (720 days)

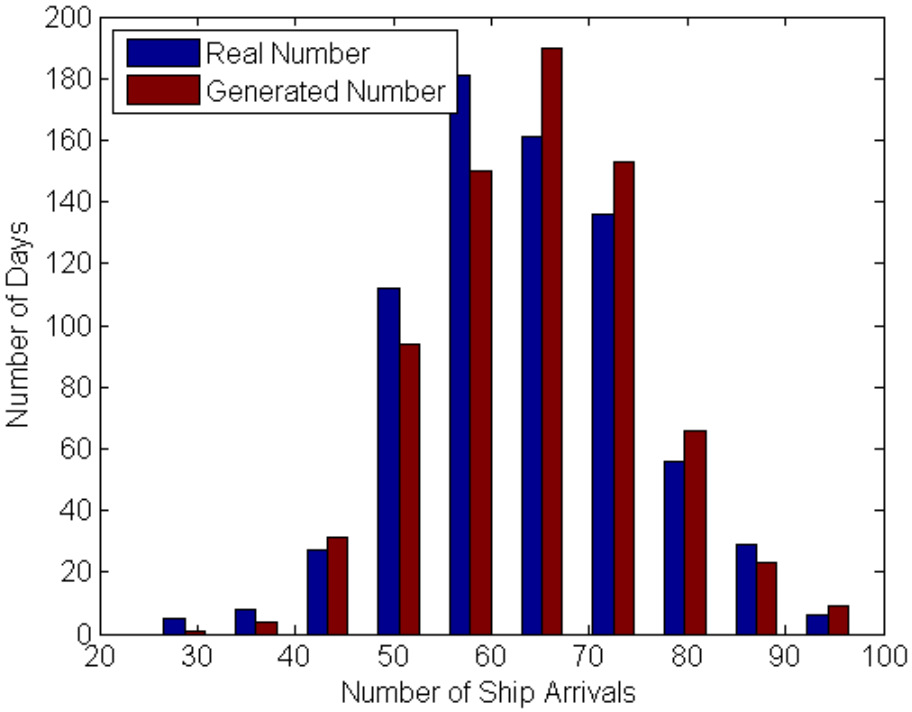

Figure III-4 Histograms of daily number of passages and generated number (720 days)

IV. CLASSIFICATIONS BASED ON GROSS TONNAGE FOR EACH TYPE OF SHIPS OTHER THAN CONTAINER SHIPS

This appendix is relevant to section 3.3.3.1. Ship type I is classified into 4 groups, see Figure IV-1 and Table IV-1. Ship type III is classified into 3 groups, see Figure IV-2 and Table IV-2. Ship type IV is classified into 2 groups, see Figure IV-3 and Table IV-3. Ship type V is classified into 3 groups, see Figure IV-4 and Table IV-4. Ship type VI is classified into 4 groups, see Figure IV-5and Table IV-5. Ship type VII is classified into 4 groups, see Figure IV-6 and Table IV-6. Ship type VIII is classified into 3 groups, see Figure IV-7and Table IV-7.

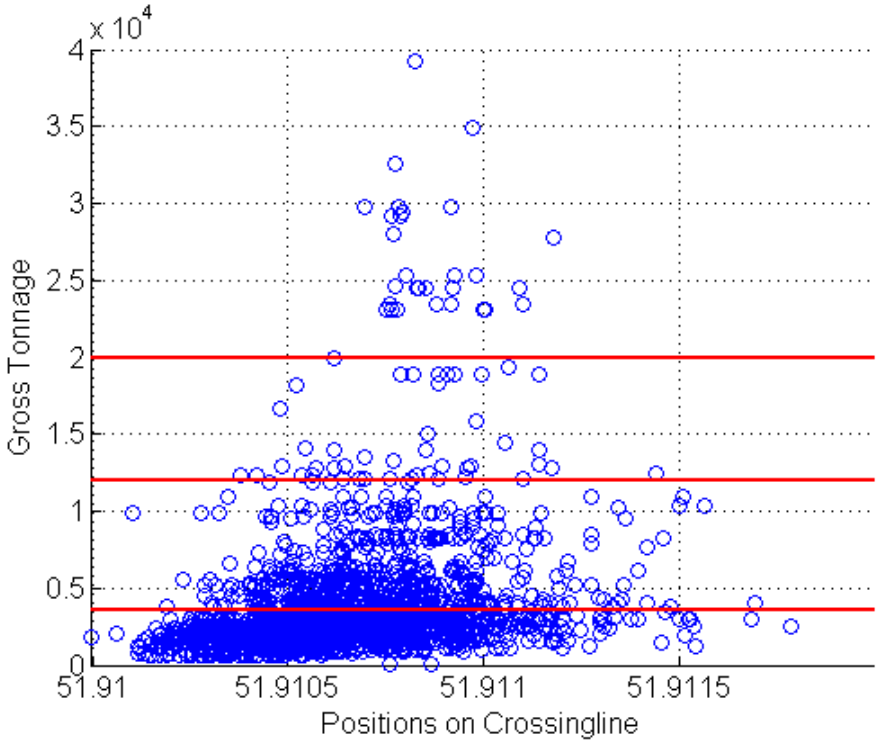

Figure IV-1 Scatter points of ship position and gross tonnage for ship type I (based on 2000 passages)

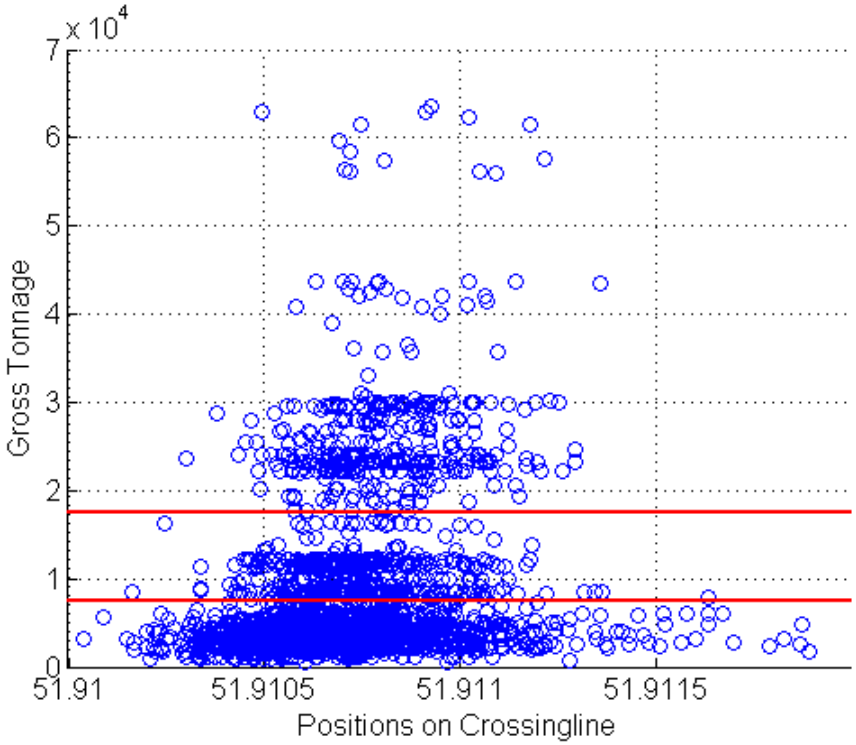

Figure IV-2 Scatter points of ship position and gross tonnage for ship type III (based on 2000 passages)

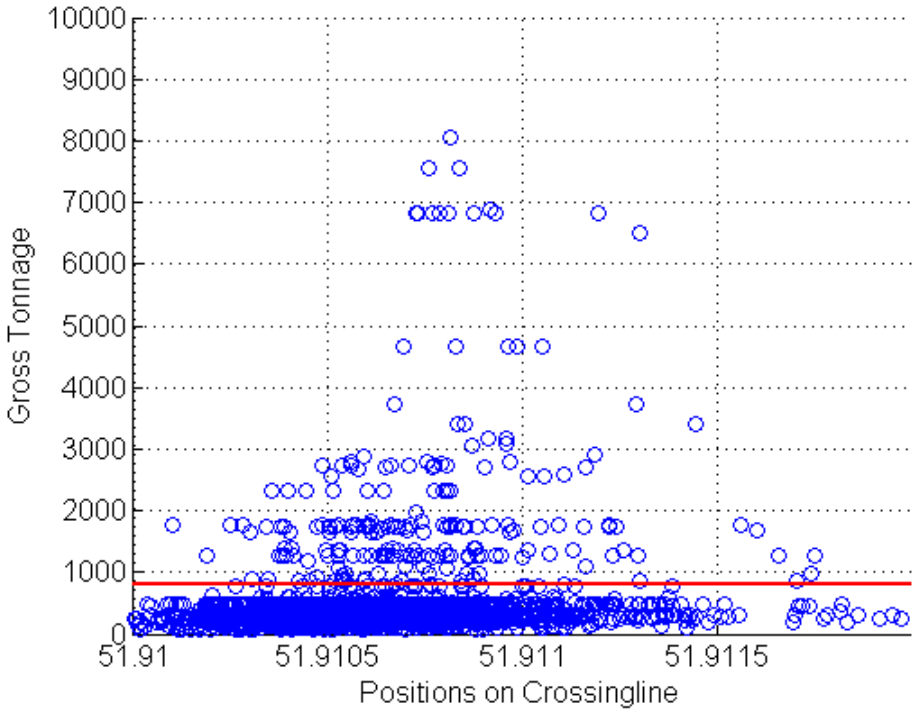

Figure IV-3 Scatter points of ship position and gross tonnage for ship type IV (based on 2000 passages)

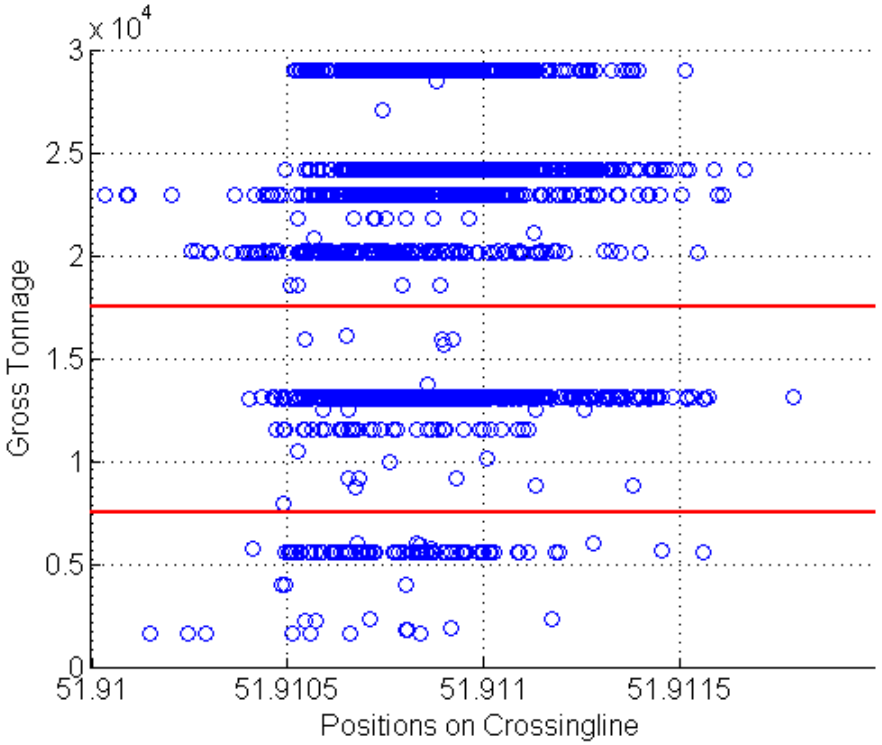

Figure IV-4 Scatter points of ship position and gross tonnage for ship type V (based on 2000 passages)

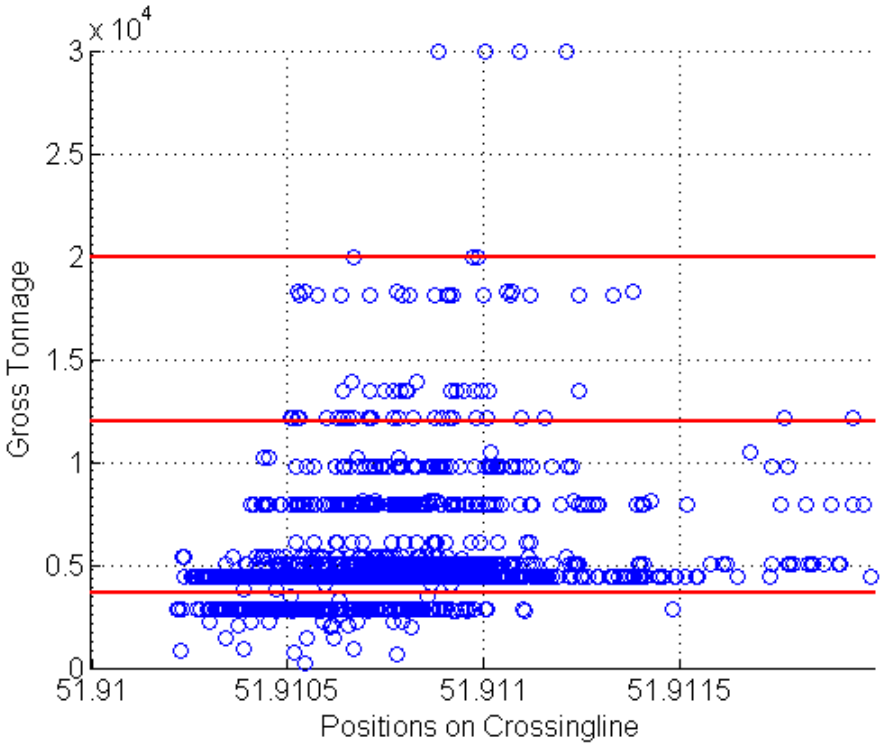

Figure IV-5 Scatter points of ship position and gross tonnage for ship type VI (based on 2000 passages)

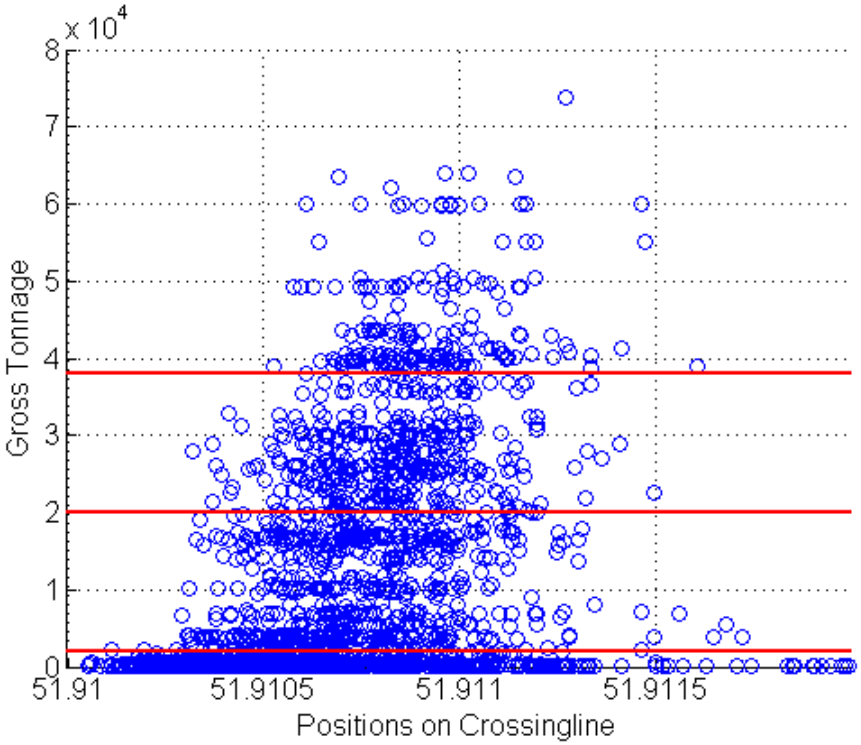

Figure IV-6 Scatter points of ship position and gross tonnage for ship type VII (based on 2000 passages)

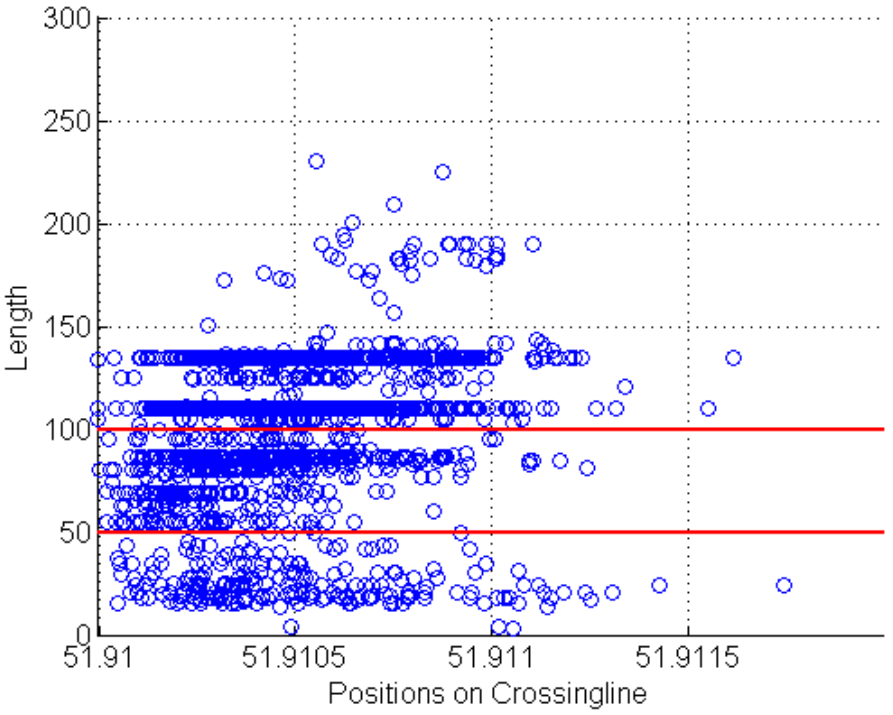

Figure IV-7 Scatter points of ship position and gross tonnage for ship type VIII (based on 2000 passages)

Table IV-1 Classification of ships type I by gross tonnage

Class	Class 1	Class 2	Class 3	Class 4
Gross tonnage (t)	<3600	3601-12000	12001-20000	>20000

Table IV-2 Classification of ships type III by gross tonnage

	Class 1	Class 2	Class 3
Gross tonnage (t)	<7500	7501-17500	>17500

Table IV-3 Classification of ships type IV by gross tonnage

Class	Class 1	Class 2
Gross tonnage (t)	<800	>800

Table IV-4 Classification of ships type V by gross tonnage

Class	Class 1	Class 2	Class 3
Gross tonnage (t)	<7500	7501-17500	>17500

Table IV-5 Classification of ships type VI by gross tonnage

Class	Class 1	Class 2	Class 3	Class 4
Gross tonnage (t)	<3600	3601-12000	12001-20000	>20000

Table IV-6 Classification of ships type VII by gross tonnage

Class	Class 1	Class 2	Class 3	Class 4
Gross tonnage (t)	<2000	2001-20000	20001-38000	>38000

Table IV-7 Classification of Ships type VIII by gross tonnage

Class	Class 1	Class 3
Length (m)	< 50	>51

V. AVERAGED VESSEL PATH AND SPEED FOR DIFFERENT CATEGORIES OF SHIPS

This appendix is relevant to section 3.3.3.1. As the part of studied area is comparatively straight waterway, so the ship tracks look straight too, except for beginning of a waterway bend at the crossing-line 9. However, the average speeds are very different, vessels increase speed in the straight waterway and they decrease speed before waterway bend. The following graphs show the details of average paths and speed for different categories of ships.

V.1 Ship type I (General Cargo Ships)

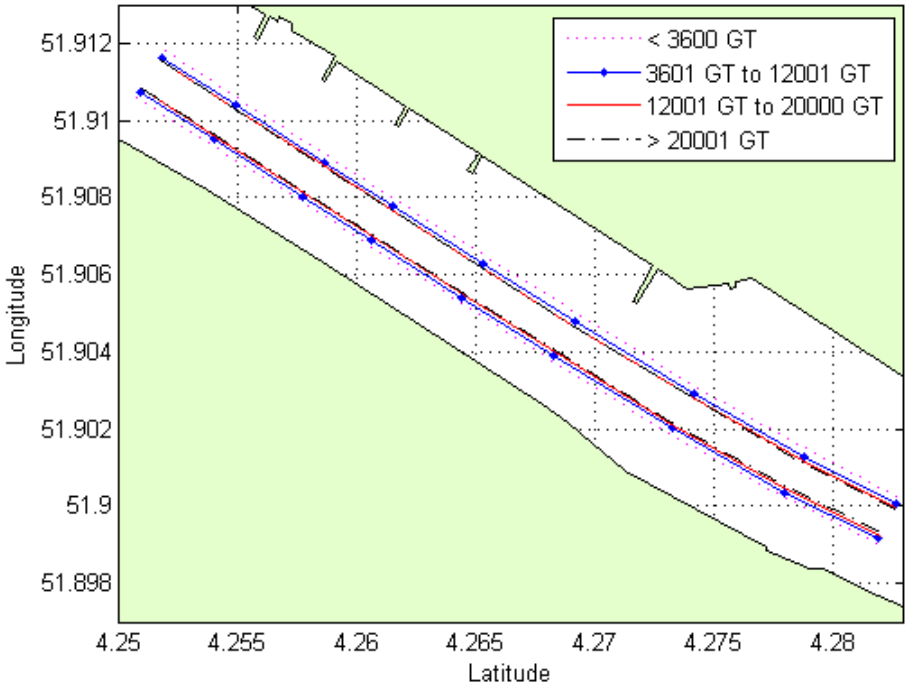

Figure V-1 Average vessel paths for ship type I on both incoming and outgoing directions

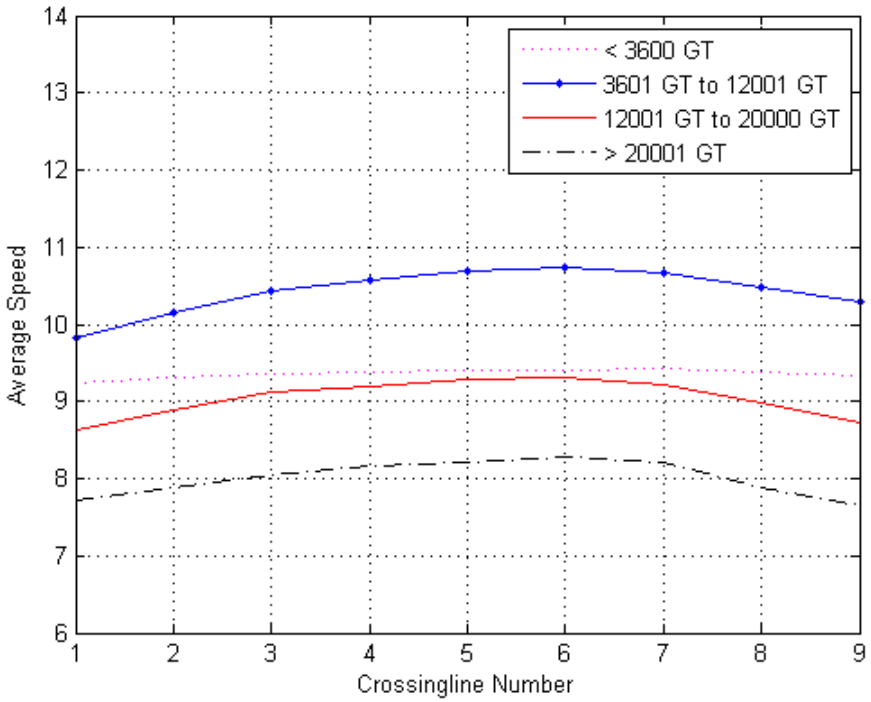

Figure V-2 Average speed for ship type I of incoming direction

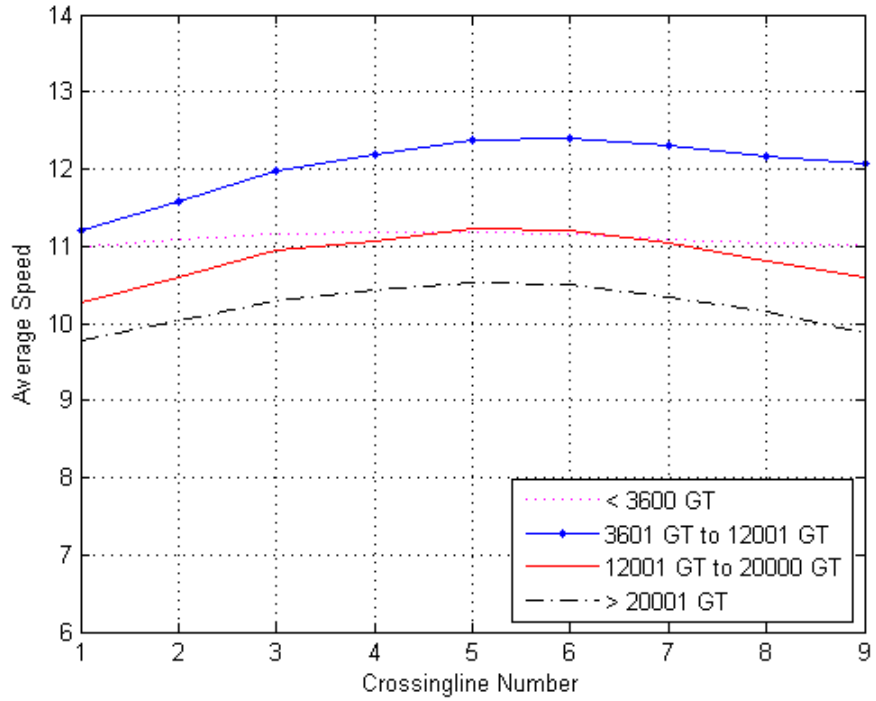

Figure V-3 Average speed for ship type I of outgoing direction

V.2 Ship type II (Containers ships)

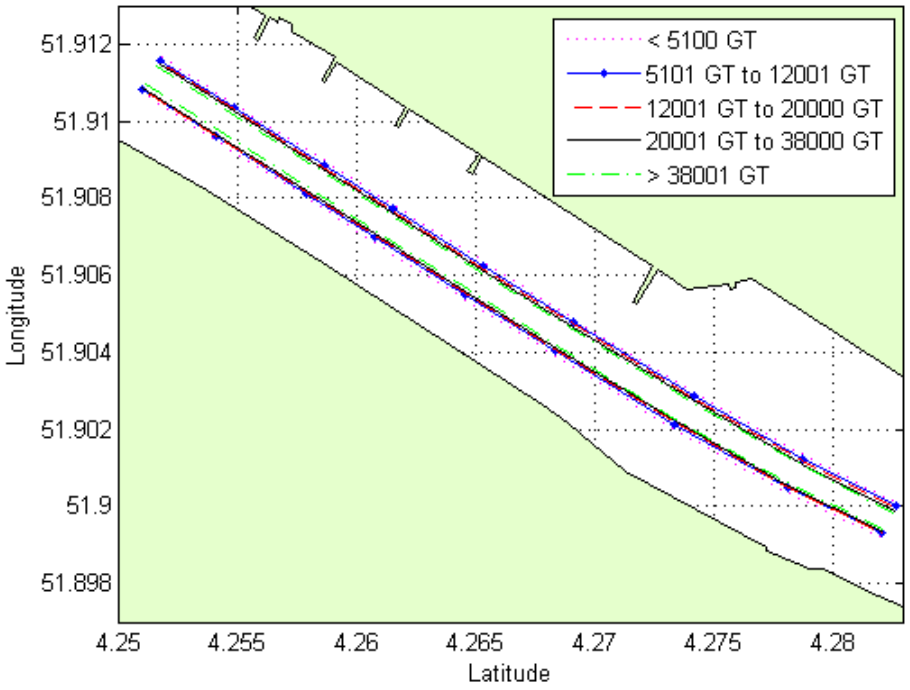

Figure V-4 Average vessel paths for ship type II on both incoming and outgoing directions

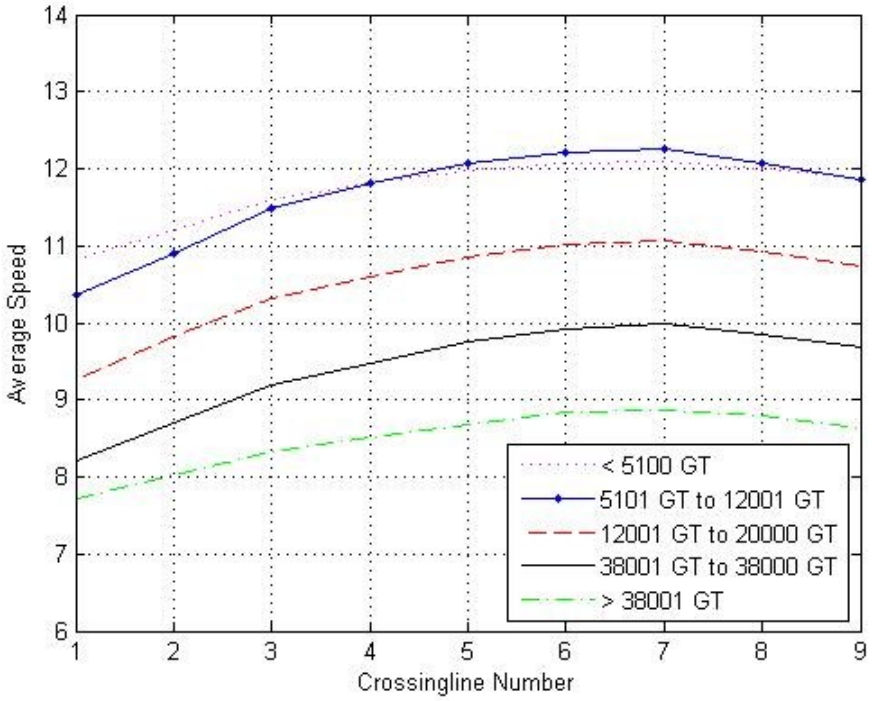

Figure V-5 Average speed for ship type II of on incoming direction

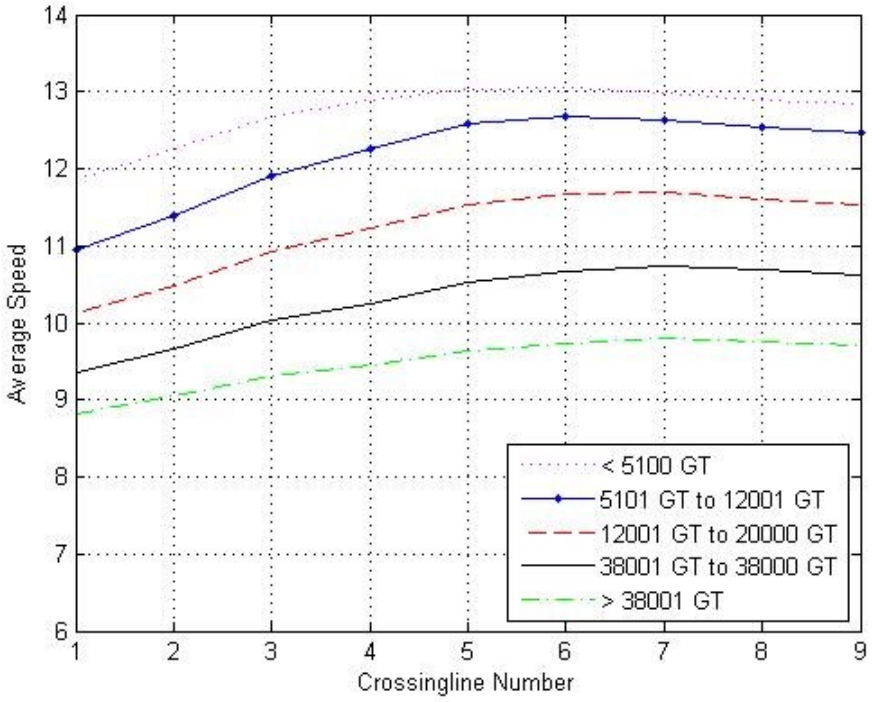

Figure V-6 Average speed for ship type II of for outgoing direction

V.3 Ship type III (Chemical ships, LPG, LNG and Oil tanker)

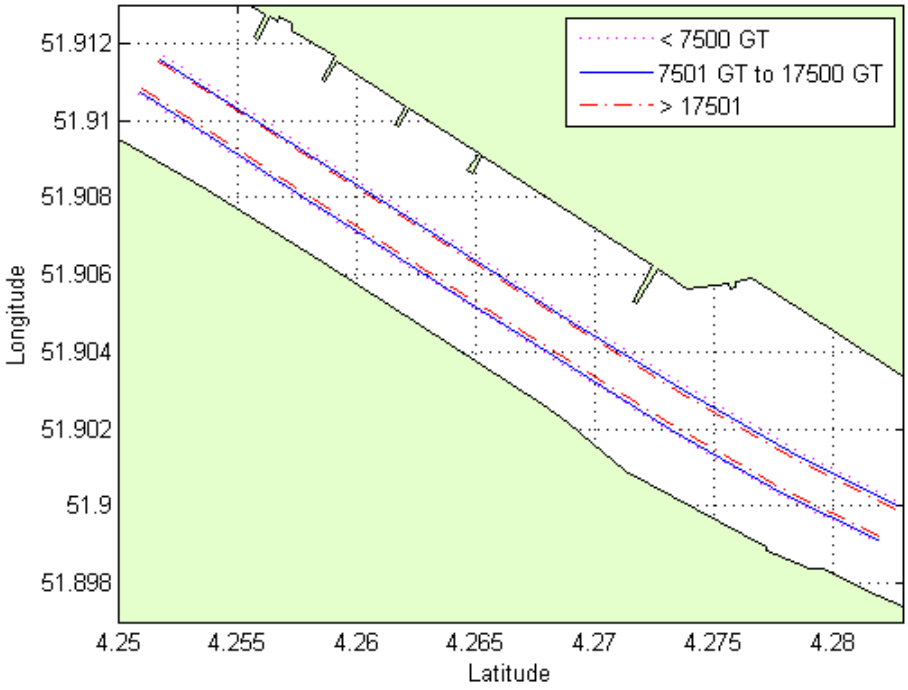

Figure V-7 Average vessel paths for ship type III on both incoming and outgoing directions

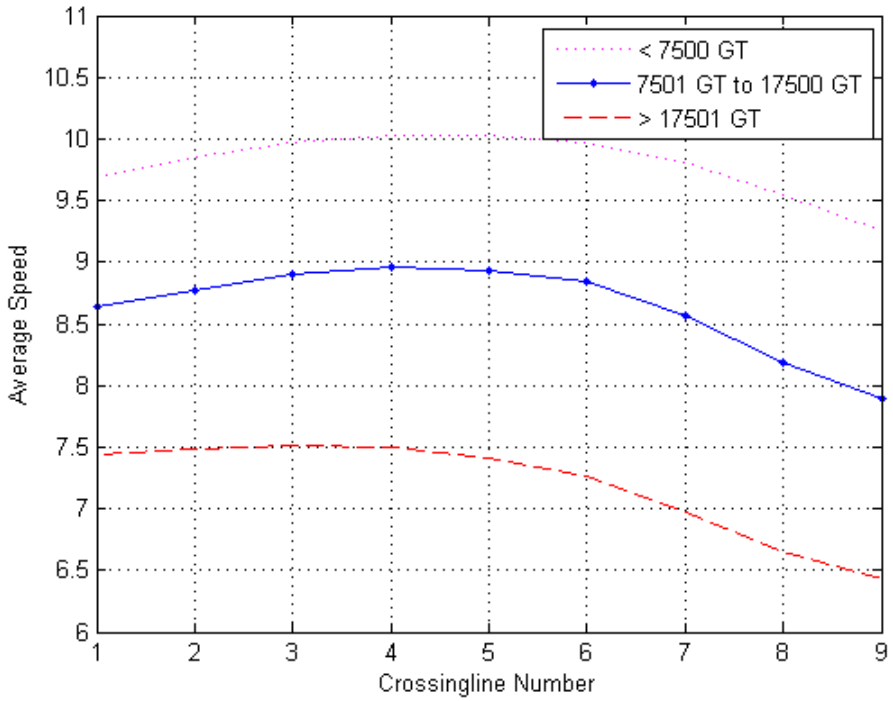

Figure V-8 Average speed for ship type III of on incoming direction

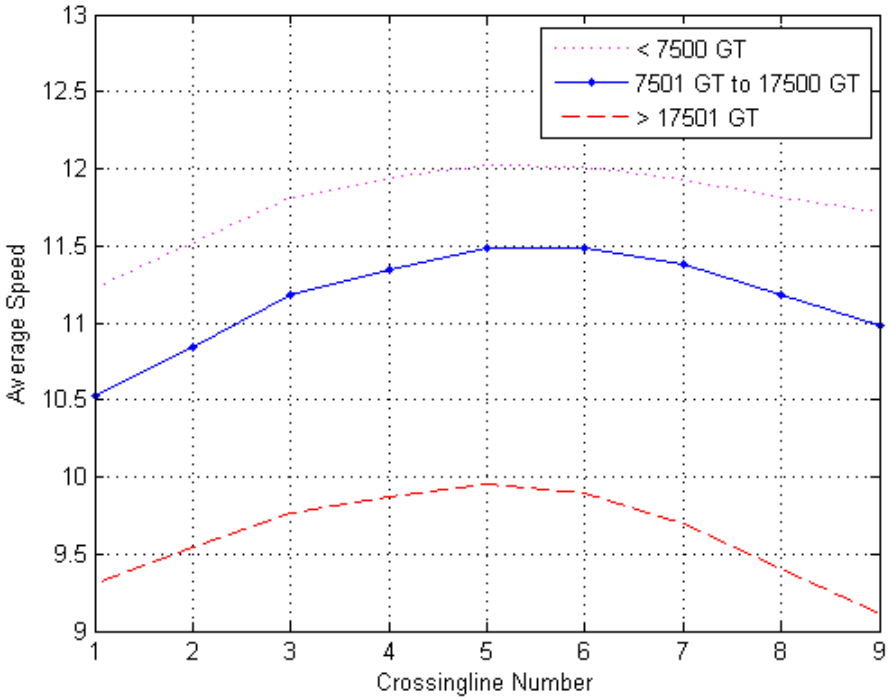

Figure V-9 Average speed for ship type III of for outgoing direction

V.4 Ship type IV (Tugs)

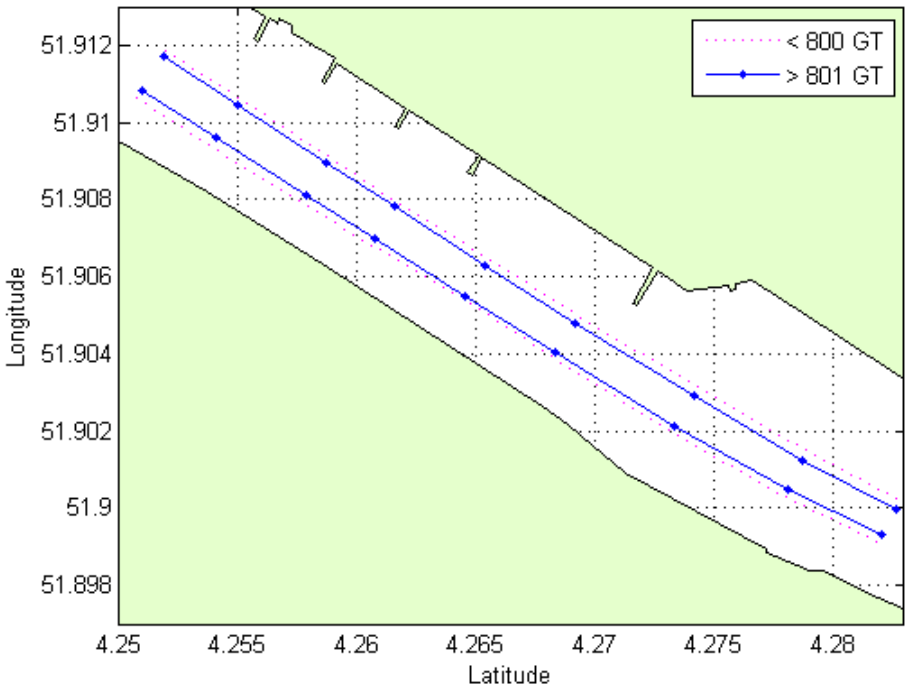

Figure V-10 Average vessel paths for ship type IV on both incoming and outgoing directions

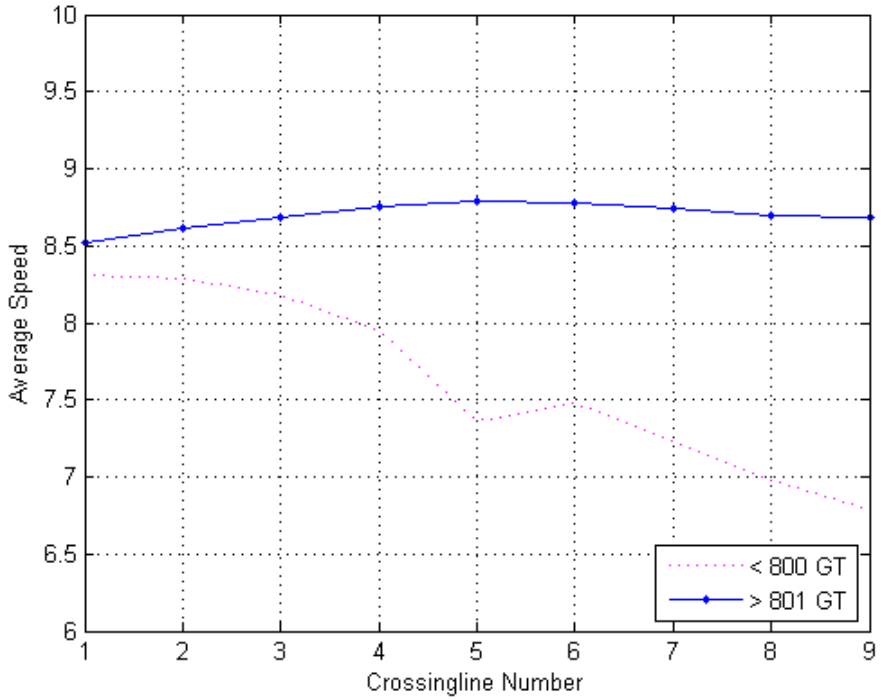

Figure V-11 Average speed for ship type IV of on incoming direction

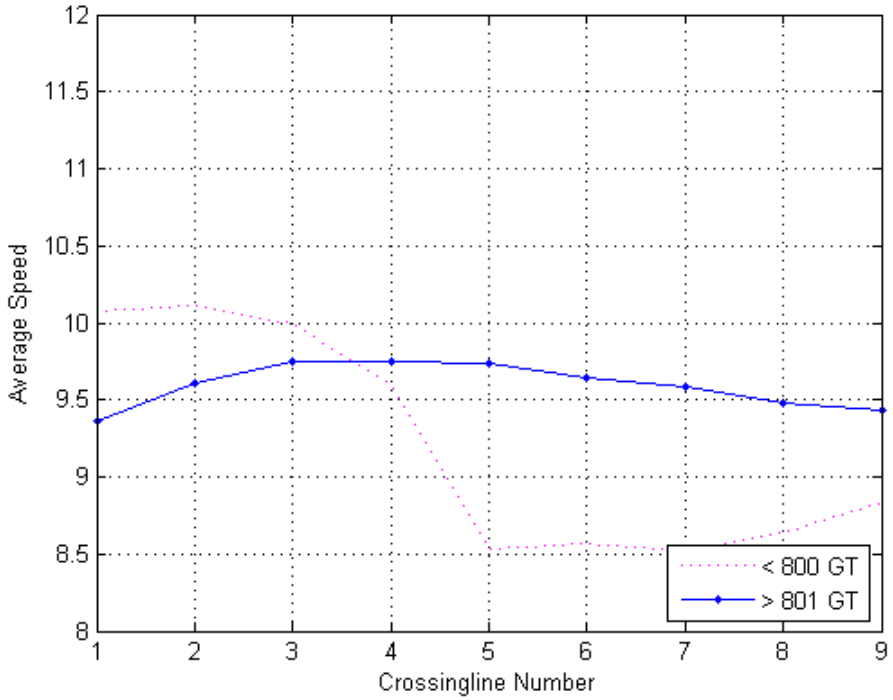

Figure V-12 Average speed for ship type IV of for outgoing direction

V.5 Ship type V (RoRo ships)

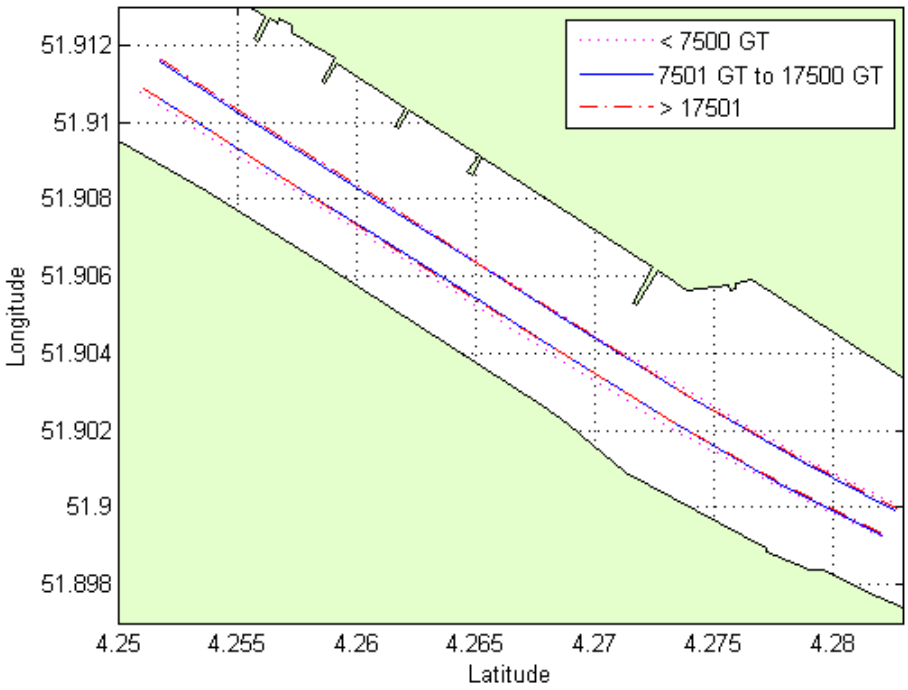

Figure V-13 Average vessel paths for ship type V on both incoming and outgoing directions

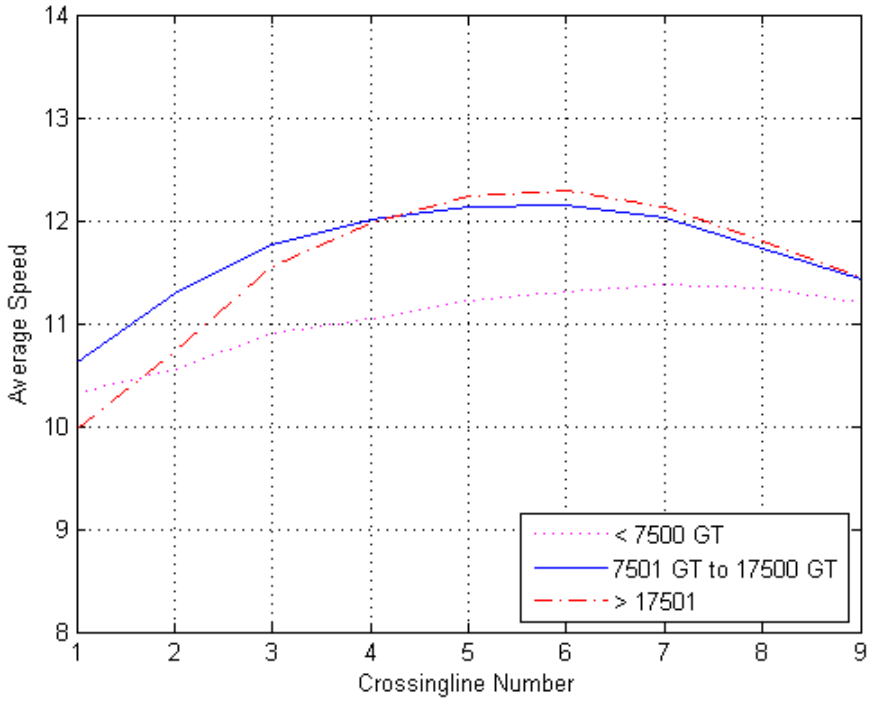

Figure V-14 Average speed for ship type V of incoming direction

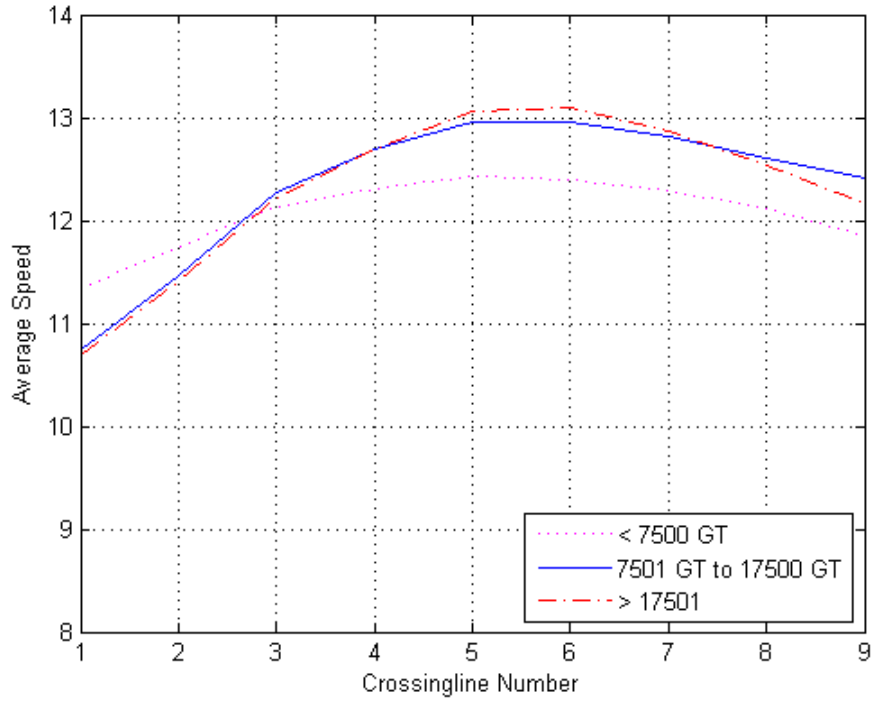

Figure V-15 Average speed for ship type V of outgoing direction

V.6 Ship type VI (Dredgers)

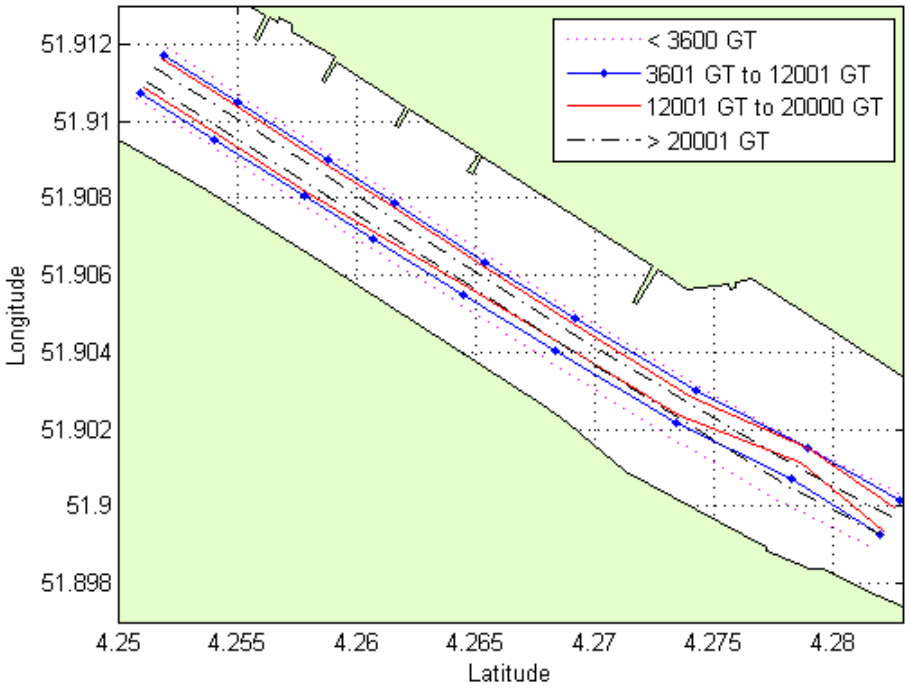

Figure V-16 Average vessel paths for ship type VI on both incoming and outgoing directions

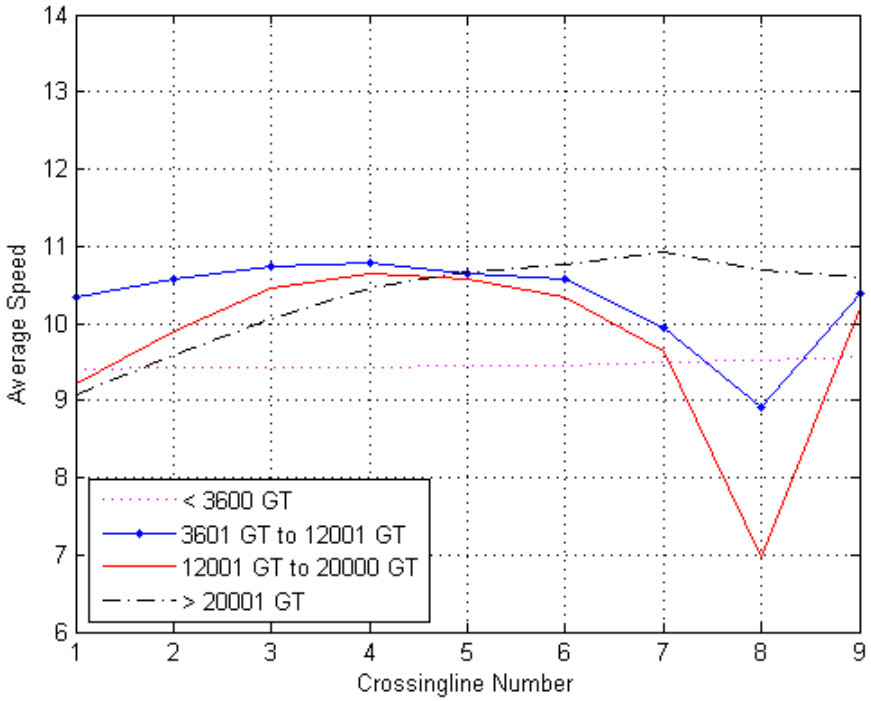

Figure V-17 Average speed for ship type VI of incoming direction

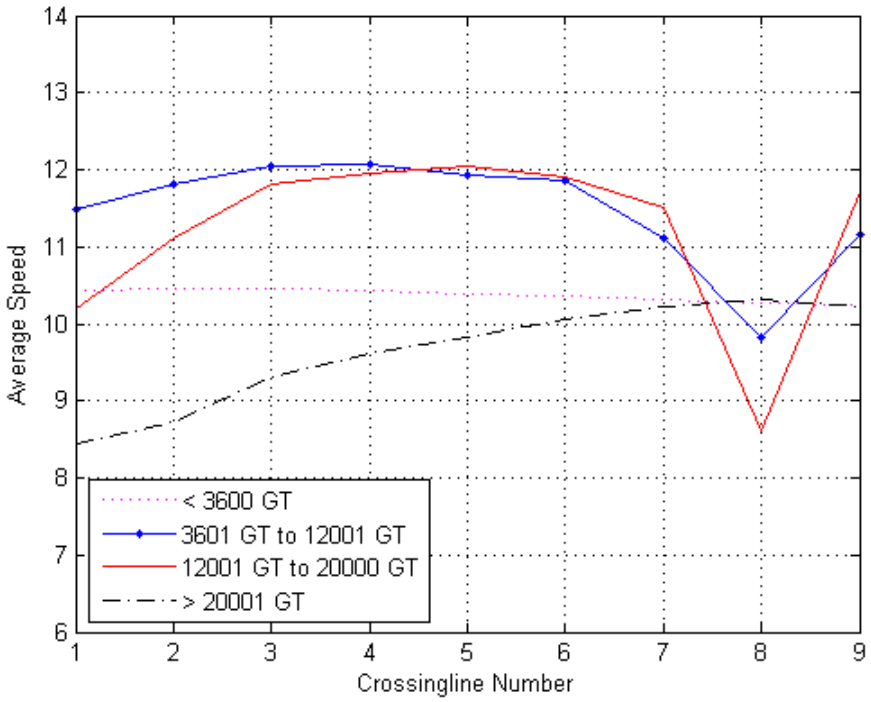

Figure V-18 Average speed for ship type VI of outgoing direction

V.7 Ship type VII (Others ships)

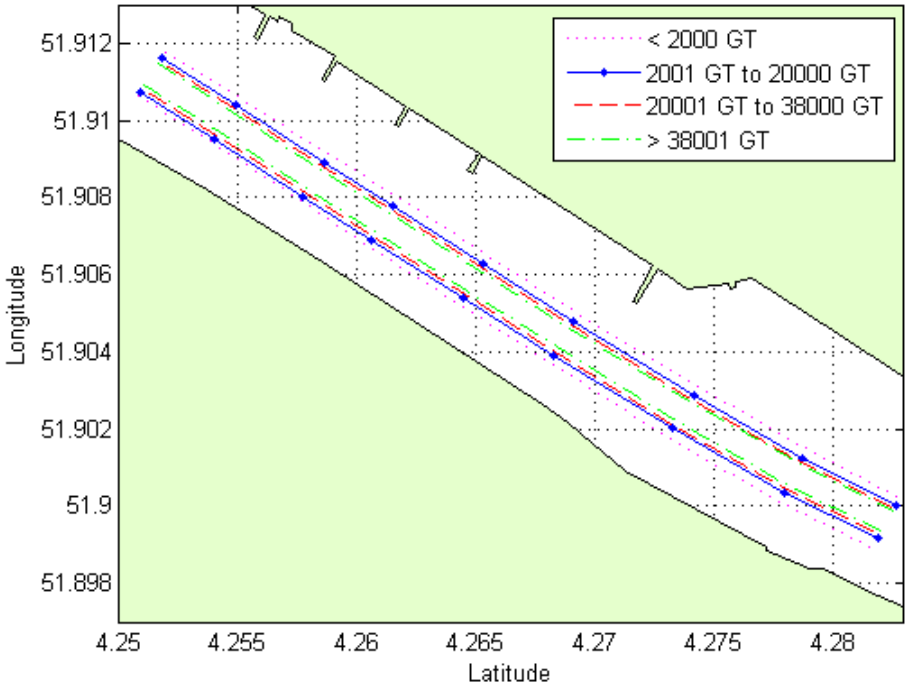

Figure V-19 Average vessel paths for ship type VII on both incoming and outgoing directions

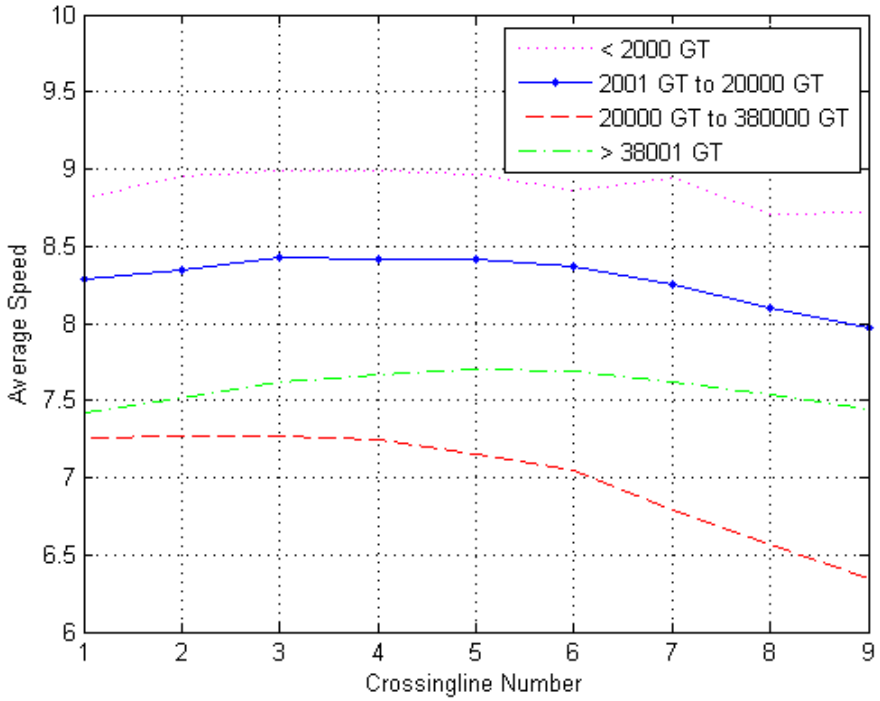

Figure V-20 Average speed for ship type VII of on incoming direction

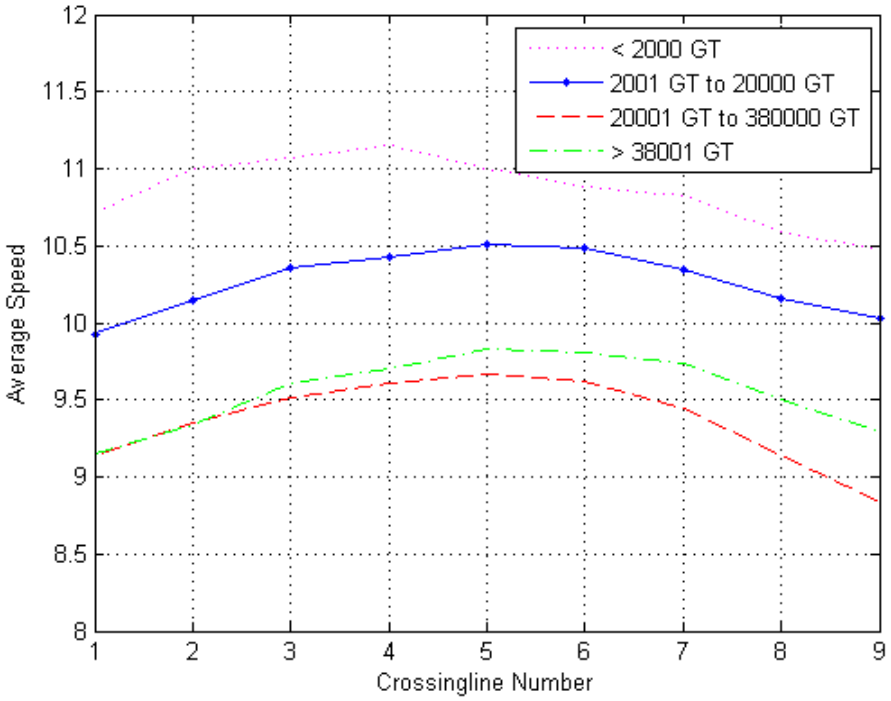

Figure V-21 Average speed for ship type VII of for outgoing direction

V.8 Ship type VIII (Unknown ship type)

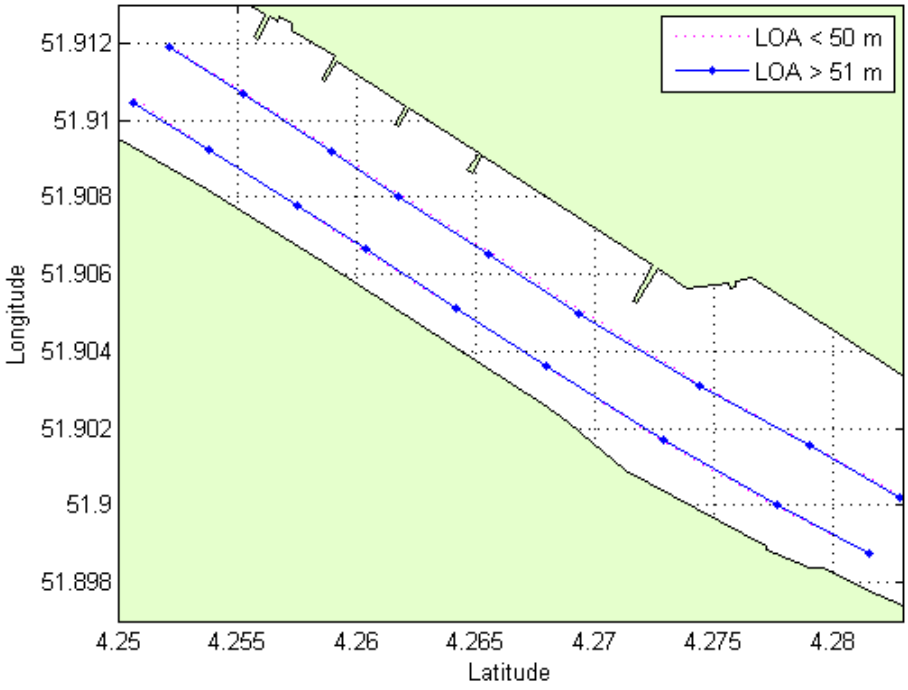

Figure V-22 Average vessel paths for ship type VIII on both incoming and outgoing directions

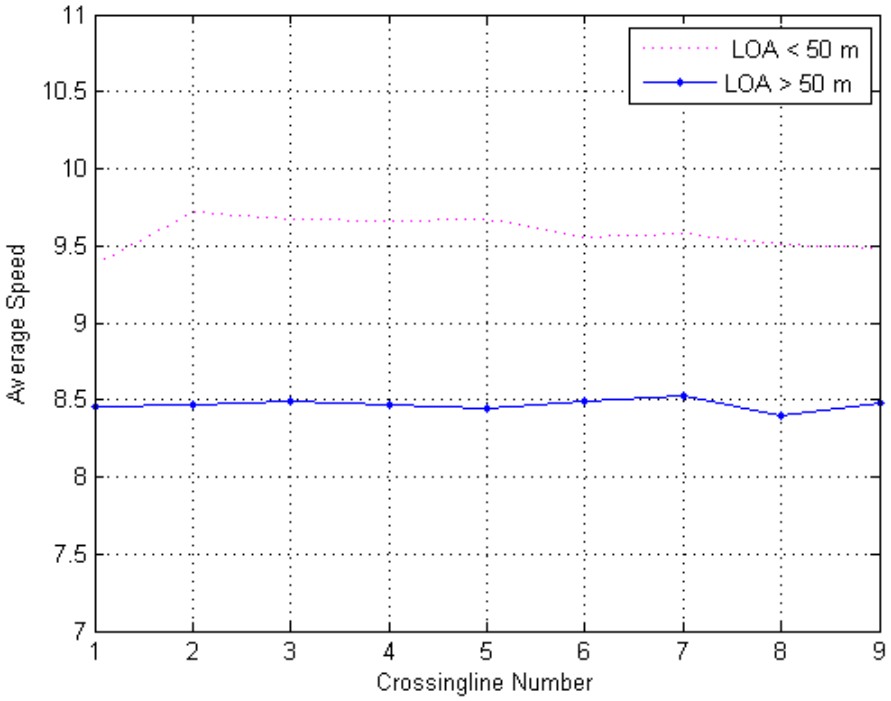

Figure V-23 Average speed for ship type VIII of on incoming direction

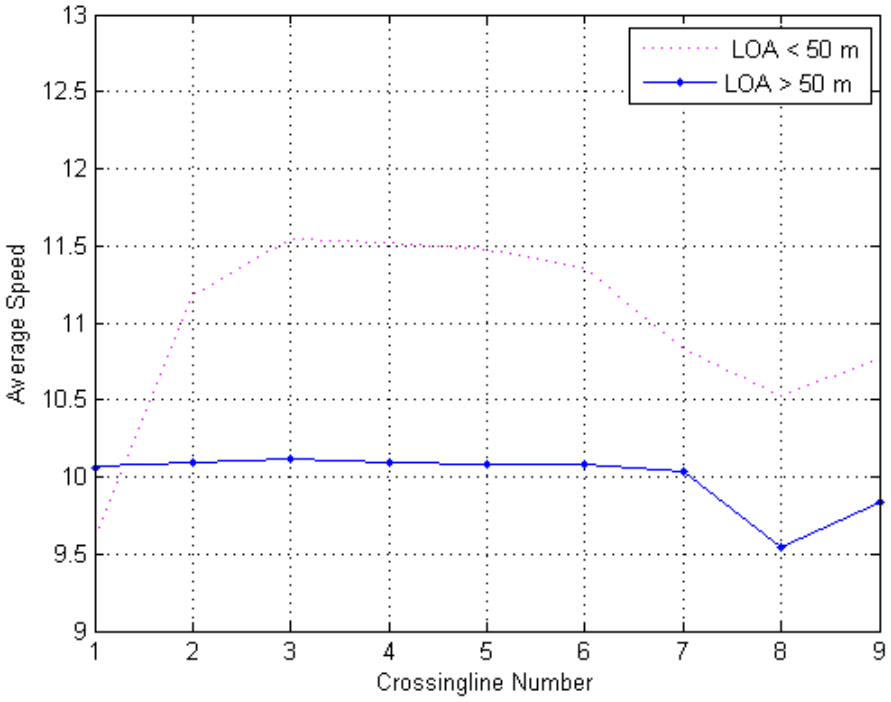

Figure V-24 Average speed for ship type VIII of for outgoing direction

VI. MATRIX OF COORDINATE COEFFICIENT ANALYSIS

We use a matrix of correlation coefficients analysis to select the parameters for equations of artificial forces. The factors in the first row and first column in the matrix are the factors that can be observed from the AIS ship tracks. The matrix of the results is presented in two different ways, a matrix with valued cells and a matrix with colored cells. The colored cells are transformed from the valued cells and this makes the analysis easier. The red and blue cells stand for strong correlations between two variables in the matrix. The lighter colors in the middle of the "color map" denote low correlations.

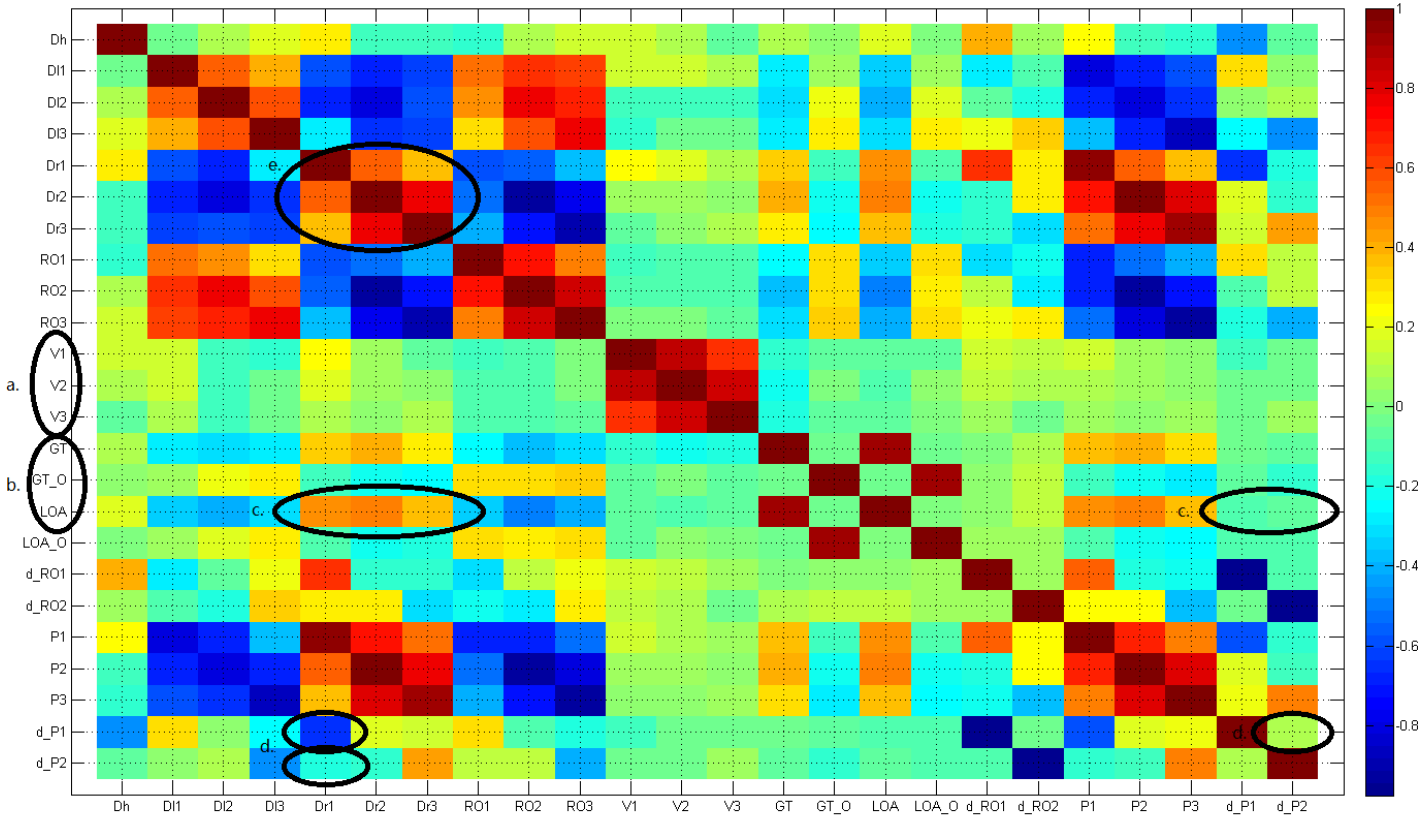

Figure VI-1 Matrix of correlation coefficient analysis results for different factors in head-on encounters (colored cells)

Table VI-1 Matrix of correlation coefficient analysis results for different factors in head-on encounters (cells with values)

	Dh	Dl1	Dl2	Dl3	Dr1	Dr2	Dr3	RO1	RO2	RO3	V1	V2	V3	GT	GT_O	LOA	LOA_O	d_RO1	d_RO2	P1	P2	P3	d_P1	d_P2
Dh	1.00	-0.03	0.09	0.17	0.28	-0.11	-0.13	-0.17	0.08	0.14	0.16	0.10	-0.06	0.10	0.04	0.18	0.00	0.41	0.05	0.24	-0.12	-0.15	-0.45	-0.08
Dl1	-0.03	1.00	0.56	0.40	-0.60	-0.69	-0.63	0.54	0.65	0.61	0.14	0.16	0.09	-0.28	0.06	-0.35	0.05	-0.27	-0.10	-0.81	-0.69	-0.59	0.32	0.03
Dl2	0.09	0.56	1.00	0.58	-0.67	-0.79	-0.60	0.45	0.76	0.66	-0.11	-0.13	-0.12	-0.30	0.20	-0.41	0.17	-0.07	-0.20	-0.68	-0.81	-0.66	0.02	0.09
Dl3	0.17	0.40	0.58	1.00	-0.28	-0.65	-0.63	0.30	0.59	0.76	-0.15	-0.05	-0.03	-0.27	0.28	-0.30	0.27	0.23	0.34	-0.37	-0.67	-0.86	-0.25	-0.45
Dr1	0.28	-0.60	-0.67	-0.28	1.00	0.56	0.37	-0.60	-0.57	-0.38	0.24	0.17	0.10	0.33	-0.14	0.45	-0.09	0.66	0.26	0.95	0.55	0.36	-0.66	-0.20
Dr2	-0.11	-0.69	-0.79	-0.65	0.56	1.00	0.75	-0.53	-0.92	-0.79	0.07	0.07	0.04	0.39	-0.21	0.49	-0.21	-0.17	0.27	0.70	1.00	0.79	0.17	-0.14
Dr3	-0.13	-0.63	-0.60	-0.63	0.37	0.75	1.00	-0.40	-0.71	-0.91	-0.05	0.02	0.08	0.27	-0.25	0.37	-0.19	-0.17	-0.32	0.52	0.76	0.93	0.15	0.44
RO1	-0.17	0.54	0.45	0.30	-0.60	-0.53	-0.40	1.00	0.70	0.50	-0.12	-0.10	-0.09	-0.24	0.32	-0.36	0.30	-0.32	-0.22	-0.67	-0.53	-0.39	0.32	0.12
RO2	0.08	0.65	0.76	0.59	-0.57	-0.92	-0.71	0.70	1.00	0.83	-0.11	-0.11	-0.10	-0.37	0.30	-0.51	0.29	0.13	-0.28	-0.69	-0.92	-0.73	-0.10	0.13
RO3	0.14	0.61	0.66	0.76	-0.38	-0.79	-0.91	0.50	0.83	1.00	0.01	0.01	-0.06	-0.31	0.34	-0.41	0.30	0.21	0.27	-0.52	-0.80	-0.94	-0.19	-0.39
V1	0.16	0.14	-0.11	-0.15	0.24	0.07	-0.05	-0.12	-0.11	0.01	1.00	0.86	0.66	-0.17	-0.07	-0.08	-0.06	0.15	0.11	0.15	0.07	0.03	-0.12	-0.05
V2	0.10	0.16	-0.13	-0.05	0.17	0.07	0.02	-0.10	-0.11	0.01	0.86	1.00	0.83	-0.22	-0.01	-0.09	0.02	0.11	0.10	0.09	0.06	0.03	-0.05	-0.05
V3	-0.06	0.09	-0.12	-0.03	0.10	0.04	0.08	-0.09	-0.10	-0.06	0.66	0.83	1.00	-0.17	-0.05	-0.05	-0.02	0.06	-0.02	0.05	0.03	0.05	-0.04	0.05
GT	0.10	-0.28	-0.30	-0.27	0.33	0.39	0.27	-0.24	-0.37	-0.31	-0.17	-0.22	-0.17	1.00	-0.04	0.91	-0.03	0.00	0.09	0.36	0.39	0.31	-0.05	-0.05
GT_O	0.04	0.06	0.20	0.28	-0.14	-0.21	-0.25	0.32	0.30	0.34	-0.07	-0.01	-0.05	-0.04	1.00	-0.03	0.91	0.02	0.12	-0.14	-0.22	-0.29	-0.06	-0.17
LOA	0.18	-0.35	-0.41	-0.30	0.45	0.49	0.37	-0.36	-0.51	-0.41	-0.08	-0.09	-0.05	0.91	-0.03	1.00	-0.01	0.04	0.13	0.47	0.49	0.38	-0.09	-0.07
LOA_O	0.00	0.05	0.17	0.27	-0.09	-0.21	-0.19	0.30	0.29	0.30	-0.06	0.02	-0.02	-0.03	0.91	-0.01	1.00	0.07	0.06	-0.11	-0.21	-0.25	-0.09	-0.11
d_RO1	0.41	-0.27	-0.07	0.23	0.66	-0.17	-0.17	-0.32	0.13	0.21	0.15	0.11	0.06	0.00	0.02	0.04	0.07	1.00	0.06	0.56	-0.19	-0.22	-0.96	-0.10
d_RO2	0.05	-0.10	-0.20	0.34	0.26	0.27	-0.32	-0.22	-0.28	0.27	0.11	0.10	-0.02	0.09	0.12	0.13	0.06	0.06	1.00	0.24	0.26	-0.37	-0.04	-0.98
P1	0.24	-0.81	-0.68	-0.37	0.95	0.70	0.52	-0.67	-0.69	-0.52	0.15	0.09	0.05	0.36	-0.14	0.47	-0.11	0.56	0.24	1.00	0.68	0.50	-0.58	-0.16
P2	-0.12	-0.69	-0.81	-0.67	0.55	1.00	0.76	-0.53	-0.92	-0.80	0.07	0.06	0.03	0.39	-0.22	0.49	-0.21	-0.19	0.26	0.68	1.00	0.80	0.19	-0.13
P3	-0.15	-0.59	-0.66	-0.86	0.36	0.79	0.93	-0.39	-0.73	-0.94	0.03	0.03	0.05	0.31	-0.29	0.38	-0.25	-0.22	-0.37	0.50	0.80	1.00	0.22	0.50
d_P1	-0.45	0.32	0.02	-0.25	-0.66	0.17	0.15	0.32	-0.10	-0.19	-0.12	-0.05	-0.04	-0.05	-0.06	-0.09	-0.09	-0.96	-0.04	-0.58	0.19	0.22	1.00	0.08
d_P2	-0.08	0.03	0.09	-0.45	-0.20	-0.14	0.44	0.12	0.13	-0.39	-0.05	-0.05	0.05	-0.05	-0.17	-0.07	-0.11	-0.10	-0.98	-0.16	-0.13	0.50	0.08	1.00

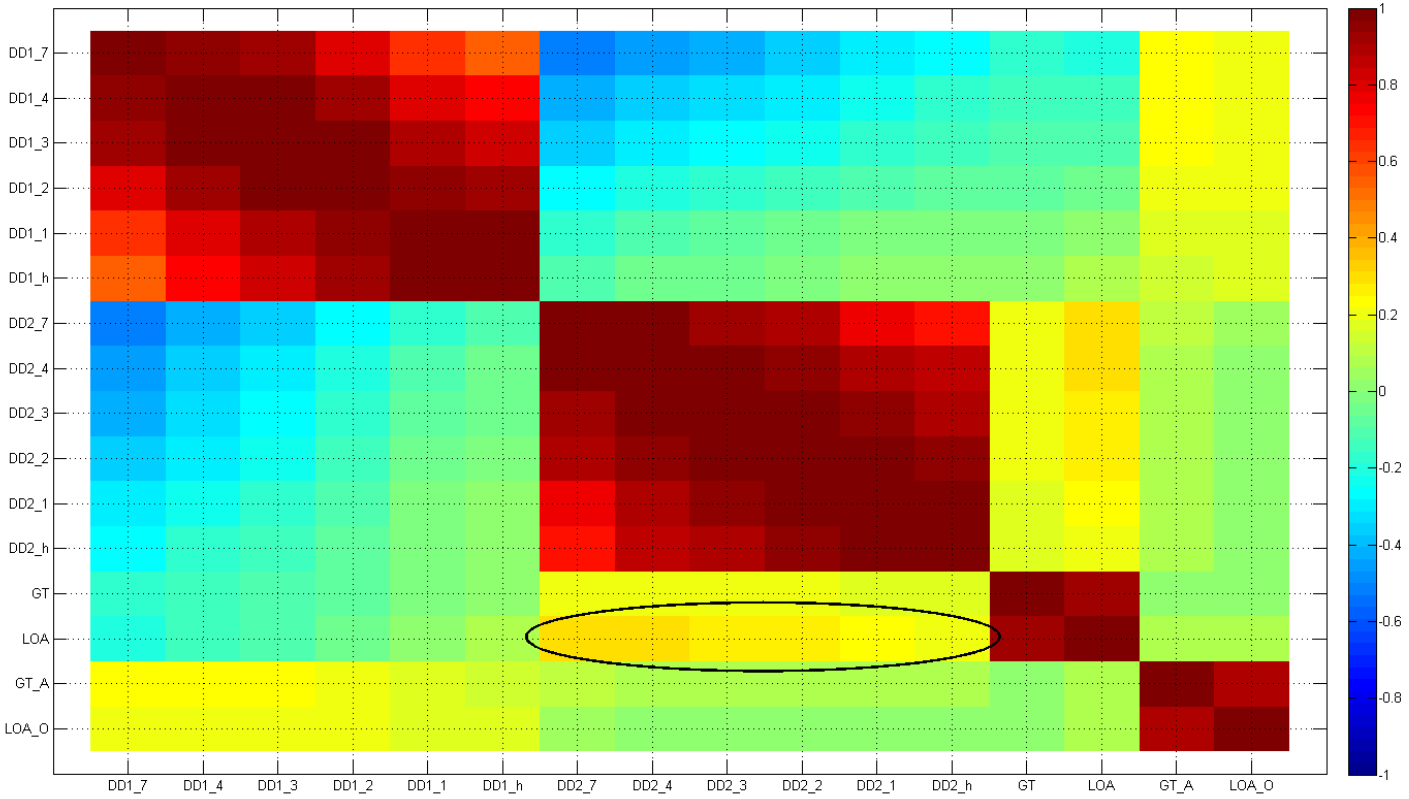

Figure VI-2 Matrix of correlation coefficient analysis results in head-on situation for deriving exponent n (colored cells)

Table VI-2 Matrix of correlation coefficient analysis results in head-on situation for deriving exponent n (cells with values)

	DD1_7	DD1_4	DD1_3	DD1_2	DD1_1	DD1_h	DD2_7	DD2_4	DD2_3	DD2_2	DD2_1	DD2_g	GT	LOA	GT_A	LOA_O
DD1_7	1.00	0.96	0.91	0.81	0.64	0.54	-0.50	-0.45	-0.42	-0.37	-0.30	-0.26	-0.17	-0.20	0.24	0.20
DD1_4	0.96	1.00	0.99	0.93	0.81	0.73	-0.42	-0.36	-0.33	-0.28	-0.22	-0.18	-0.14	-0.15	0.23	0.21
DD1_3	0.91	0.99	1.00	0.98	0.89	0.83	-0.36	-0.30	-0.27	-0.23	-0.17	-0.14	-0.12	-0.11	0.22	0.20
DD1_2	0.81	0.93	0.98	1.00	0.97	0.93	-0.27	-0.21	-0.18	-0.15	-0.10	-0.07	-0.07	-0.05	0.21	0.20
DD1_1	0.64	0.81	0.89	0.97	1.00	0.99	-0.16	-0.11	-0.08	-0.05	-0.02	0.00	-0.01	0.03	0.18	0.18
DD1_h	0.54	0.73	0.83	0.93	0.99	1.00	-0.10	-0.05	-0.03	-0.01	0.02	0.03	0.02	0.07	0.15	0.17
DD2_7	-0.50	-0.42	-0.36	-0.27	-0.16	-0.10	1.00	0.97	0.94	0.88	0.78	0.72	0.21	0.28	0.10	0.04
DD2_4	-0.45	-0.36	-0.30	-0.21	-0.11	-0.05	0.97	1.00	0.99	0.96	0.90	0.85	0.22	0.28	0.07	0.01
DD2_3	-0.42	-0.33	-0.27	-0.18	-0.08	-0.03	0.94	0.99	1.00	0.99	0.94	0.90	0.21	0.27	0.07	0.01
DD2_2	-0.37	-0.28	-0.23	-0.15	-0.05	-0.01	0.88	0.96	0.99	1.00	0.98	0.96	0.20	0.25	0.08	0.01
DD2_1	-0.30	-0.22	-0.17	-0.10	-0.02	0.02	0.78	0.90	0.94	0.98	1.00	0.99	0.19	0.22	0.09	0.01
DD2_h	-0.26	-0.18	-0.14	-0.07	0.00	0.03	0.72	0.85	0.90	0.96	0.99	1.00	0.17	0.20	0.09	0.01
GT	-0.17	-0.14	-0.12	-0.07	-0.01	0.02	0.21	0.22	0.21	0.20	0.19	0.17	1.00	0.92	0.00	0.02
LOA	-0.20	-0.15	-0.11	-0.05	0.03	0.07	0.28	0.28	0.27	0.25	0.22	0.20	0.92	1.00	0.07	0.09
GT_A	0.24	0.23	0.22	0.21	0.18	0.15	0.10	0.07	0.07	0.08	0.09	0.09	0.00	0.07	1.00	0.89
LOA_O	0.20	0.21	0.20	0.20	0.18	0.17	0.04	0.01	0.01	0.01	0.01	0.01	0.02	0.09	0.89	1.00

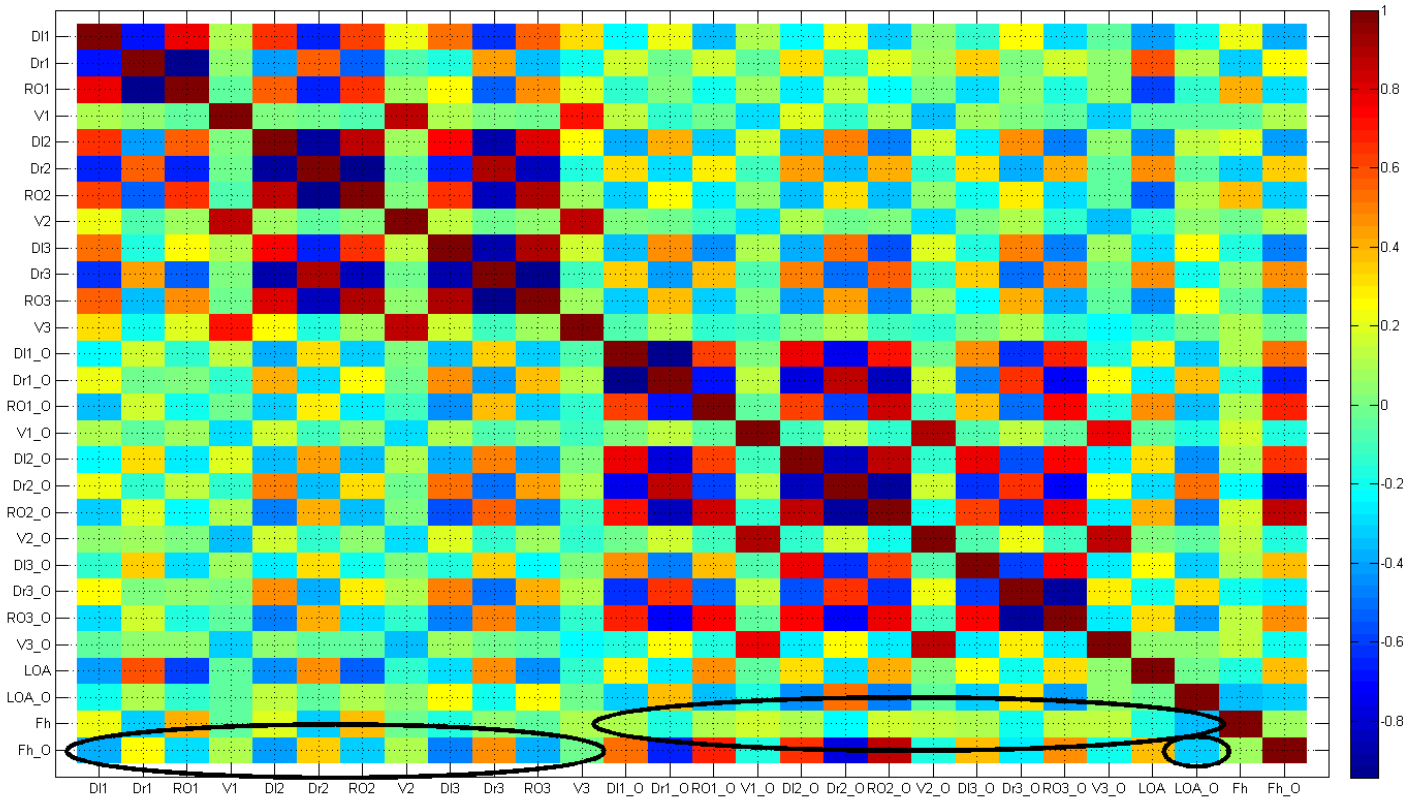

Figure VI-3 Matrix of correlation coefficient analysis results for factors that contribute to $\mathrm{F_{head-on}}$ (colored cells)

Table VI-3 Matrix of correlation coefficient analysis results for factors that contribute to $F_{head-on}$ (cells with values)

	Dl1	Dr1	RO1	V1	Dl2	Dr2	RO2	V2	Dl3	Dr3	RO3	V3	Dl1_O	Dr1_O	RO1_O	V1_O	Dl2_O	Dr2_O	RO2_O	V2_O	Dl3_O	Dr3_O	RO3_O	V3_O	LOA	LOA_O	Fh	Fh_O
Dl1	1.00	-0.68	0.77	0.12	0.64	-0.66	0.61	0.24	0.54	-0.62	0.57	0.33	-0.23	0.22	-0.35	0.11	-0.23	0.22	-0.31	0.06	-0.14	0.25	-0.29	-0.04	-0.42	-0.20	0.22	-0.37
Dr1	-0.68	1.00	-0.92	0.03	-0.41	0.55	-0.54	-0.08	-0.16	0.44	-0.36	-0.20	0.16	-0.03	0.17	-0.05	0.31	-0.13	0.20	0.07	0.35	0.01	0.17	0.04	0.59	0.10	-0.31	0.24
RO1	0.77	-0.92	1.00	-0.04	0.55	-0.67	0.66	0.07	0.26	-0.54	0.47	0.18	-0.13	0.02	-0.19	0.07	-0.26	0.14	-0.22	0.03	-0.29	0.05	-0.18	0.03	-0.60	-0.13	0.41	-0.28
V1	0.12	0.03	-0.04	1.00	0.01	-0.01	-0.09	0.85	0.09	0.01	-0.02	0.72	0.12	-0.13	-0.03	-0.31	0.19	-0.13	0.10	-0.34	0.07	0.01	-0.06	-0.34	-0.05	-0.06	-0.06	0.11
Dl2	0.64	-0.41	0.55	0.01	1.00	-0.91	0.87	0.09	0.73	-0.86	0.81	0.27	-0.38	0.42	-0.33	0.15	-0.36	0.51	-0.48	0.15	-0.26	0.48	-0.46	0.06	-0.43	0.13	0.21	-0.43
Dr2	-0.66	0.55	-0.67	-0.01	-0.91	1.00	-0.92	-0.04	-0.67	0.88	-0.82	-0.17	0.31	-0.30	0.30	-0.10	0.43	-0.35	0.41	-0.13	0.33	-0.39	0.42	-0.04	0.45	-0.04	-0.32	0.35
RO2	0.61	-0.54	0.66	-0.09	0.87	-0.92	1.00	0.00	0.65	-0.84	0.88	0.09	-0.31	0.27	-0.25	0.04	-0.35	0.32	-0.35	0.05	-0.21	0.29	-0.30	-0.05	-0.53	0.11	0.36	-0.31
V2	0.24	-0.08	0.07	0.85	0.09	-0.04	0.00	1.00	0.12	-0.03	0.06	0.86	0.01	-0.01	-0.12	-0.29	0.11	-0.02	0.01	-0.30	0.02	0.09	-0.13	-0.36	-0.13	0.05	-0.03	0.09
Dl3	0.54	-0.16	0.26	0.09	0.73	-0.67	0.65	0.12	1.00	-0.88	0.88	0.16	-0.34	0.47	-0.43	0.10	-0.40	0.52	-0.56	0.20	-0.17	0.49	-0.48	0.09	-0.30	0.27	-0.16	-0.48
Dr3	-0.62	0.44	-0.54	0.01	-0.86	0.88	-0.84	-0.03	-0.88	1.00	-0.94	-0.10	0.35	-0.40	0.38	-0.08	0.49	-0.51	0.55	-0.14	0.34	-0.49	0.50	-0.03	0.46	-0.19	0.04	0.48
RO3	0.57	-0.36	0.47	-0.02	0.81	-0.82	0.88	0.06	0.88	-0.94	1.00	0.07	-0.33	0.37	-0.32	0.03	-0.42	0.44	-0.47	0.08	-0.22	0.40	-0.38	-0.05	-0.44	0.25	-0.04	-0.39
V3	0.33	-0.20	0.18	0.72	0.27	-0.17	0.09	0.86	0.16	-0.10	0.07	1.00	-0.09	0.10	-0.14	-0.12	0.02	0.11	-0.09	-0.15	0.02	0.12	-0.15	-0.23	-0.14	-0.03	0.09	-0.03
Dl1_O	-0.23	0.16	-0.13	0.12	-0.38	0.31	-0.31	0.01	-0.34	0.35	-0.33	-0.09	1.00	-0.93	0.63	0.01	0.76	-0.75	0.73	-0.01	0.47	-0.62	0.67	-0.16	0.30	-0.31	0.11	0.53
Dr1_O	0.22	-0.03	0.02	-0.13	0.42	-0.30	0.27	-0.01	0.47	-0.40	0.37	0.10	-0.93	1.00	-0.70	0.14	-0.78	0.86	-0.84	0.17	-0.46	0.66	-0.71	0.26	-0.25	0.36	-0.18	-0.65
RO1_O	-0.35	0.17	-0.19	-0.03	-0.33	0.30	-0.25	-0.12	-0.43	0.38	-0.32	-0.14	0.63	-0.70	1.00	-0.06	0.63	-0.60	0.84	-0.12	0.38	-0.52	0.73	-0.18	0.46	-0.34	0.09	0.69
V1_O	0.11	-0.05	0.07	-0.31	0.15	-0.10	0.04	-0.29	0.10	-0.08	0.03	-0.12	0.01	0.14	-0.06	1.00	-0.10	0.13	-0.14	0.90	-0.07	0.14	-0.05	0.78	-0.05	-0.16	0.17	-0.16
Dl2_O	-0.23	0.31	-0.26	0.19	-0.36	0.43	-0.35	0.11	-0.40	0.49	-0.42	0.02	0.76	-0.78	0.63	-0.10	1.00	-0.82	0.86	-0.14	0.77	-0.57	0.73	-0.27	0.30	-0.43	0.12	0.65
Dr2_O	0.22	-0.13	0.14	-0.13	0.51	-0.35	0.32	-0.02	0.52	-0.51	0.44	0.11	-0.75	0.86	-0.60	0.13	-0.82	1.00	-0.91	0.16	-0.63	0.64	-0.72	0.26	-0.30	0.52	-0.23	-0.78
RO2_O	-0.31	0.20	-0.22	0.10	-0.48	0.41	-0.35	0.01	-0.56	0.55	-0.47	-0.09	0.73	-0.84	0.84	-0.14	0.86	-0.91	1.00	-0.20	0.61	-0.61	0.78	-0.27	0.40	-0.49	0.16	0.87
V2_O	0.06	0.07	0.03	-0.34	0.15	-0.13	0.05	-0.30	0.20	-0.14	0.08	-0.15	-0.01	0.17	-0.12	0.90	-0.14	0.16	-0.20	1.00	-0.07	0.21	-0.12	0.86	0.01	-0.06	0.14	-0.18
Dl3_O	-0.14	0.35	-0.29	0.07	-0.26	0.33	-0.21	0.02	-0.17	0.34	-0.22	0.02	0.47	-0.46	0.38	-0.07	0.77	-0.63	0.61	-0.07	1.00	-0.60	0.74	-0.27	0.26	-0.33	0.09	0.39
Dr3_O	0.25	0.01	0.05	0.01	0.48	-0.39	0.29	0.09	0.49	-0.49	0.40	0.12	-0.62	0.66	-0.52	0.14	-0.57	0.64	-0.61	0.21	-0.60	1.00	-0.90	0.30	-0.20	0.31	-0.20	-0.27
RO3_O	-0.29	0.17	-0.18	-0.06	-0.46	0.42	-0.30	-0.13	-0.48	0.50	-0.38	-0.15	0.67	-0.71	0.73	-0.05	0.73	-0.72	0.78	-0.12	0.74	-0.90	1.00	-0.27	0.32	-0.40	0.13	0.46
V3_O	-0.04	0.04	0.03	-0.34	0.06	-0.04	-0.05	-0.36	0.09	-0.03	-0.05	-0.23	-0.16	0.26	-0.18	0.78	-0.27	0.26	-0.27	0.86	-0.27	0.30	-0.27	1.00	0.03	0.06	0.13	-0.20
LOA	-0.42	0.59	-0.60	-0.05	-0.43	0.45	-0.53	-0.13	-0.30	0.46	-0.44	-0.14	0.30	-0.25	0.46	-0.05	0.30	-0.30	0.40	0.01	0.26	-0.20	0.32	0.03	1.00	-0.02	-0.18	0.37
LOA_O	-0.20	0.10	-0.13	-0.06	0.13	-0.04	0.11	0.05	0.27	-0.19	0.25	-0.03	-0.31	0.36	-0.34	-0.16	-0.43	0.52	-0.49	-0.06	-0.33	0.31	-0.40	0.06	-0.02	1.00	-0.35	-0.31
Fh	0.22	-0.31	0.41	-0.06	0.21	-0.32	0.36	-0.03	-0.16	0.04	-0.04	0.09	0.11	-0.18	0.09	0.17	0.12	-0.23	0.16	0.14	0.09	-0.20	0.13	0.13	-0.18	-0.35	1.00	0.08
Fh_O	-0.37	0.24	-0.28	0.11	-0.43	0.35	-0.31	0.09	-0.48	0.48	-0.39	-0.03	0.53	-0.65	0.69	-0.16	0.65	-0.78	0.87	-0.18	0.39	-0.27	0.46	-0.20	0.37	-0.31	0.08	1.00

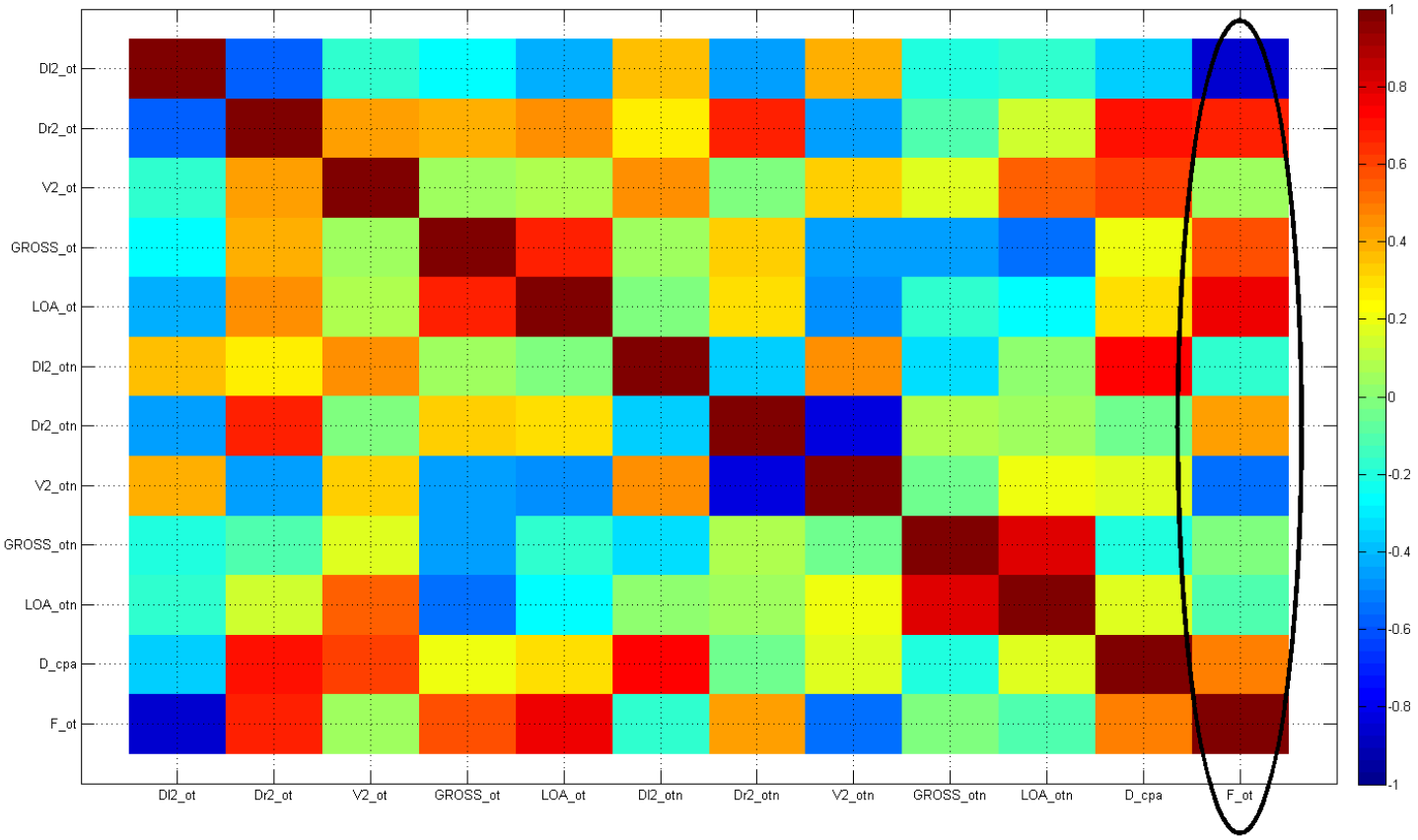

Figure VI-4 Matrix of correlation coefficient analysis results for factors in overtaking encounters that contribute to $\mathrm{F}_{\mathrm{overtaking}}$ (colored cells)

Table VI-4 Matrix of correlation coefficient analysis results for factors in overtaking encounters that contribute to $F_{overtaking}$ (cells with values)

	Dl2_ot	Dr2_ot	V2_ot	GROSS_ot	LOA_ot	Dl2_otn	Dr2_otn	V2_otn	GROSS_otn	LOA_otn	D_cpa	F_ot
Dl2_ot	1.00	-0.59	-0.16	-0.26	-0.43	0.37	-0.45	0.40	-0.19	-0.18	-0.36	-0.87
Dr2_ot	-0.59	1.00	0.43	0.40	0.44	0.28	0.67	-0.47	-0.10	0.15	0.70	0.66
V2_ot	-0.16	0.43	1.00	0.05	0.09	0.46	-0.02	0.32	0.16	0.56	0.60	0.06
GROSS_ot	-0.26	0.40	0.05	1.00	0.68	0.03	0.33	-0.45	-0.45	-0.56	0.22	0.57
LOA_ot	-0.43	0.44	0.09	0.68	1.00	-0.01	0.30	-0.49	-0.17	-0.28	0.31	0.75
Dl2_otn	0.37	0.28	0.46	0.03	-0.01	1.00	-0.37	0.44	-0.33	0.03	0.73	-0.16
Dr2_otn	-0.45	0.67	-0.02	0.33	0.30	-0.37	1.00	-0.83	0.08	0.04	-0.05	0.43
V2_otn	0.40	-0.47	0.32	-0.45	-0.49	0.44	-0.83	1.00	-0.05	0.21	0.17	-0.53
GROSS_otn	-0.19	-0.10	0.16	-0.45	-0.17	-0.33	0.08	-0.05	1.00	0.81	-0.21	-0.03
LOA_otn	-0.18	0.15	0.56	-0.56	-0.28	0.03	0.04	0.21	0.81	1.00	0.16	-0.11
D_cpa	-0.36	0.70	0.60	0.22	0.31	0.73	-0.05	0.17	-0.21	0.16	1.00	0.48
F_ot	-0.87	0.66	0.06	0.57	0.75	-0.16	0.43	-0.53	-0.03	-0.11	0.48	1.00

VII. TABLE OF K′ AND T′ INDICES OF SHIPS

This appendix provides 47 ships from literature with non-dimensional K and T (K′ and T′), ship types, loading conditions and dimensions (Table VII-1). The table is used for deriving the formula for K and T indices for simulation in section 6.3.1.2.

Table VII-1 statistics of K′ and T′ indices and other factors

Number	ship type	Δt	L(m)	B(m)	d(m)	V(kn)	C_b	Ld/A_R	K'	T'
1	Multi-purpose ship	9296	140	22	5	15.6	0.65	32	1.09	0.8
2	Container	20380	189	28	6	19	0.64	32	1.16	1.34
3	Container	6851	114	21	4	15.9	0.65	33	0.97	0.59
4	Container	15700	158	28	6	18.5	0.61	33	2.5	2.37
5	RORO	9660	135	23	5	17.7	0.61	28	1.17	1.29
6	RORO	8255	130	23	5	19.6	0.58	44	1.51	1.88
7	RORO	13830	160	27	6	19.9	0.56	43	1.9	2.53
8	bulk carrier	23365	175	31	6	15.8	0.75	30	0.95	0.69
9	bulk carrier	12013	145	27	4	16	0.70	25	0.81	1.11
10	bulk carrier	22773	183	32	5	17.2	0.75	26	0.98	0.88
11	oil tank	72915	219	32	12	15.4	0.83	65	4.08	5.39
12	oil tank	80684	220	36	12	14.7	0.83	67	1.93	2.84
13	general cargo ship	5400	120	18	4	18	0.63	33	0.96	0.76
14	general cargo ship	13085	130	19	8	12.5	0.65	77	1.82	2.7
15	general cargo ship	11800	149	23	5	16.3	0.65	32	1.21	1.09
16	general cargo ship	19000	150	21	9	18	0.66	61	1.25	1.55
17	general cargo ship (with ballast)	9140	150	21	5	19	0.59	35	0.92	0.72
18	general cargo ship (half loaded)	13840	150	21	7	18.5	0.63	47	1	1.22
19	general cargo ship	15160	133	19	8	14.5	0.74	65	1.59	2.77
20	general cargo ship	4493	86	13	6	8.5	0.72	64	2.07	2.06
21	general cargo ship	320	22	6	3	5.8	0.77	26	1.25	1.21
22	oil tank	43000	192	27	10	15	0.78	74	1.57	3.37
23	oil tank (with ballast)	13000	192	27	4	16	0.60	30	0.87	0.42
24	oil tank	241000	326	50	18	16	0.82	63	2	4.2
25	oil tank	222000	290	48	19	15.5	0.84	72	2.8	5.3

26	oil tank	162000	276	43	17	16.5	0.81	68	3.2	6.2
27	oil tank	89760	245	33	13	17.8	0.82	73	1.7	3.5
28	oil tank	67200	220	31	12	16.5	0.83	77	4.5	1.3
29	oil tank	4115	79	13	5	12.5	0.74	57	1.4	2.8
30	Container (light loaded)	33200	245	32	8	29	0.52	32	1.7	2.1
31	RORO	6050	127	23	5	22	0.44	39	1	1
32	patrol boat	534	52	8	3	13	0.49	40	1.66	1.62
33	oil tank	122800	257	39	15	16.5	0.81	71	3.21	6.01
34	oil tank	110204	242	37	15	16	0.82	72	2.79	6.02
35	oil tank	60000	210	31	12	17	0.79	74	3	6.08
36	cargo ship	16000	157	20	8	17	0.61	24	1.29	1.48
37	cargo ship	16050	140	19	8	15	0.70	59	1.7	1.93
38	oil tank	166200	265	44	17	15.3	0.83	59	2.3	3.6
39	oil tank	43100	192	27	10	16	0.79	71	1.7	3.44
40	oil tank	20583	154	20	9	12	0.72	71	2.3	3
41	oil tank	37695	185	25	10	15.5	0.77	75	1.7	3
42	oil tank (with ballast)	125300	313	48	10	15.5	0.81	35	1.37	1.15
43	general cargo ship (with ballast)	6100	128	18	4	13	0.66	32	1.11	0.61
44	oil tank	262000	310	54	19	16	0.80	60	2.6	4.97
45	oil tank	161900	265	44	17	16.5	0.82	65	2.47	7.4
46	oil tank	126100	251	41	15	15	0.82	67	3.25	7.53
47	oil tank	250300	313	48	19	16	0.84	67	3.8	10.39

VIII. FACE VALIDATION OF THE TRAJECTORIES OF SHIP TRAFFIC FROM THE DUTCH CASE

This appendix is relevant to section 7.4.1.2. The figures are face validation of the overall ship trajectories.

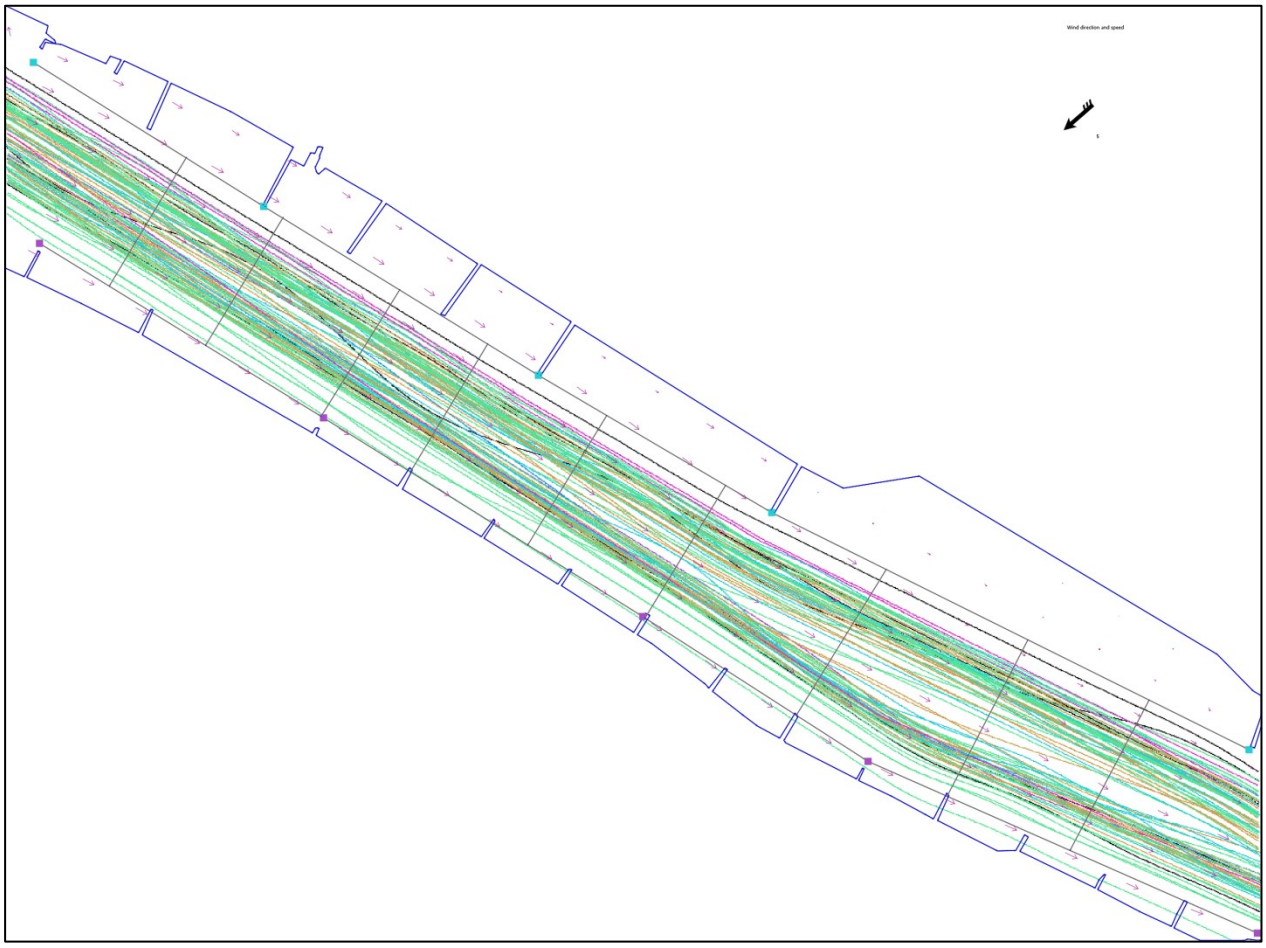

Figure VIII-1 ship trajectories from the simulation results from the Dutch case

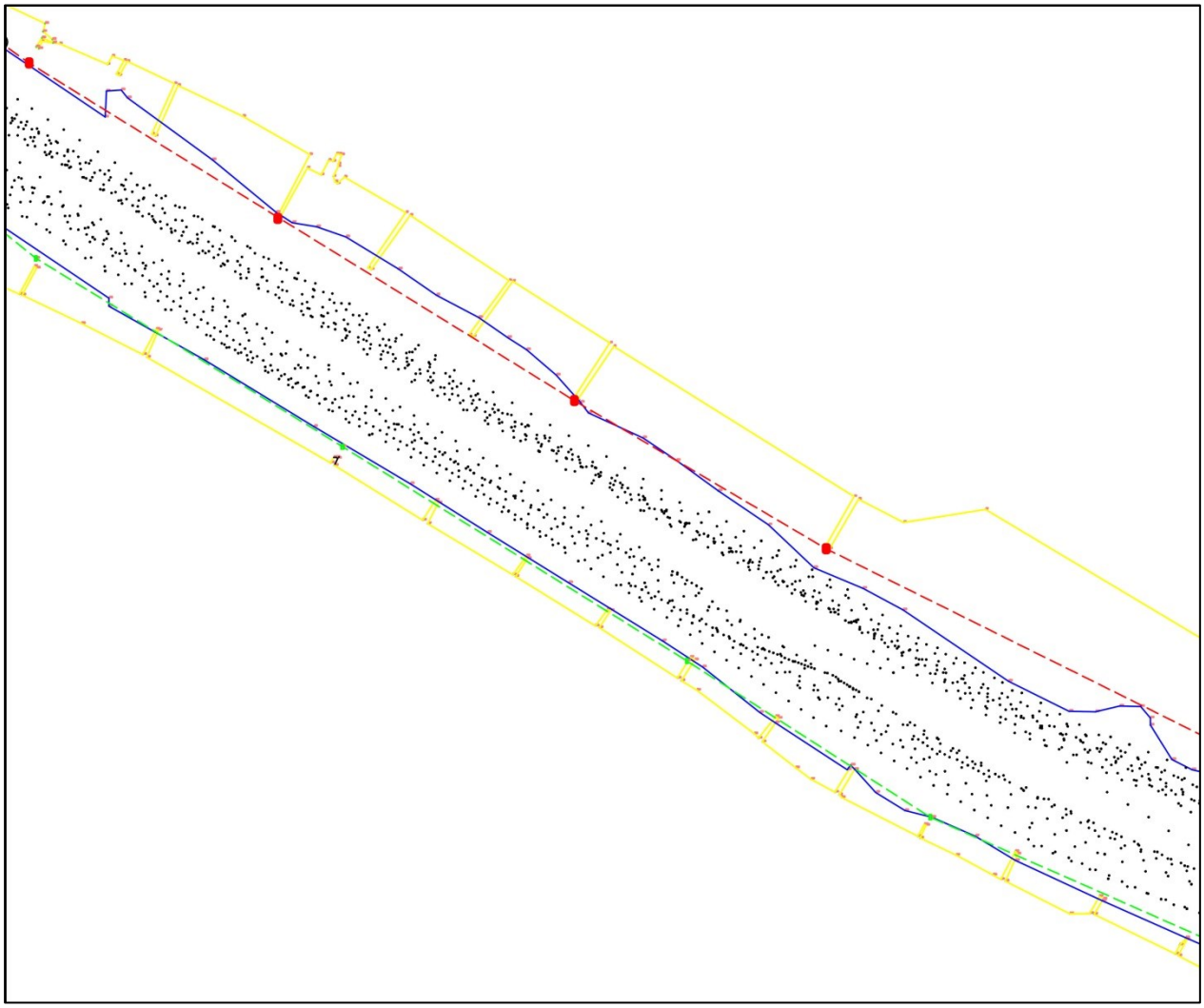

Figure VIII-2 ship trajectories (dots with 9 seconds of time interval) from the AIS data of the Dutch case

IX. CALIBRATED PARAMETERS

This appendix is relevant to section 7.3. The tables provide the calibrated parameters in the relevant random process.

Table IX-1 Calibrated values at the boundary of the simulation for each category of general cargo ships (random numbers can be generated with the parameters of μ and б, $X \sim \aleph(\mu, \epsilon)$, unless otherwise specified; for generating random gross tonnages, only the numbers in the range of specific categories are acceptable in simulation)

	Calibrated values							
Ship categories based on gross tonnages	**[0, 3600]**		**(3600, 12000]**		**(12000, 20000]**		**(20000, +∞)**	
Parameters	μ	б	μ	б	μ	б	μ	б
Gross tonnage (t)	2134	865	-23052	7743	12340	891	20671[1]	6577
Speed of incoming ships (kn)	9.10	2.17	9.79	1.58	8.65	1.53	7.76	1.33
y-coordinate in NetLogo for incoming ships	337.1	16.31	347.7	15.29	352.2	15.88	355.9	10.13
Speed of outgoing ships (kn)	11.16	1.93	12.27	2.03	10.81	2.24	10.05	2.25
y-coordinate in NetLogo for outgoing ships	-380.7	17.38	-392.6	15.93	-398.4	15.99	-401.3	14.04

Note: [1] the generated number is restrained in (20000, 56738), as 56738 t ships is the largest ship observed in AIS data.

Table IX-2 Calibrated values at the boundary of the simulation for each category of container ships (random numbers can be generated with the parameters of μ and б, $X \sim \aleph(\mu, \epsilon)$, unless otherwise specified; for generating random gross tonnages, only the numbers in the range of specific categories are acceptable in simulation)

	Calibrated values									
Ship categories based on gross tonnages (t)	**(0, 5100]**		**(5100, 12000]**		**(12000, 20000]**		**(20000,38000]**		**(38000, +∞)**	
Parameters	μ	б	μ	б	μ	б	μ	б	μ	б
Gross tonnage (t)	N/A[2]		7427	833	N/A[3]		N/A[4]		-171750	58726
Speed of incoming ships (kn)	10.76	1.19	10.20	1.27	9.29	1.36	8.14	1.36	7.76	1.29
y-coordinate in NetLogo for incoming ships	349.8	14.73	353.9	13.87	356.1	13.82	359.8	12.92	367.2	11.86
Speed of outgoing ships (kn)	13.00	2.04	12.50	1.73	11.55	1.90	10.67	1.69	9.71	1.56
y-coordinate in NetLogo for outgoing ships	-389.3	15.56	-394.6	14.93	-398.6	14.22	-405.5	14.63	-407.0	12.77

Note: [2] Here, we generate random number for this category using the uniform distribution, $X \sim U(2035,5068)$.
[3] In this category, we use two distributions to generate random numbers: a. $X \sim U(14000,14664)$, b. $X \sim \aleph(17444,589)$, $X \epsilon (15000,20000)$.

[4] In this category, we generate random number using the uniform distribution, $X \sim U(21025, 28000)$.

Table IX-3 Calibrated values at the boundary of the simulation for each category of chemical & oil ships (random numbers can be generated with the parameters of μ and б, $X \sim \aleph(\mu, \text{б})$, unless otherwise specified; for generating random gross tonnages, only the numbers in the range of specific categories are acceptable in simulation)

	Calibrated values					
Ship categories based on gross tonnages (t)	**(0, 7500]**		**(7500, 17500]**		**(17500, +∞)**	
Parameters	μ	б	μ	б	μ	б
Gross tonnage (t)	3383	1543	-7315	9099	24882	4681
Speed of incoming ships (kn)	9.71	1.64	8.62	1.45	7.46	1.41
y-coordinate in NetLogo for incoming ships	343.6	14.71	348.9	12.47	354.7	13.56
Speed of outgoing ships (kn)	11.85	1.81	11.11	2.04	9.08	1.90
y-coordinate in NetLogo for outgoing ships	-387.7	16.53	-395.8	15.57	-402.0	14.77

Table IX-4 Calibrated values at the boundary of the simulation for each category of tugs (random numbers can be generated with the parameters of μ and б, $X \sim \aleph(\mu, \text{б})$, unless otherwise specified; for generating random gross tonnages, only the numbers in the range of specific categories are acceptable in simulation)

	Calibrated values			
Ship categories based on gross tonnages (t)	**(0, 800]**		**(800, +∞)**	
Parameters	μ	б	μ	б
Gross tonnage (t)	292	105	N/A[5]	
Speed of incoming ships (kn)	8.45	2.54	9.02	1.48
y-coordinate in NetLogo for incoming ships	336.6	19.67	347.2	17.28
Speed of outgoing ships (kn)	9.28	3.25	10.11	1.85
y-coordinate in NetLogo for outgoing ships	-374.4	23.07	-395.1	20.09

Note: [5] Here, we generate random number for this category using the exponential distribution, written as $X \sim \text{Exp}(961), X \epsilon (800, +\infty)$.

Table IX-5 Calibrated values at the boundary of the simulation for each category of RoRo ships (random numbers can be generated with the parameters of μ and б, $X \sim \aleph(\mu, \text{б})$, unless otherwise specified; for generating random gross tonnages, only the numbers in the range of specific categories are acceptable in simulation)

	Calibrated values					
Ship categories based on gross tonnages (t)	**(0, 7500]**		**(7500, 17500]**		**(17500, +∞)**	
Parameters	μ	б	μ	б	μ	б
Gross tonnage (t)	5599	157	12856	177	24596	2499
Speed of incoming ships (kn)	10.26	1.37	10.54	1.37	10.03	1.19
y-coordinate in NetLogo for incoming ships	350.7	14.45	356.6	13.38	357.4	14.11
Speed of outgoing ships (kn)	12.05	1.64	12.43	1.80	11.99	1.91
y-coordinate in NetLogo for outgoing ships	-391.3	19.70	-399.5	15.81	-397.0	15.46

Table IX-6 Calibrated values at the boundary of the simulation for each category of dredging ships (random numbers can be generated with the parameters of μ and б, $X \sim \aleph(\mu, \text{б})$, unless otherwise specified; for generating random gross tonnages, only the numbers in the range of specific categories are acceptable in simulation)

	Calibrated values					
Ship categories based on gross tonnages (t)	**(0, 3600]**		**(3600, 12000]**		**(12000, +∞)**	
Parameters	μ	б	μ	б	μ	б
Gross tonnage (t)	2952	107	4872	230	12083	889
Speed of incoming ships (kn)	8.94	1.88	10.37	1.72	9.74	1.52
y-coordinate in NetLogo for incoming ships	334.8	13.44	343.7	14.56	354.4	19.32
Speed of outgoing ships (kn)	10.25	1.73	11.94	1.30	11.52	2.12
y-coordinate in NetLogo for outgoing ships	-372.7	17.79	-382.2	16.14	-398.7	17.91

Table IX-7 Calibrated values at the boundary of the simulation for each category of all the others ships not mentioned in the previous types (random numbers can be generated with the parameters of μ and б, $X \sim \aleph(\mu, \text{б})$, unless otherwise specified; for generating random gross tonnages, only the numbers in the range of specific categories are acceptable in simulation)

	Calibrated values							
Ship categories based on gross tonnages (t)	**(0, 2000]**		**(2000, 20000]**		**(20000, 38000]**		**(38000, +∞)**	
Parameters	μ	б	μ	б	μ	б	μ	б
Gross tonnage (t)	N/A[6]		N/A [7]		N/A [8]		N/A[9]	
Speed of incoming ships (kn)	8.62	2.82	8.27	1.89	7.21	1.35	7.18	1.57
y-coordinate in NetLogo for incoming ships	332.9	20.17	347.6	15.87	356.1	13.79	361.4	12.73
Speed of outgoing ships (kn)	10.80	2.99	10.28	2.34	8.68	1.84	9.46	2.51
y-coordinate in NetLogo for outgoing ships	-372.9	23.36	-396.1	16.95	-401.6	16.89	-407.4	13.25

Note: [6] Here, we generate random number for this category using the exponential distribution, written as $X \sim \text{Exp}(311), X \epsilon (48, 2000)$.
[7] In this category, we generate random number using the uniform distribution, $X \sim U(2000,20000)$.
[8] In this category, we generate random number using the uniform distribution, $X \sim U(20000,38000)$.
[9] Here, we generate random number for this category using the exponential distribution, written as $X \sim \text{Exp}(9438), X \epsilon (38000, +\infty)$.

Table IX-8 Calibrated values at the boundary of the simulation for each category of Unknown ships (random numbers can be generated with the parameters of μ and б, $X \sim \aleph(\mu, \text{б})$, unless otherwise specified; for generating random gross tonnages, only the numbers in the range of specific categories are acceptable in simulation)

	Calibrated values			
Ship categories based on LOA (m)	**(0, 50]**		**(50, +∞)**	
Parameters	μ	б	μ	б
Gross tonnage (t)	24[10]	9	114	22
Speed of incoming ships (kn)	8.03	2.60	8.21	2.01
y-coordinate in NetLogo for incoming ships	326.7	19.61	326.9	16.87
Speed of outgoing ships (kn)	10.50	3.04	10.13	2.04
y-coordinate in NetLogo for outgoing ships	-366.3	23.93	-375.4	20.27

Note: [10] Here, as ship tonnage should larger than 2 t, $X \sim \aleph(24,9), X \epsilon (2, 50)$.

Table IX-9 Calibrated values of speed accelerations for container ship of with Gross Tonnage less than 5100 t

Geographical sections	Speed acceleration for outgoing ships (m/s)	Speed acceleration for incoming ships (m/s)
Crossing-line1 to crossing-line2	0.004317	-0.005090
Crossing-line2 to crossing-line3	0.003965	-0.004674
Crossing-line3 to crossing-line4	0.002737	-0.003004
Crossing-line4 to crossing-line5	0.001670	-0.001599
Crossing-line5 to crossing-line6	0.000884	-0.000220
Crossing-line6 to crossing-line7	0.000190	0.000662
Crossing-line7 to crossing-line8	-0.000714	0.000800
Crossing-line8 to crossing-line9	-0.001327	0.000449

Table IX-10 Calibrated values for artificial forces in different encountering situations with different thresholds of distances for actions (random numbers can be generated with the parameters of μ and б, $X \sim \aleph(\mu, \text{б})$, only the numbers in the specific range are acceptable in simulation)

Parameters	μ	б	Range
$\mathbf{F}_{head-on}$	2.27	6.8	X ϵ (-14, +∞)
$\mathbf{F}_{overtaking}$	6.87	6.3	X ϵ (3, +∞)
$\mathbf{F}_{overtaken}$	2.27	6.8	X ϵ (-14, +∞)
$\mathbf{D}_{head-on}$ **(m)**	1548	706	X ϵ (500, 3500)
$\mathbf{D}_{overtaking}$ **(m)**	384	358	X ϵ (150, 1000)
$\mathbf{D}_{overtaking\_after}$ **(m)**	308	182	X ϵ (100, 900)

X. THE EXPECTED VARIANCES AND VARIANCES IN THE SIMULATION OUTPUT FOR WEEKLY SHIP ARRIVALS AND DAILY SHIP ARRIVALS

This appendix is relevant to section 7.4.1. The tables show the differences between real data and simulation data for weekly and daily variances of expected ship arrivals.

As is shown in Figure 6-3, the weekly variances of expected ship arrivals is based on random normal process introduced in Section 3.3.2.2. However, when the random number is coupled with the hourly variances and random process for time intervals, the weekly variances of ship arrivals get amplified in the simulation Figure X-2.

Similarly, the daily variance is amplified in a similar way. As is shown in Figure X-3, the daily variance of expected ship arrivals is based on random normal process introduced in Section 3.3.2.3. However, when the random number is coupled with the hourly variances and random process for time intervals, the weekly variances of ship arrivals get amplified in the simulation (Figure X-4).

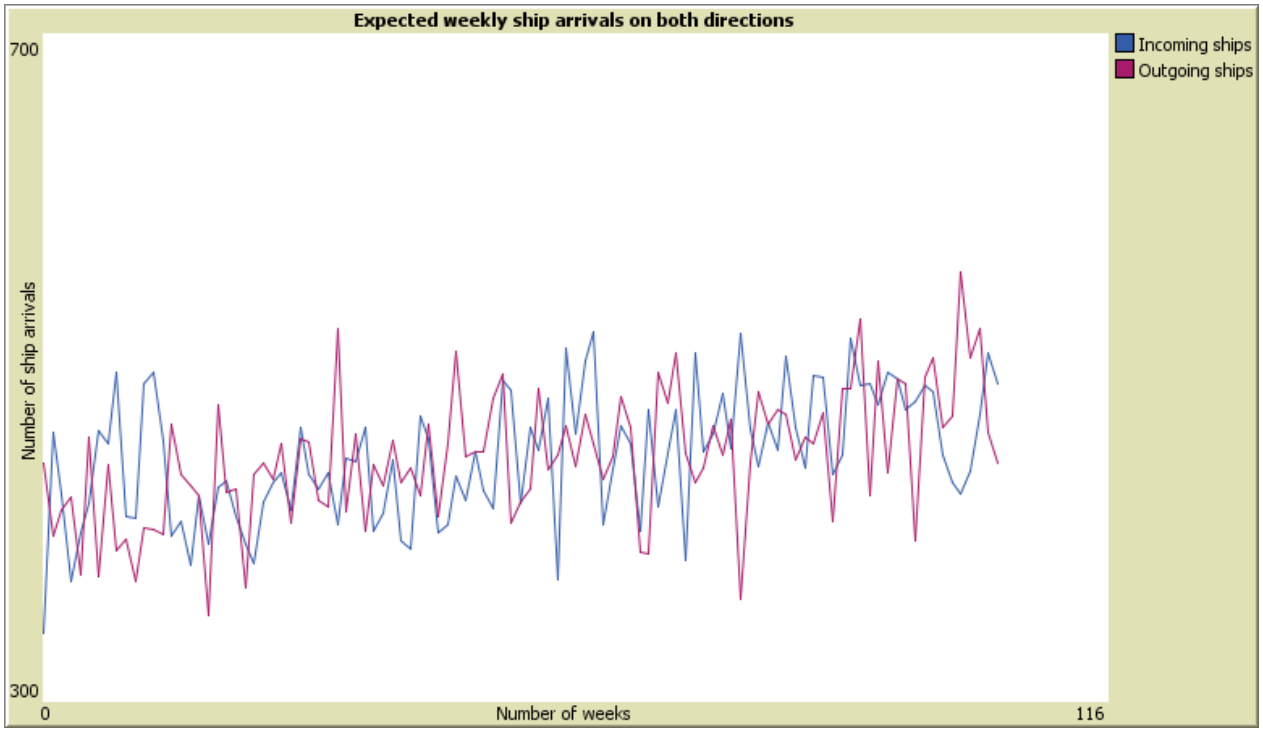

Figure X-1 The expected weekly variance of ship arrivals that is recorded in the simulation process

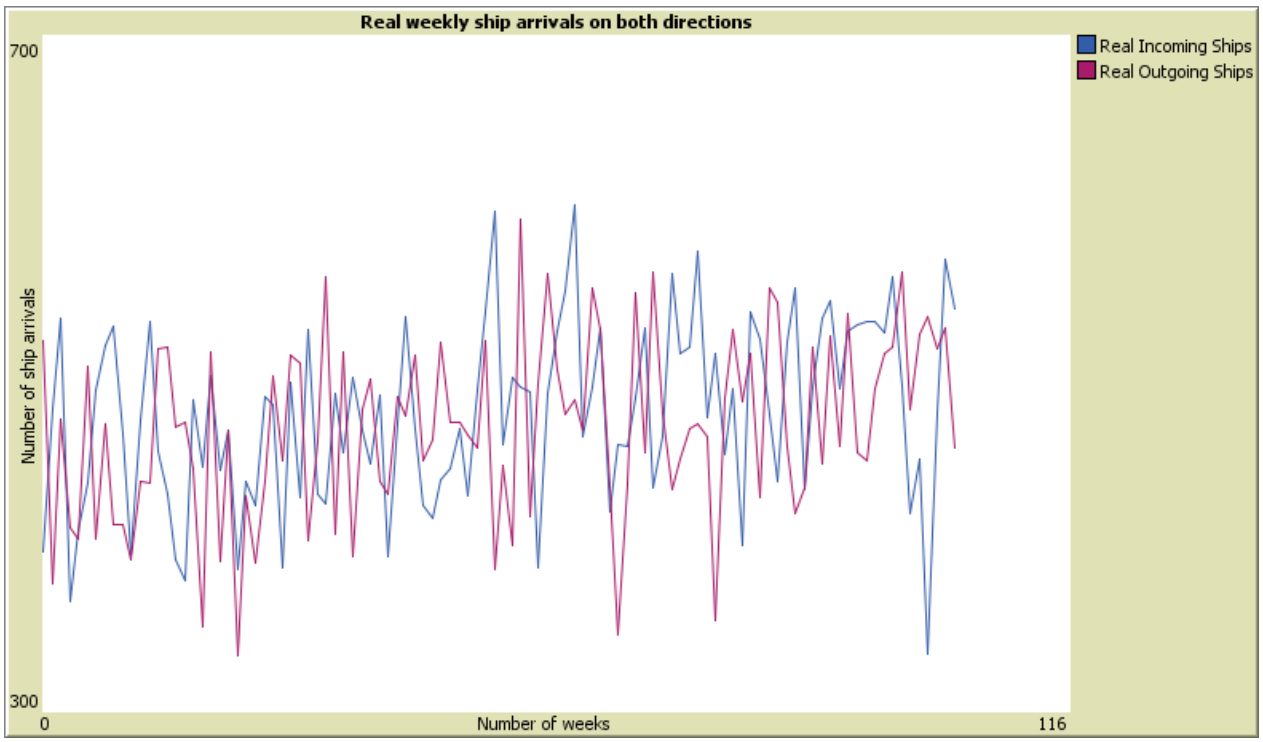

Figure X-2 The weekly variance of ship arrivals that is recorded in the simulation output

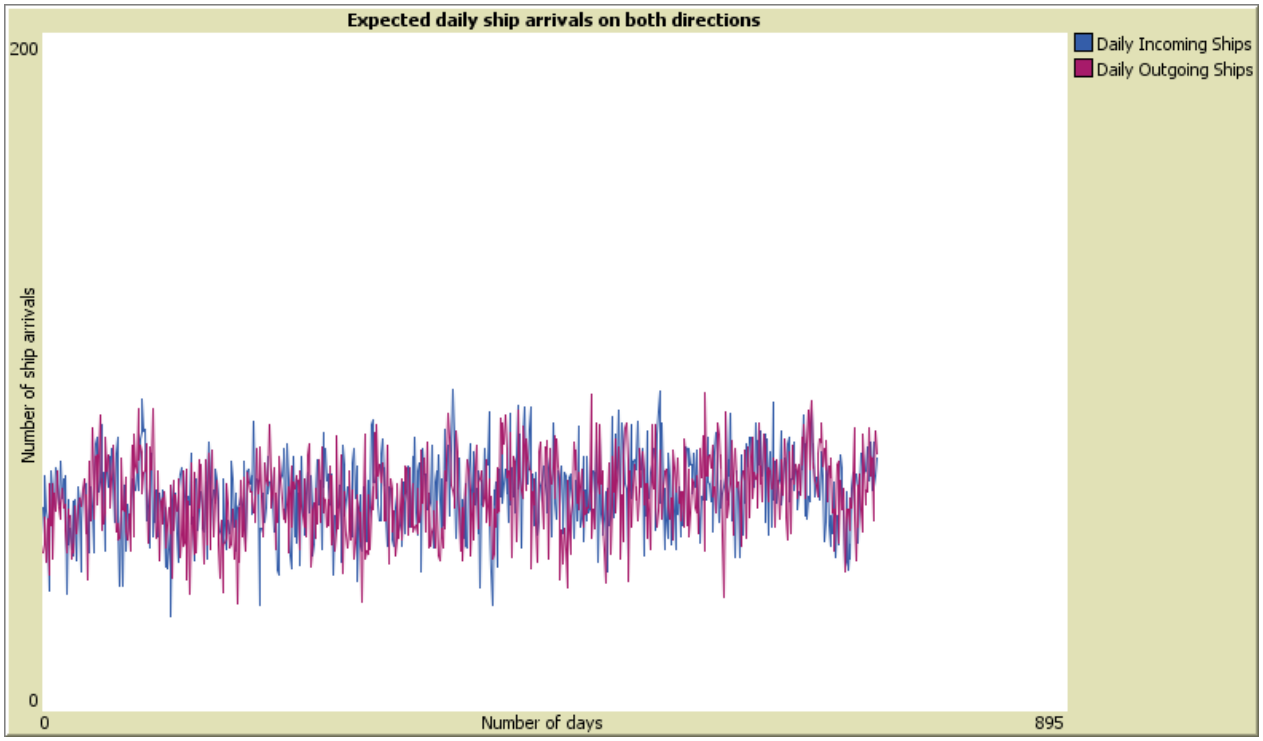

Figure X-3 The expected daily variance of ship arrivals that is recorded in the simulation process

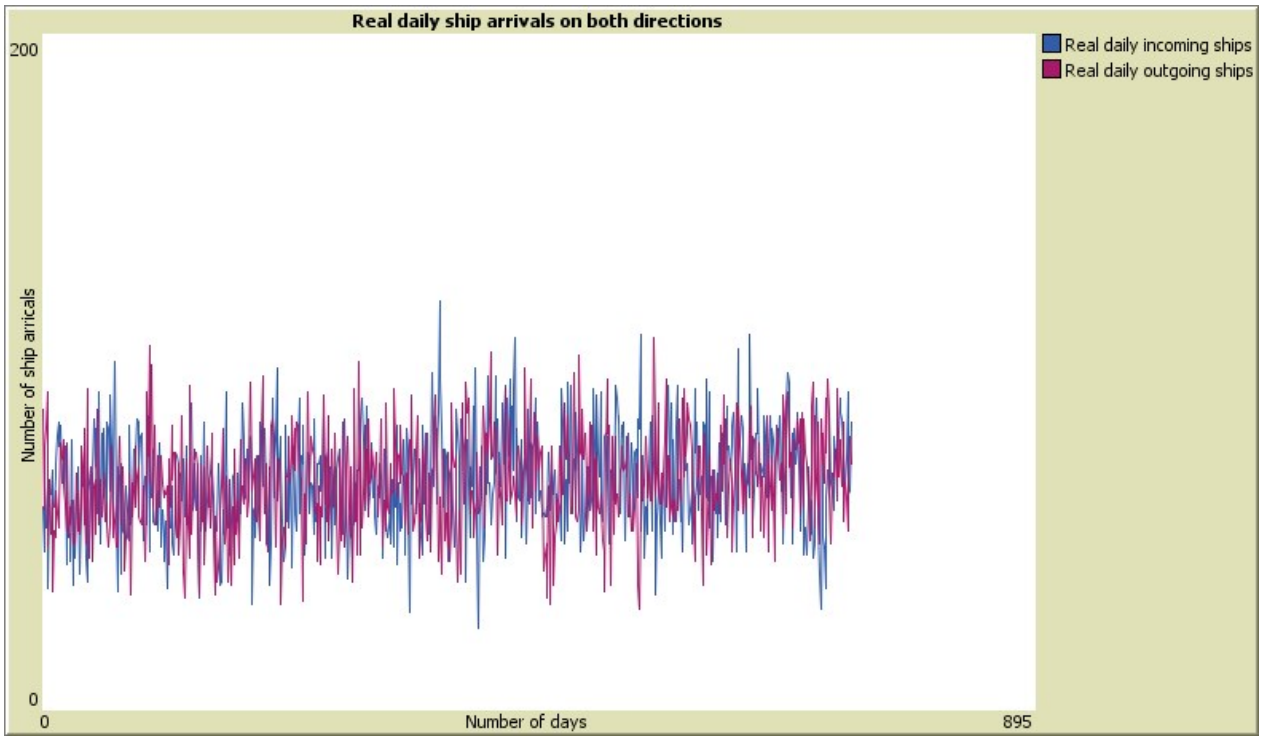

Figure X-4 The daily variance of ship arrivals that is recorded in the simulation output

XI. CASES OF ENCOUNTERS FOR VALIDATION OF INDIVIDUAL SHIP BEHAVIOR

This appendix provides additional cases of individual ship level of validation, which is relevant to section 7.4.2.

Table XI-1 Initial parameters for the ships in head-on encounter scenario (Case 2)

Parameters	Chemical (Incoming)	Chemical (Outgoing)
xcor	-699.063	532.4243
ycor	334.9902	-305.69955
LOA (m)	170.15	131.85
Gross Tonnage (t)	17401	7260
Speed (kn)	6	11.9
heading (°)	124	290
Dr1 (m)	86	139
Dr2 (m)	87	101
Dr3 (m)	110	97
d_{head} (m)	2462	1373

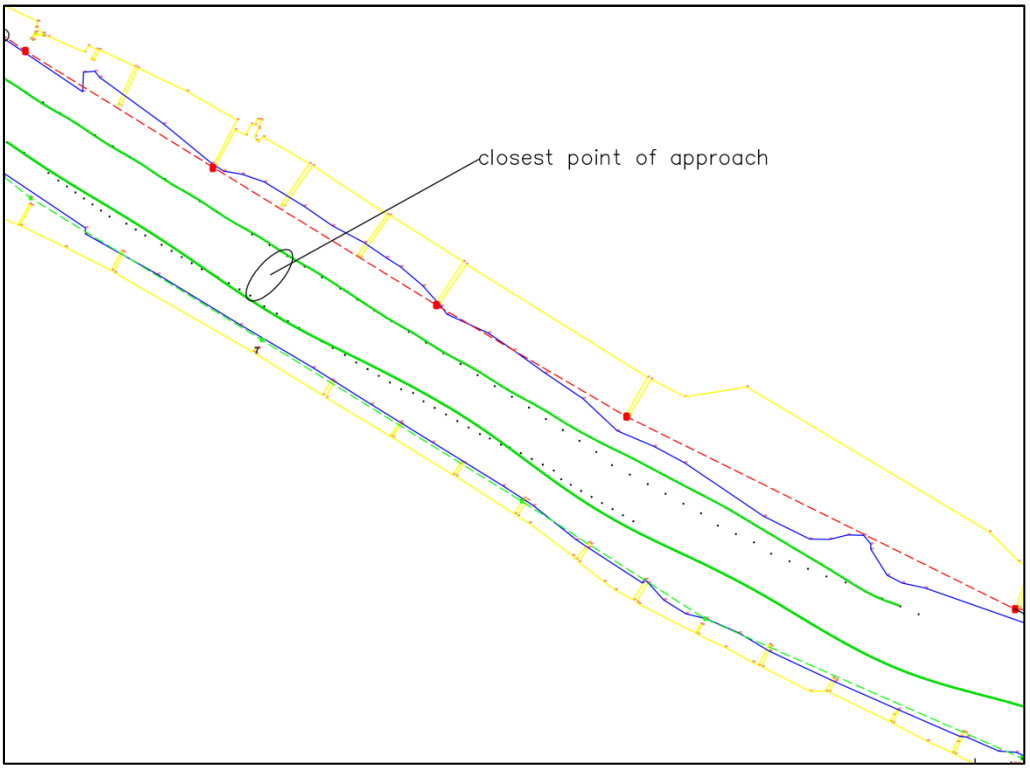

Figure XI-1 Comparing ship tracks of head-on encounter between AIS data (black dots) and results from simulation (green lines) (case 2)

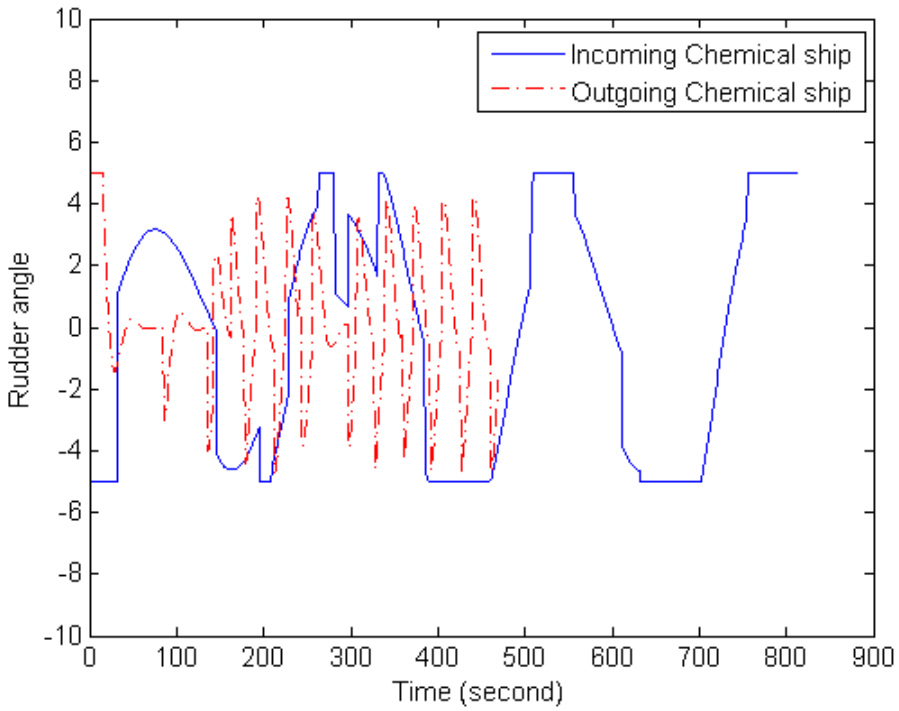

Figure XI-2 Rudder angles used in head-on encounter (a positive value means rudder angle to starboard) (case 2)

Table XI-2 Initial parameters for the ships in head-on encounter scenario (Case 3)

Parameters	container (Incoming)	container (Outgoing)
xcor	-700.603	199.9637
ycor	350.5386	-119.2434
LOA (m)	140.64	139.6
Gross Tonnage (t)	7852	8246
Speed (kn)	9.5	11.7
heading (°)	125	303
Dr1 (m)	98	207
Dr2 (m)	88	82
Dr3 (m)	167	87
d_{head} (m)	749	2920

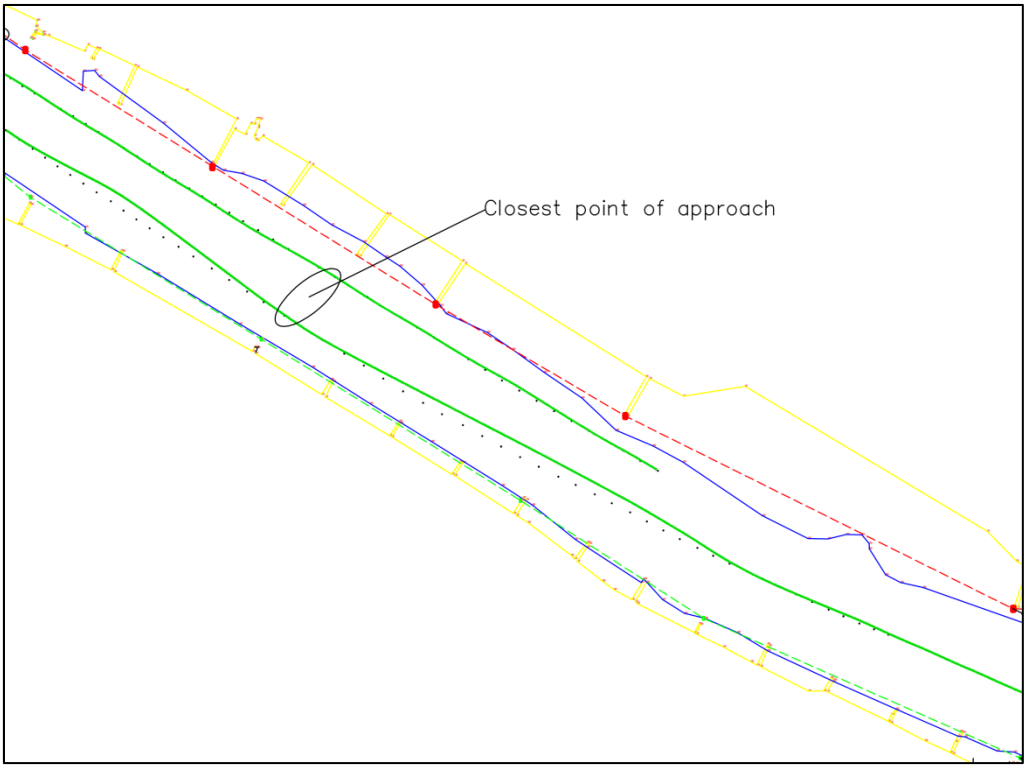

Figure XI-3 Comparing ship tracks of head-on encounter between AIS data (black dots) and results from simulation (green lines) (case 3)

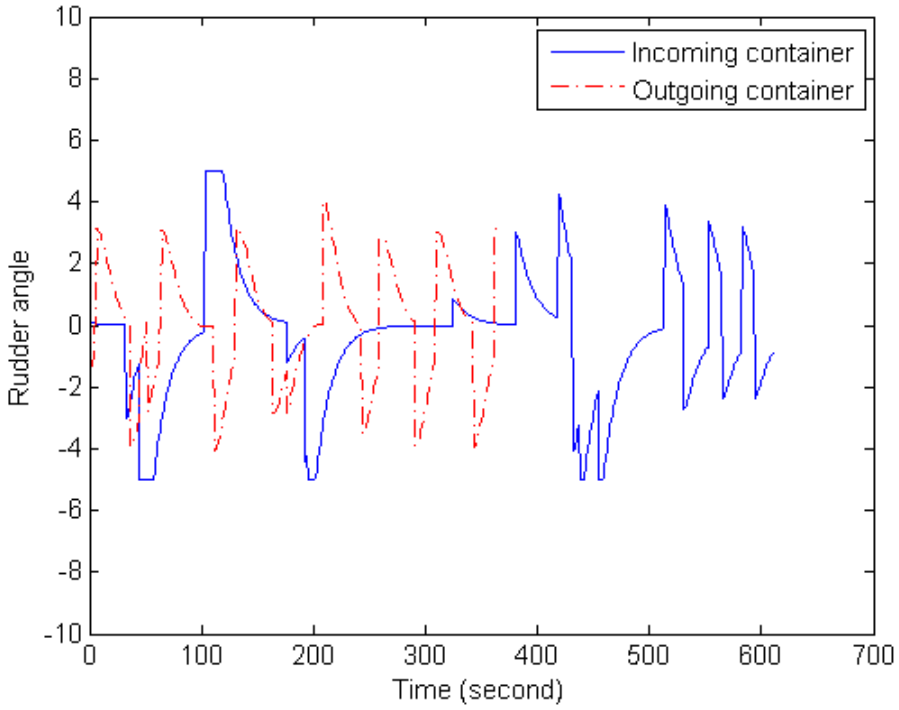

Figure XI-4 Rudder angles used in head-on encounter (a positive value means rudder angle to starboard) (case 3)

Table XI-3 initial parameters for the ships in overtaking encounter scenario (Case 2)

parameters	Dredging (overtaken)	Container (overtaking)
xcor	-499.9183	-589.2691
ycor	193.0659	327.6964
LOA (m)	91.46	129.58
Gross Tonnage (t)	2854	7465
Speed (kn)	8.4	11.9
heading (°)	121	125
Dr2 (m)	83	N/A
Dr3 (m)	106	162
Dl2 (m)	N/A	144
Dovertaking (m)	500	500
dovertaking_after (m)	483	302

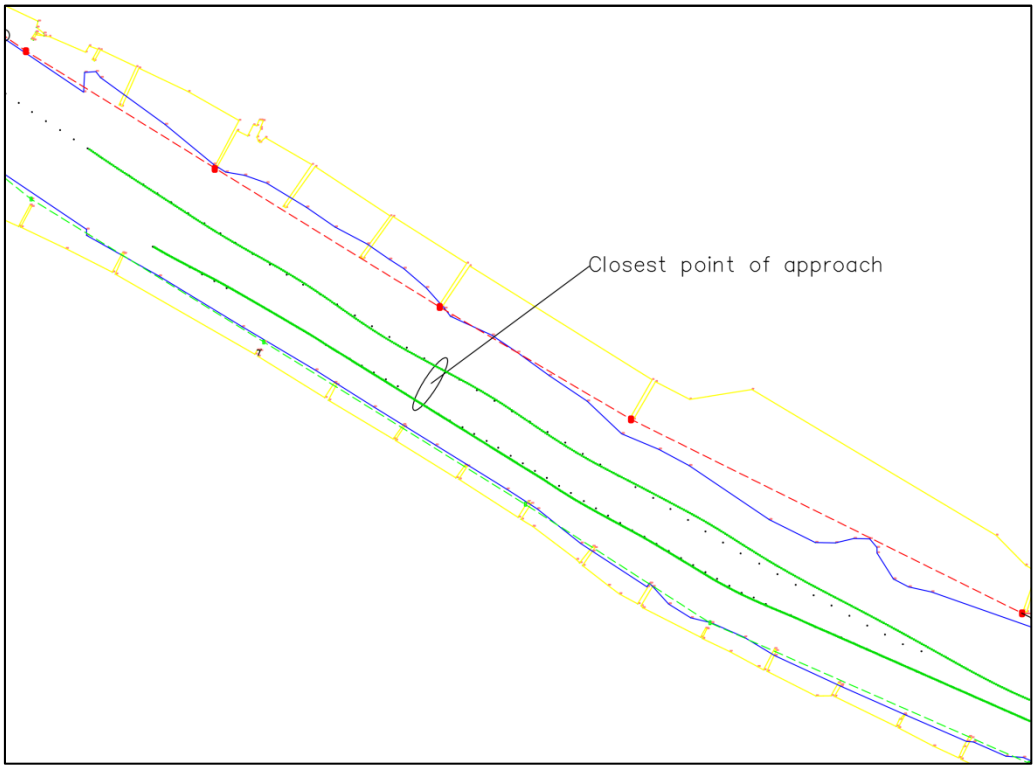

Figure XI-5 Comparing ship tracks of overtaking encounter between AIS data (black dots) and results from simulation (black lines) (case 2)

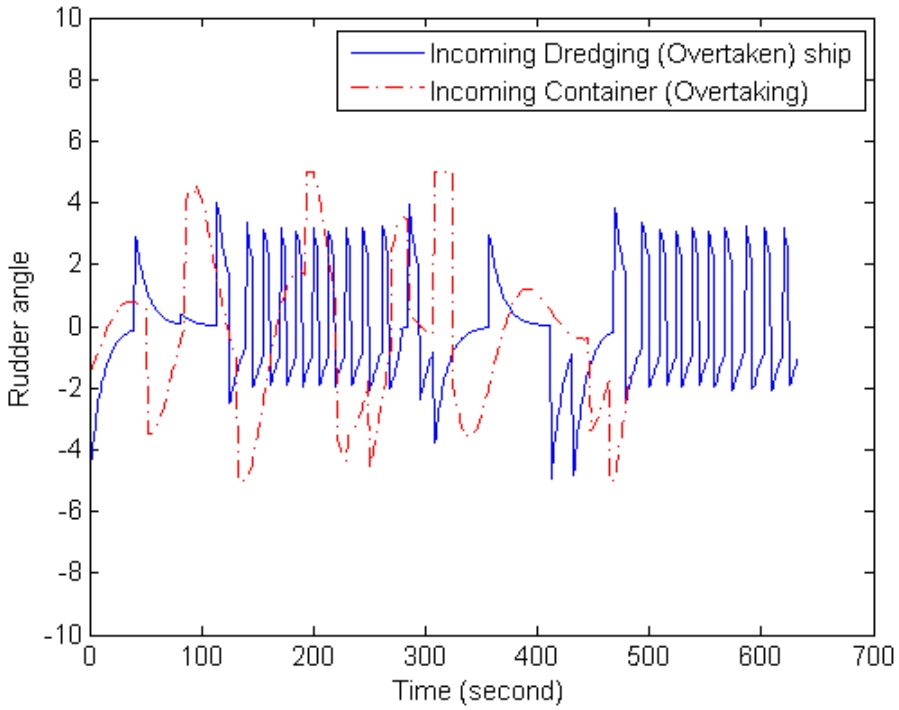

Figure XI-6 Rudder angles used in overtaking encounter (a positive value means rudder angle to starboard) (case 2)

Table XI-4 initial parameters for the ships in overtaking encounter scenario (Case 3)

parameters	Chemical (overtaken)	Chemical (overtaking)
xcor	-572.19595	-683.2875
ycor	259.0162	363.9069
LOA (m)	170	85
Gross Tonnage (t)	19420	1756
Speed (kn)	6.2	11.5
heading (°)	122	120
Dr2 (m)	101	N/A
Dr3 (m)	120	153
Dl2 (m)	N/A	130
$D_{overtaking}$ (m)	500	500
$d_{overtaking\_after}$ (m)	863	190

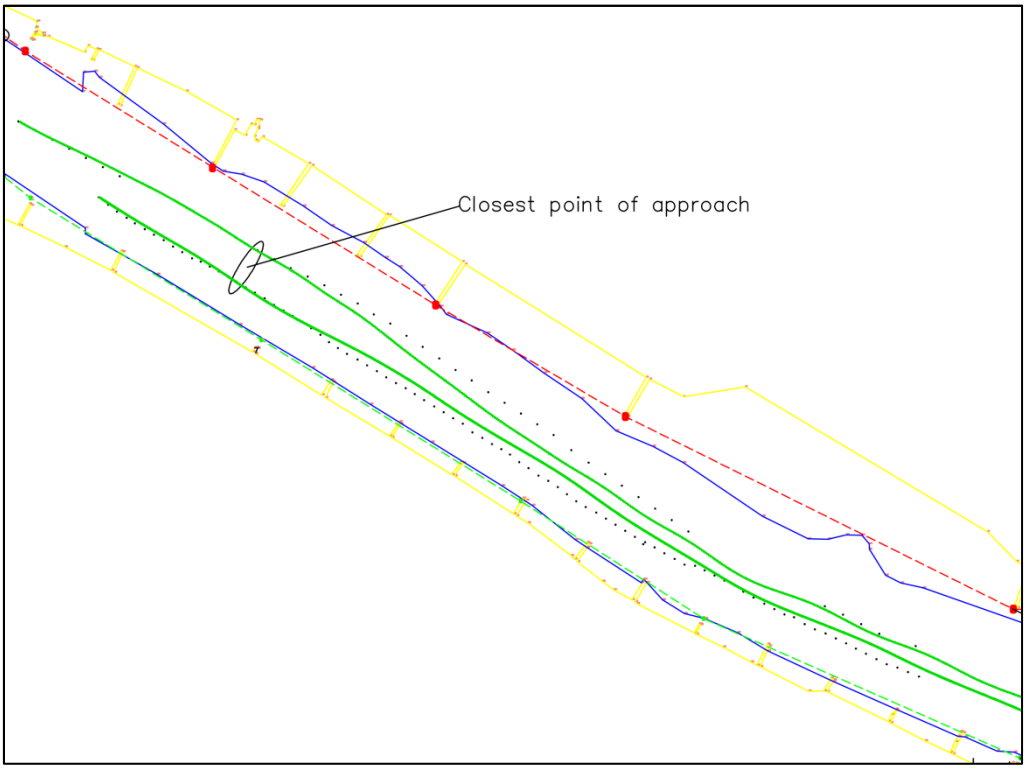

Figure XI-7 Comparing ship tracks of overtaking encounter between AIS data (black dots) and results from simulation (black lines) (case 3)

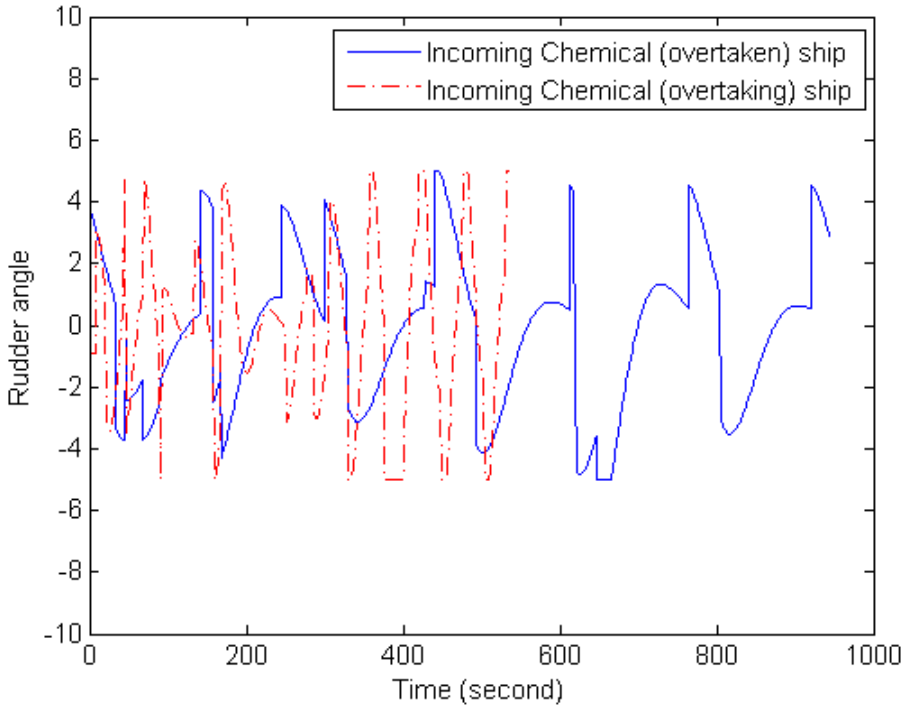

Figure XI-8 Rudder angles used in overtaking encounter (a positive value means rudder angle to starboard) (case 3)

XII. FACE VALIDATION OF THE TRAJECTORIES OF SHIP TRAFFIC FROM THE CHINESE CASE

This appendix is relevant to section 8.6.1. The figures are face validation of the overall ship trajectories.

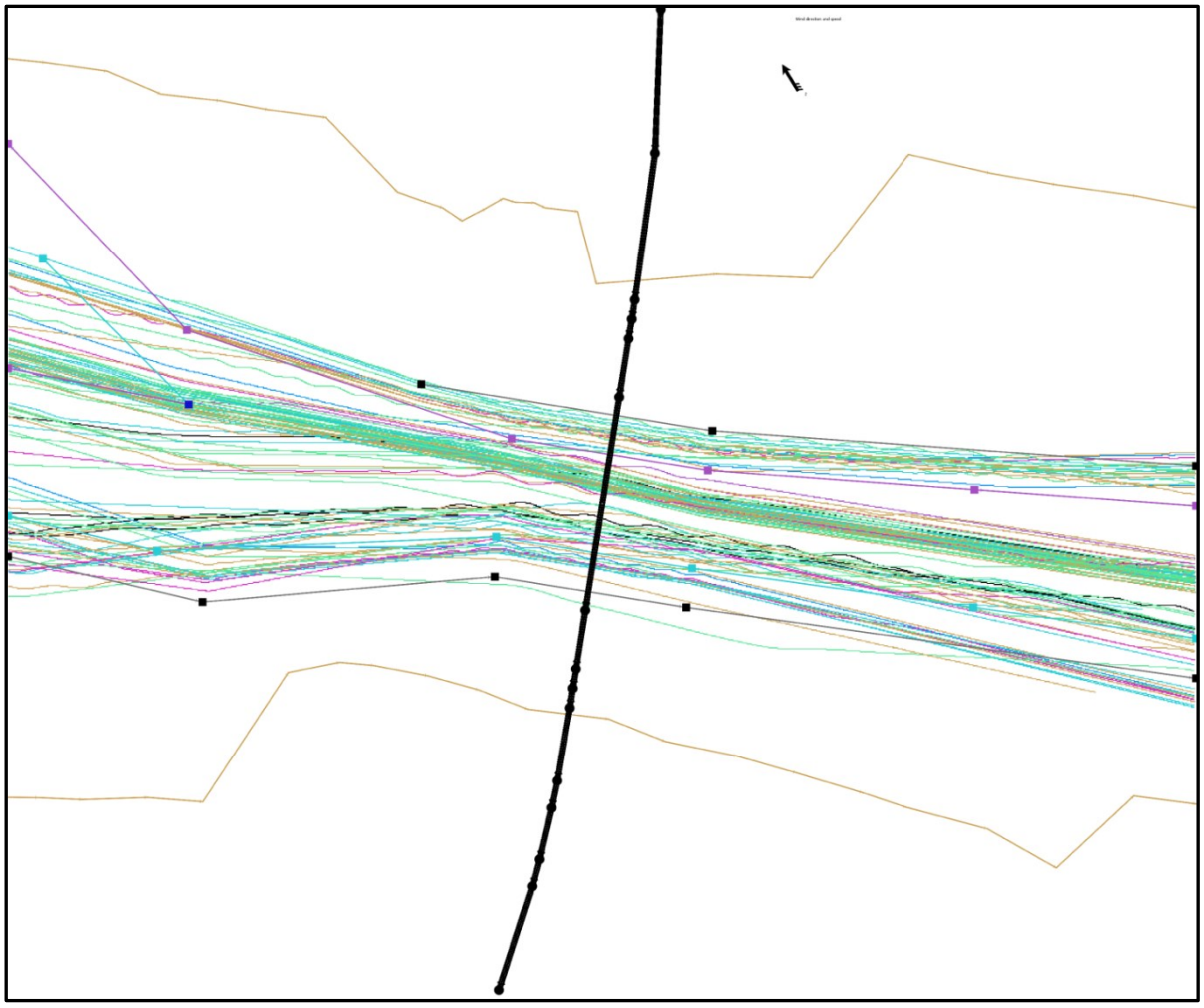

Figure XII-1 Ship trajectories from the simulation results of the Chinese case

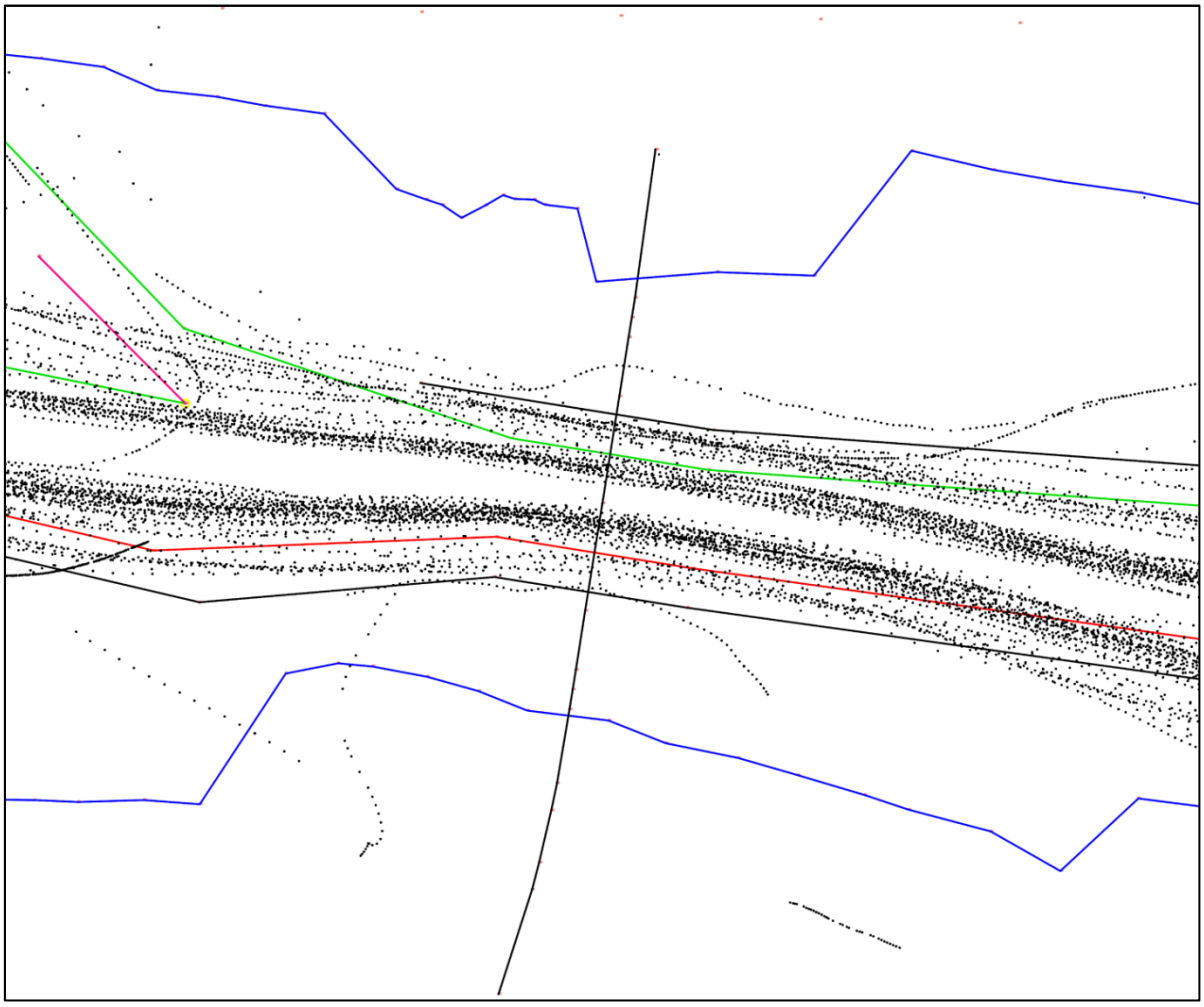

Figure XII-2 Ship trajectories from the AIS data of the Chinese case

XIII. THE SHIP TRACKS WITH MALFUNCTIONS HAPPENED ONBOARD

This appendix is relevant to section 9.2.2 and section 9.2.3. The figures show the ship tracks with engine failures and rudder failures individually.

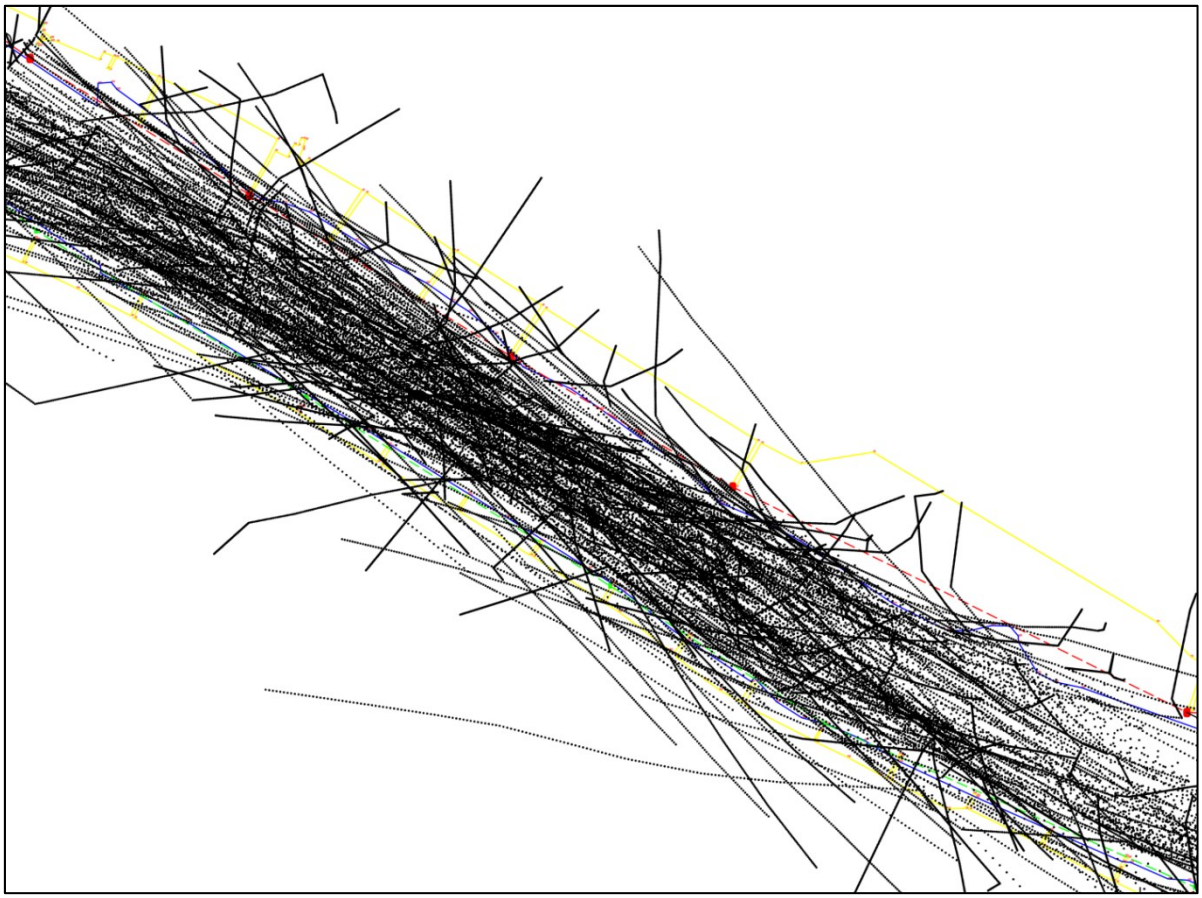

Figure XIII-1 A snapshot of groundings with engine failure onboard in the simulation

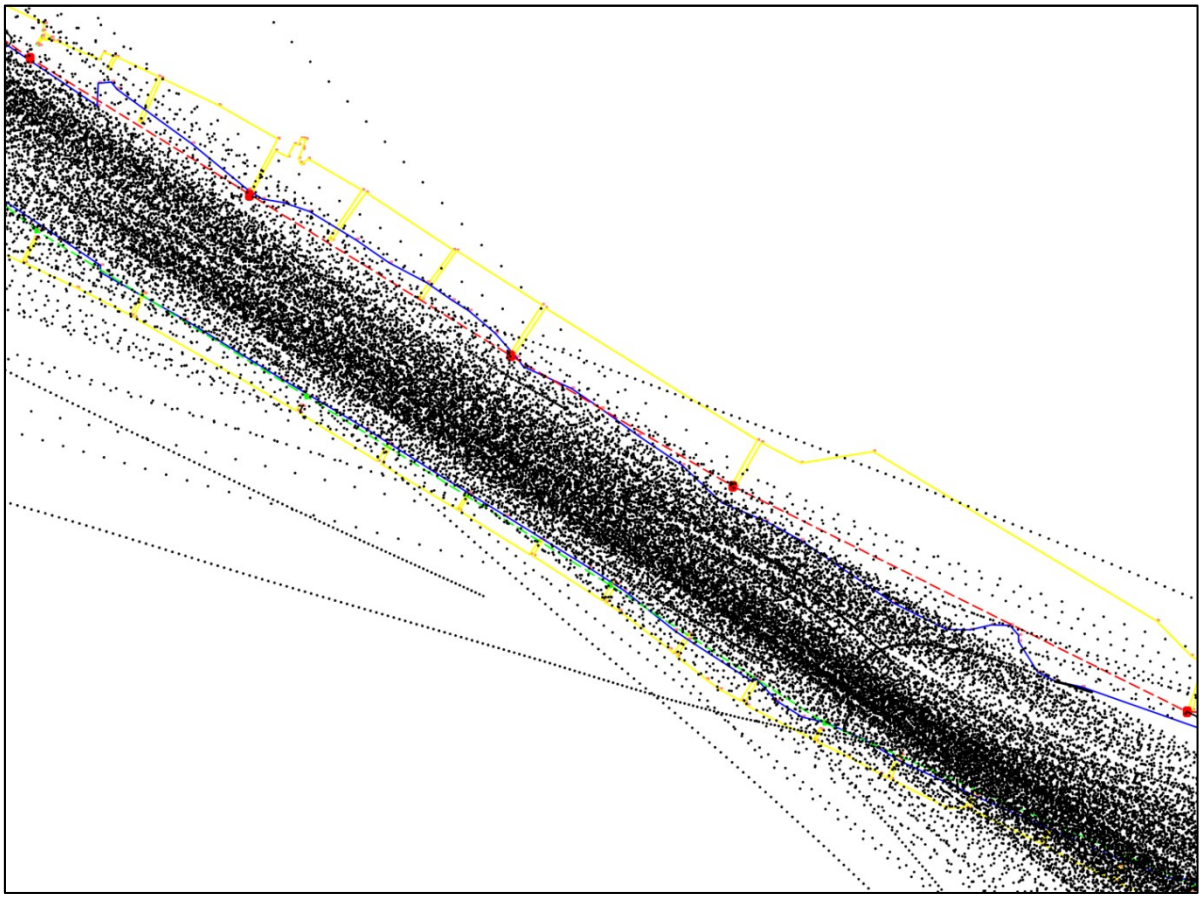

Figure XIII-2 A snapshot of groundings with rudder failure onboard in the simulation

REFERENCES

AASHTO (2004). *AASHTO LRFD bridge design specifications - SI units. 3rd edition*. American Association of State Highway and Transportation Officials.

Ahn, J. H., Rhee, K. P. and You, Y. J. (2012). A study on the collision avoidance of a ship using neural networks and fuzzy logic. *Applied Ocean Research*, **37**, 162-173.

Ale, B. J. M., Bellamy, L. J., van der Boom, R., Cooper, J., Cooke, R. M., Goossens, L. H. J., Hale, A. R., Kurowicka, D., Morales, O., Roelen, A. L. C. and Spouge, J. (2009). Further development of a Causal model for Air Transport Safety (CATS): Building the mathematical heart. *Reliability Engineering & System Safety*, **94**, 1433-1441.

Biehl, F., Dalhoff, P. and Povel, D. (2007). *Collision Risk Analysis and Collision Friendly Design of Offshore Wind Farms*.

Bin, L. (2006). Behavior of Ship Officers in Maneuvering to Prevent a Collision. *Journal of marine science and technology*, **14**, 225-230.

Davis, P., Dove, M. and Stockel, C. (1980). A computer simulation of marine traffic using domains and arenas. *The journal of Navigation*, **33**, 215-222.

De Boer, T. (2010). *Application of AIS data in a nautical traffic model*. Delft University of Tecknology.

Fang, J., Xu, Y., Liu, M., Zhang, J. and Li, B. (2009). Study on dangerous collision area of ships out of control in Sutong Bridge area. *ENGINEERING SCIENCES*, **7**, 83-86.

Fowler, T. G. and Sorgard, E. (2000). Modeling ship transportation risk. *Risk Analysis*, **20**, 225-244.

Frandsen, A. G., Olsen, D., Lund, H. T. and Bach, P. (1991). *Evaluation of minimum bridge span openings applying ship domain theory*. Transportation Research Board.

Friis-Hansen, A. (2000). *Bayesian Networks as a Decision Support Tool in Marine Applications*. Department of Naval Architecture and Offshore Engineering, Technical University of Denmark.

Gardenier, J. S. Safety of Bridges and Offshore Structures – the Role of Ship Simulation. Proceedings of the Ship Collision with Bridges and Offshore Structures, Introductory Report, IABSE COLLOQUIUM, Copenhagen/Denmark

Geng, B. (2007). *Safety Assessment of Bridges Due to Vessel Impact*. Tongji University.

Geng, B., Wang, H. and Wang, J. (2008). Probabilistic Model of Influence Parameters for Vessel-Bridge Collisions in Three-Gorges Reservoir. *JOURNAL OF TONGJI UNIVERSITY(NATURAL SCIENCE)*, 477-482.

Goerlandt, F. and Kujala, P. (2011). Traffic simulation based ship collision probability modeling. *Reliability Engineering & System Safety*, **96**, 91-107.

Goerlandt, F. and Kujala, P. (2014). On the reliability and validity of ship–ship collision risk analysis in light of different perspectives on risk. *Safety Science*, **62**, 348-365.

Goodwin, E. M. (1975). A Statistical Study of Ship Domains. *The journal of Navigation*, **28**, 328-344.

Grabowski, M., Merrick, J. R. W., Harrold, J., Massuchi, T. and van Dorp, J. (2000). Risk modeling in distributed, large-scale systems. *Systems, Man and Cybernetics, Part A: Systems and Humans, IEEE Transactions on*, **30**, 651-660.

Grimm, V., Berger, U., Bastiansen, F., Eliassen, S., Ginot, V., Giske, J., Goss-Custard, J., Grand, T., Heinz, S. K., Huse, G., Huth, A., Jepsen, J. U., Jørgensen, C., Mooij, W. M., Müller, B., Pe'er, G., Piou, C., Railsback, S. F., Robbins, A. M., Robbins, M. M., Rossmanith, E., Rüger, N., Strand, E., Souissi, S., Stillman, R. A., Vabø, R., Visser, U. and DeAngelis, D. L. (2006). A standard protocol for describing individual-based and agent-based models. *Ecological Modelling*, **198**, 115-126.
Grimm, V., Berger, U., DeAngelis, D. L., Polhill, J. G., Giske, J. and Railsback, S. F. (2010). The ODD protocol: A review and first update. *Ecological Modelling*, **221**, 2760-2768.
Gucma, L. (2009). Method of ship-bridge collision safety evaluation. *Reliability & Risk Analysis: Theory & Applications*, **2**, 50-63.
Gucma, L. and Schoeneich, M. (2008). Probabilistic Model of Underkeel Clearance in Decision Making Process of Port Captain. *TransNav, the International Journal on Marine Navigation and Safety of Sea Transportation*, **2**, 167-171.
Hänninen, M. and Kujala, P. (2010). The Effects of Causation Probability on the Ship Collision Statistics in the Gulf of Finland. *International Journal on Marine Navigation and Safety of Sea Transportation*, **Vol. 4**, 79-84.
Harati-Mokhtari, A., Wall, A., Brooks, P. and Wang, J. (2007). Automatic Identification System (AIS): data reliability and human error implications. *Journal of navigation*, **60**, 373.
Harrald, J. R., Mazzuchi, T. A., Spahn, J., Van Dorp, R., Merrick, J., Shrestha, S. and Grabowski, M. (1998). Using system simulation to model the impact of human error in a maritime system. *Safety Science*, **30**, 235-247.
Hasegawa, K., Shigemori, Y. and Ichiyama, Y. Feasibility study on intelligent marine traffic system. Proceedings of the 5th IFAC Conference on Maneuvering and Control of Marine Craft (MCMC), Denmark
Helbing, D. and Molnar, P. (1995). Social force model for pedestrian dynamics. *Physical review E*, **51**, 4282.
Hu, S. P., Cai, C. Q. and Fang, Q. G. (2008). Risk Bayesian Assessment Approach to HOF-based Ship Operation in Harbour. *Ieem: 2008 International Conference on Industrial Engineering and Engineering Management*, **Vols 1-3**, 1954-1960.
IALA (2010). *Technical characteristics for an automatic identification system using time division multiple access in the VHF maritime mobile band*. International Telecommunications Union.
Itoh, H., Mitomo, N., Matsuoka, T. and Murohara, Y. An Extension of M-Shel Model for Analysis of Human Factors at Ship Operation. Proceedings of the 3rd International Conference on Collision and Grounding of Ships (ICCGS 2004), Izu, Japan
Jarque, C. M. and Bera, A. K. (1987). A test for normality of observations and regression residuals. *International Statistical Review/Revue Internationale de Statistique*, 163-172.
Karamouzas, I., Heil, P., van Beek, P. and Overmars, M. (2009). A predictive collision avoidance model for pedestrian simulation. *Motion in Games*, 41-52.
Karmarkar, J. and Vargus, R. A Multi-Threat Avoidance Maneuver Generator. Proceedings of the OCEANS'80, Seattle, WA
Kawaguchi, A., Xiong, X., Inaishi, M. and Kondo, H. A computerized navigation support for maneuvering clustered ship groups in close proximity. Proceedings of the Best session paper in the 10th International Conference on Information Systems Analysis and Synthesis (ISAS'04), Orlando, Florida
Kiriya, N. (2001). Statistical Study on Reliability of Ship Equipment and Safety Management– Reliability Estimation for Failures on Main Engine System by Ship Reliability Database System. *Bulletin of the JIME*, **29**, P64-70.
Koldenhof, Y., Van der Tak, C. and Glansdorp, C. Risk Awareness: a model to calculate the risk of a ship dynamically. Proceedings of the XIII International Scientific and Technical Conference on Marine Traffic Egineerng, Molmo, Sweden

Köse, E., Başar, E., Demirci, E., Güneroğlu, A. and Erkebay, Ş. (2003). Simulation of marine traffic in Istanbul Strait. *Simulation Modelling Practice and Theory*, **11**, 597-608.
Kujala, P., Hanninen, M., Arola, T. and Ylitalo, J. (2009). Analysis of the marine traffic safety in the Gulf of Finland. *Reliability Engineering & System Safety*, **94**, 1349-1357.
Kunz, C. Ship bridge collision in river traffic, analysis and design practice. Proceedings of the Ship Collision Analysis: Proceedings of the International Symposium on Advances in Ship Collision, Copenhagen, Denmark
Łącki, M., Weintrit, A., Neumann, T., Formela, K., Kalina, T., Piala, P., Boykov, A., Katenin, V., Demchenkov, O. and Gucma, L. (2012). Neuroevolutionary Ship Handling System in a Windy Environment. *International Journal on Marine Navigation and Safety of Sea Transportation*, **6**, 453-458.
Laheld, P. Statistics on Collision Accidents Involving Offshore Structures. Proceedings of the Ship Collision with Bridges and Offshore Structures, Introductory Report, IABSE COLLOQUIUM, Copenhagen/Denmark
Larsen, O. D. Ship Collision Risk Assessment for Bridge. Proceedings of the Ship Collision with Bridges and Offshore Structures, Introductory Report, IABSE COLLOQUIUM, Copenhagen/Denmark
Larsen, O. D. (1993). *Ship Collision with Bridges: The Interaction Between Vessel Traffic and Bridge Structures*. International Association for Bridge and Structural Engineering.
Li, Q. and Fan, H. (2012a). A Simulation Model for Detecting Vessel Conflicts Within a Seaport. *TransNav - International Journal on Marine Navigation and Safety of Sea Transportation*, **6**, 11-17.
Li, S. Y., Meng, Q. and Qu, X. B. (2012b). An Overview of Maritime Waterway Quantitative Risk Assessment Models. *Risk Analysis*, **32**, 496-512.
Li, Z. (2008). *Research on Speed Loss during Ships' Turning*. Dalian Maritime University.
Li, Z. B., Zhang, X. K. and Zhang, Y. (2007). Prediction of maneuver ability indecis for ships using SPSS (in Chinese). *MARINE TECHNOLOGY*, **5**, 1-5.
Lin, T., Wang, J. and Chen, A. (2007). Construction of Probability Models About Ship Collision with Bridge Piers Based on Accident Records. *JOURNAL OF TONGJI UNIVERSITY(NATURAL SCIENCE)*, 181-186.
Lopes, R. H. C., Reid, I. and Hobson, P. R. The two-dimensional Kolmogorov-Smirnov test. Proceedings of the XI International Workshop on Advanced Computing and Analysis Techniques in Physics Research, Amsterdam, the Netherlands
Macal, C. M. and North, M. J. (2010). Tutorial on agent-based modelling and simulation. *Journal of Simulation*, **4**, 151-162.
Merrick, J. R. W., van Dorp, J. R., Blackford, J. P., Shaw, G. L., Harrald, J. and Mazzuchi, T. A. (2003). A traffic density analysis of proposed ferry service expansion in San Francisco Bay using a maritime simulation model. *Reliability Engineering & System Safety*, **81**, 119-132.
Merrick, J. R. W., van Dorp, J. R. and Dinesh, V. (2005). Assessing uncertainty in simulation-based maritime risk assessment. *Risk Analysis*, **25**, 731-743.
Merrick, J. R. W., van Dorp, J. R., Harrald, J., Mazzuchi, T., Spahn, J. E. and Grabowski, M. (2000). A systems approach to managing oil transportation risk in Prince William Sound. *Systems Engineering*, **3**, 128-142.
Merrick, J. R. W., van Dorp, J. R., Mazzuchi, T., Harrald, J. R., Spahn, J. E. and Grabowski, M. (2002). The Prince William Sound risk assessment. *Interfaces*, **32**, 25-40.
Merrick, J. R. W. and van Dorp, R. (2006). Speaking the truth in maritime risk assessment. *Risk Analysis*, **26**, 223-237.
Montewka, J., Hinz, T., Kujala, P. and Matusiak, J. (2010). Probability modelling of vessel collisions. *Reliability Engineering & System Safety*, **95**, 573-589.
Mou, J. M., Tak, C. and Ligteringen, H. (2010). Study on collision avoidance in busy waterways by using AIS data. *Ocean Engineering*, **37**, 483-490.

Murakami, Y., Minami, K., Kawasoe, T. and Ishida, T. Multi-agent simulation for crisis management. Proceedings of the Proceedings IEEE Workshop on Knowledge Media Networking,
Nguyen, M. Q. (2008). *Approach channels: risk- and simulation-based design*. Delft University of Tecknoledge.
Nyman, T., Porthin, M. and Karppinen, S. (2010). *Collision and grounding frequency analyses in the Gulf of Finland*. Technical Research Centre of Finland.
Parikh, R. (1994). Vagueness and utility: The semantics of common nouns. *Linguistics and Philosophy*, **17**, 521-535.
Pedersen, P. T. (2002). Collision risk for fixed offshore structures close to high-density shipping lanes. *Proceedings of the Institution of Mechanical Engineers, Part M: Journal of Engineering for the Maritime Environment*, **216**, 29-44.
Pedersen, P. T., Valsgård, S., Olsen, D. and Spangenberg, S. (1993). Ship impacts: Bow collisions. *International Journal of Impact Engineering*, **13**, 163-187.
Pedersen, P. T. and Zhang, S. The mechanics of ship impacts against bridges. Proceedings of the Ship Collision Analysis: Proceedings of the International Symposium on Advances in Ship Collision, Copenhagen, Denmark
PIANC (2001). *Ship Collision due to the Presence of Bridge, Report of Working Group 19 of the INLAND NAVIGATION COMMISION*. PIANC General Secretariat, 2001.
Pietrzykowski, Z. and Uriasz, J. (2009). The Ship Domain – A Criterion of Navigational Safety Assessment in an Open Sea Area. *The journal of Navigation*, **62**, 93-108.
Pietrzykowski, Z., Wielgosz, M. and Siemianowicz, M. Ship domain in the restricted area–simulation research.
Pimontel, L. A. (2007). *A study into maritime collision probability*. TU Delft.
Priadi, A. A., Tjahjono, T. and Benabdelhafid, A. (2012). Assessing Safety of Ferry Routes by Ship Handling Model through AHP and Fuzzy Approach. *Intelligent Information Management*, **4**, 277-283.
Railsback, S. F., Lytinen, S. L. and Jackson, S. K. (2006). Agent-based simulation platforms: Review and development recommendations. *Simulation*, **82**, 609-623.
Razali, N. M. and Wah, Y. B. (2011). Power comparisons of shapiro-wilk, kolmogorov-smirnov, lilliefors and anderson-darling tests. *Journal of Statistical Modeling and Analytics*, **2**, 21-33.
Reynolds, C. W. Steering behaviors for autonomous characters. Proceedings of the Game Developers Conference,
Ribeiro, M. I. (2005). Obstacle avoidance. *Instituto de Sistemas e Robótica, Instituto Superio Técnico*, 1.
Roeleven, D., Kokc, M., Stipdonk, H. I. and De Vries, W. A. (1995). Inland waterway transport: Modelling the probability of accidents. *Safety Science*, **19**, 191-202.
Samuelides, M. S., Tabri, K., Incecik, A. and Dimou, D. (2008). Scenarios for the assessment of the collision behavior of ships. *International Shipbuilding Progress*, **55**, 145-162.
Shen, W. (2012). *A statistical analysis of average vessel behaviour by AIS data*. UNESCO-IHE Institute.
Shu, Y., Daamen, W., ligteringen, H. and Hoogendoorn, S. (2013a). *AIS DATA ANALYSIS FOR VESSEL BEHAVIOUR UNDER CURRENT AND ENCOUNTERS IN THE BOTLEK AREA IN THE PORT OF ROTTERDAM*. Delft University of Technology.
Shu, Y., Daamen, W., ligteringen, H. and Hoogendoorn, S. (2013b). Vessel Speed, Course, and Path Analysis in the Botlek Area of the Port of Rotterdam, Netherlands. *Transportation Research Record: Journal of the Transportation Research Board*, **2330**, 63-72.
Sii, H. S., Ruxton, T. and Wang, J. (2001). A fuzzy-logic-based approach to qualitative safety modelling for marine systems. *Reliability Engineering & System Safety*, **73**, 19-34.
Szwed, P., van Dorp, J. R., Merrick, J. R. W., Mazzuchi, T. A. and Singh, A. (2006). A Bayesian paired comparison approach for relative accident probability assessment with covariate information. *European Journal of Operational Research*, **169**, 157-177.
Teahan, W. J. (2010). *Cars Guessing Game NetLogo model*. Ventus Publishing Aps.

Trucco, P., Cagno, E., Ruggeri, F. and Grande, O. (2008). A Bayesian Belief Network modelling of organisational factors in risk analysis: A case study in maritime transportation. *Reliability Engineering & System Safety*, **93**, 845-856.
Ulusçu, Ö. S., Özbaş, B., Altıok, T. and Or, İ. (2009). Risk analysis of the vessel traffic in the strait of Istanbul. *Risk Analysis*, **29**, 1454-1472.
Van den Berg, J., Lin, M. and Manocha, D. Reciprocal velocity obstacles for real-time multi-agent navigation. Proceedings of the Robotics and Automation, 2008, Pasadena, CA
van der Rijken, W. W. J. L. (2008). Capability statement of mscn simulators.
van Dorp, J. R. and Merrick, J. R. W. (2011). On a risk management analysis of oil spill risk using maritime transportation system simulation. *Annals of Operations Research*, **187**, 249-277.
van Dorp, J. R., Merrick, J. R. W., Harrald, J. R., Mazzuchi, T. A. and Grabowski, M. (2001). A risk management procedure for the Washington state ferries. *Risk Analysis*, **21**, 127-142.
van Manen, S. E. (2001). *Ship collisions due to the presence of bridge*. PIANC General Secretariat.
van Manen, S. E. and Frandsen, A. G. (1998). Ship collision with bridges, review of accidents. *Ship collision analysis*, 3-11.
Vaněk, O., Jakob, M., Hrstka, O. and Pěchouček, M. (2012). Using multi-agent simulation to improve the security of maritime transit. *Multi-Agent-Based Simulation XII*, 44-58.
Vrouwenvelder, A. C. W. M. Design for Ship Impact according to Eurocode 1, Part 2.7. Proceedings of the Ship Collision Analysis: Proceedings of the International Symposium on Advances in Ship Collision Analysis, Copenhagen, Denmark
Wang, G., Ji, C., Kujala, P., Lee, S.-G., Marino, A., Sirkar, J., Suzuki, K., Pedersen, P. T., Vredeveldt, A. W. and Yuriy, V. ISSC Committee V.1: Collision and Grounding. Proceedings of the 16th International Ship and Offshore Structures Congress, Southampton
Wang, J. and Geng, B. (2010). *Probabilistic Risk Assessment and Safety measurement of bridge under vessel collisions*. China Communications Press.
Webster, W. C. (1992). *Shiphandling simulation: Application to waterway design*. National Academies Press.
Wilensky, U. (1999). Netlogo. http://ccl.northwestern.edu/netlogo/., Center for Connected Learning and Computer-Based Modeling. *Northwestern University: Evanston, IL, USA*.
Xiao, F., Ligteringen, H., van Gulijk, C. and Ale, B. (2012). Artificial Force Fields for Multi-agent Simulations of Maritime Traffic: A Case Study of Chinese Waterway. *Procedia Engineering*, **45**, 807-814.
Xiao, F. L., Ale, B. and Jagtman, E. (2010). Overview of Methods on Modeling Risks of Ship in the Presence of Bridge. *Progress in Safety Science and Technology, Vol. Viii, Pts a and B*, **8**, 1905-1916.
Xiao, Y., Zhang, H. and Li, S. Dynamic Data Driven Multi-agent Simulation in Maritime Traffic. Proceedings of the International Conference on Computer and Automation Engineering, Thailand
Ylitalo, J. (2009). *Ship-ship collision probability of the crossing area between Helsinki and Tallinn*.
Ylitalo, J. (2010). *Modelling Marine Accident Frequency*. Aalto University School of Science and Technology.
Zhang, F., Li, J. and Zhao, Q. Single-lane traffic simulation with multi-agent system. Proceedings of the 2005 IEEE Proceedings on Intelligent Transportation Systems, Vienna, Austria
Zhang, H., Xiao, Y. and Li, S. Agent Based Simulation Architecture for Ship's Routeing. Proceedings of the International Conference on Computer and Automation Engineering, Bangkok
Zheng, B., Xia, S., Chen, J. and Jin, Y. Human Factor Analysis on Marine Accidents Based on Attribute Reduction. Proceedings of the International Conference on Measuring Technology and Mechatronics Automation, Zhangjiajie, Hunan